EXPERIMENTAL SPINDLE TORQUE AND OPEN-WATER PERFORMANCE OF TWO SKEWED CONTROLLABLE-PITCH PROPELLERS

DAVID W. TAYLOR NAVAL SHIP RESEARCH AND DEVELOPMENT CENTER

DECEMBER 1975

DAVID W. TAYLOR NAVAL SHIP RESEARCH AND DEVELOPMENT CENTER

Bethesda, Md. 20084

EXPERIMENTAL SPINDLE TORQUE AND OPEN-WATER PERFORMANCE OF TWO SKEWED CONTROLLABLE-PITCH PROPELLERS

by
R.J. Boswell
J.J. Nelka
R.D. Kader

SHIP PERFORMANCE DEPARTMENT
RESEARCH AND DEVELOPMENT REPORT

December 1975

Report 4753

MAJOR DTNSRDC ORGANIZATIONAL COMPONENTS

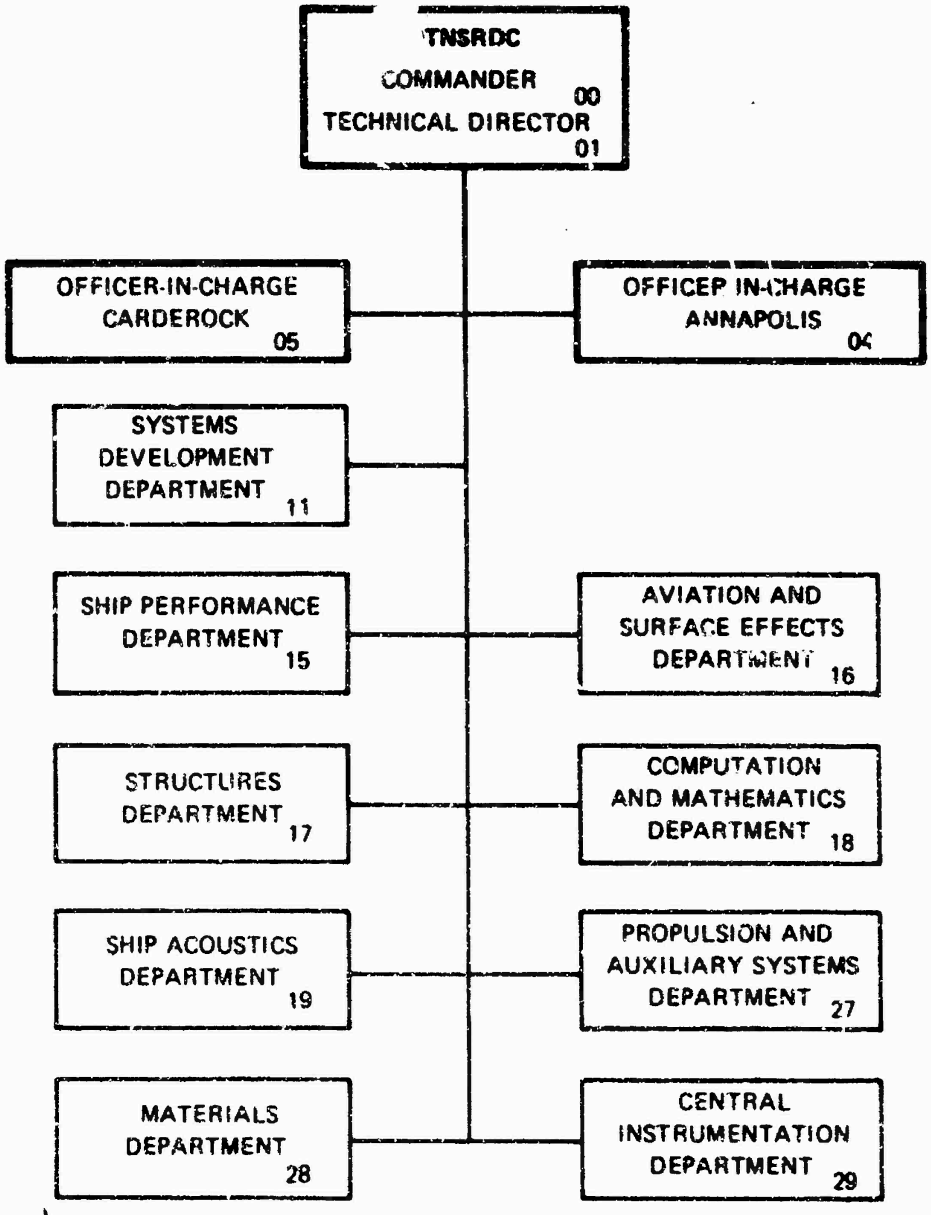

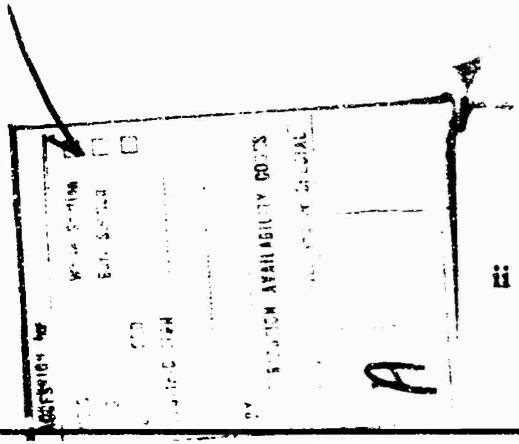

UNCLASSIFIED
SECURITY CLASSIFICATION OF THIS PAGE (When Data Entered)

REPORT DOCUMENTATION PAGE		READ INSTRUCTIONS BEFORE COMPLETING FORM
1. REPORT NUMBER 4753	2. GOVT ACCESSION NO.	3. RECIPIENT'S CATALOG NUMBER
4. TITLE (and Subtitle) EXPERIMENTAL SPINDLE TORQUE AND OPEN-WATER PERFORMANCE OF TWO SKEWED CONTROLLABLE-PITCH PROPELLERS		5. TYPE OF REPORT & PERIOD COVERED Final 6. PERFORMING ORG. REPORT NUMBER
7. AUTHOR(s) Robert J. Boswell, John J. Nelka and Richard D. Kader		8. CONTRACT OR GRANT NUMBER(s)
9. PERFORMING ORGANIZATION NAME AND ADDRESS David W. Taylor Naval Ship Research and Development Center Bethesda, Maryland 20084		10. PROGRAM ELEMENT, PROJECT, TASK AREA & WORK UNIT NUMBERS Program Element 63508N Task Area S4622, Task 17425 Work Unit 1-1544-278
11. CONTROLLING OFFICE NAME AND ADDRESS Naval Sea Systems Command (S0331G) Washington, D.C. 20362		12. REPORT DATE December 1975 13. NUMBER OF PAGES 174
14. MONITORING AGENCY NAME & ADDRESS(if different from Controlling Office)		15. SECURITY CLASS. (of this report) 15a. DECLASSIFICATION/DOWNGRADING SCHEDULE

16. DISTRIBUTION STATEMENT (of this Report)

APPROVED FOR PUBLIC RELEASE: DISTRIBUTION UNLIMITED

17. DISTRIBUTION STATEMENT (of the abstract entered in Block 20, if different from Report)

18. SUPPLEMENTARY NOTES

19. KEY WORDS (Continue on reverse side if necessary and identify by block number)

Skewed Propeller
Controllable-Pitch Propeller
Spindle Torque
Propulsion

20. ABSTRACT (Continue on reverse side if necessary and identify by block number)

Experimental results are presented on the spindle torque and open-water performance of two skewed controllable-pitch propellers. Both [illegible] have radial distributions of skew specified so that the section midchord is forward of the spindle axis at the inner radii and aft of the spindle axis at the outer radii. One propeller has no rake and the other has substantial forward rake. The experiments were conducted at steady

(Continued on reverse)

DD FORM 1 JAN 73 1473 EDITION OF 1 NOV 65 IS OBSOLETE
S/N 0102-014-6601

UNCLASSIFIED
SECURITY CLASSIFICATION OF THIS PAGE (When Data Entered)

(Block 20, Continued)

conditions in uniform flow in a towing basin over a range of positive and negative pitch ratios and a range of positive and negative advance coefficients so that the complete maneuvering envelope of the ship was simulated in a quasi-steady manner.

The experimental open-water performance was correlated with calculated values based on a least-squares fit to previous systematic experimental data. The correlation indicates that the calculation procedure may be adequate for preliminary dynamic simulation studies in cases where open-water data are not available on a similar model propeller.

The experimental hydrodynamic spindle torque results are generally consistent with previously reported experimental results. These results suggest that realistic highly skewed propellers can be designed with spindle torque characteristics comparable to those of equivalent propellers without significant skew. No definite conclusions could be drawn regarding the effect of forward rake on spindle torque. The experimental values of centrifugal spindle torque generally agreed with analytically calculated values over a range of pitch ratios.

TABLE OF CONTENTS

LIST OF FIGURES

LIST OF TABLES

NOTATION

A_E	Expanded blade area
A_0	Propeller disk area, $\pi D^2/4$
C_L	Lift coefficient of blade section
C_Q^*	Torque index, $Q/[(\rho/2)(V_R^*)^2 A_0 D]$
C_T^*	Thrust index, $T/[(\rho/2)(V_R^*)^2 A_0]$
C_{Th}	Thrust loading coefficient, $T/[(\rho/2)\ V_A^2\ A_0]$
c	Blade section chord length
D	Propeller diameter
f_M	Camber of propeller blade section
J	Advance coefficient, $J = V_A/nD$
J'	Modified advance coefficient, $V_A/[V_A^2 + n^2D^2]^{1/2}$
K_Q	Torque coefficient, $Q/(\rho n^2 D^5)$
K_{SC}	Centrifugal blade spindle torque coefficient, $Q_{SC}/(\rho_p n^2 D^5)$
K_{SH}^*	Hydrodynamic blade spindle torque index, $Q_{SH}/[(\rho/2)(V_R^*)^2 A_0 D]$
K'_{SH}	Modified hydrodynamic blade spindle torque coefficient, $Q_{SH}/[\rho D^3 (V_A^2 + n^2D^2)]$
K_T	Thrust coefficient, $T/(\rho n^2 D^4)$

n	Propeller revolutions per unit time
p	Propeller blade section pitch
Q	Propeller torque
Q_S	Blade spindle torque arising from hydrodynamic and centrifugal loading
Q_{SA}	Blade spindle torque arising from aerodynamic loading
Q_{SC}	Blade spindle torque arising from centrifugal loading
Q_{SH}	Blade spindle torque arising from hydrodynamic loading
R	Propeller radius
R_n	Reynolds number, $c_{0.7}V_R^*/\nu$
r	Radial coordinate from propeller axis
S	Skew back of propeller blade section measured from the spindle axis to the midchord point of the blade section, positive towards trailing edge
T	Thrust of propeller, positive forward
t	Maximum thickness of propeller blade section
V_A	Propeller speed of advance
V_L	Circumferential mean longitudinal velocity at local radius
V_R^*	Vector sum of speed of advance and rotational velocity at the 0.7 radius, $[V_A^2 + (0.7\ \pi nD)^2]^{1/2}$

x	Nondimensional radial position, $x = r/R$
Z	Number of blades
Z_R	Rake of propeller blade section measured from the propeller plane (plane normal to propeller axis and containing spindle axis) to the generator line (intersection of pitch helices and the plane containing the spindle axis and propeller axis), positive aft
Z_T	Total rake, $Z_R + \theta_s \tan \phi$
β^*	Propeller advance angle at 0.7R, $\tan^{-1}[V_A/(0.7\pi nD)]$
θ_s	Skew angle measured from spindle axis to projection of blade section midchord onto propeller plane (plane normal to propeller axis and containing spindle axis), positive towards trailing edge, $(S \cos \phi)/r$
ν	Kinematic viscosity of water
ρ	Mass density of water
ρ_A	Mass density of air
ρ_P	Mass density of propeller blade
ϕ	Pitch angle of propeller blade section, $\tan^{-1}[P/(\pi xD)]$

Subscripts

D	Value at design conditions
h	Value at the propeller hub
0.7	Value at the 0.7 radius

ABSTRACT

Experimental results are presented on the spindle torque and open-water performance of two skewed controllable-pitch propellers. Both propellers have radial distributions of skew specified so that the section midchord is forward of the spindle axis at the inner radii and aft of the spindle axis at the outer radii. One propeller has no rake and the other has substantial forward rake. The experiments were conducted at steady conditions in uniform flow in a towing basin over a range of positive and negative pitch ratios and a range of positive and negative advance coefficients so that the complete maneuvering envelope of the ship was simulated in a quasisteady manner.

The experimental open-water performance was correlated with calculated values based on a least-squares fit to previous systematic experimental data. The correlation indicates that the calculation procedure may be adequate for preliminary dynamic simulation studies in cases where open-water data are not available on a similar model propeller.

The experimental hydrodynamic spindle torque results are generally consistent with previously reported experimental results. These results suggest that realistic highly skewed propellers can be designed with spindle torque characteristics comparable to those of equivalent propellers without significant skew. No definite conclusions could be drawn regarding the effect of forward rake on spindle torque. The experimental values of centrifugal spindle torque generally agreed with analytically calculated values over a range of pitch ratios.

ADMINISTRATIVE INFORMATION

The work reported herein was funded by the Naval Sea Systems Command (NAVSEA 033) Program Element 63508N, Task Area [illegible] Task 17425. The work was performed under David W. Taylor Naval Ship Research and Development Center (DTNSRDC) Work Unit 1-1544-278.

INTRODUCTION

Controllable-reversible pitch (CP) propellers can achieve astern thrust by reversing pitch while maintaining ahead shaft rotation and therefore do not require reversing gearboxes. Such propellers are of

interest for ships powered by gas turbines and also offer several advantages for ships which must operate over a range of conditions, i.e., over a range of propeller thrust loading coefficients. For these applications, pitch control may enable the propeller to operate efficiently at off-design advance coefficients with less cavitation than fixed-pitch propellers. CP propellers are ideally suited for power plants which have high efficiencies over a limited range of rpm and for high-speed craft in which weight is critical and shaft reversal gearing is to be avoided if possible. CP propellers also have an advantage over fixed-pitch propellers for maneuvering and stopping since the propeller blades can be rotated to astern pitch with the full power of the ahead turbine available. Background information on CP propellers is available in the technical literature.[1-4]

Design problems for CP propeller blades are similar to those for fixed-pitch propellers except for (1) the additional parameter of spindle torque and (2) the restrictions on blade outline shape dictated by the requirement that the blades must pass through zero pitch to achieve pitch reversal. At the design condition, strength (with the additional complication at the palm), cavitation, and propeller-induced vibratory forces can be handled by exactly the same methods used for conventional propellers. At off-design pitch, performance (thrust as a function of

---

[1]Rusetskiy, A.A. "Hydrodynamics of Controllable-Pitch Propellers," Shipbuilding Publishing House, Leningrad (1968) (in Russian). A complete listing of references is given on page 161.

[2]Gunsteren, L.A., van, "Hydrodynamics of Controllable-Pitch Propellers," in Design and Economical Consideration on Shipbuilding and Shipping, Report of the Post Graduate Course, May 1969, University of Delft, the Netherlands, H. Veenman En Zonen N.V., Wageningen, the Netherlands (1970) pp. 212–252; also presented as "Design and Performance of Controllable-Pitch Propellers," New York Metropolitan Section, Society of Naval Architects and Marine Engineers (Mar 1970).

[3]Schanz, F., "The Controllable Pitch Propeller as an Integral Part of the Ship's Propulsion System," Transactions Society of Naval Architects and Marine Engineers, Vol. 75, pp. 194–223 (1967).

[4]Boatwright, G.M. and J. Strandell, "Controllable-Pitch Propellers," Fourth Annual Technical Symposium, Association of Senior Engineers, Naval Ship Systems Command, Washington, D.C. (31 Mar 1967).

pitch, rpm, and speed of advance) can be estimated from uniform flow experiments of previous designs.[5-8] Strom-Tejsen and Porter[9] have presented analytical expressions for estimating the off-design performance of CP propellers based on the experimental data of Gutsche and Schroeder.[8]

The problems associated with propulsion, cavitation, strength, and vibration-excitation forces are aggravated by the pitch-changing and reversing requirements of CP propellers. The requirement that the blades must pass through zero pitch limits the maximum blade area and generally leads to blade shapes which are narrow at the root and wide in the tip region. Neither the total blade area limitation nor the resulting chord length distribution are favorable for delaying or preventing blade cavitation, erosion, and performance breakdown. CP propellers which are designed to absorb high power and/or operate in a wake with significant circumferential variation generally have thick blade root sections for strength purposes. The combination of small blade chord and large root thickness produces blade root sections with high thickness/chord ratios which are subject to cavitation and erosion, particularly when the propeller is applied to high-speed vessels.

The magnitude of the spindle torque is, of course, an important consideration in the design of a CP propeller. Three phenomena contribute to the net spindle torque which must be overcome in order to change the pitch:

1. Friction in the pitch-changing mechanism.
2. Distribution of hydrodynamic loading on the blade.
3. Distribution of centrifugal loading on the blade.

The friction in the pitch-changing mechanism is essentially independent of the design of the propeller blades. Therefore the design of the

---

[5]Tsuchida, K., "Design Diagrams of Three-Bladed Controllable-Pitch Propellers," Proceedings, Fourth ONR Symposium on Naval Hydrodynamics, Washington, D.C. (Aug 1962).

[6]Yazaki, A., "Model Tests on Four-Bladed Controllable-Pitch Propellers," Ship Research Institute, Toyko, Japan, Paper 1, (Mar 1964).

[7]Yazaki, A. and S. Nobuo, "Further Model Tests on Four-Bladed Controllable-Pitch Propellers," Ship Research Institute, Tokyo, Japan, Paper 16 (Aug 1966).

[8]Gutsche, F. and G. Schroeder, "Freifahrversuche an Propellern mit festen und verstellbaren Flugeln voraus und zuruck (Open Water Tests on Fixed-Bladed and Controllable-Pitch Propellers in Forward and Backing Operations), Schiffbauforschung, Vol. 2, No. 4 (1963).

[9]Strom-Tejsen, J. and R.R. Porter, "Prediction of Controllable-Pitch Propeller Performance in Off-Design Conditions," Third Ship Control Systems Symposium, Bath, England (Aug 1972).

external propeller can significantly influence only those components of spindle torque produced by the hydrodynamic and centrifugal loading on the blades. The primary design objective related to spindle torque is generally to minimize the magnitude of the largest spindle torque to be encountered in the operating profile of the propeller. Depending on the design application, it is often a secondary design objective to obtain a min-imum or slightly positive hydrodynamic plus centrifugal spindle torque at the design condition where positive spindle torque tends to rotate the blade toward higher ahead pitch. If a positive spindle torque is obtained, then a failure in the pitch-control mechanism will result in a tendency of the blade to rotate toward a positive pitch condition, which will allow the ship to proceed in the ahead direction.

The achievement of the desired spindle torque depends on (1) an accurate technique for predicting spindle torque as a function of design variables and (2) design tradeoffs with efficiency, strength, cavitation, and unsteady forces. Prediction techniques are discussed later. Design tradeoffs primarily involve hydrodynamic spindle torque because it is much more sensitive than is the centrifugal component to variables over which the designer has some reasonable control. Hydrodynamic spindle torque is essentially the product of the component of hydrodynamic net force on the blade normal to the spindle axis and the distance between this force and the spindle axis. Therefore, the controlling geometric parameters are (in approximate descending order of importance) skew, spindle axis location, blade width, rake, and design pitch. Centrifugal spindle torque depends only on the geometry of the blade and propeller rotational speed. For all practical cases, it is directed such that it tends to change the blade pitch to small positive values. Within constraints dictated by considerations of efficiency, strength, cavitation, and unsteady forces, the only significant control which the designer has over centrifugal spindle torque is in the selection of rake and spindle axis location.

Analytical techniques for calculating spindle torque have been developed by several investigators including Rusetskiy,[1] Tsao,[10] Boswell,[11] and Klaasen and Arnoldus.[12] As stated previously, the centrifugal component of spindle torque is a function only of the geometry and propeller rotational speed; therefore, it is fairly straightforward to develop an analytical technique for calculating this component. However, any calculation of the hydrodynamic spindle torque requires accurate knowledge of the distribution of hydrodynamic loading over the blade. At the present state-of-the-art, the distribution of hydrodynamic loading can be accurately calculated at design pitch setting and advance coefficient, but is has not been demonstrated that it can be accurately calculated at substantially off-design pitch and/or advance coefficient. The recently developed procedure described by Tsao[10] is the most refined technique known to the authors for calculating off-design loading and spindle torque. However, this technique has not been correlated with experimentally determined spindle torque. Further, it is not reasonable to expect a technique which is based on potential flow to accurately predict hydrodynamic spindle torque under conditions at which the blade sections are stalled, i.e., under simulated crash-astern or crash-ahead conditions.

Therefore, although existing techniques should yield reasonable predictions of centrifugal spindle torque at all conditions and hydrodynamic spindle torque at or near design conditions, hydrodynamic spindle torque at maneuvering conditions must presently be determined experimentally because the hydrodynamic load distribution cannot be predicted with sufficient accuracy. For design purposes it is obviously desirable to have a method that can predict the hydrodynamic component over the entire operating profile of the propeller, including crash-astern and crash-ahead maneuvers.

An experimental program was therefore undertaken at DTNSRDC to measure thrust, torque, and spindle torque on a systematic series of

---

[10] S.S. Tsao, "Documentation of Programs for the Analysis of Performance and Spindle Torque of Controllable-Pitch Propellers," Massachusetts Institute of Technology, Department of Ocean Engineering Report 75-8 (May 1975).

[11] Boswell, R.J., "A Method of Calculating the Spindle Torque of a Controllable-Pitch Propeller at Design Conditions," David Taylor Model Basin Report 1529 (Aug 1961).

[12] Klaasen and Arnoldus, "Actuating Forces in Controllable-Pitch Propellers," Transactions Institute of Marine Engineers, Vol. 76, No. 6 (Jun 1964).

propellers in the towing basin* over a wide range of pitches and over a complete range of advance coefficients from locked shaft ahead to locked shaft astern, including the bollard pull condition. Experimental results under the first phase of this program have already been reported.[16,17] In that phase, thrust, torque, and spindle torque were measured on four propellers which were investigated to evaluate the effects of blade width and skew. The parent propeller of this series was almost identical to the propeller evaluated by Denny and Nelka.[15] The present report presents the experimental results under the second phase of this program.

DESCRIPTION OF PROPELLERS

Two existing models, designated DTNSRDC Propellers 4572 and 4575, were evaluated in the phase of the investigation reported here; see Figures 1 and 2 and Tables 1 and 2. These two propellers were designed independently for separate specific applications and therefore do not represent a strict systematic variation of any single design parameter. They were selected for evaluation because they represent a rational extension of the systematic series of propellers on which spindle torque had been measured previously;[16,17] see Figures 3-6 and Tables 3-7. The new parameters evaluated in these propellers are rake and different

*Earlier experiments[13-15] had revealed that hydrodynamic spindle torque cannot be properly determined in a water tunnel under simulated crash-astern and crash-ahead maneuvers because under such conditions, the tunnel walls significantly influence the flow into the propeller, thereby exerting a first order influence on the spindle torque. To avoid these wall effects, subsequent experiments[16] were conducted in a towing basin. Moreover, the balance employed in some of the earlier measurements[13,14] was found to cause a significant interaction between spindle torque and other components of blade loading (thrust, tangential force, radial force and two components of bending moment about axes normal to the spindle axis). Since that interaction tended to reduce the accuracy of the measurements, later experiments[15,16] and the present study were conducted with a balance which had no measurable influence of the other components of blade loading on spindle torque.

[13]Miller, M.L., "Spindle Torque Tests of Four CRP Propeller Blade Designs for MSO-421," David Taylor Model Basin Report 1837 (Jul 1964).

[14]Hansen, E.O., "Thrust and Blade Spindle Torque Measurements for Five Controllable-Pitch Propeller Designs for MSO-421," David Taylor Model Basin Report 2325 (Apr 1967).

[15]Denny, S.B. and J.J. Nelka, "Blade Spindle Moment on a Five-Bladed Controllable-Pitch Propeller," NSRDC Report 3729 (Jan 1972).

[16]Denny, S.B. and H.G. Stephens, "Blade Spindle Moment on Controllable-Pitch Propellers," NSRDC SPD Report 011-14 (Jul 1974).

[17]Stephens, H.G., "Open Water Performance of a Controllable-Pitch (C-P) Propeller Series," NSRDC SPD Report 011-13 (Jul 1974).

distributions of skew. In addition, these two propellers were designed by lifting surface procedures[18,19] and were candidates for Fleet applications.[20]

Both Propellers 4572 and 4575 were designed so that the spindle axis coincided with the propeller reference line, and with the radial distributions of skew specified so that the midchord position is forward of the spindle axis at the inner radii and aft of the spindle axis at the outer radii. Such distributions of skew are called "balanced" skew distributions. A balanced skew distribution may be necessary to simultaneously meet the following three design objectives:

1. To reduce propeller-induced vibration excitation below values for an unskewed propeller[21,22] (depending on the distribution of velocity in the propeller plane).

2. To provide for attaching the section at the blade root to the palm in such a manner that it possesses sufficient strength without blade overhang at the leading edge.

3. To ensure a zero or small positive value of spindle torque resulting from hydrodynamic and centrifugal loading at design conditions (positive spindle torque tends to increase ahead pitch).

The third design objective required locating the center of pressure sufficiently forward of the spindle axis so that the hydrodynamic spindle torque will counteract the centrifugal spindle torque which inherently tends to reduce pitch to small positive values.[11] Positive net spindle torque is desirable so that the blades will tend to go to a large ahead pitch in the event of a hydraulic failure in the pitch-changing system.

The projected skew angle θ_s measured from the spindle axis to the section midchord varies for Propeller 4572 from -9.7 deg at the

---

[18]Cheng, H.M., "Hydrodynamic Aspect of Propeller Design Based on Lifting-Surface Theory," Part 1, David Taylor Model Basin Report 1802 (Sep 1964) and Part 2 DTMB Report 1803 (Jun 1965).

[19]Kerwin, J.E. and R. Leopold, "A Design Theory for Subcavitating Propellers," Transactions, Society of Naval Architects and Marine Engineers, Vol. 72, pp. 294-335 (1964).

[20]Denny, S.B. et al., "Hydrodynamic Design Considerations for the Controllable-Pitch Propeller for the Guided Missile Frigate," Naval Engineers Journal, pp. 72-81 (Apr 1975).

[21]Cumming, R.A. et al., "Highly Skewed Propellers," Transactions, Society of Naval Architects and Marine Engineers, Vol. 80 (1972).

[22]Boswell, R.J. and G.G. Cox, "Design and Model Evaluation of a Highly Skewed Propeller for a Cargo Ship," Marine Technology, Vol. 11, No. 1, pp. 73-89 (Jan 1974).

50-percent radius to +24.7 deg at the blade tip (skewback is positive). For Propeller 4575, θ_s varies from -5.9 deg at the 50-percent radius to +11.6 deg at the blade tip.

Propeller 4572 has zero rake, but a nonlinear radial distribution of rake was specified for Propeller 4575 so that the locus of the midchords of the blade sections would lie in a circular conical surface with the axis coincident with the propeller axis and with the surface generator line 5.0 deg forward of the propeller plane. (The propeller plane is the plane normal to the propeller axis and contains the propeller reference line which, for Propellers 4572 and 4575, coincides in the spindle axis.) Thus, the total rake for Propeller 4575 is defined by

$$Z_T = -r\,[\tan(5\ \text{deg}) + \theta_s(r)\tan\phi(r)]$$

where θ_s is in radians.

Forward rake is beneficial from strength considerations because with forward rake the bending moment arising from centrifugal force is of opposite sense to the bending moment arising from the hydrodynamic loading for ahead operation. Thus forward rake tends to reduce the maximum principal stress in the blade for ahead operation. It is thought that forward rake also tends to increase the algebraic value of both centrifugal[11] and hydrodynamic spindle torque. This speculated variation of hydrodynamic spindle torque with rake results, in part, from a spindle torque component arising from drag of the blade sections. The use of forward rake is especially attractive for propellers with skewback because it may be desirable to have zero or small positive values of spindle torque at design ahead conditions, as discussed previously. Forward rake also increases the clearance between the propeller and rudder and thus may substantially reduce the effort required to remove the propeller from the tailshaft.

EXPERIMENTAL APPARATUS

FACILITY

All spindle torque measurements were performed by using the open-water propeller boat and Carriage I of the David Taylor Model Basin. In the experimental setup (Figure 7) the blades of each propeller were mounted in the spindle torque hub and the hub was mounted on a hollow propeller shaft which fitted through the contrarotating end of the propeller boat. All experiments were conducted in uniform flow with the propeller fixed to an upstream shaft; i.e., the propeller was upstream of the boat and shafting.

The blade pitches were set manually by using a construction template which matched the blade surface along the plane normal to the spindle axis and intersecting the spindle axis at 0.7 radius. The template was attached to a vernier scribed angle-setting device at the fairwater end of the dynamometer hub.

DYNAMOMETRY

Propeller thrust and torque were measured by using a variable reluctance 150-in-lb transmission dynamometer (Serial 112). The transmission dynamometer was positioned between the slipring assembly and the drive motors, and thrust and torque data were acquired concurrently with the spindle torque data. Power to rotate the propeller was supplied by two d-c servomotors (Model MT-5045-039A) connected in series. The torque rating of each motor is 3 ft-lb for continuous operation and 12 ft-lb for peak operation. These motors were selected to match the capabilities of the transmission dynamometer and for their ability to control the shaft rotation rate during negative torque conditions. Propeller rpm and propeller boat velocity were respectively determined by a Hewlett-Packard roto-pulser and a revolution-speed-time recorder. Propeller depth of submergence during the entire experiment was approximately 13 in. at the shaft centerline. This submergence was 1.42 times the diameter of Propeller 4572 and 1.32 times that of Propeller 4575. The strut arrangements and towing gear were such that the propeller

could be lifted clear of the water for pitch setting and for air-spin experiments conducted to determine the centrifugal spindle torque.

Figure 8 is a schematic of the propeller, slipring assembly, transmission dynamometer, and motors as assembled in the open-water propeller boat.

The blade spindle mechanism and spindle torque dynamometer are shown in Figures 9 and 10. The spindle torque dynamometer consists of a spindle torque flexure and a hub designed specifically to house both the spindle torque flexture and the blade spindle. The hub, blade spindle, and bearings (Barden Corporation Types A539X80 and SF2) are of stainless steel. The bearings are intended to isolate the spindle from the dynamometer hub and to carry the thrust, centrifugal, and torque forces of the propeller blade and spindle. A single blade is attached to the blade spindle. The spindle torque measuring element is a strain-gaged tempered-steel flexure employed as a cantilever beam. A clamp at one end of the flexure is attached to the center section of the spindle and can be adjusted from outside the propeller hub to allow blade pitch to be set at any desired value. The other end of the flexure rests in a close-tolerance ground slot. The flexure lies along the axis of the propeller hub in order to avoid deflection of the flexure due to centrifugal forces on it.

The flexure was instrumented with 120-ohm strain gages. Excitation voltage and gage output were transmitted via slipring assemblies with leads through a hollow propeller shaft.

CALIBRATION

Prior to the series of measurements, the spindle-torque dynamometer was statically calibrated in air at its installed position in the propeller boat. Positive values of spindle torque (tending to increase ahead pitch) and negative values of spindle torque were applied incrementally to the spindle over a range of spindle torque from -30 to +30

in-lb, the maximum limits expected during the experiment. The response of the strain gage was both linear and instantaneous with applied torque. No hysteresis characteristics were observed in the output signal. There was no measurable interaction with other loading components, as indicated by the fact that the signal remained unchanged over the entire spindle torque range as pure centrifugal, thrust, and torque forces were applied to the spindle. A static calibration following completion of the experiments showed no changes in response characteristics from the original spindle-torque flexure calibration.

The transmission dynamometer was also statically calibrated over a range of thrust (100 to +100 lb) and torque (150 to +150 in-lb). The response of the transmission dynamometer for both thrust and torque remained linear with applied load, which agreed with the previous calibration.

At each pitch setting, air-spin experiments to determine the centrifugal component of spindle torque were conducted over a range of rotational speeds from 2.0 to 20.0 rps for both right- and left-hand rotation. The spindle torque due to aerodynamic loading at $V_A = 0$ was determined from the measured hydrodynamic spindle torque at the bollard pull conditions, $V_A = 0$. Since the "hydrodynamic" blade spindle torque index is independent of the fluid, it follows that:

$$Q_{SA} = Q_{SH}\left(\frac{\rho}{\rho_A}\right)\left(\frac{n_{water}}{n_{air}}\right)^2 \quad \text{at } V_A = 0$$

where Q_{SA} is the spindle torque due to aerodynamic loading and Q_{SH} is the spindle torque due to hydrodynamic loading. However, Q_{SA} was insignificant relative to Q_{SH}.

ACCURACY

The speed of advance and rotational speed were controllable within accuracies of $\pm$0.01 ft/sec and 0.01 rpm, respectively. The recorded values of thrust, torque, and spindle torque were accurate to within 0.1 lb, 0.1 in-lb, and 0.02 in-lb, respectively.

As mentioned previously, the propeller blade pitch was set manually with the aid of construction templates. The differential angle from design pitch was determined from the following equation:

$$\Delta\phi_{0.7} = \tan^{-1}\left[(P/D)_{set}/(0.7\,\pi)\right] - \tan^{-1}\left[(P/D)_{design}/(0.7\,\pi)\right]$$

with all pitch ratios defined at the 70-percent propeller radius. Previous calculations showed that for the spindle torque values measured, the actual bending of the flexure in the dynamometer produced less than $\pm$0.1 deg of pitch change.

EXPERIMENTAL PROCEDURE

EXPERIMENTAL CONDITIONS

Experiments were conducted in uniform flow over a range of positive and negative advance coefficients for several values of ahead and astern pitch setting. Each experimental condition was run at a constant pitch setting, speed of advance, and rotational speed. Therefore, these experimental conditions represented a quasi-steady simulation of the various modes of propeller operation including steady ahead, crash astern, crash ahead, and turns.

All propeller operating conditions were established in the David Taylor Model Basin by setting the propeller rpm and propeller boat velocity to achieve a given advance condition. To obtain uniform flow into the propeller, it was necessary to drive the propeller from downstream for all conditions. All experimental conditions were run in one direction in the basin; conditions with astern velocity on the ship (such as steady backing and the initial stages of crash ahead) were simulated in the experiments by rotating the blades 180 deg about the spindle axis and reversing the direction of shaft rotation. Figure 11 is a schematic of the propeller operating conditions simulated in the experiment. The propeller pitch-diameter ratios $(P/D)_{0.7}$ are listed in the operating quadrants in which they were evaluated on the model.

The lower absolute values of advance coefficients were obtained by rotating the propeller at 10 rps, with speed of advance varying from 0 to 6 knots. The higher absolute values of advance coefficients were obtained with a velocity of 6 knots over a range of values from 3.5 to 0.6 rps. The resulting range of Reynolds number was from 3.2×10^5 to 6.1×10^5. Previous data obtained in the David Taylor Model Basin had shown that this range of Reynolds number had no significant effect on spindle torque for a complete range of advance coefficients and pitch settings.[16] Therefore, each experimental condition representing a given pitch setting and advance coefficient was run at only one speed of advance and one value of rpm. Unfortunately, some conditions were unattainable due to combinations of pitch, velocity, and advance coefficient which tended to draw air to the propeller from the free surface.

Spindle torque measurements and related data were collected in the following step-by-step manner:

1. The desired pitch was set by using construction template.

2. Air-spin experiments were conducted to separate the spindle torque components due to centrifugal forces and due to hydrodynamic loading. First, the propeller shaft was submerged in water to saturate the bearings in the shaft and hub. Next, the propeller boat was raised so the propeller was completely out of the water and air-spin data were recorded over a range of rotational speeds.

3. The propeller model was submerged and no-load experiments were conducted without blades attached to determine the effect of shaft friction and propeller hub pressure forces on thrust and torque, so that

$$T = T_{measured} - T_{no\ load}$$

$$Q = Q_{measured} - Q_{no\ load}$$

4. Propeller blades were replaced and bollard-pull data (zero velocity) were recorded at n = 10 rps to monitor the spindle torque flexure for possible slippage of the blade in its mounting. (These bollard-pull conditions were repeated several times throughout the experiment.)

5. Data were collected over a range of advance coefficients by varying the speed of advance and rotational speed.

6. Pitch was changed and the above steps repeated.

DATA ACQUISITION AND ANALYSIS

All data were digitized and analyzed by using an analog-to-digital converter and an interdata minicomputer (Model 4). A block diagram of the instrumentation is presented in Figure 8. The records of spindle torque, thrust, torque, rotational speed, and speed of advance were digitized and averaged over a 5-sec time interval. Computer programs were developed for the interdata minicomputer to enable an on-line data analysis. This included subtraction of "no loads," the separation of centrifugal and hydrodynamic components of spindle torque, and nondimensionalization by the appropriate factors. The data were printed out as a function of advance conditions for immediate plotting and checking with previous results.

EXPERIMENTAL RESULTS

OPEN-WATER PERFORMANCE

There is no single standard method of presenting open-water data over the complete range of advance coefficients from locked shaft ahead ($J = +\infty$) to locked shaft astern ($J = -\infty$). Therefore, to facilitate comparison with other results, the thrust and torques data in this report are presented in two forms:

1. The system normally used at DTNSRDC:

K_T and K_Q versus J for $J < 1.0$

K_T and K_Q versus 1/J for $J \geq 1.0$

where

$$K_T = T/(\rho n^2 D^4)$$

$$K_Q = Q/(\rho n^2 D^5)$$

$$J = V_A/(nD)$$

This is the system generally used for normal ahead operation. Its disadvantage is that as n approaches zero, K_T, K_Q, and J approach plus or minus infinity.

2. The system used in Strom-Tejsen and Porter[9] and in Stephens,[17] namely:

C_T^* and C_Q^* versus β^*

where

$$C_T^* = \frac{T}{(\rho/2)(V_R^*)^2 A_0} = \frac{8T}{\pi\rho D^2[V_A^2 + (0.7\pi nD)^2]}$$

$$C_Q^* = \frac{Q}{(\rho/2)(V_R^*)^2 A_0 D} = \frac{8Q}{\pi\rho D^3[V_A^2 + (0.7\pi nD)^2]}$$

$$\beta^* = \tan^{-1}[V_A/(0.7\pi nD)]$$

$$V_R^* = [V_A^2 + (0.7\pi nD)^2]^{1/2}$$

$$A_0 = \pi R^2$$

The advantage of this system is that the magnitude of the vector sum of the speed of advance and rotational speed at 0.7 radius, i.e., V_R^*, is used to nondimensionalize the quantities C_T^* and C_Q^*. Therefore C_T^*, C_Q^*, and β^* remain finite over the complete range from locked shaft ahead ($V_A > 0$, $n = 0$) to locked shaft astern ($V_A < 0$, $n = 0$), including the bollard condition ($V_A = 0$, $n \neq 0$).

Both methods are employed to present open-water characteristics over a range of pitch settings for Propeller 4572 (Figures 12-15) and Propeller 4575 (Figures 16-19). The data presented are actual experimental points with no fairing. In the $C_T^* - C_Q^* - \beta^*$ system, experimental results are compared with predictions based on the method of Strom-Tejsen and Porter.[9] The correlation with experimental results obtained with this method are discussed in the section on discussion of results. In the $K_T - K_Q - J$ system at design pitch and ahead operation, previous experimental results obtained with a different instrumentation system are also presented. Such previous data for Propeller 4572 were reported over only a limited range of advance coefficients.

SPINDLE TORQUE

There is no standard method of presenting data for spindle torque over a complete range of advance conditions from locked shaft ahead to locked shaft astern. Therefore, to facilitate comparison with other results, the hydrodynamic spindle torque data in this report are presented in two forms:

1. The system used in unpublished results from Hydronautics, Inc. and the Massachusetts Institute of Technology:

$$K'_{SH} \text{ versus } J'$$

where

$$K'_{SH} = \frac{Q_{SH}}{\rho D^3 (V_A^2 + n^2 D^2)} = \frac{Q_{SH}}{\rho n^2 D^5 (1 + J^2)}$$

and

$$J' = \frac{V_A}{(V_A^2 + n^2D^2)^{1/2}} = \frac{J}{(1 + J^2)^{1/2}}$$

2. The system used in Denny and Stephens[16]:

$$K^*_{SH} \text{ versus } \beta^*$$

where

$$K^*_{SH} = \frac{Q_{SH}}{(\rho/2)(V^*_R)^2 A_0 D} = \frac{8Q_{SH}}{\pi\rho D^3[V_A^2 + (0.7\pi nD)^2]}$$

Both systems use a characteristic velocity which is a combination of speed of advance and rotational speed. Therefore K'_{SH}, K^*_{SH}, J', and β^* remain finite over the complete range from locked shaft ahead ($V_A > 0$, $n = 0$) to locked shaft astern ($V_A < 0$, $n = 0$) including the bollard condition ($V_A = 0$, $n \neq 0$).

Both systems are utilized to present hydrodynamic spindle torque data over a range of pitch settings for Propeller 4572 (Figures 20 and 22) and Propeller 4575 (Figures 21 and 23). The data presented in these figures are actual experimental points with no fairing.

Figures 24 and 25 present faired curves of the hydrodynamic spindle torque data in the K^*_{SH} - β^* system for Propellers 4572 and 4575, respectively. For comparison, the faired hydrodynamic spindle torque data reported by Denny and Stephens[16] (K^*_{SH} - β^* system) are presented in Figures 26-29.

Figures 30 and 31 indicate the centrifugal spindle torque coefficients for Propellers 4572 and 4575, respectively, where the centrifugal spindle torque coefficient is

$$K_{SC} = \frac{Q_{SC}}{\rho_P n^2 D^5}$$

This nondimensionalization is equivalent to that used for K'_{SH} with $V_A = 0$ except that the density of the propeller is used for K_{SC} whereas

the density of the water is used for K'_{SH}. Centrifugal spindle torque is a function only of the geometry of the blades (including pitch setting), density of the blades, and propeller rotational speed. For comparison DTNSRDC centrifugal spindle torque data reported earlier[15,16] are presented in Figures 32-36.

Figures 30-37 also present analytically calculated values of centrifugal spindle torque coefficients based on the method presented by Boswell.[11] The correlation obtained between theory and experiment is indicated in the section on discussion of results.

Table 8 presents the net hydrodynamic plus centrifugal spindle torque at design advance coefficient J_D and pitch ratio $(P/D)_{0.7_D}$ for the propellers evaluated in this report and in Reference 16. These results were derived by scaling the model experimental data to a hypothetical full-scale situation as indicated in Table 8. The material for all of the full-scale propeller blade is assumed to be nickel-aluminum-bronze.

DISCUSSION OF RESULTS

Some of the experimental data showed a slight displacement or discontinuity at the zero advance condition. This continuity appeared in torque coefficient data for both propellers at most pitch settings and was greater for Propeller 4572. In passing from negative to positive advance coefficients, the torque coefficients jumped to smaller algebraic values for Propeller 4572 and to larger algebraic values for Propeller 4575. The only noticeable discontinuity for thrust coefficient occurred at P/D = 0 for Propeller 4572, and the only noticeable discontinuity for hydrodynamic spindle torque occurred at P/D = +1.00 for Propeller 4575.

As discussed in the section on experimental procedure, the negative advance coefficients were simulated in the experiment by reversing the

direction of propeller rotation, rotating the blades 180 deg about the spindle axis, and driving the propeller in the same directions in the basin. It is unlikely that the observed discontinuities resulted from inaccuracies in pitch setting because thrust coefficients do not jump in the same manner as do torque coefficients. A careful check of torque no-loads for both right- and left-hand rotation failed to indicate any inconsistencies. In the experimental arrangement, the effective location of the propeller boat and shafting relative to the propeller blades was different for positive and negative advance coefficients; i.e., the propeller was pushing water toward the boat for one arrangement and away from the boat in the other arrangement. Any interactions between the propeller and the driving system would be opposite in the two cases and this could contribute to the observed discontinuities. The actual reason for the discontinuities is not known, and it is suggested that they be eliminated by local fairing near zero advance coefficient. Such local fairing was done as necessary in the faired spindle torque data presented in Figures 24 and 25.

There was very little scatter in the experimental data for simulated steady ahead ($(P/D)_{0.7} > 0$, $J > 0$) and steady astern ($(P/D)_{0.7} < 0$, $J < 0$). On the other hand, there was significant scatter in the data for simulated crash ahead ($(P/D)_{0.7} > 0$, $J < 0$) and crash astern ($(P/D)_{0.7} < 0$, $J > 0$), but the trends were well defined. Scatter under these conditions is to be expected because the propeller was pushing the water in a direction opposite to the incoming flow; accordingly, the blade sections were generally stalled and large-scale churning (highly unsteady flow) was set up around the propeller. There appeared to be some air drawing under crash-ahead and crash-astern operation at the highest pitch settings, but it is not known whether this influenced the experimental results.

THRUST AND TORQUE

Thrust coefficient K_T and torque coefficient K_Q determined experimentally under the present project were compared in Figures 12b, 13b, 16b, and 17b with experimental values obtained previously (data not formally reported) only at design pitch and over a limited range of positive advance coefficients. These comparisons indicated generally satisfactory agreement between the two sets of experimental results. However, the thrust coefficient determined under the present project for Propeller 4575 was approximately 10 percent higher than the previously measured value for advance coefficient in the range $0 < J < 0.6$. Both sets of experiments were carefully reviewed, but the reason for this disagreement is unknown. Based on comparison with systematic series data [23] it is judged that the thrust coefficient determined under the present project is more accurate than the previously measured values.

Figures 14, 15, 18, and 19 compare the experimental values of thrust index C_T^* and torque index C_Q^* with predictions based on the method of Strom-Tejsen and Porter[9] over the complete range of advance angle (-90 deg $\leq \beta^* \leq +90$ deg) for most pitch settings experimentally evaluated. The method of Strom-Tejsen and Porter is based on an analytical least-squares approximation to the experimental data presented by Gutsche and Schroeder[8] and employs orthogonal polynomials and a Fourier Series expansion. It is assumed in this method that C_T^* and C_Q^* can be adequately represented as a function of only expanded area ratio A_E/A_0, pitch setting $(P/D)_{0.7}$, and advance angle β^*. Such other parameters as number of blades, design pitch, radial distribution of pitch, skew, rake, radial distribution of chord length, and location of spindle axis are considered of secondary importance and are not included in the predictions by that method.

The agreement between the analytical predictions and the experimental results for Propellers 4572 and 4575 was good for some combinations of β^* and $(P/D)_{0.7}$ and rather poor for others. Agreement was generally

---

[23] Van Lammeren, W.P.A. et al, "The Wageningen B-Screw Series," Transactions, Society of Naval Architects and Marine Engineers, Vol 77, pp. 269–317 (1969).

better for $|\beta^*| \leq 60$ deg than for $|\beta^*| > 60$ deg, better for $(P/D)_{0.7} \geq 0$ than for $(P/D)_{0.7} < 0$, and better when β^* and $(P/D)_{0.7}$ had the same sign than when of opposite sign.

For most conditions, agreement became rather poor for $|\beta^*| > 60$ deg. This is equivalent to $|J| > 3.81$ and more than three times the design J for Propellers 4572 and 4575. Therefore, if these conditions were encountered on the ship, they would be at quite low values of rotational speed n ($n/n_D < |V/(3V_n)|$) which tends to suggest that thrust and torque would not be high at these conditions. Therefore the poor agreement between predicted values and experimental results for $|\beta^*| > 60$ deg is not considered serious. For most conditions, either the analytical predictions or the experimental results indicated stall at high values of β^*. To a large extent, the disagreement at $|\beta^*| > 60$ deg resulted from difference in the value of β^* at which stall was predicted. The stall angle may be different on the full-scale propeller at sea under crash-astern or crash-ahead conditions than it is on the model propeller under noncavitating steady-state conditions in uniform flow. Therefore both the predictions based on the Strom-Tejsen and Porter method (which are based on noncavitating steady model data in uniform flow) and the experimental results presented in this report may be subject to scale effects for $|\beta^*| > 60$ deg.

The agreement was generally better for $(P/D)_{0.7} \geq 0$ than for $(P/D)_{0.7} < 0$. In part, this may be because the prediction method[9] neglects the effects of skew, rake, and spindle axis location. Recall that for $(P/D)_{0.7} < 0$, the blades had been rotated from design pitch settings through large angles about the spindle axis. As the blades are rotated about the spindle axis to change pitch, different parts of the blade intersect a circular cylinder concentric with the propeller axis. As a result, the shape of a constant-radius cross section of the blade changes with pitch setting. At substantially off-design pitch setting, the constant radius sections are characterized by a significant S-shaped camber with inflection point approximately in the plane containing the propeller axis and spindle axis.[1,2,10] Therefore the effective camberline

at $(P/D)_{0.7} < 0$ was influenced to a first order by the location of the spindle axis relative to the blade section; i.e., it was influenced by skew and rake. Over a range of conditions for $(P/D)_{0.7} < 0$ and $\beta^* < 0$ (such as steady-astern operation) the blade has low angle of attack and a significant amount of lift is produced by camber; therefore, the values of C_T^* and C_Q^* are significantly influenced by the magnitude and distribution of camber.

For $(P/D)_{0.7} \leq -1.5$, the prediction method[9] gave large oscillations in the variation of C_T^* and C_Q^* with β^*, even in the region $-60 \text{ deg} < \beta < 0$ where these oscillations should not occur (since $(\phi_{0.7} - \beta^*)$ is small, stall is not expected in this region). These oscillations were extreme for Propeller 4572 at $(P/D)_{0.7} = -2.15$ and therefore are not presented. The fact that the numerical expressions derived by using Reference 9 are not valid for $(P/D)_{0.7} \leq -1.5$ agrees with the applicable range of $(P/D)_{0.7}$ cited in that reference.

In the regions where $\beta^* > 0$ and $(P/D)_{0.7} < 0$ (simulated crash astern) and $\beta^* < 0$ and $(P/D)_{0.7} > 0$ (simulated crash ahead), the agreement was generally not as good as for $\beta^* > 0$ and $(P/D)_{0.7} > 0$ (simulated steady ahead) and for $\beta^* < 0$ and $(P/D)_{0.7} < 0$ (simulated steady astern). In general, the agreement deteriorated as $|\phi_{0.7} - \beta^*|$ increased, especially in regions in which the data indicated that the blade sections had stalled, i.e., for $|(P/D)_{0.7}| > 1.0$ with β^* and $(P/D)_{0.7}$ of opposite signs or for $|\beta^*| > 60$ deg. As discussed previously, scaling problems may exist in regions for which the data indicated blade section stall. In some cases the differences between analytical and experimental values of C_T^* and C_Q^* at a given value of $(P/D)_{0.7}$ and β^* was greater than a factor of two. However, the differences between analytical and experimental values of maximum C_T^* and C_Q^* and minimum C_T^* and C_Q^* for a given value of $(P/D)_{0.7}$ was generally less than 20 percent for $|\beta^*| < 60$ deg and $(P/D)_{0.7} > -1.5$.

In summary, the comparison between analytical predictions and experimental results for Propellers 4572 and 4575 indicates that the thrust and torque predicted by the method of Strom-Tejsen and Porter[9] are probably sufficiently accurate for preliminary analyses of propulsion system dynamic simulation. Such analyses are important for the design of the control system of CP propellers so that the propeller rotational speed and pitch ratio $(P/D)_{0.7}$ are varied in a manner which does not overload the propeller during severe crash-astern and crash-ahead maneuvers. For final propulsion system dynamic analyses, it is, of course, desirable to conduct open-water experiments on a model of the design propeller over a suitable range of pitch settings and advance angles.

HYDRODYNAMIC SPINDLE TORQUE

The composite plots of Figures 24 and 25 presented faired values of experimental hydrodynamic spindle torque index K^*_{SH} as a function of pitch ratio $(P/D)_{0.7}$ and advance angle β^* for the two propellers. These results were, in general, consistent with the experimental results presented by Denny and Stephens;[16] see Figures 26-29. However, hydrodynamic spindle torque is thought to be sensitive to a number of geometric parameters including (in approximate descending order of importance) maximum skew, spindle axis location, blade width, radial distribution of skew, maximum rake, radial distribution of rake, radial distribution of chord length, design meanline, design pitch, and radial distribution of pitch loading. The values for each of these parameters were different for Propellers 4572 and 4575 and also different than the values of propellers in the other study[16] (the only exceptions were the design meanline for all propellers and rake for all but Propeller 4575); see Tables 1-6 and Figures 1-6. For many of these parameters, however, the values for Propellers 4572 and 4575 were within the range covered by the systematic series of propellers evaluated by Denny and Stephens.[16]

Therefore, comparison of the results of the present study with those of Reference 16 can be made only in a general sense, and careful consideration must be given to the difference in the pertinent geometric characteristics of the different propellers.

The hydrodynamic spindle torque can be represented as the product of the net force component normal to the spindle axis and the distance from the force component to the spindle axis. For a given operating condition (given values of $(P/D)_{0.7}$ and β^*), this distance is controlled largely by skew and spindle axis location. These two parameters reduce to one parameter if skew is defined from the spindle axis to a specified chordwise position, such as the midchord. Tables 1-6 showed the radial distribution of skew to diameter ratio S/D, defined from the spindle axis to the midchord, for the propellers evaluated earlier[16] and in the present study. The skew at the tip for both Propellers 4572 and 4575 was within the range covered by the previous series; however, both had significant forward skew at the inner radii whereas the other propellers[16] did not.

Chord length is another parameter which significantly affects the distance from the net force on the blade to the spindle axis. Since all the propellers have five blades, expanded area ratio A_E/A_0 is a direct measure of average chord length. The values of A_E/A_0 for Propellers 4572 and 4575 fell within the range covered by the propellers evaluated by Denny and Stephens.[16]

Rake influences the distance from the net force to the spindle axis in two ways:

1. It provides a distance component normal to the hydrodynamic drag so that with rake, the drag significantly contributes to the spindle torque. This could be important at off-design conditions where the drag may be substantial.

2. It changes the distance component normal to the hydrodynamic lift; see Boswell.[11] All propellers evaluated in Reference 16 and Propeller 4572 have zero rake; in contrast, Propeller 4575 has substantial forward rake.

In addition to the parameters previously indicated as important at all operating conditions, the design radial distribution of pitch and design chordwise distribution of camber are important at design pitch-ratio P/D and advance angle β^*. These parameters largely control the spanwise and chordwise center of hydrodynamic force on the blade near design P/D and β^* since most of the lift is usually developed by camber for these conditions. At substantially off-design P/D and β^*, the dominant amount of lift is developed by angle of attack; therefore, the relative importance of design pitch distribution and camberline is greatly diminished. All propellers in the previous[16] and present study were designed to have a chordwise distribution of lift at design P/D and β^* which is the same as that produced by an NACA a = 0.8 meanline at ideal angle of attack in two-dimensional flow. At design P/D and β^*, the intended chordwise distribution of loading will be achieved only if the propeller is designed with the proper tools; i.e., by using lifting surface procedures which accurately consider all pertinent variables. The propellers of Reference 16 and Propeller 4572 of this study were designed by using the lifting surface procedure of Pien and Cheng[18] with thickness corrections by the method of Kerwin and Leopold.[19] Propeller 4575 was designed by using both the lifting surface and thickness corrections based on the method of Kerwin and Leopold.[19] Propeller 4575 has substantial forward rake; however, the Kerwin-Leopold design procedure does not consider the effect of rake on propeller pitch and camber required to produce a specified distribution of lift. Since the effect of rake may be substantial,[24,25] the chordwise distribution of loading on this propeller at design P/D and β^* may be substantially different than that produced by an NACA a = 0.8 meanline in two-dimensional flow at ideal angle of attack.

---

[24]Kerwin, J.E., "Computer Techniques for Propeller Blade Section Design," Proceedings, Second LIPS Propeller Symposium, Drunen, Holland, pp. 7-31 (May 1973).

[25]Nelka, J.J., "Experimental Evaluation of a Series of Skewed Propellers with Forward Rake: Open-Water Performance, Cavitation Performance, Field-Point Pressures, and Unsteady Propeller Loading," NSRDC Report 4113 (Jul 1974).

For a propeller with a given number of blades, the magnitude of the net force on a blade suitably nondimensionalized at a given operating condition (given values of $((P/D)_{0.7}$ and β^*) depends primarily on the value of A_E/A_0. All propellers evaluated in the present investigation and in Reference 16 have five blades. The expanded area ratios for Propellers 4572 and 4575 fell within the range covered by the other propellers.[16]

Based on the differences in geometry between the various propellers as discussed, only a general comparison can be made between the values of hydrodynamic spindle torque index measured on the propellers of the present investigation and on the systematic series of propellers studied by Denny and Stephens.[16] Although Propellers 4575 and 4536 had approximately the same blade width A_E/A_0 = 0.65 and 0.62, respectively, Propeller 4575 has a balanced skew and forward rake whereas Propeller 4536 has a small amount of skewback and no rake (see Figures 2 and 4 and Tables 2 and 4). The radial distribution of chord length is also somewhat different for these two propellers; Propeller 4575 has wider blades from the 40- to the 80-percent radius and narrower blades near the root and near the tip. Therefore, for a given $(P/D)_{0.7}$ and β^*, the difference in hydrodynamic spindle torque indices K^*_{SH} for these two propellers stems primarily from the effects of skew, rake, and radial distribution of chord length.

Figures 25 and 27 indicate that the variation of K^*_{SH} with β^* and $(P/D)_{0.7}$ was somewhat similar for these two propellers. However, the magnitudes of the extreme values of K^*_{SH} and the variation of K^*_{SH} with β^* and $(P/D)_{0.7}$ were substantially greater for Propeller 4575. For most combinations of β^* and $(P/D)_{0.7}$, the magnitude of K^*_{SH} for Propeller 4575 was of the order of twice its value for Propeller 4536. For both propellers, K^*_{SH} was very small at design conditions, i.e., at $(P/D)_{0.7_D}$ and β^*_D. In general, for $\beta^* > \beta^*_D$, K^*_{SH} (Propeller 4575) < K^*_{SH} (Propeller 4536) and for $\beta^* < \beta^*_D$, K^*_{SH} (Propeller 4575) > K^*_{SH} (Propeller 4536). For a high value of advance angle β^* relative to pitch angle $\phi_{0.7}$, the blade

sections operate at less than the ideal angle of attack and there is a negative component of lift coefficient C_L due to the angle of attack concentrated near the 0.25 chord position. Conversely, for low value of β^* relative to $\phi_{0.7}$, the blade sections operate at greater than the ideal angle of attack and there is a positive component of C_L due to the angle of attack concentrated near the 0.25 chord position. Therefore, the relative variation of K^*_{SH} with β^* for Propellers 4575 and 4536, as shown in Figures 25 and 27, indicate that the effective center of lift due to angle of attack on Propeller 4575 is further forward relative to the spindle axis than for Propeller 4536. For example, for $(P/D)_{0.7} = 1.5$ at $\beta^* = 60$ deg, the experimental data from the present investigation and References 16 and 17 show the following

Parameter	Propeller 4575	Propeller 4536
C^*_T	-0.52	-0.54
C^*_Q	-0.110	-0.116
K^*_{SH}	-0.0088	-0.0027

Therefore, Propeller 4575 is not nearly as effective as Propeller 4536 for minimizing $|K^*_{SH}|$ over a range of β^* and $(P/D)_{0.7}$. Since the magnitude and radial distribution of skew, rake, and chord length are all different for these two propellers, available data are insufficient to isolate the effects of these three parameters on the measured differences in K^*_{SH} for these two propellers.

These data do not conclusively determine whether a CP propeller can be designed with substantial skew (to reduce propeller-induced vibratory forces[21,22,24]) so that the maximum $|K^*_{SH}|$ over the pertinent range of β^* and $(P/D)_{0.7}$ is no greater than it is for a comparable propeller without significant skew. However, it appears that the maximum $|K^*_{SH}|$ for Propeller 4575 could be reduced by increasing the

skewback at the outer radii and/or increasing the chord length at the outer radii. Such a revised distribution of skew may also be advantageous for reducing propeller-induced vibratory forces, depending on the circumferential distribution of wake in the propeller plane; however, it would reduce the algebraic value of K^*_{SH} at design conditions. Depending on the design application, increasing the chord length near the tip may have disadvantages regarding propulsive efficiency, cavitation, and propeller-induced vibratory forces. Therefore, it appears that a highly skewed propeller could be designed so that spindle torque over the entire operating profile would be comparable to that of a propeller with little or no skew.

Propeller 4572 has no rake and a radial distribution of skew which is similar to that of Propeller 4575 but approximately twice as large. The expanded area ratio A_E/A_0 of Propeller 4572 ($A_E/A_0 = 0.73$) is larger than that of Propeller 4536 ($A_E/A_0 = 0.62$) and Propeller 4575 ($A_E/A_0 = 0.65$) and smaller than that of Propellers 4496, 4517, and 4536 ($A_E/A_0 = 0.83$).

The variation of K^*_{SH} with β^* and $(P/D)_{0.7}$ for Propeller 4572 is generally consistent with the other propellers evaluated in the present investigation and in Reference 16. This variation of K^*_{SH} for Propeller 4572 is more nearly like that of Propeller 4496 than any of the other propellers. This similarity apparently results from cancellation of the effects of skew and chord length. The narrower blades of Propeller 4572 should tend to reduce the variation of K^*_{SH} (this is demonstrated by the experimental results for Propellers 4496 and 4536) whereas the skew may tend to increase the variation of K^*_{SH} (this is qualitatively demonstrated by the experimental results for Propellers 4536 and 4575).

The variation of K^*_{SH} for the two propellers of the present study exhibited the same trend but in most regions, $|K^*_{SH}|$ was larger for Propeller 4572. This is consistent since these two propellers have similar radial distributions of skew and chord length, but Propeller 4572 has approximately 13 percent greater chord length and approximately twice as much skew. Based on other results, as previously discussed, both the wider blades and larger skew of Propeller 4572 may tend to increase K^*_{SH}.

All spindle torque results presented in this report are for noncavitating conditions. However, neglecting the effects of cavitation generally tends to yield a conservative prediction of the maximum value of spindle torque. The effects of cavitation tend to be most severe at off-design conditions, i.e., at off-design values of $(P/D)_{0.7}$ and β^*, where a substantial amount of lift is produced by angle of attack. For these conditions cavitation tends to reduce the high lift developed near the leading edge and thereby to move the center of pressure of a typical blade section further aft of the leading edge. Since the center of pressure is usually forward of the spindle axis for these conditions, the moment arm from the spindle axis to the center of lift is reduced. Therefore, the absolute value of the net spindle torque on the blade is reduced.

Cavitation usually reduces the maximum spindle torque, but it can actually increase it for some unusual combinations of propeller geometry and operating conditions. For example, in propellers with substantial unbalanced skewback relative to the spindle axis (such as Propeller 4535), the center of pressure under noncavitating conditions may be aft of the spindle axis at conditions where substantial lift is produced by angle of attack. When the high lift near the leading edge is reduced by cavitation, the center of pressure moves further aft of the spindle axis. The net change in spindle torque resulting from cavitation depends on a change in moment arm (which for this case is increased by cavitation) and a change in lift force (which is decreased by cavitation). Therefore, for this case spindle torque may either increase or decrease with cavitation depending on the relative change in lift and moment arm. However, the sensitivity of spindle torque to cavitation is much greater for the more usual situation in which both lift and moment arm (and thus spindle torque) decrease with increasing cavitation.

CENTRIFUGAL SPINDLE TORQUE

For centrifugal spindle torque, the agreement between analytical predictions[11] and experimental results was excellent for all pitch settings of Propeller 4572 (Figure 30); it was also excellent for zero and negative pitch settings of Propeller 4575 but not nearly as good for positive pitch settings (Figure 31). There is no known reason why agreement in this region was not better; however, the variation of the experimental results with pitch setting was not as smooth as for Propeller 4572, which suggests that these experimental data may be questionable.

The absolute values of the centrifugal spindle torque coefficients K_{SC} for Propeller 4572 was almost twice as large as those for Propeller 4575. This apparently resulted from the combination of wider blades and higher skew for Propeller 4572 and the use of forward rake for Propeller 4575.

Figures 32-36 compare the experimental results of K_{SC} versus $(P/D)_{0.7}$ presented in References 15 and 16 with analytical predictions.[11] The agreement between theory and experiment was excellent for some propellers and poor for others. The reason for this inconsistency is not known but possibly some of the experimental data may have been in error, as indicated by the experimental results. For example, Propellers 4496 and 4402 which are quite similar (see Tables 1 and 7) had virtually identical values for K_{SC} as calculated analytically yet the experimental values for Propeller 4496 were substantially different both from the analytical predictions and from the experimental results for Propeller 4402. Therefore, it appears that the experimental results for Propeller 4496 are in error.

The experimental $|K_{SC}|$ was approximately 30 percent lower than the analytically calculated value (Figure 34) for Propeller 4535 which has higher skew than any of the other propellers evaluated. However, since no systematic deviation between theory and experiment was apparent with increasing skew, the reason for the poor agreement between theory and experiment for this propeller is not known.

In general, the correlation between analytical and experimental values of K_{SC} substantiate the validity of the analytical technique for a range of blade width, skew, and rake. Figure 37 which compares the analytical values of K_{SC} for the propellers evaluated in the present investigation and earlier[15,16] gives an indication of the effect of various geometric parameters on K_{SC}. However, a more direct measure of the influence of individual design parameters on K_{SC} can be obtained by exercising the analytical technique described in Reference 11 over a range for one parameter while holding the others constant.

SPINDLE TORQUE AT DESIGN CONDITIONS

The total (hydrodynamic plus centrifugal) spindle torque on the full-scale propeller depends on the values of K^*_{SH} and K^*_{SC} and on the dimensional operating and geometric conditions of the propeller, i.e., on V_A n, D, $(P/D)_{0.7}$, and ρ_P. Therefore, in order to compare the total spindle torque at design conditions on the various propellers evaluated in this report and in Reference 16, the spindle torque coefficients were converted to dimensional spindle torques; see Table 8. In order to illustrate the magnitude of the spindle torques for realistic propellers, these dimensional spindle torques are presented for hypothetical full-scale propellers geometrically similar to the model propellers. All these hypothetical full-scale propellers have the same diameter, speed of advance, and density, and all operate at their design advance coefficient. However, all do not operate at the same rpm since they were designed for different advance coefficients.

The results show that the two propellers with balanced skew (Propellers 4572 and 4575) and the two propellers with small skew (Propellers 4496 and 4536) had small values of spindle torque ($|Q_s| \leq$ 17,700 ft-lb), whereas the two propellers with substantial skewback without balancing forward skew had large negative (depitching) spindle torques ($Q_s \leq$ -105,000 ft-lb). This demonstrates that by using balanced skew, small values of spindle torque at design conditions can be obtained with substantial variation in skew angle with propeller radius. The large

negative values of spindle torque for the highly skewed propellers without forward balancing skew arises because this type of skew distribution places the center of pressure of the blade significantly aft of the spindle axis.

The results indicate that except for Propeller 4575, all the propellers evaluated developed negative, or depitching, spindle torque at design pitch and design advance coefficient. However, when a propeller operates in a realistic wake, the spindle torque fluctuates due to the circumferential nonuniform inflow velocity; therefore, it is anticipated that all the propellers evaluated would experience negative spindle torque at some blade angular positions. Positive spindle torque at design conditions is desirable so that the blade will tend to rotate toward high ahead pitch in the event of loss of hydraulic pressure in the pitch-changing mechanism. However, if the absolute value of the net hydrodynamic plus centrifugal spindle torque is less than the spindle torque arising from static friction in the hub mechanism, the blade will not rotate following loss of hydraulic pressures in the pitch-changing mechanism. Therefore, small negative values of net hydrodynamic plus centrifugal spindle torque present no serious problems regarding blade pitch upon loss of hydraulic pressure.

The results shown in Table 8 are based on model experimental runs conducted to determine hydrodynamic spindle torque in uniform flow. Inasmuch as these propellers were designed for a small radial variation of the circumferential mean longitudinal velocity (see Tables 1-6); the results shown in Table 8 do not represent precisely the design condition. However, it is anticipated that the effect of this small velocity gradient on spindle torque would be small. In addition, although the deviation between theoretical and experimental centrifugal spindle torque is greater for some propellers than for others, it is not sufficiently large to significantly affect the trends shown in Table 8 for the net spindle torque.

SUMMARY

Experimental spindle torque and open-water performance were investigated for two skewed controllable-pitch propellers. Both propellers have radial distributions of skew specified so that the section midchord is forward of the spindle axis at the inner radii and aft of the spindle axis at the outer radii. One propeller has no rake and the other has substantial forward rake. The experiments were conducted at steady conditions in uniform flow in a towing basin over a range of positive and negative pitch ratios and a range of positive and negative advance coefficients so that the complete maneuvering envelope of the ship was simulated in a quasi-steady manner.

The experimental open-water performance was correlated with calculated values based on a least-squares fit to previous systematic experimental data. The correlation indicates that the calculation procedure may be adequate for preliminary dynamic simulation studies in cases for which open-water data are not available on a simular model propeller.

The experimental spindle torque results are generally consistent with previously reported experimental results. These results suggest that realistic highly skewed propellers can be designed with spindle torque characteristics comparable to those of equivalent propellers without significant skew. No definite conclusions could be drawin regarding the effect of forward rake on spindle torque. The experimental values of centrifugal spindle torque generally agree with analytically calculated values over a range of pitch ratio.

RECOMMENDATIONS

Based on the results of this investigation, the following recommendations are made:

1. The effect of forward rake on spindle torque should be further evaluated. This should include model experimental evaluation of a raked

propeller designed by lifting surface procedures which properly account for rake. This propeller should be identical to one of the unraked propellers evaluated in this report or in Reference 16 except for rake and for pitch and camber corrections arising from rake.

2. The analytical technique described by Tsao[10] for calculating hydrodynamic spindle torque over a range of pitch settings and advance coefficients should be evaluated by correlation with the experimental results presented in the present report and in Denny and Stephens.[16] If necessary, depending on this correlation, a semieimpirical technique should be developed for predicting spindle torque over the entire operating profile. This may supplement the analytical technique and may involve techniques similar to those used by Strom-Tejsen and Porter for predicting thrust and torque.

3. Spindle torque and other components of blade loading should be measured behind a model hull for various simulated operating conditions including dynamic crash astern and crash ahead. This would determine the influence of the propeller-hull interactions and time variation of conditions on the spindle torque and other components of blade loading.

ACKNOWLEDGMENTS

The authors are grateful to Mr. Stephen B. Denny for general guidance on the experimental procedure, to Messrs Dennis Crown and Michael Chambers for their help in conducting the experiments, to Mr. John Leahy for setting up the instrumentation, and to Mr. Richard M. Norton for developing the computer program for plotting the data.

The first author was primarily responsible for the interpretations of the data and text presented here. His coauthors refined the experimental technique, conducted the experiments described, and reduced the data.

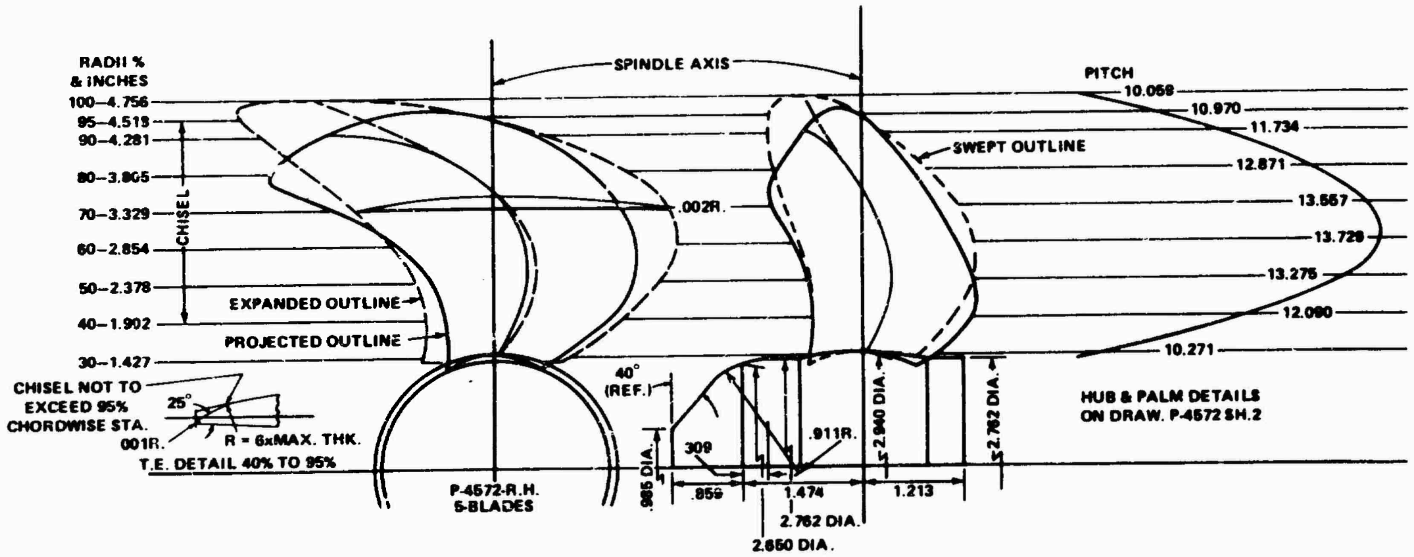

Figure 1 - DTNSRDC Model Propeller 4572

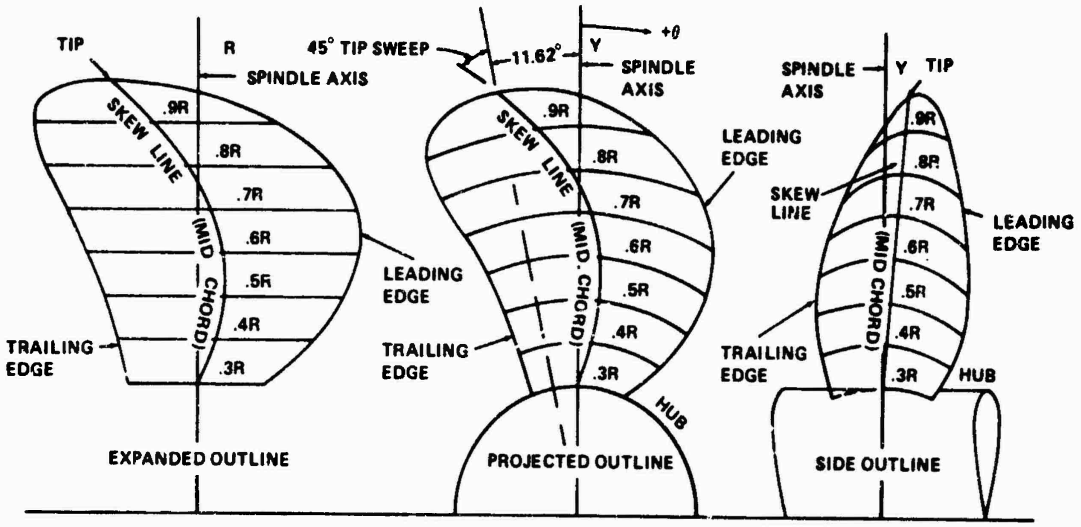

Figure 2 - DTNSRDC Model Propeller 4575

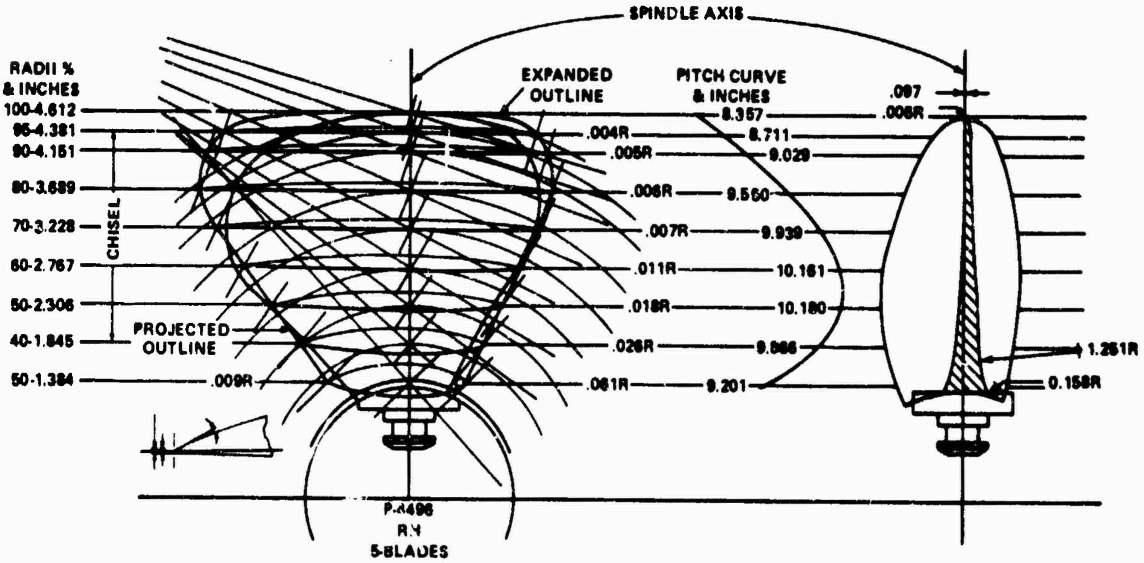

Figure 3 - DTNSRDC Model Propeller 4496

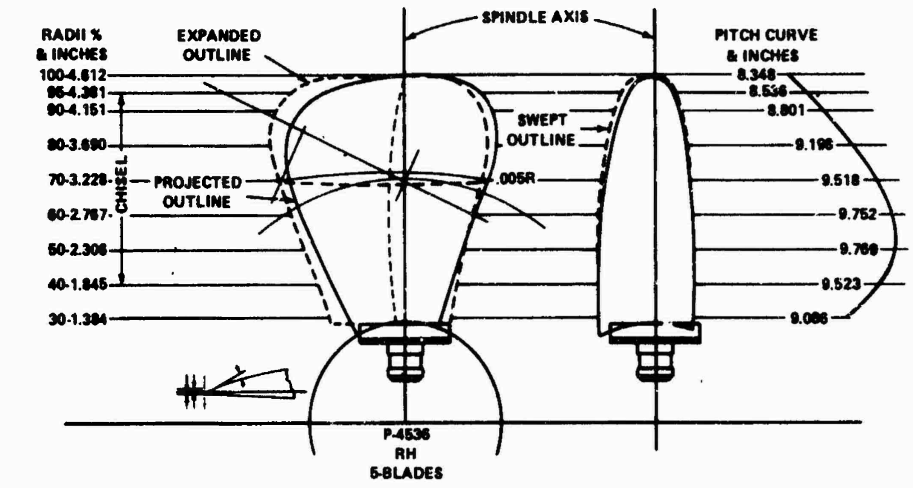

Figure 4 - DTNSRDC Model Propeller 4536

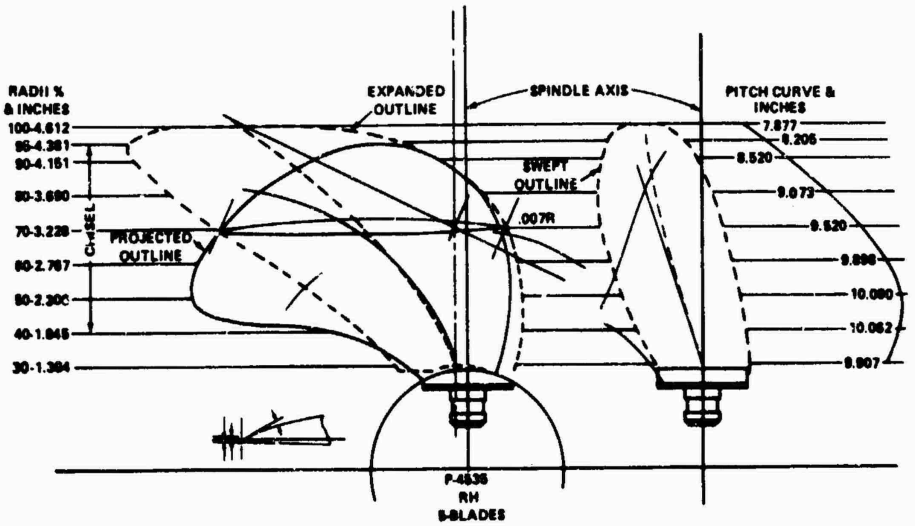

Figure 5 - DTNSRDC Model Propeller 4535

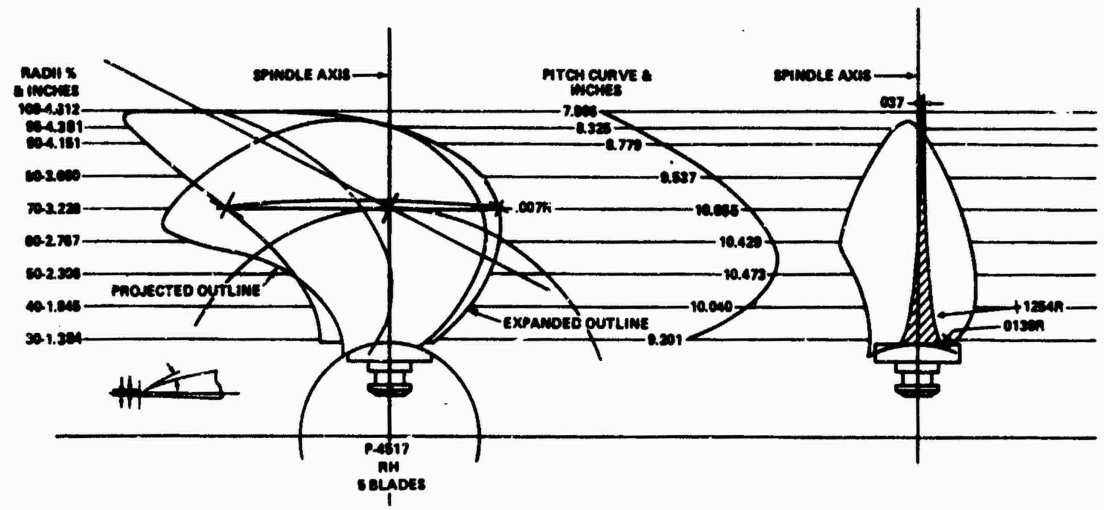

Figure 6 - DTNSRDC Model Propeller 4517

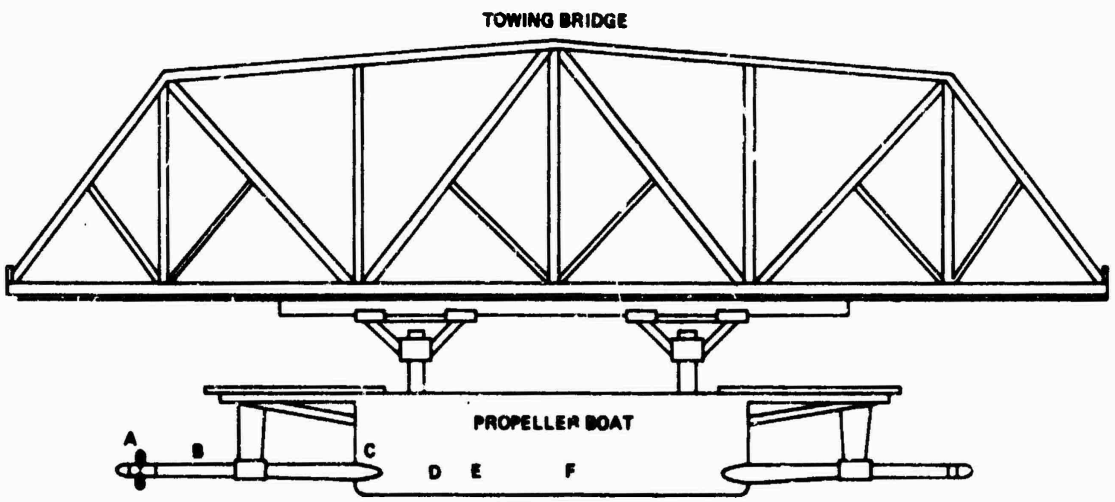

A. PROPELLER, SPINDLE TORQUE DYNAMOMETER
B. HOLLOW SHAFT
C. SLIPRINGS
D. THRUST AND TORQUE TRANSMISSION DYNAMOMETER
E. PERMANENT MAGNET FIELD DRIVE MOTORS
F. SHAFT REVOLUTION COUNTER

Figure 7 - Arrangement of Experimental Equipment

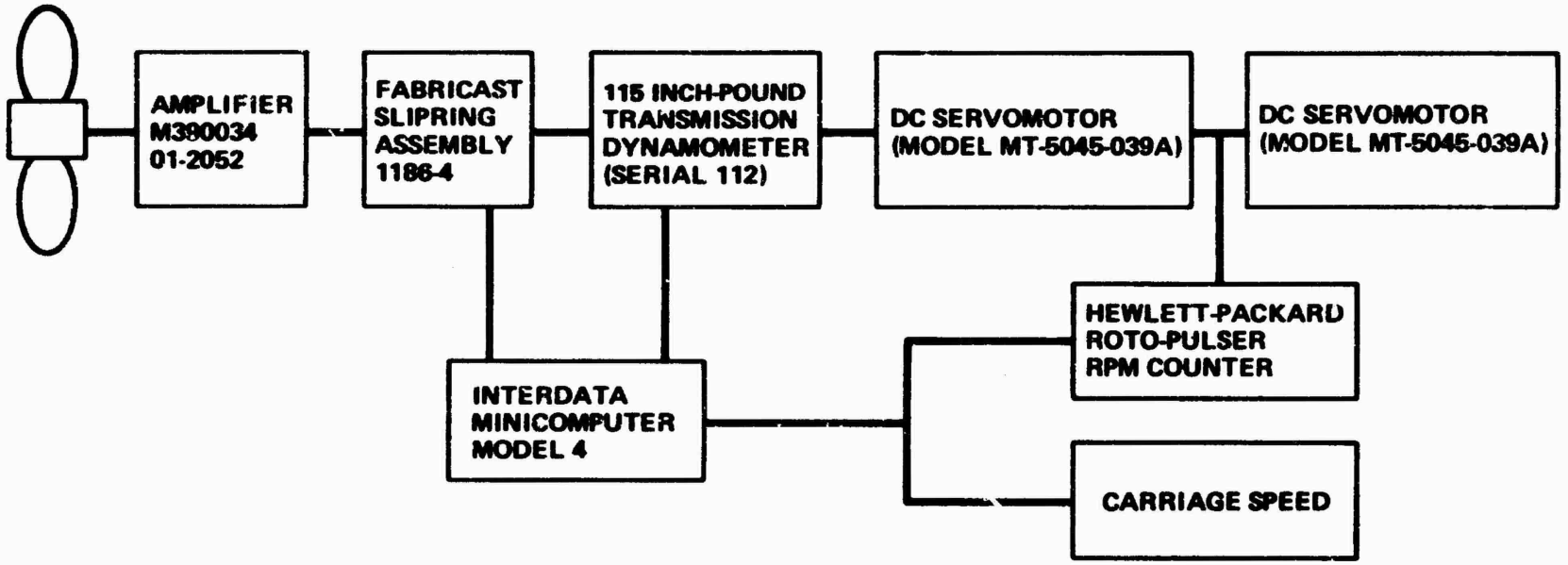

Figure 8 - Instrumentation for Spindle Torque Experiment

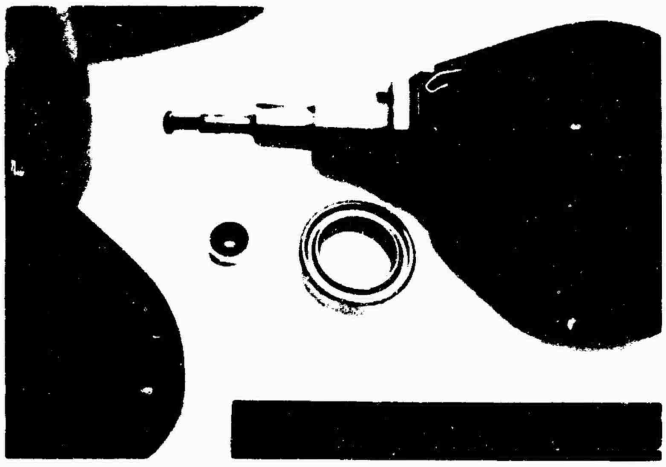

Figure 9 - Blade Spindle Mechanism

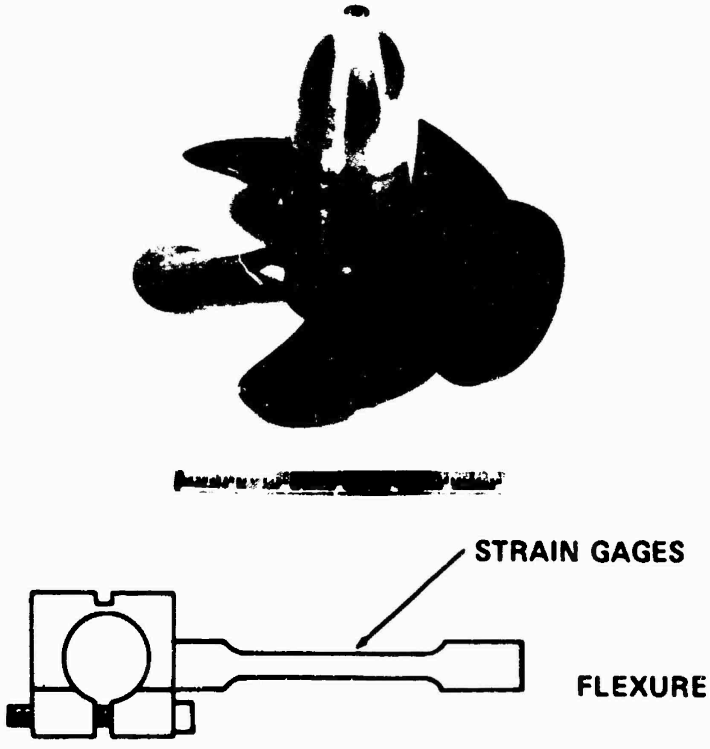

Figure 10 - Spindle Torque Dynamometer

Figure 11 - Pitch Settings and Experimental Operating Conditions

(All conditions are shown as simulated during the model experiments. The propeller was always driven from downstream.)

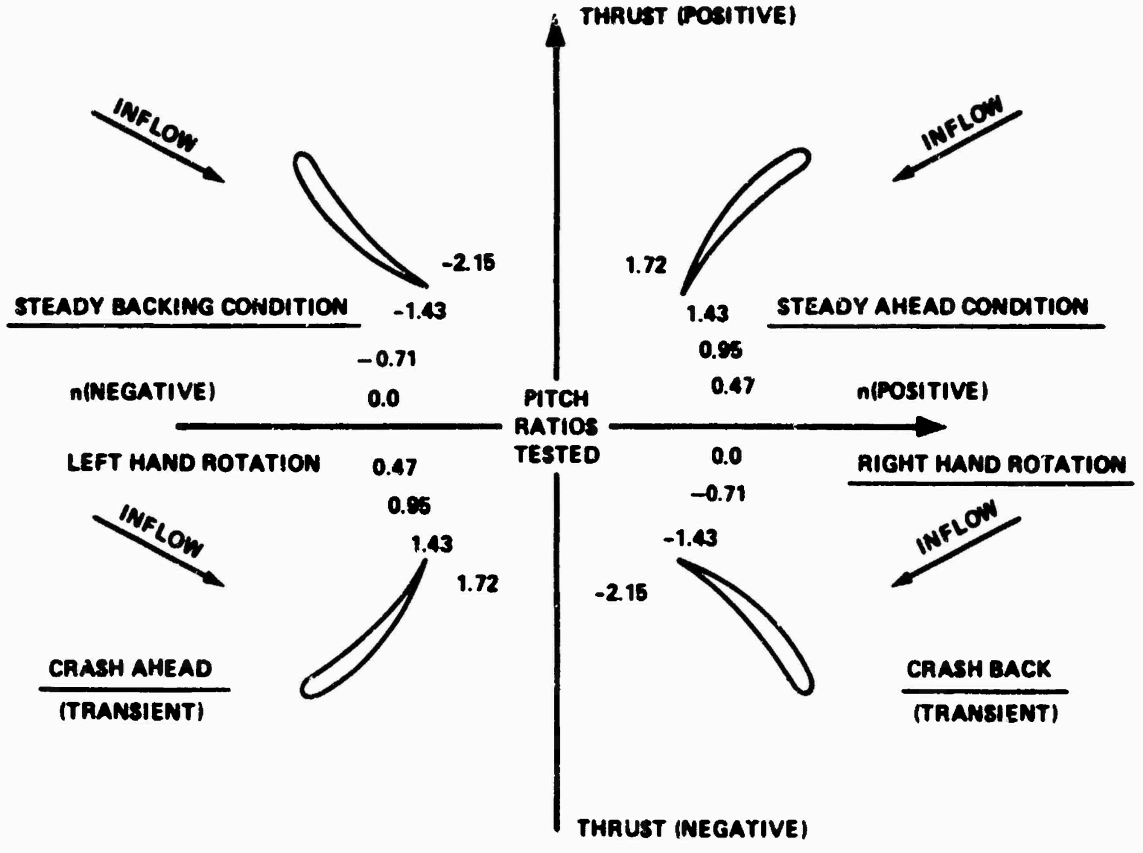

Figure 11a - For Propeller 4572

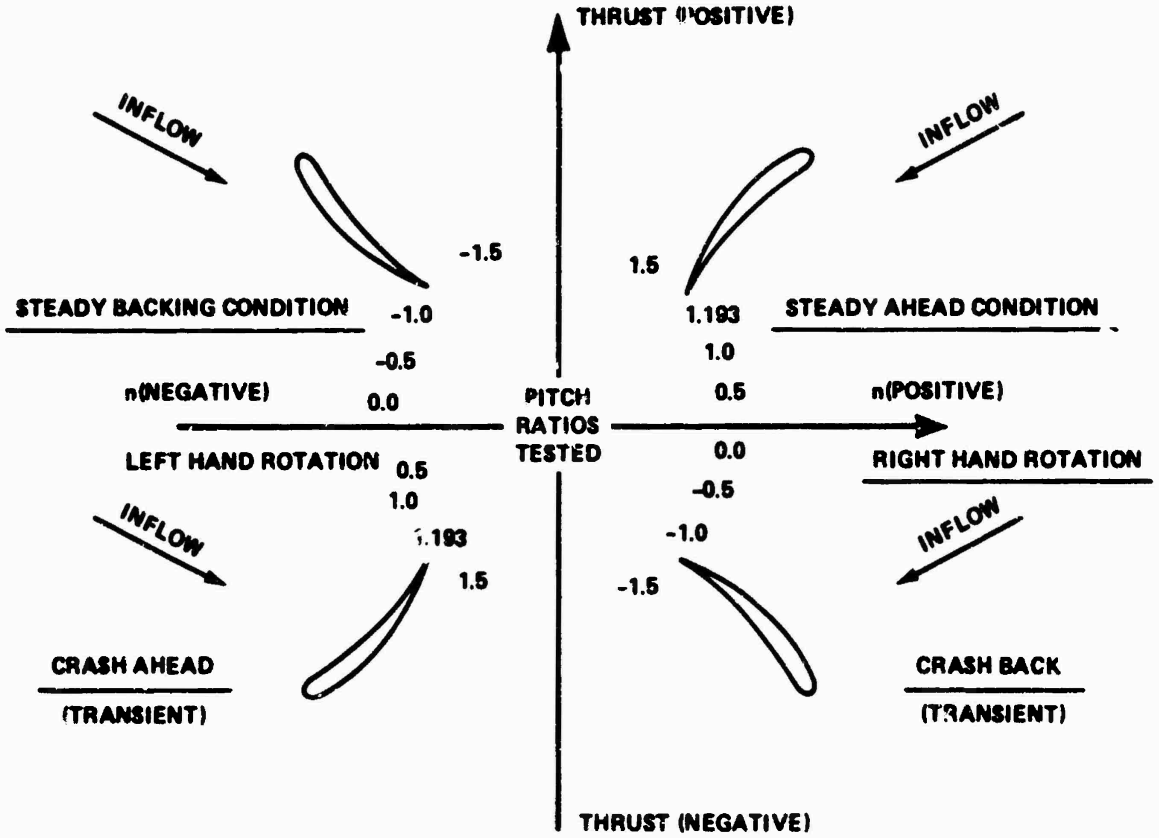

Figure 11b - For Propellers 4575

Figure 12 - Variation of Thrust Coefficient K_T with Advance Coefficient J for Propeiler 4572

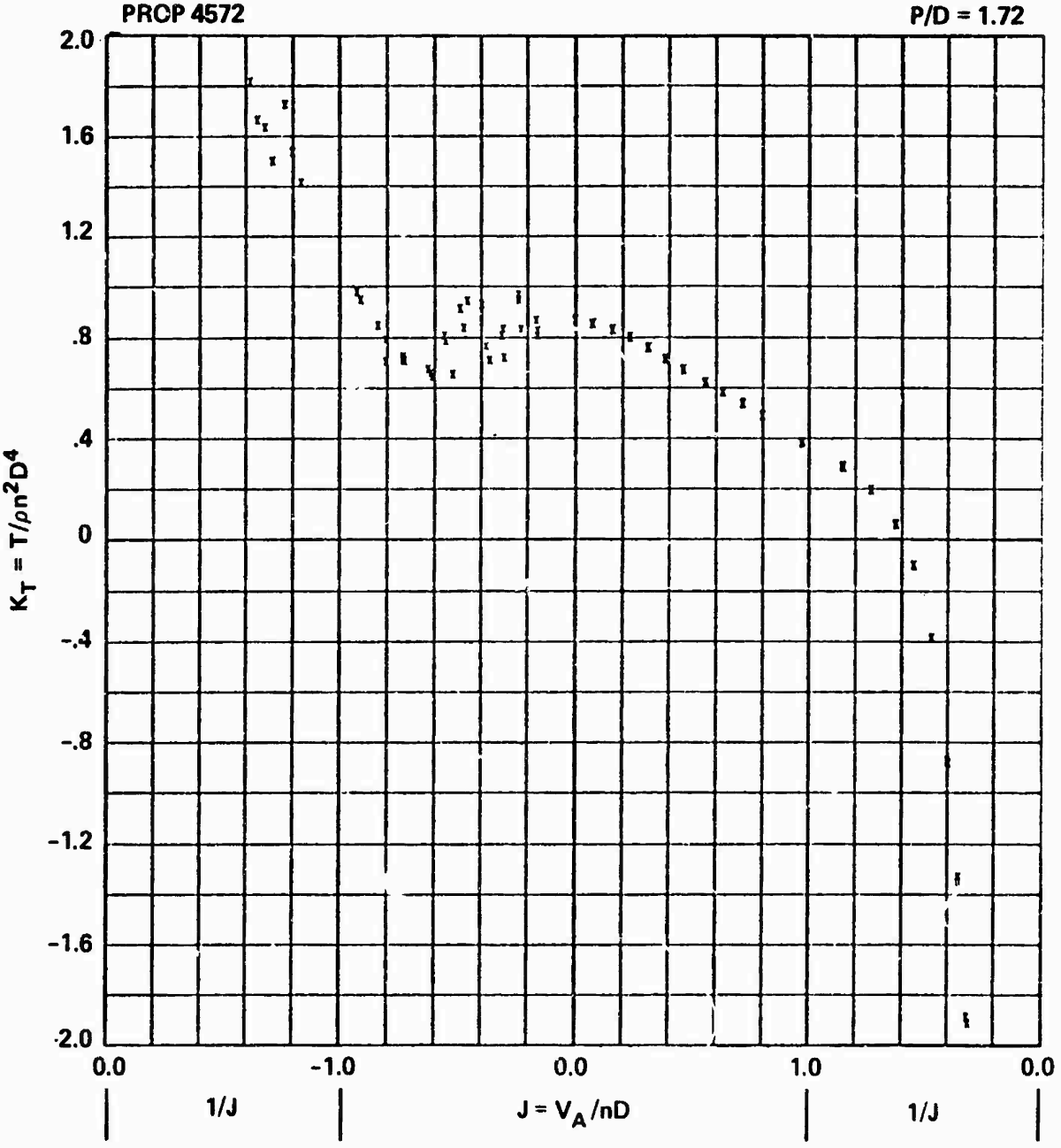

Figure 12a - At P/D = 1.72

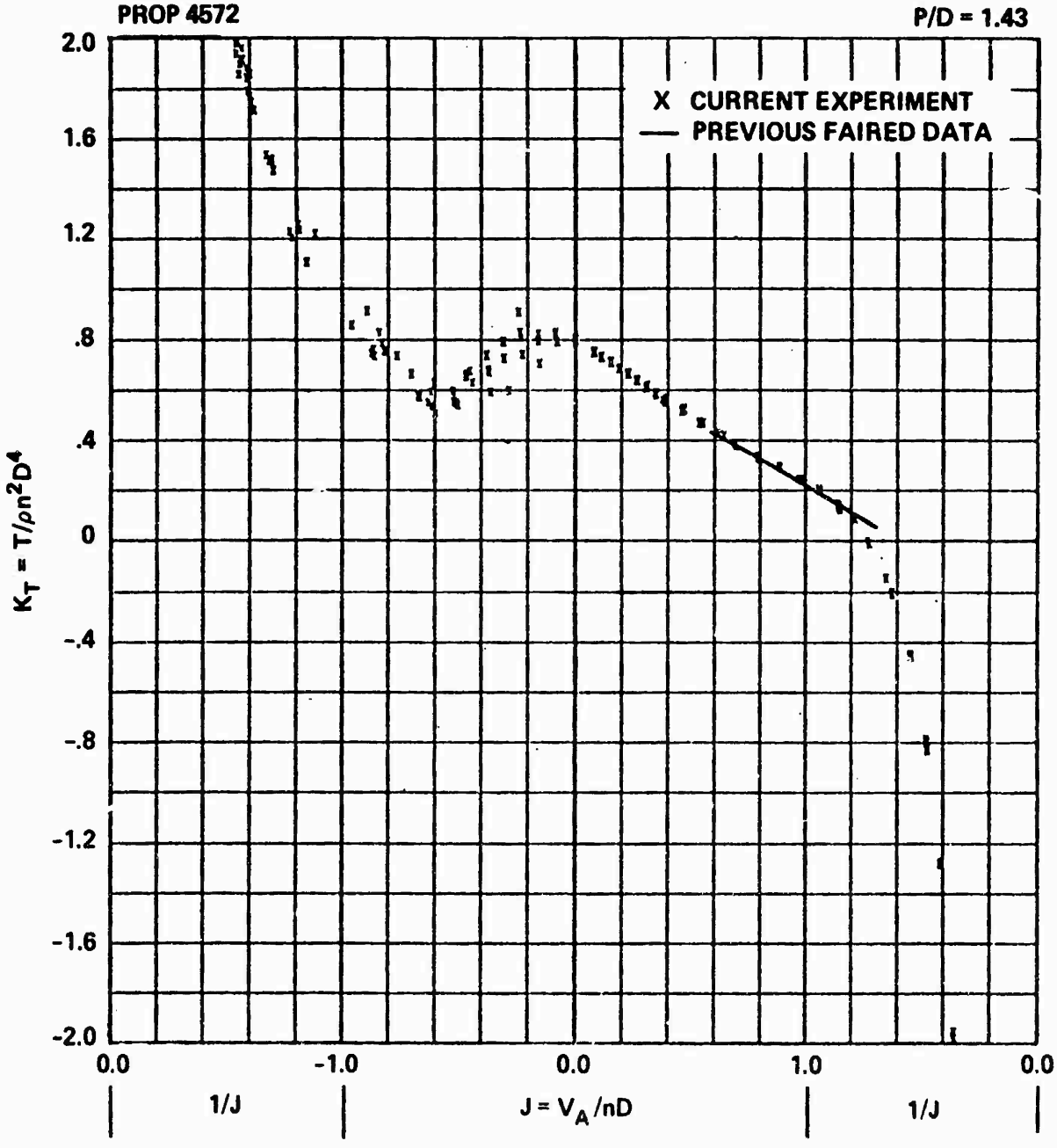

Figure 12b - At P/D = 1.43

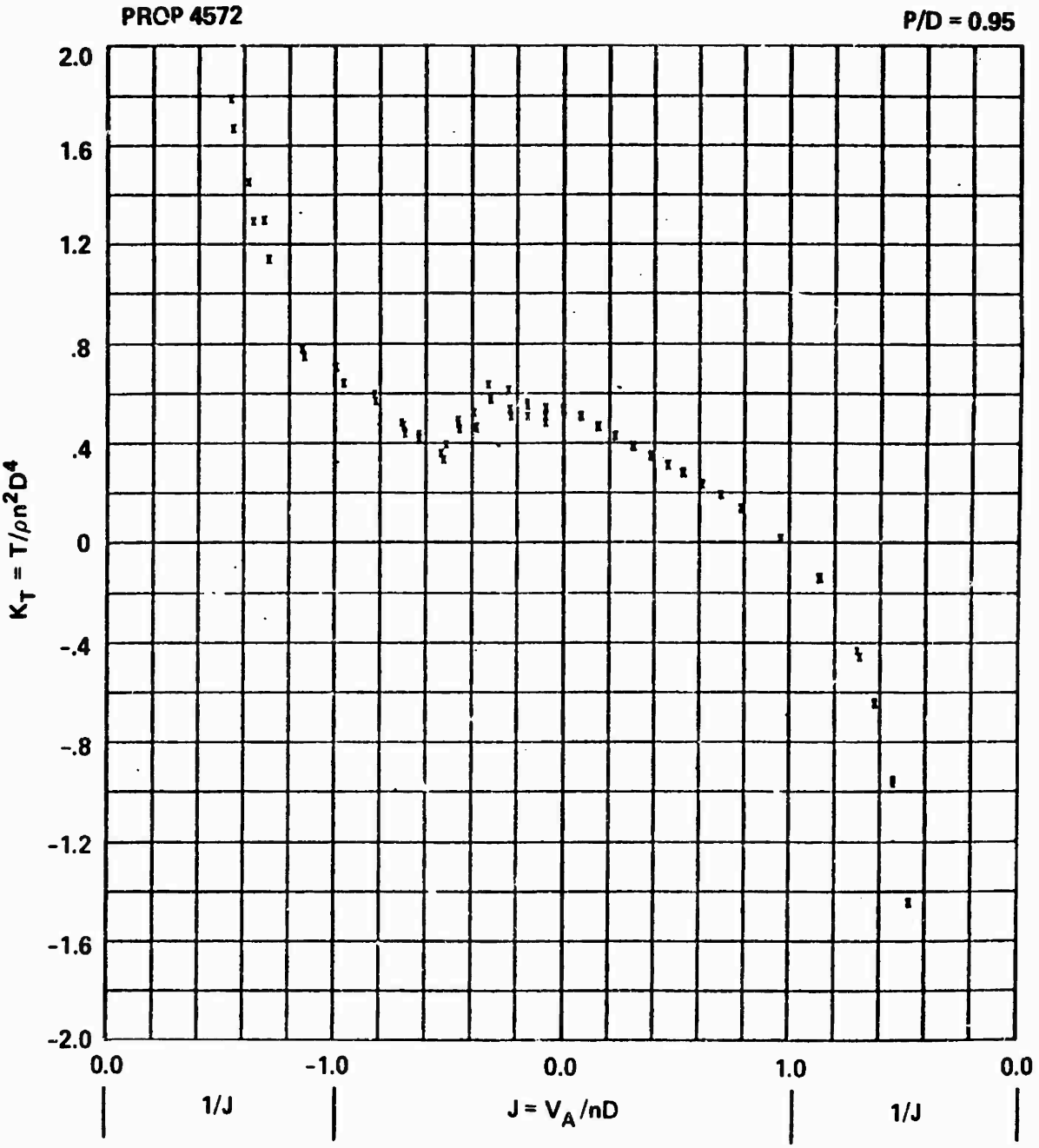

Figure 12c - At P/D = 0.95

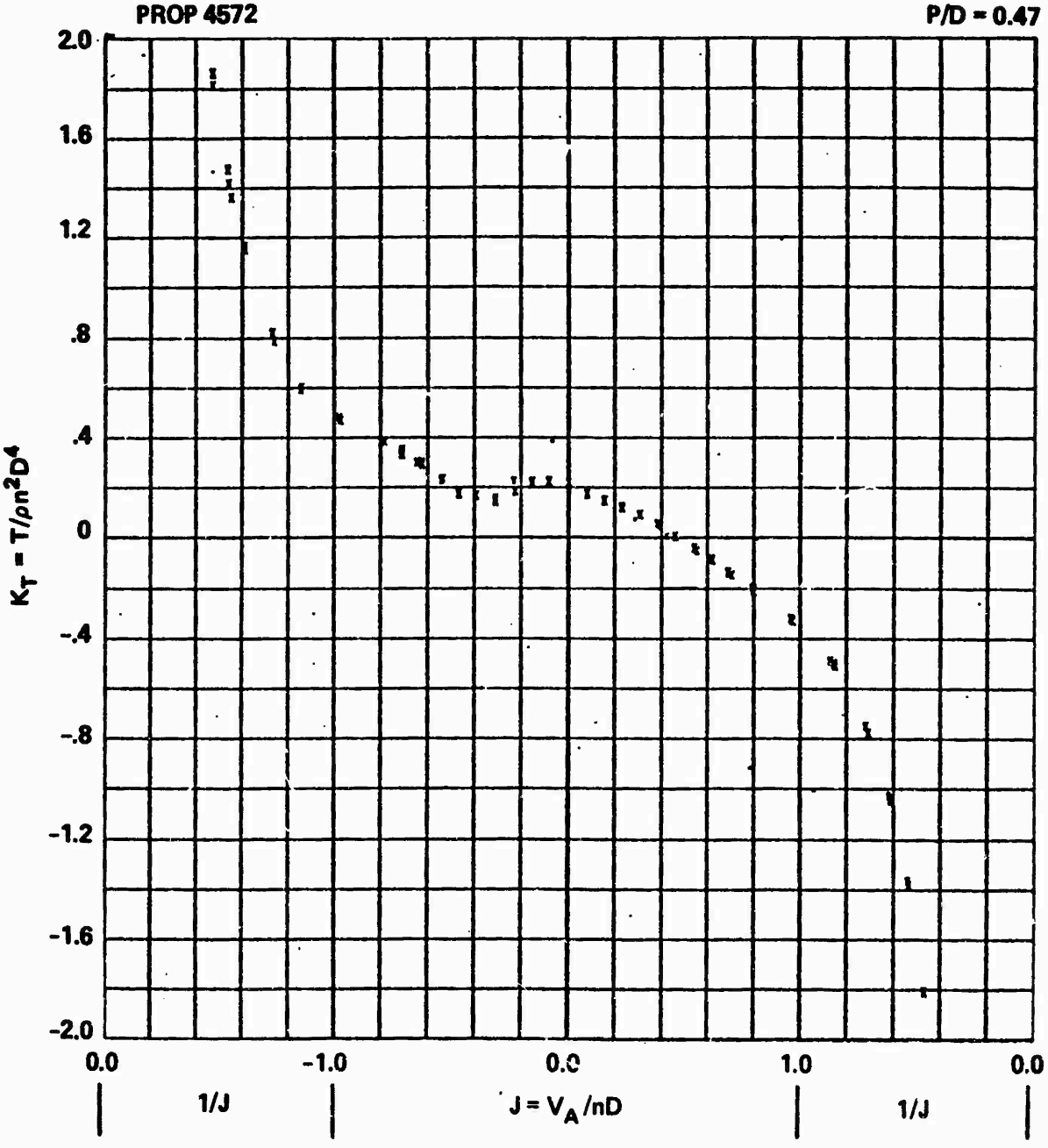

Figure 12d - At P/D = 0.47

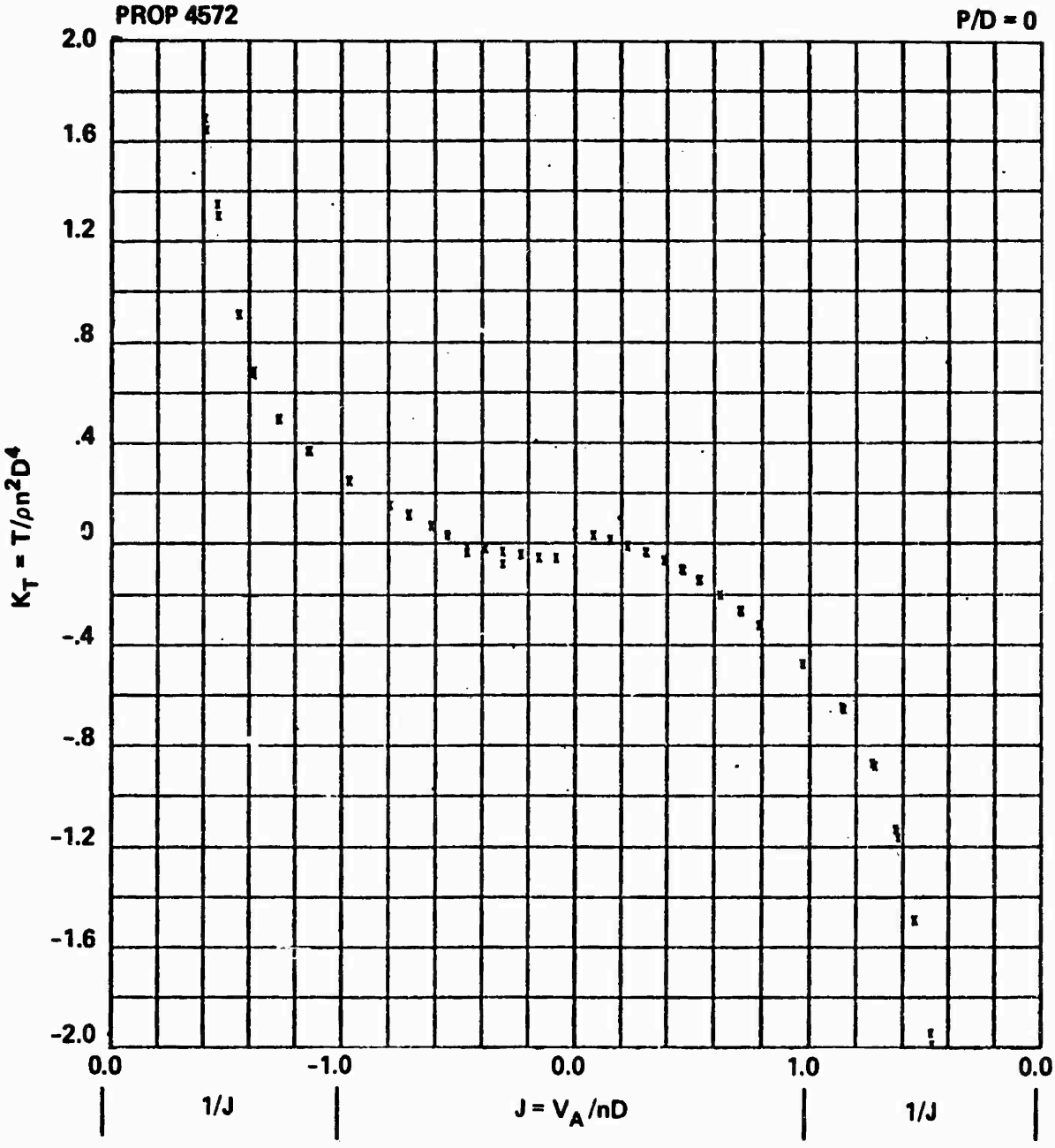

Figure 12e - At P/D = 0

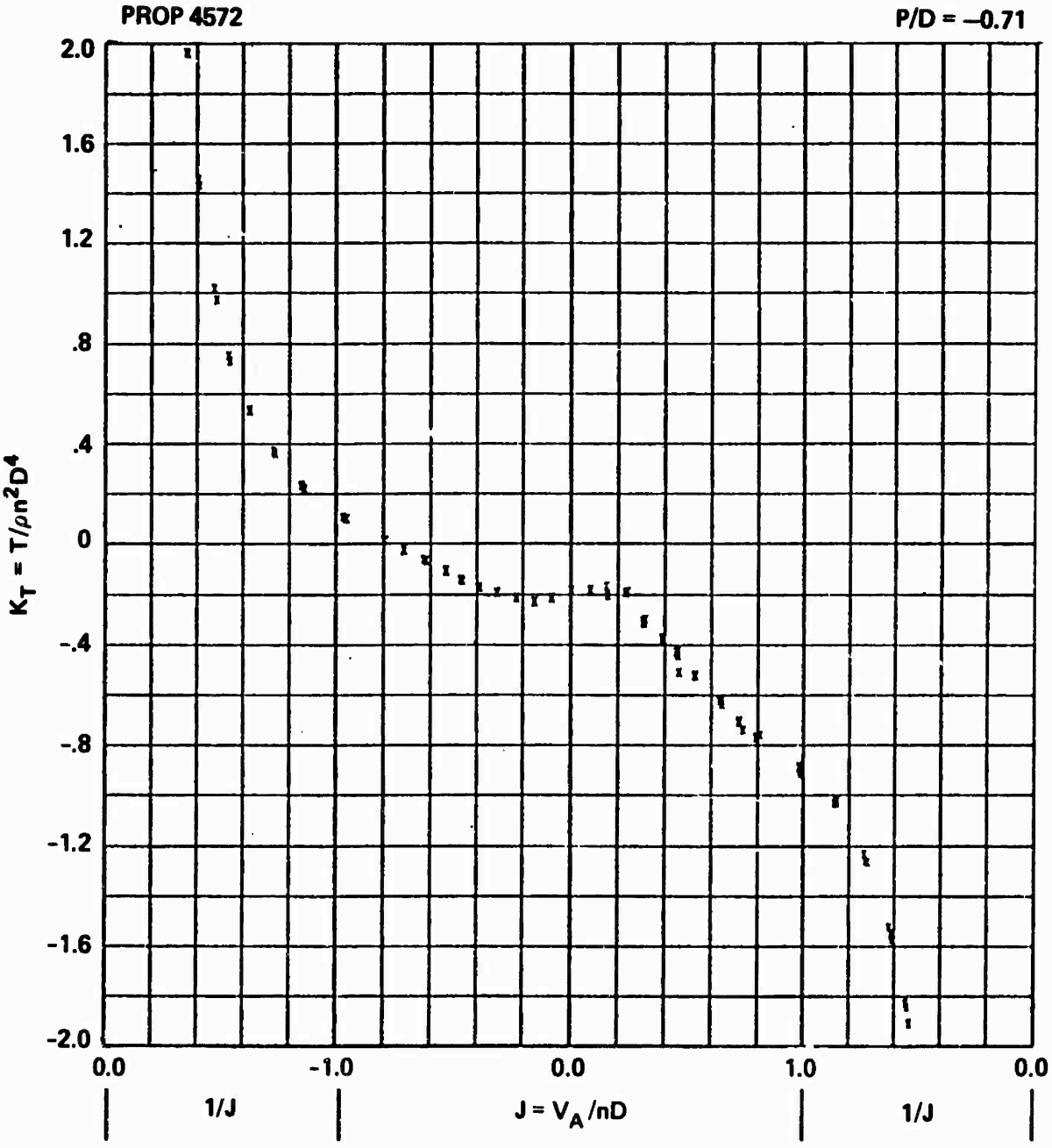

Figure 12f - At P/D = -0.71

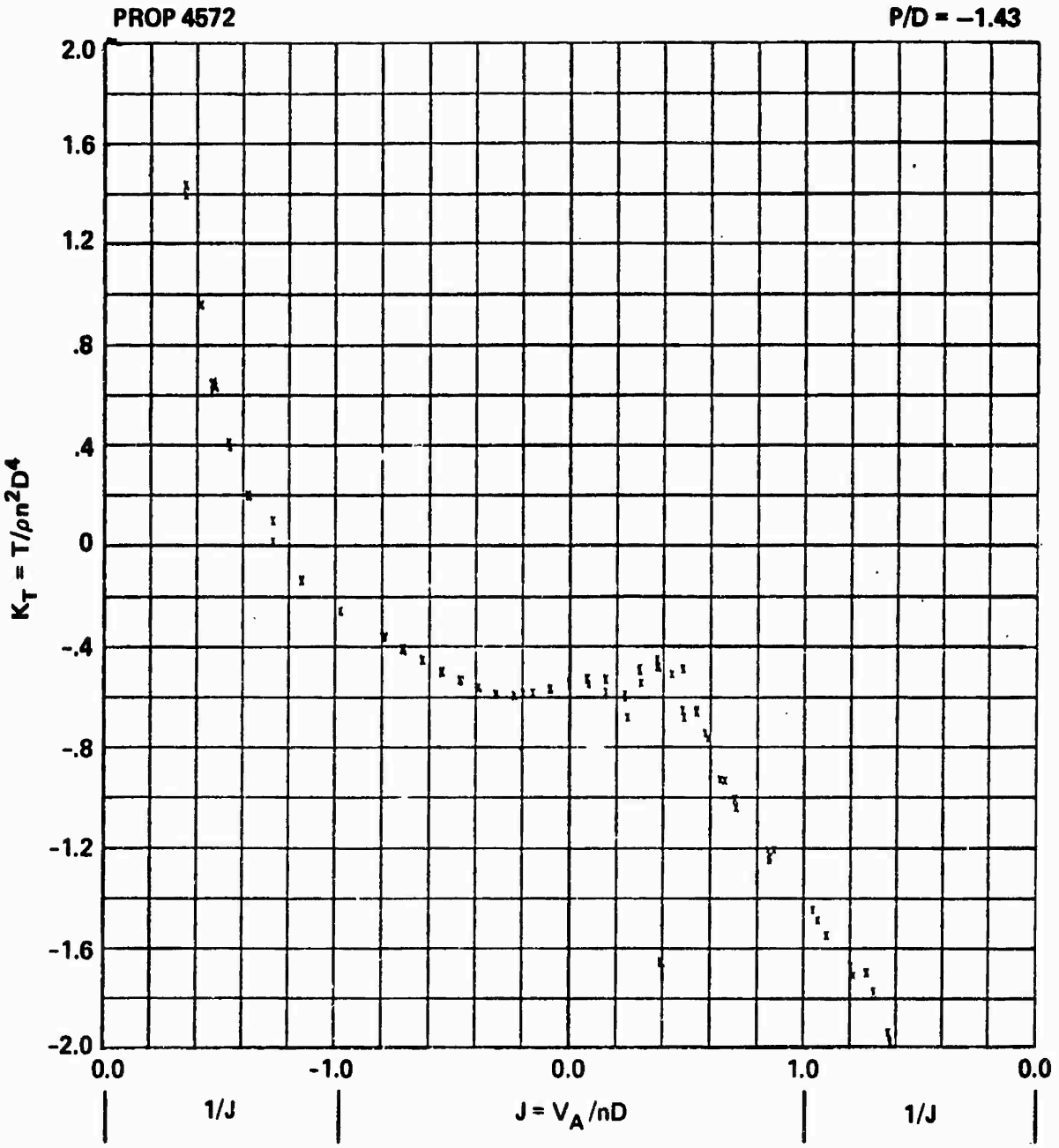

Figure 12g - At P/D = - 1.43

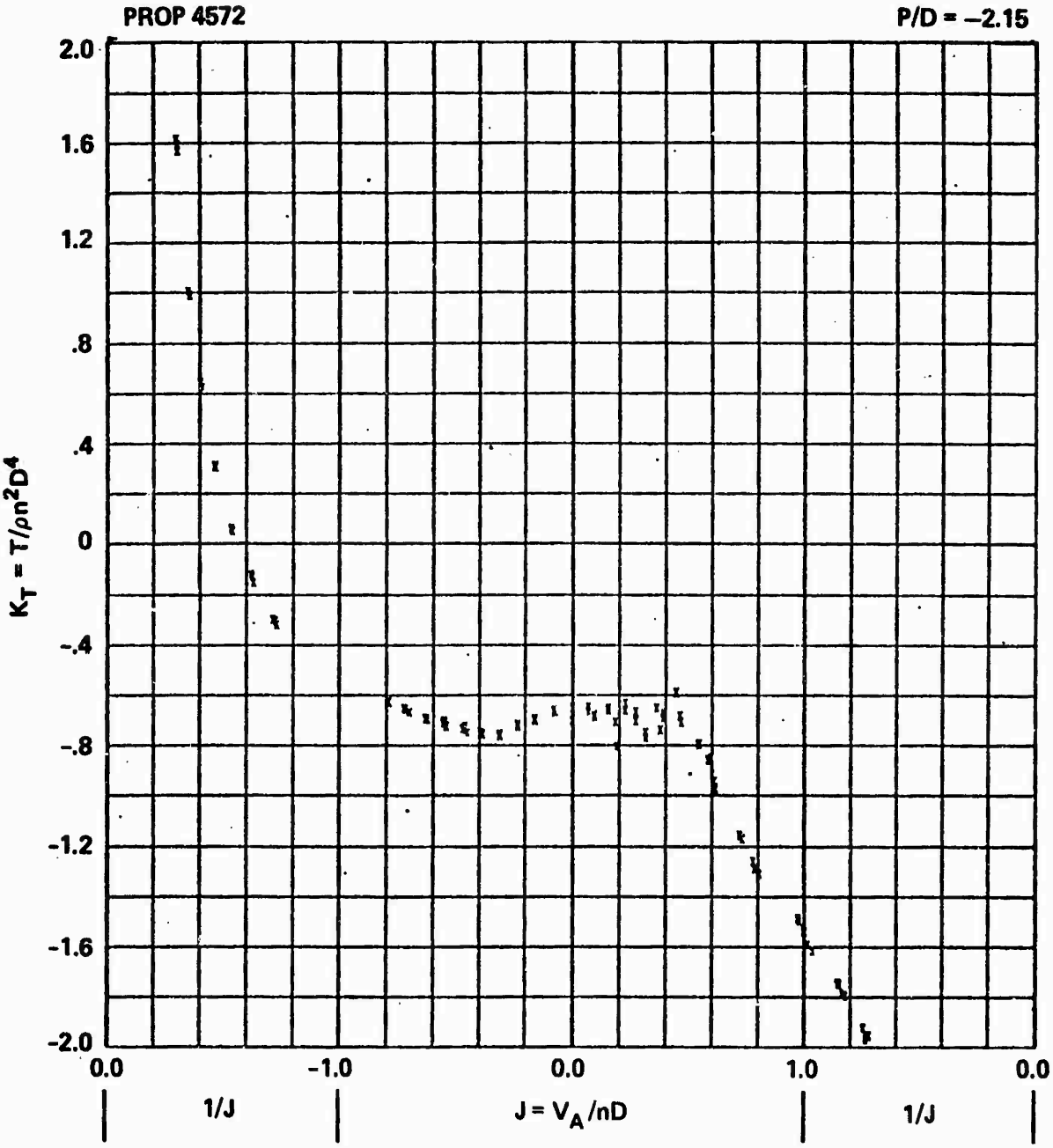

Figure 12h - At P/D = -2.15

Figure 13 - Variation of Torque Coefficient K_Q with Advance Coefficient J for Propeller 4572

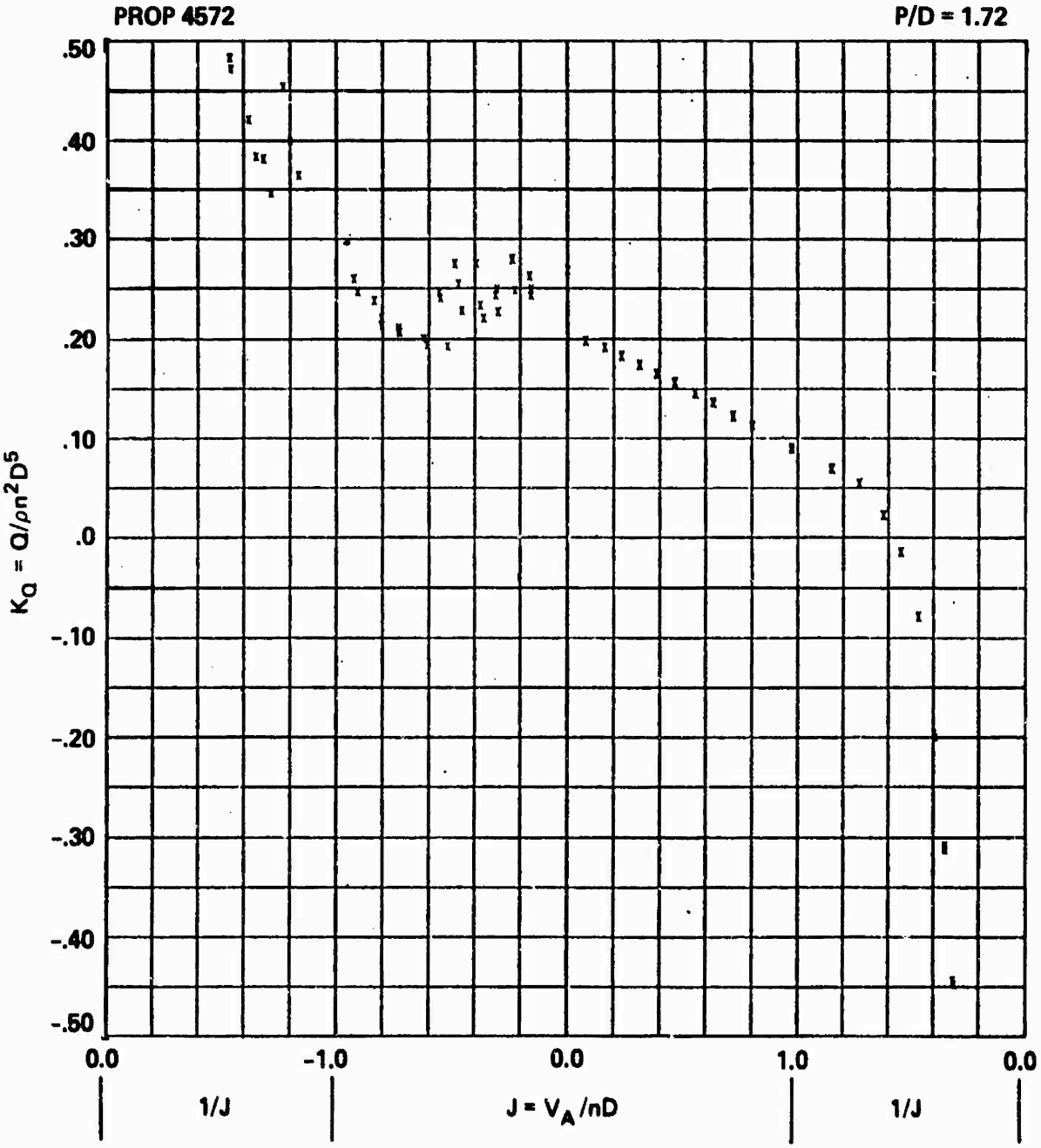

Figure 13a - At P/D = 1.72

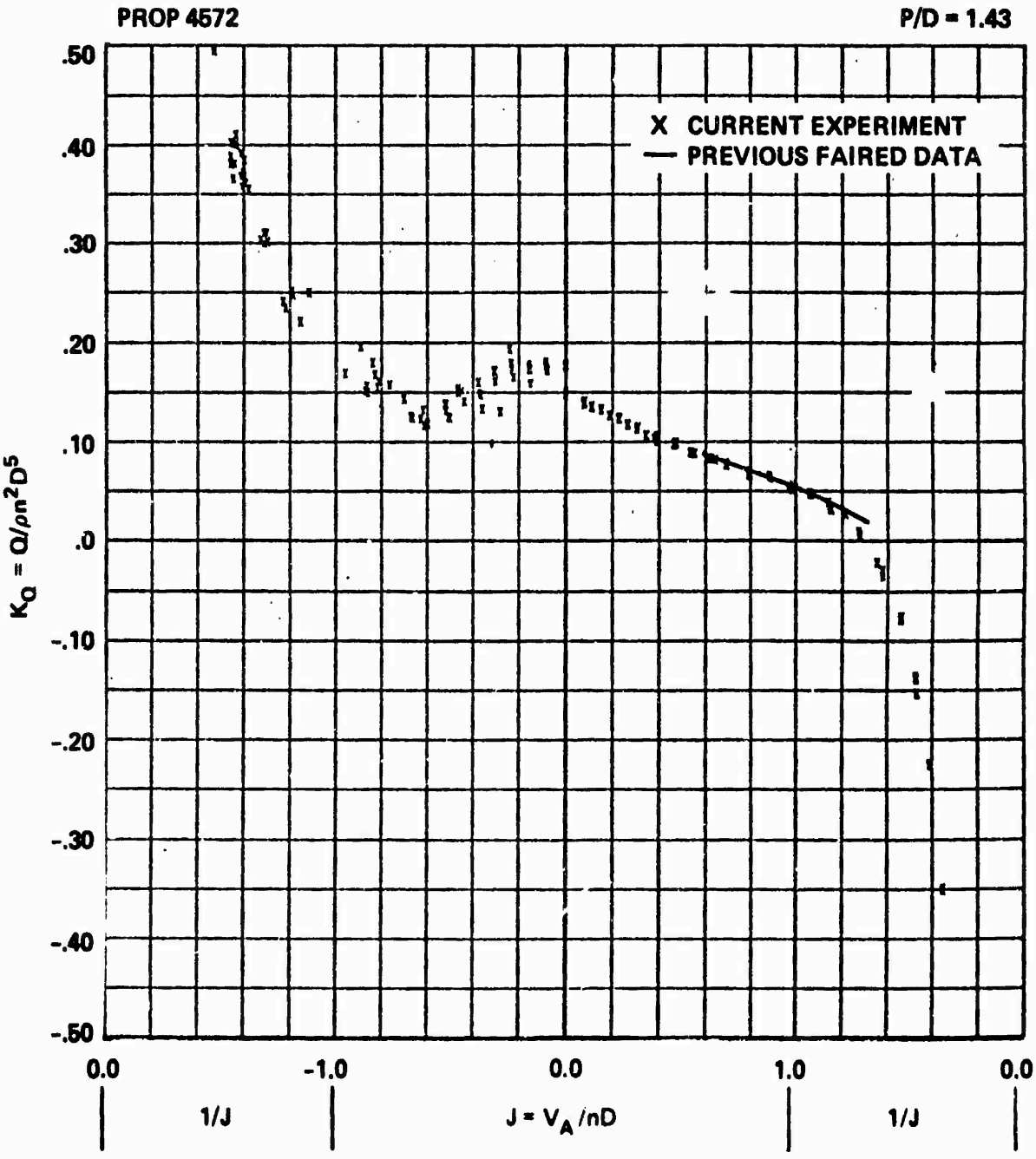

Figure 13b - At P/D = 1.43

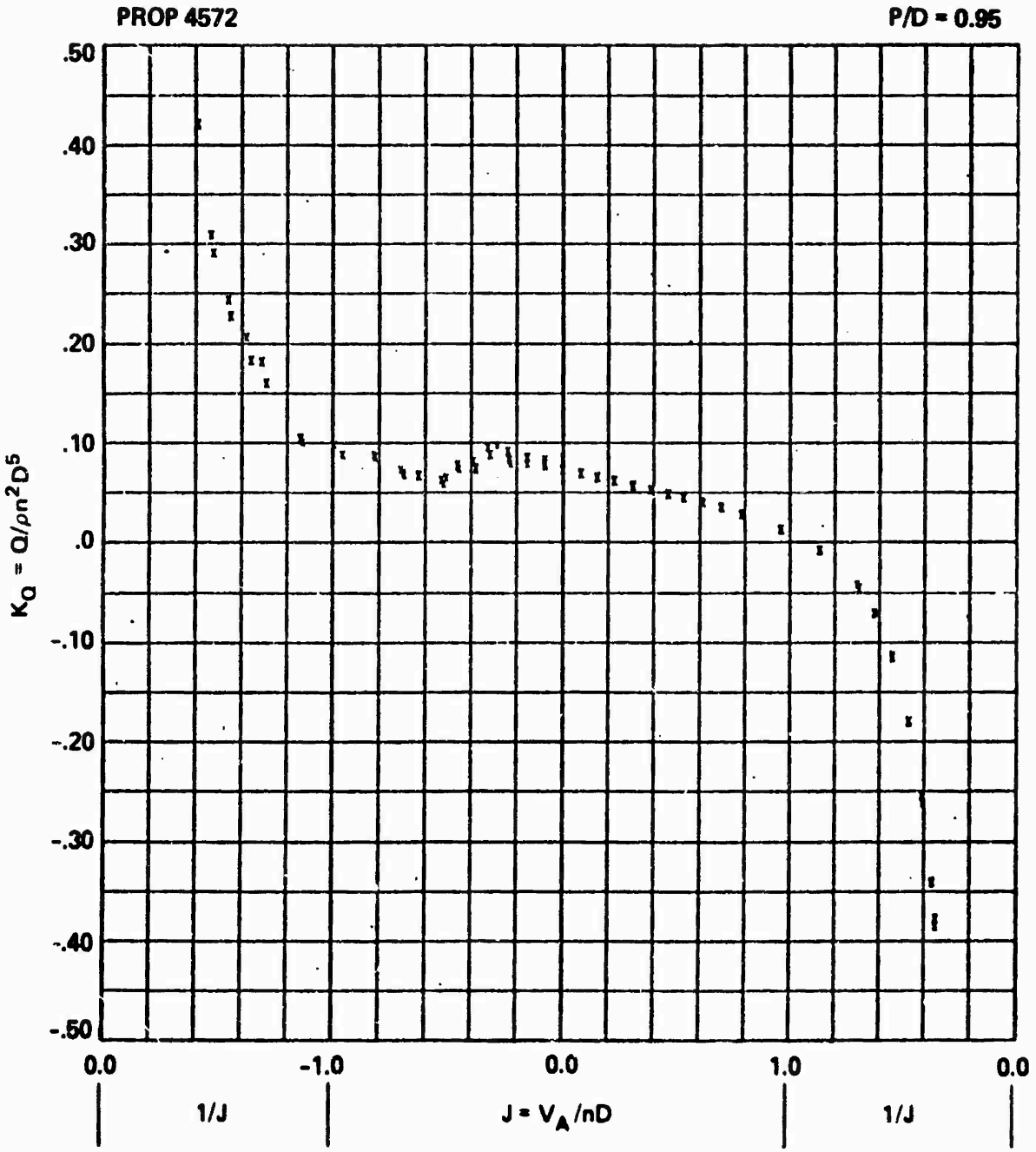

Figure 13c - At P/D = 0.95

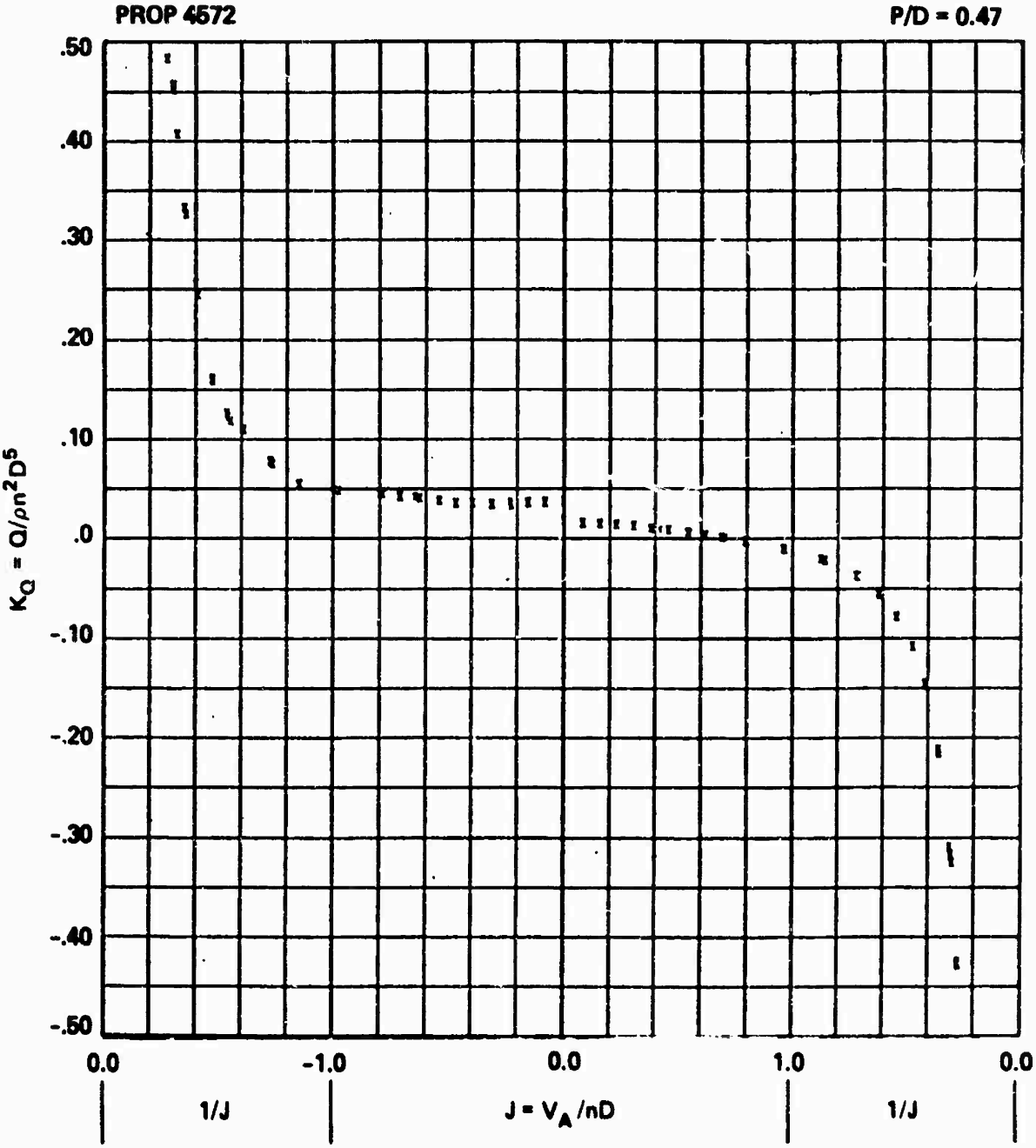

Figure 13d - At P/D = 0.47

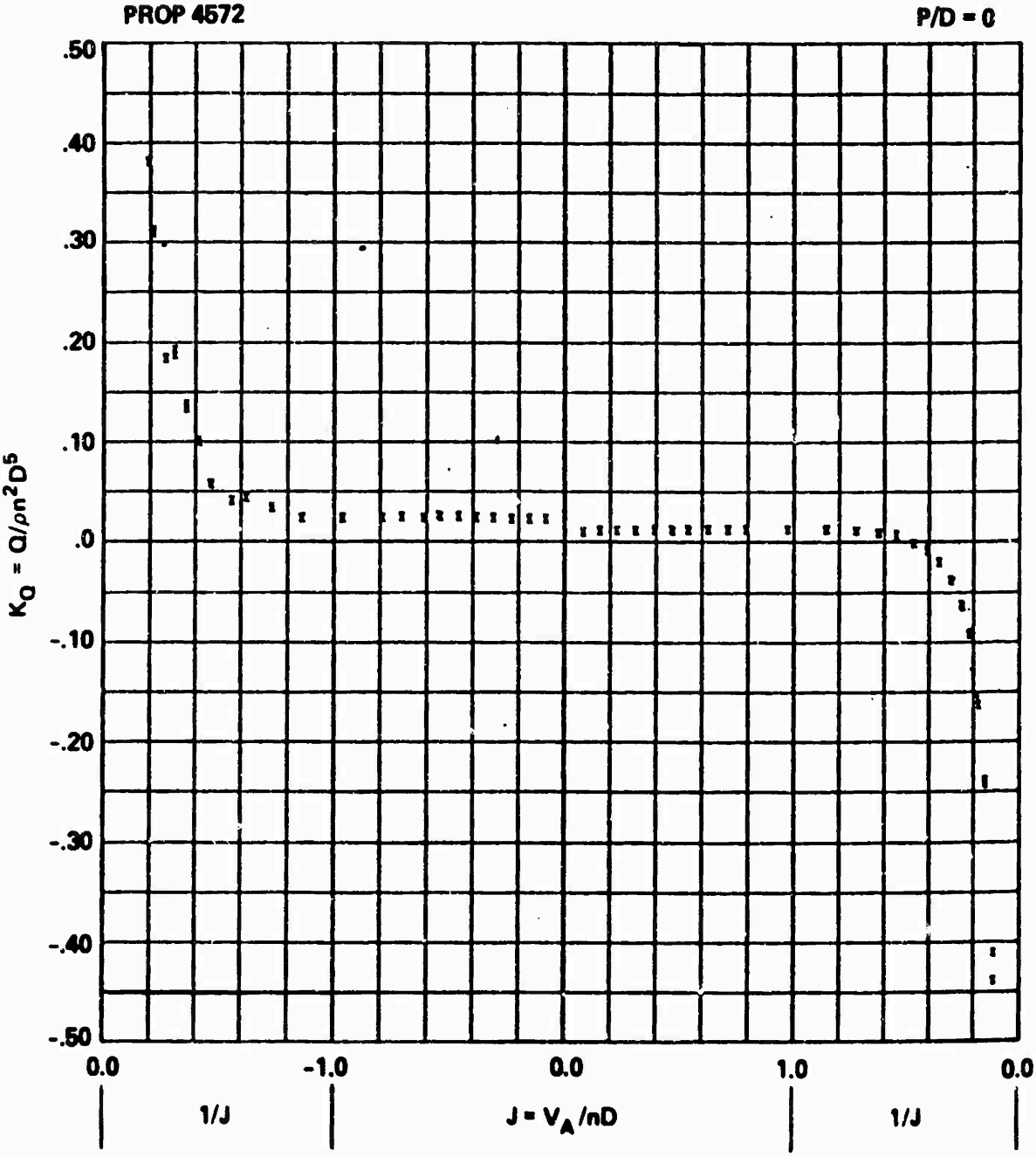

Figure 13e - At P/D = 0

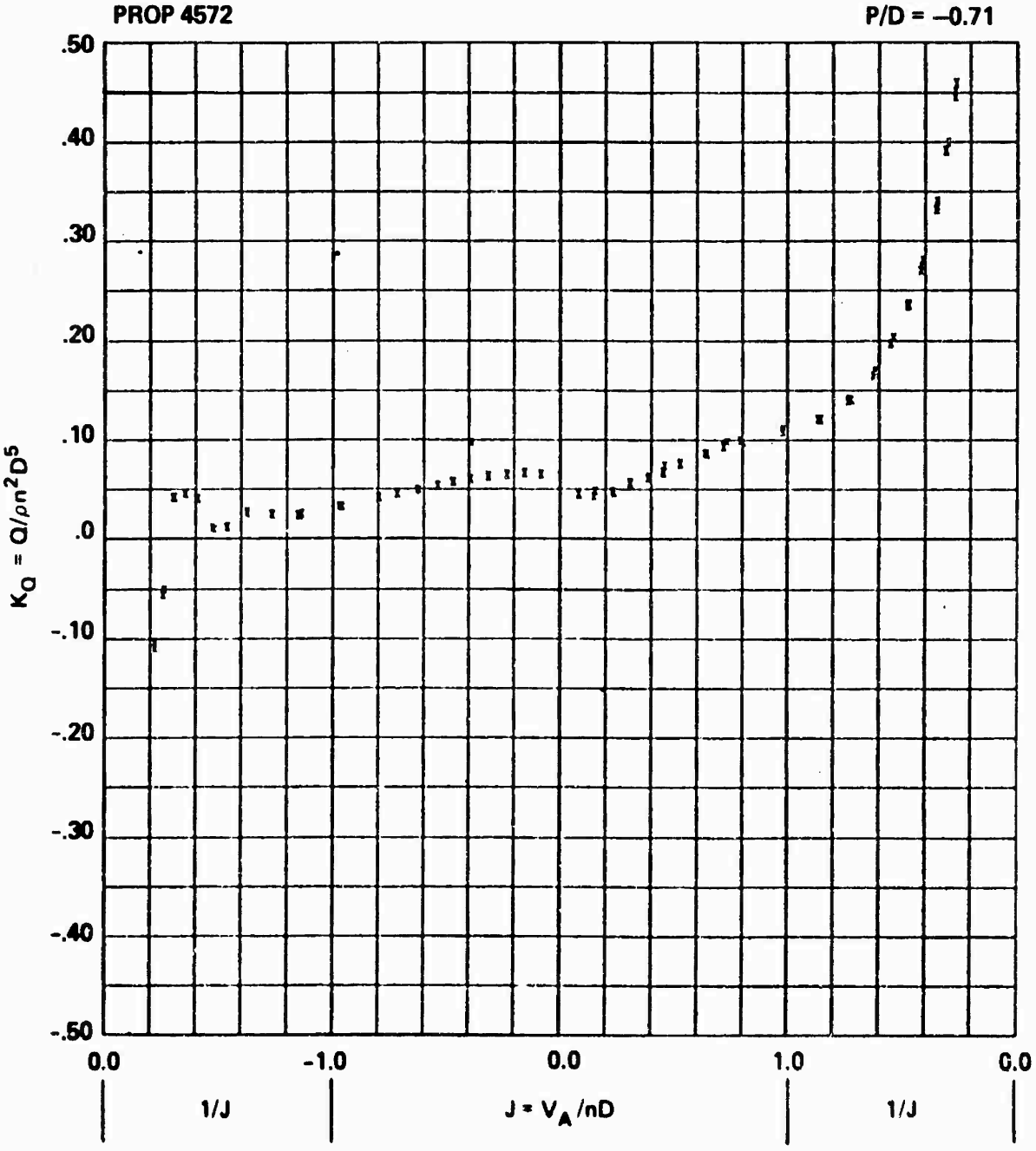

Figure 13f - At P/D = -0.71

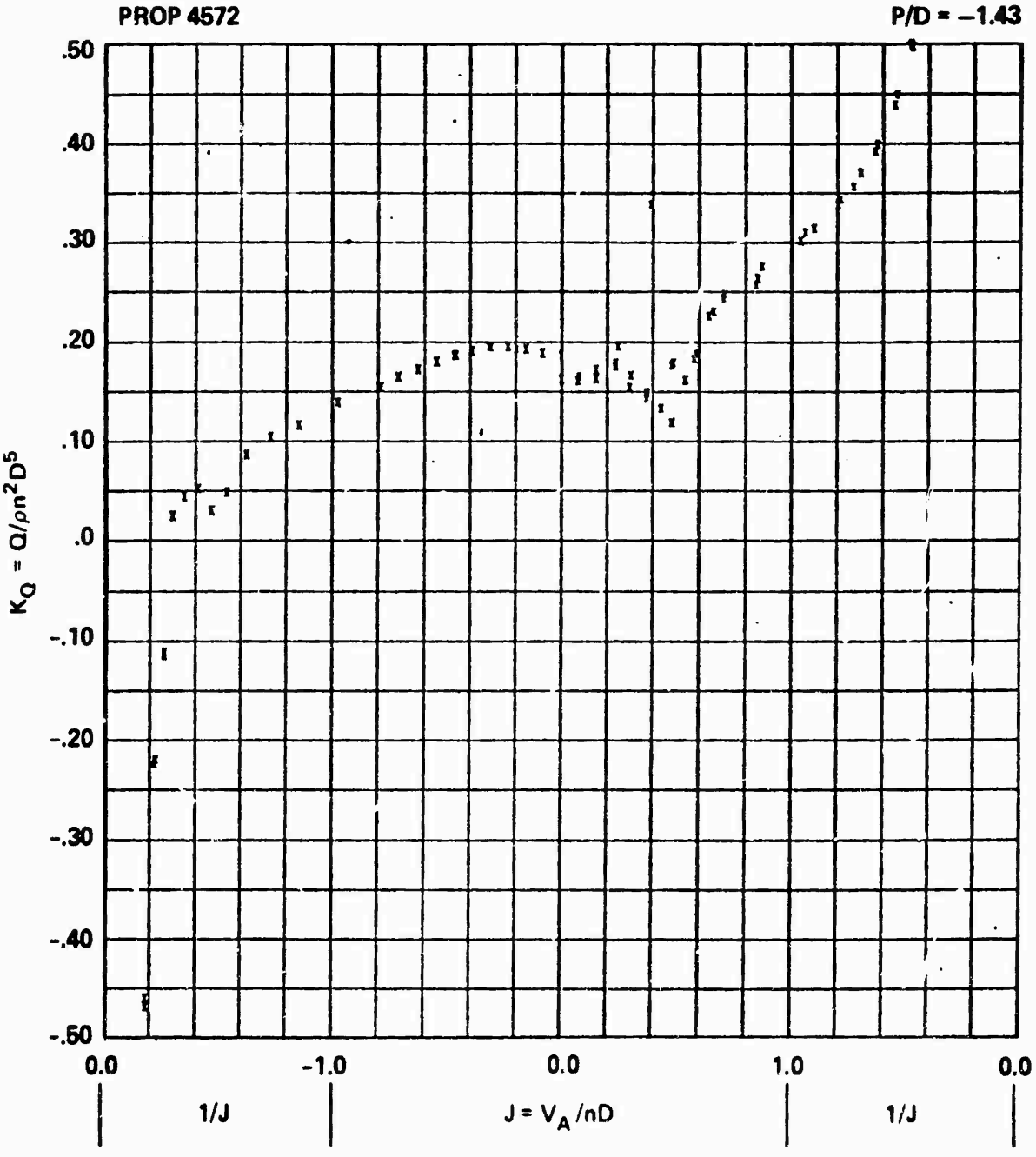

Figure 13g - At P/D = -1.43

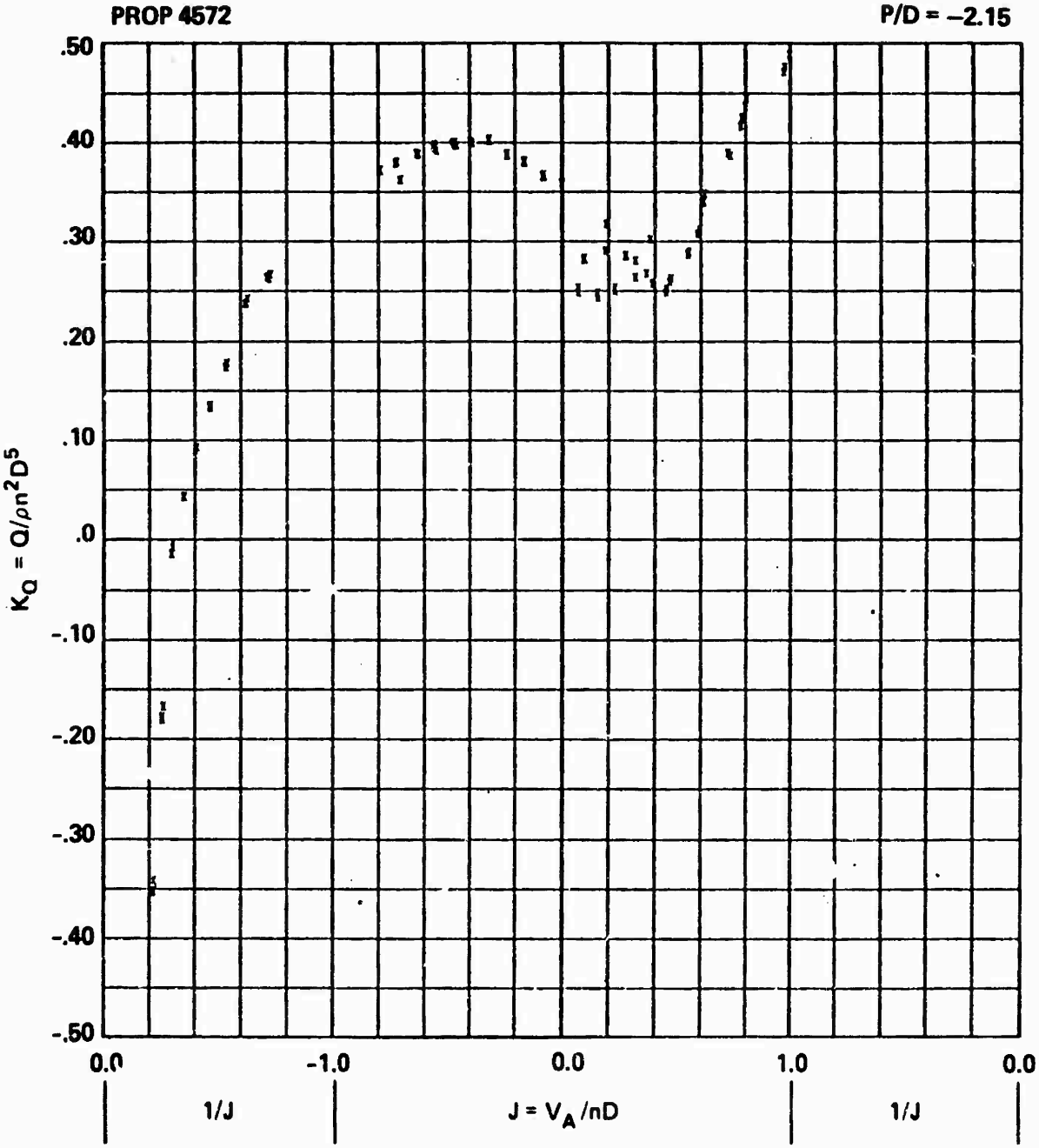

Figure 13h - At P/D = -2.15

Figure 14 - Variation of Thrust Index C_T^* with Advance Angle β^* for Propeller 4572

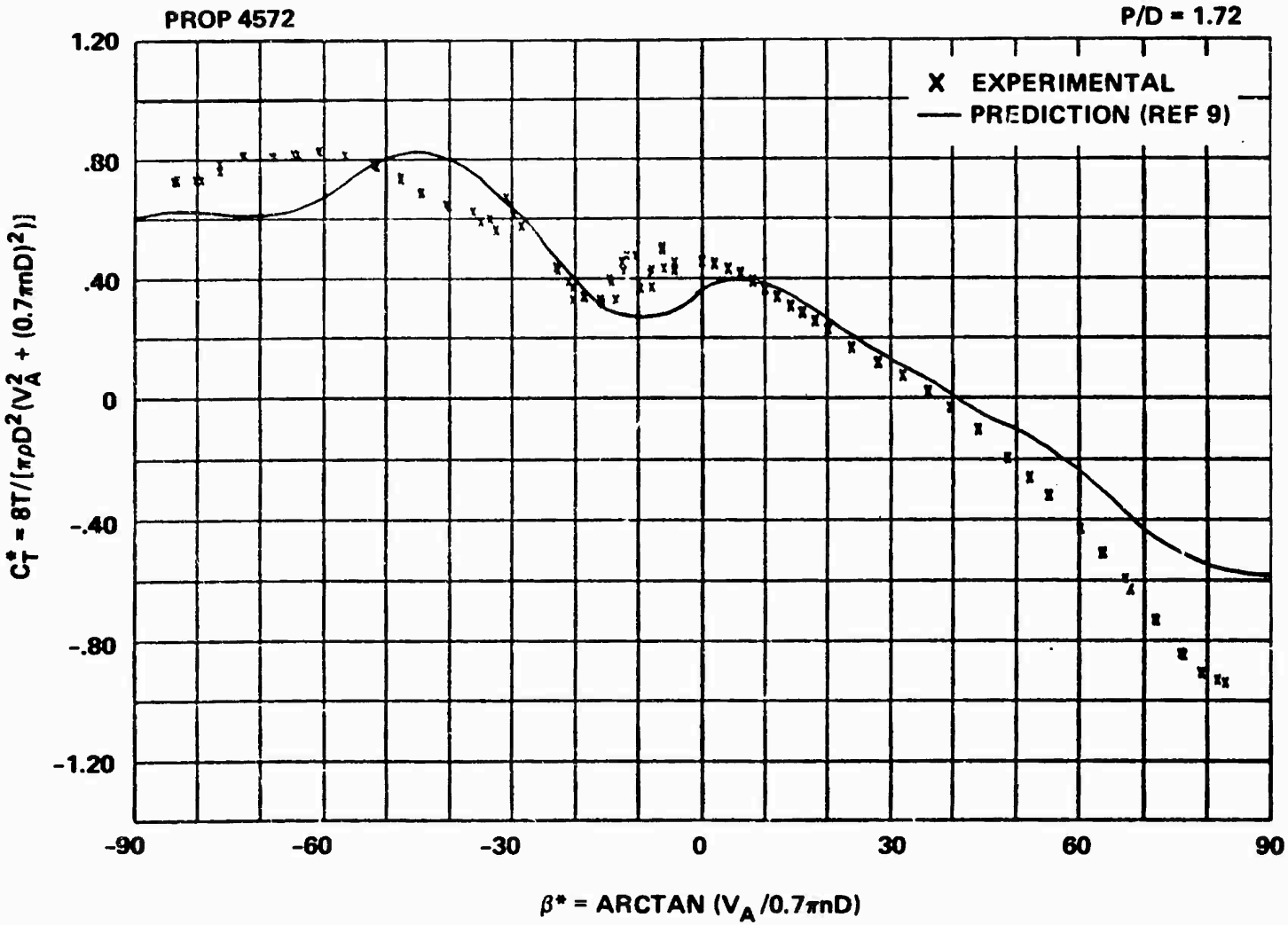

Figure 14a - At P/D = 1.72

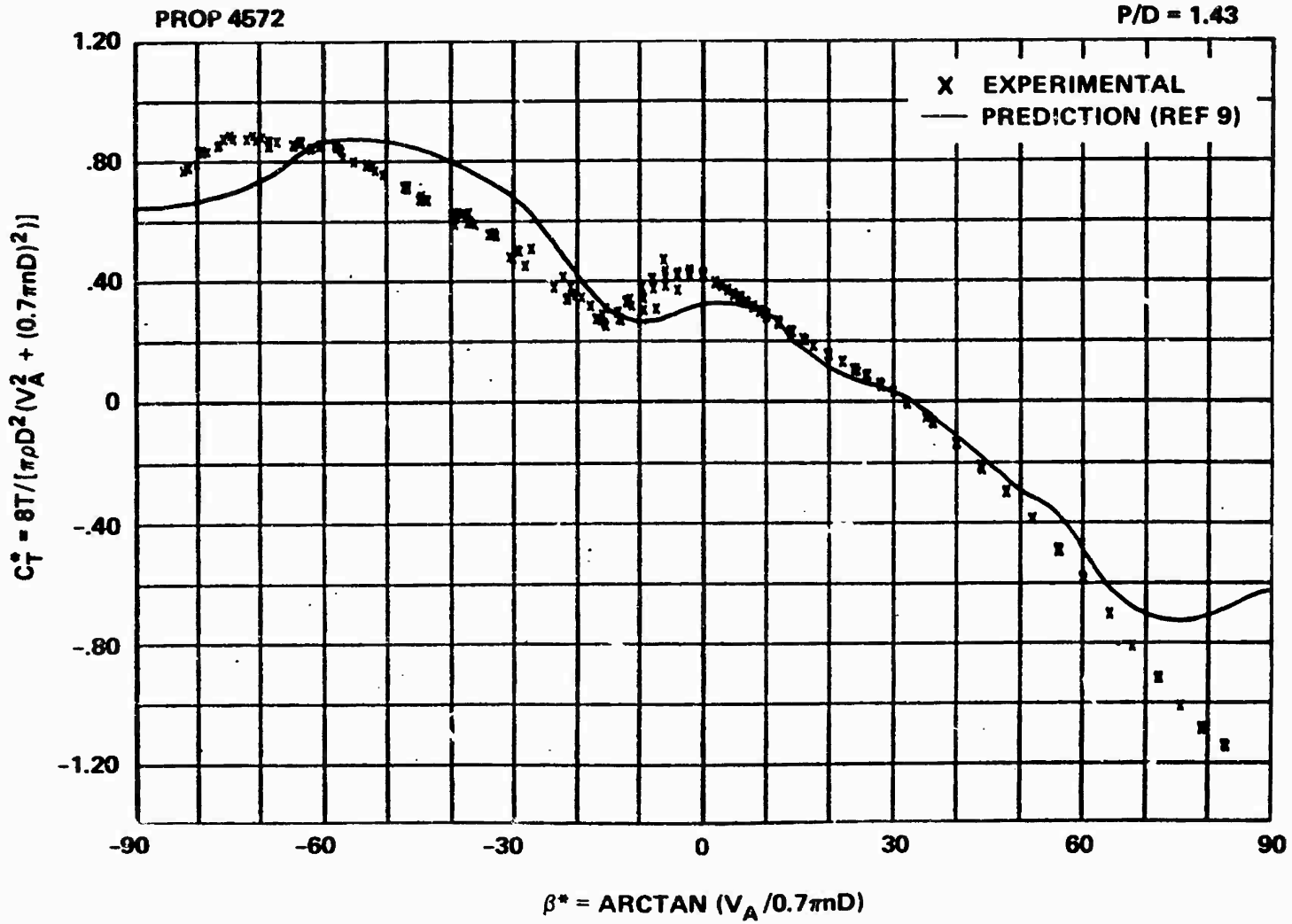

Figure 14b - At P/D = 1.43

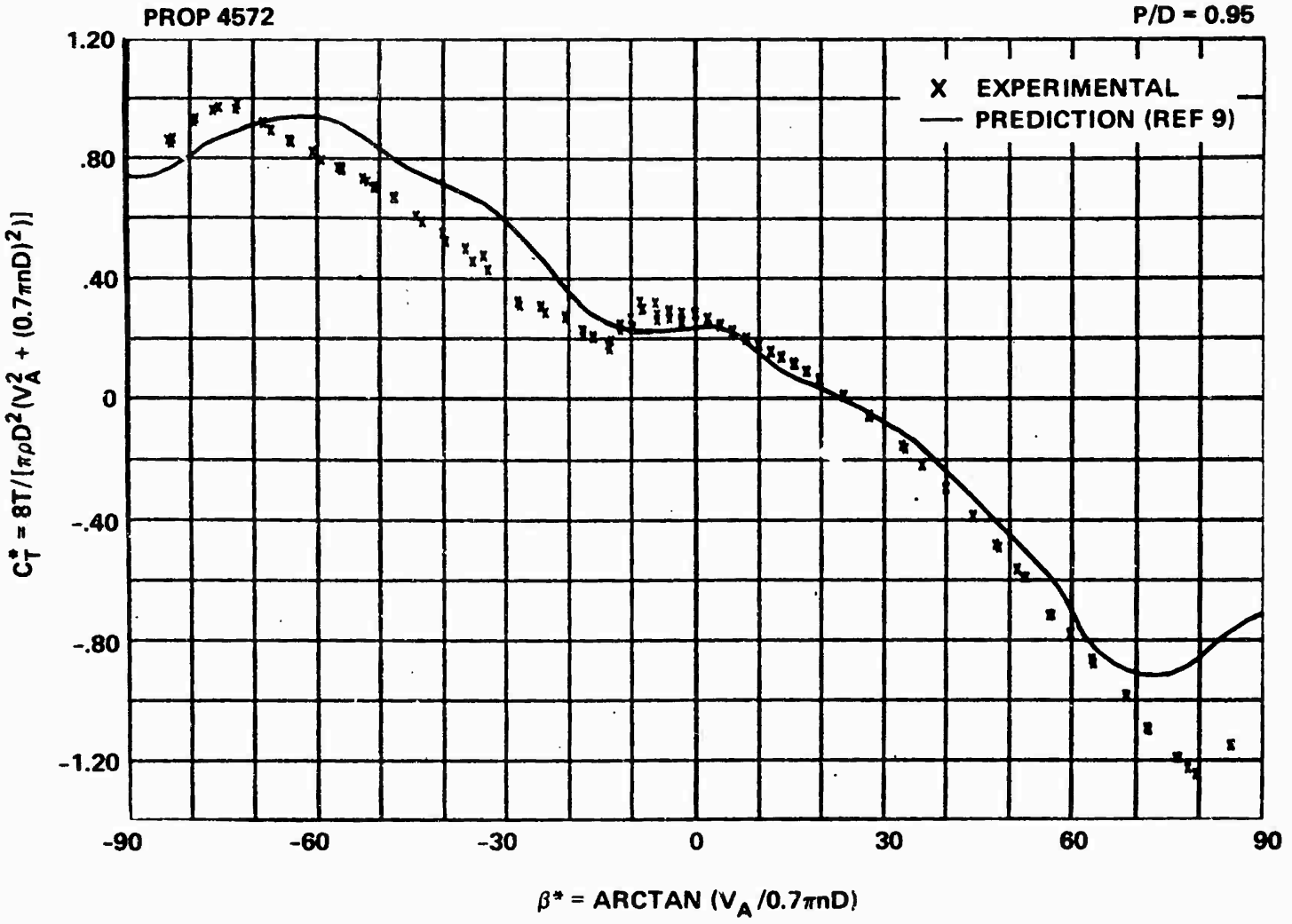

Figure 14c - At P/D = 0.95

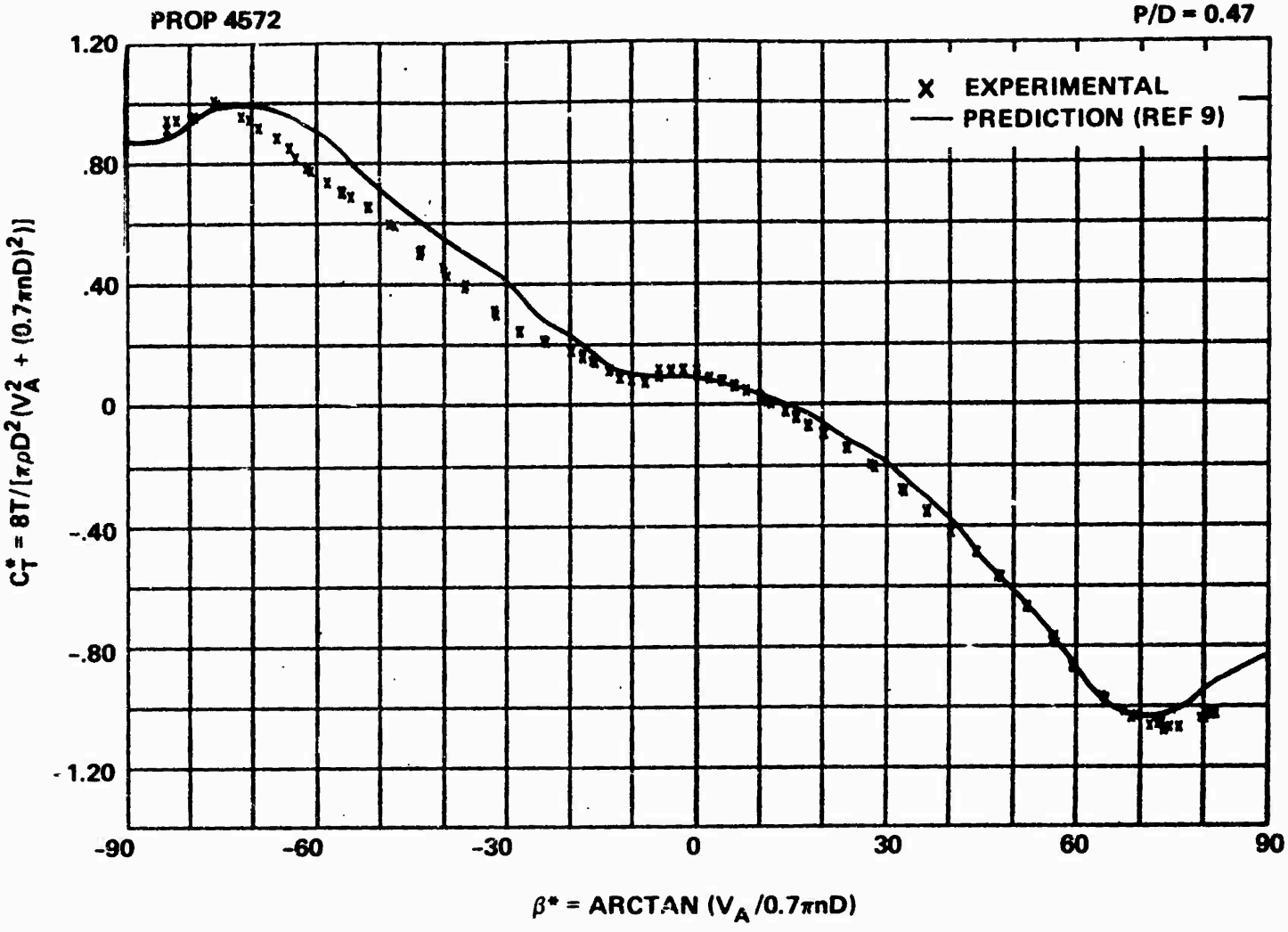

Figure 14d - At P/D = 0.47

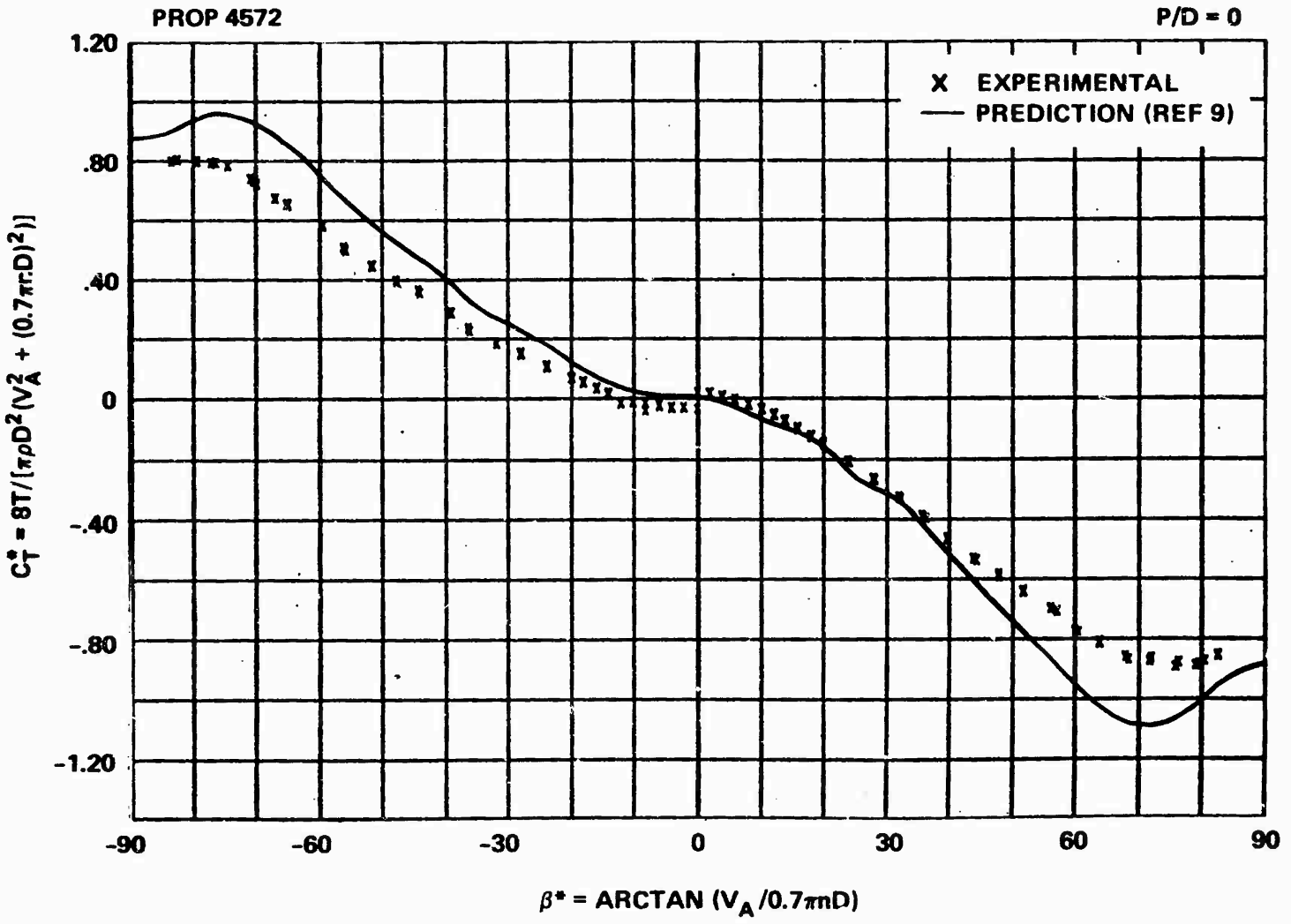

Figure 14e - At P/D = 0

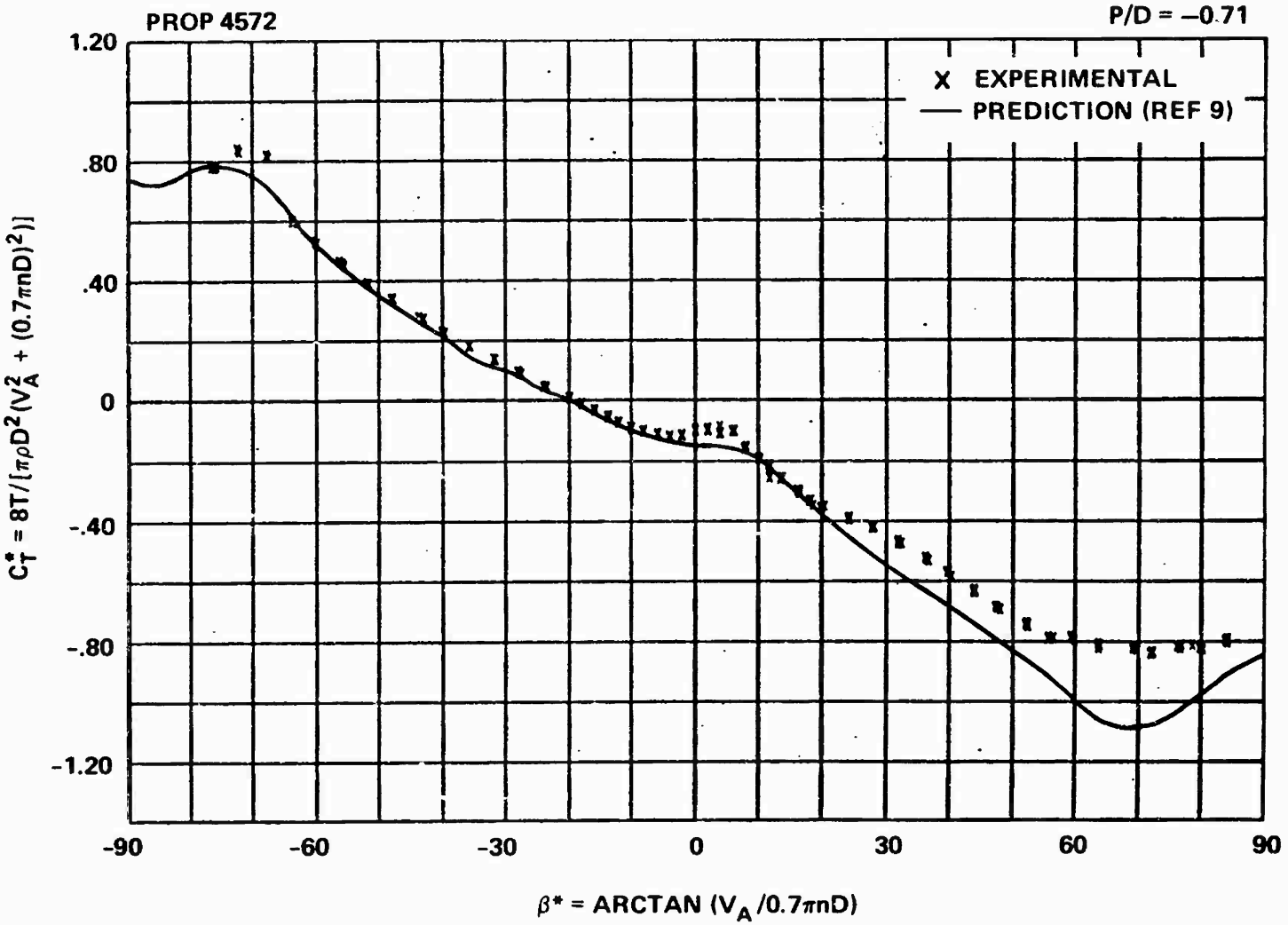

Figure 14f - At P/D = -0.71

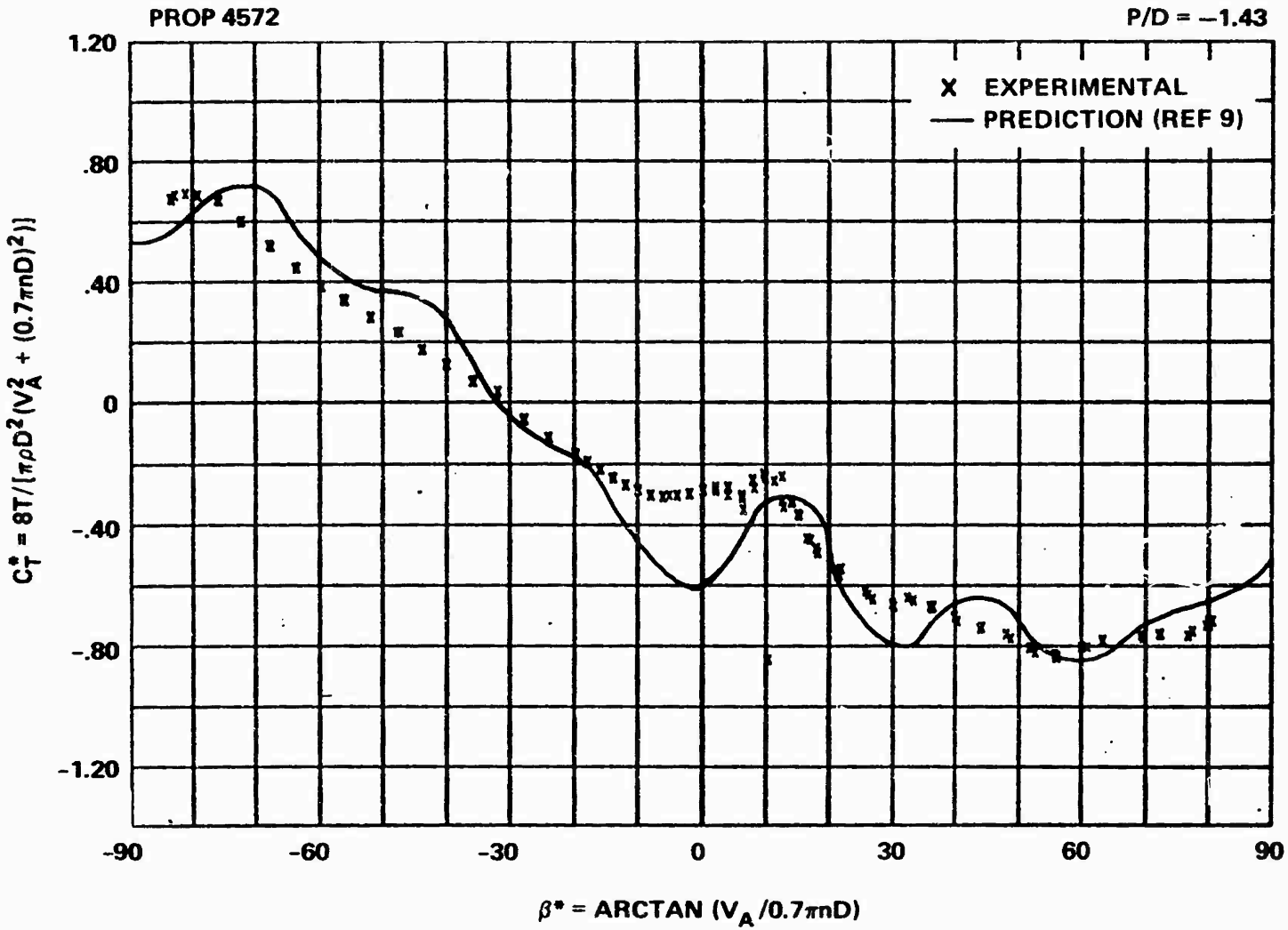

Figure 14g - At P/D = -1.43

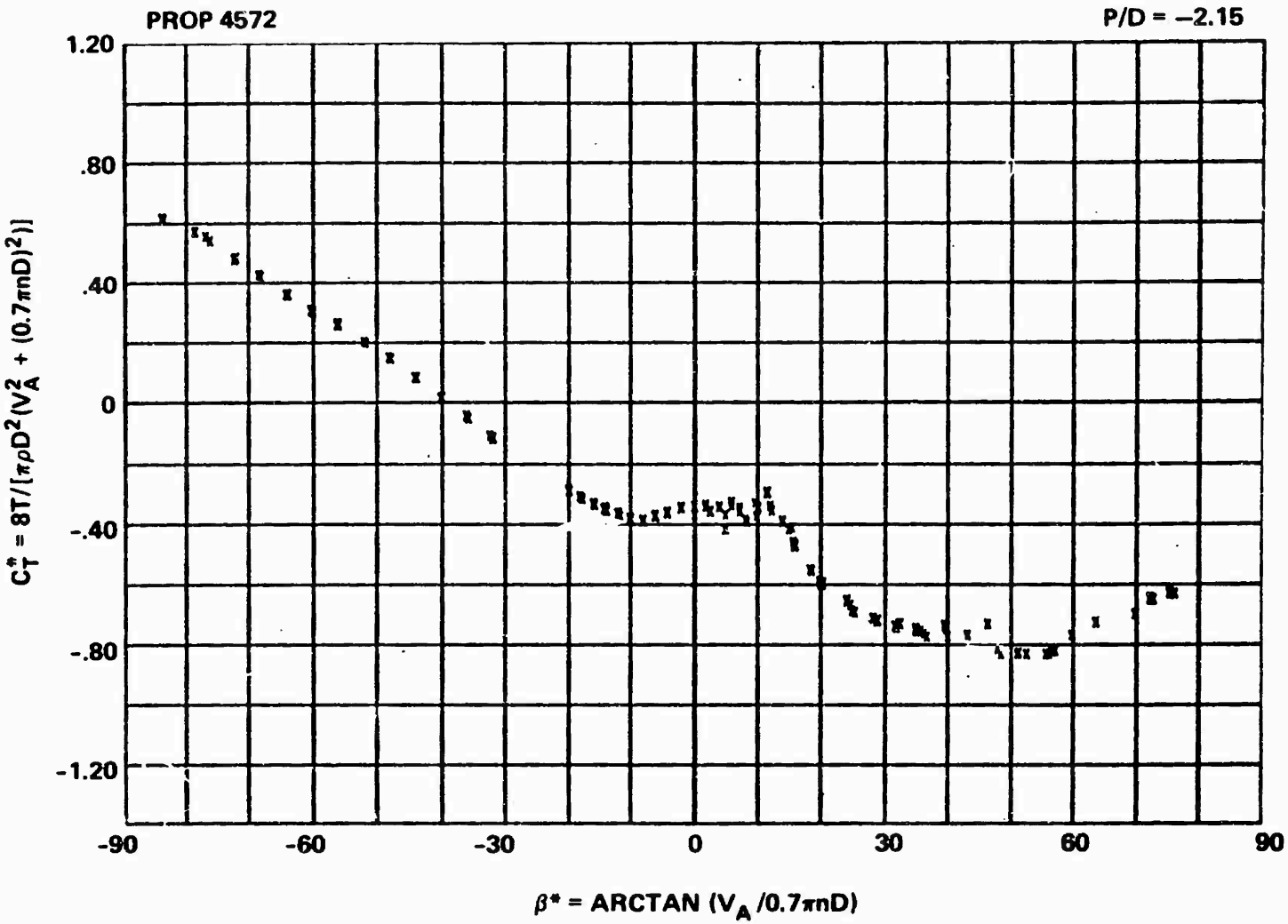

Figure 14h - At P/D = -2.15

Figure 15 - Variations of Torque Index C_Q^* with Advance Angle β^* for Propeller 4572

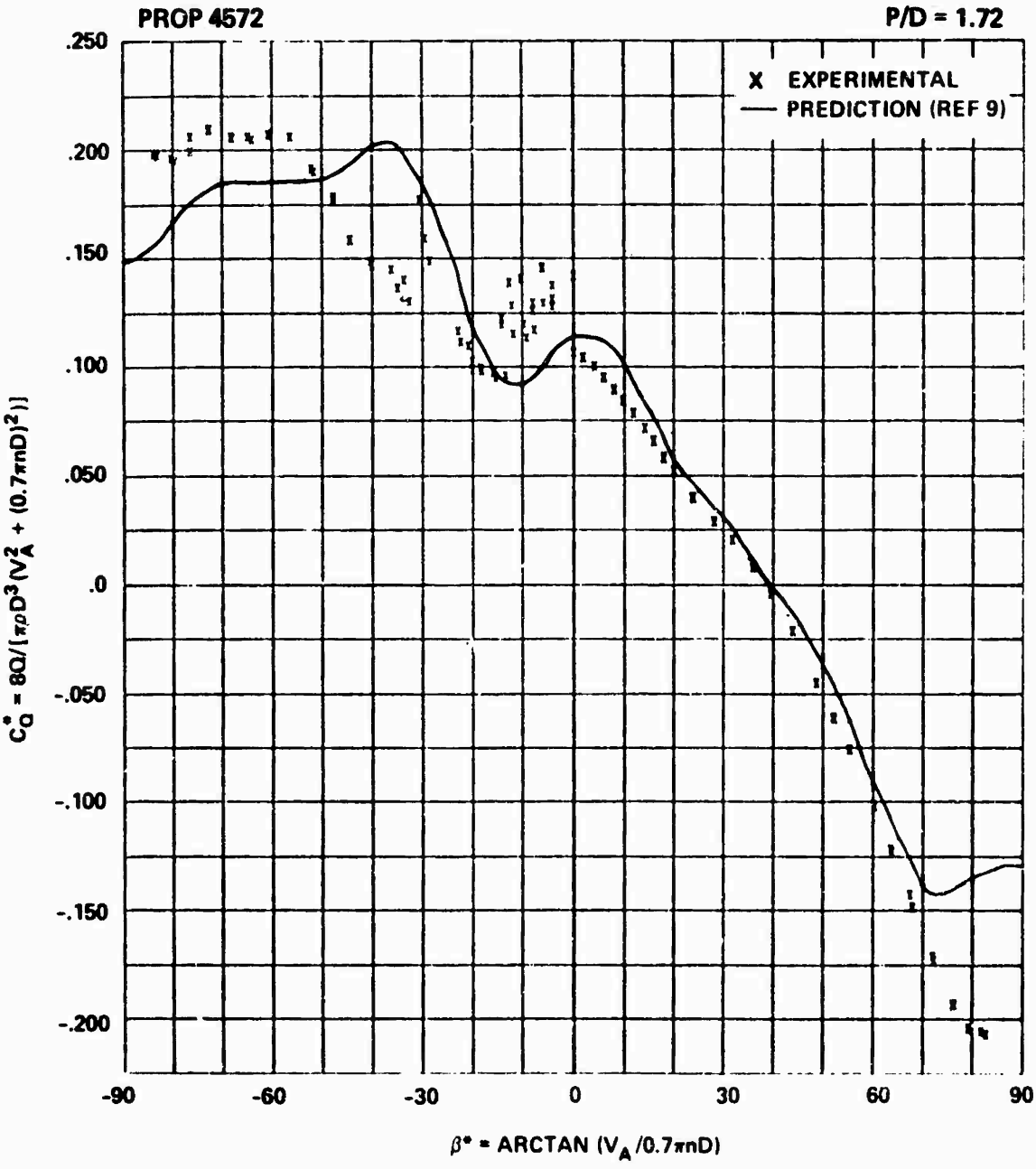

Figure 15a - At P/D = 1.72

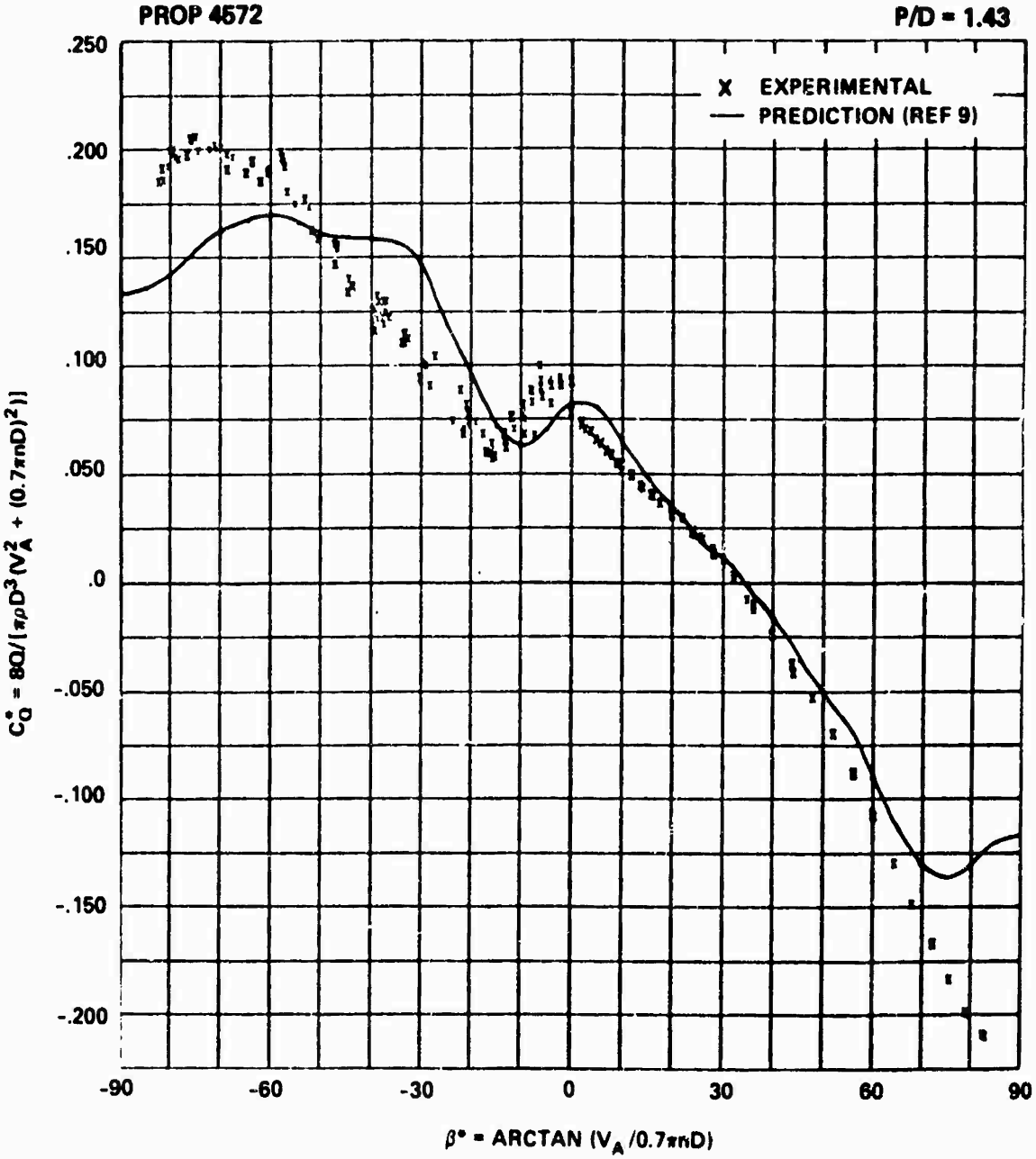

Figure 15b - At P/D = 1.43

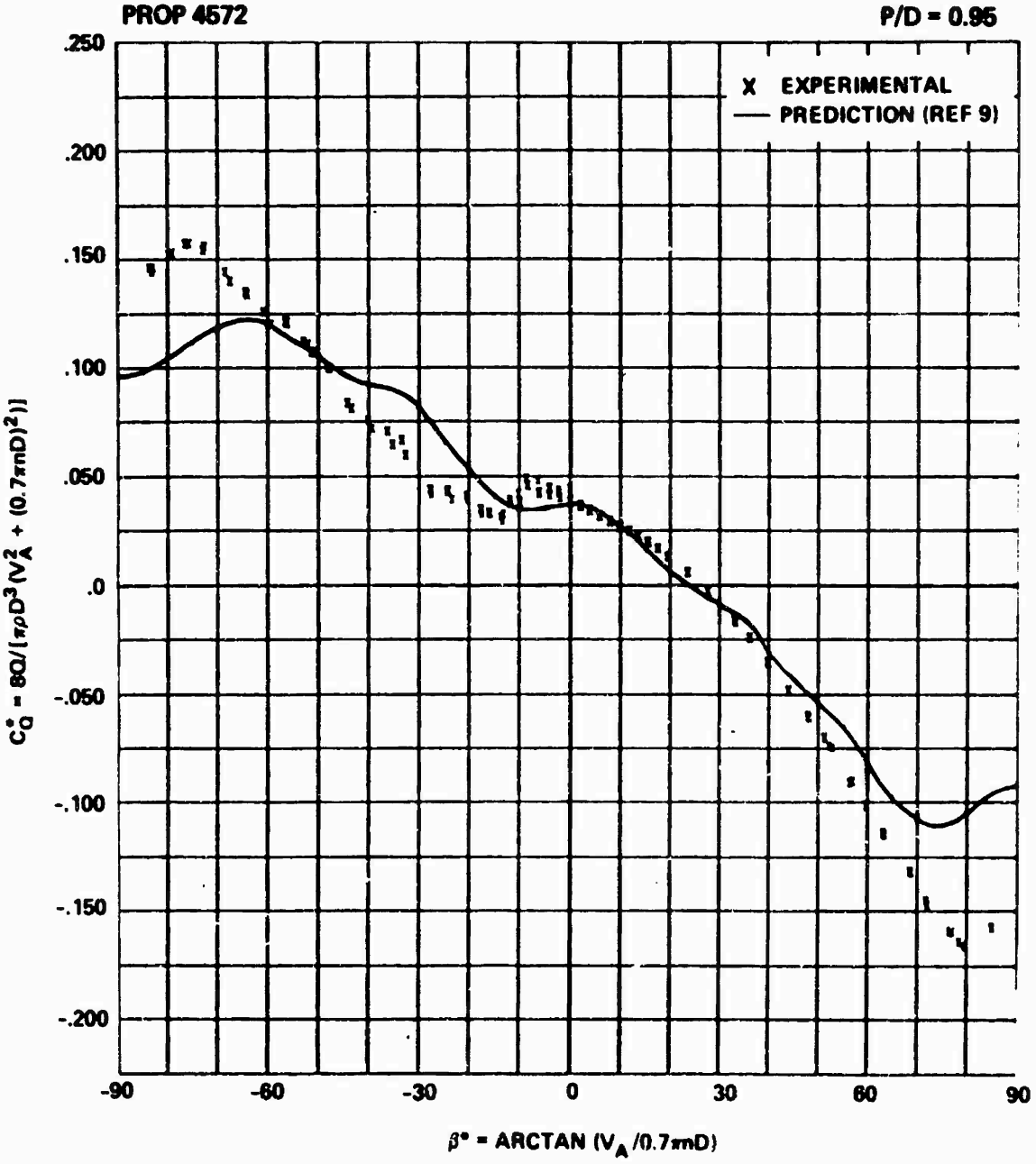

Figure 15c - At P/D = 0.95

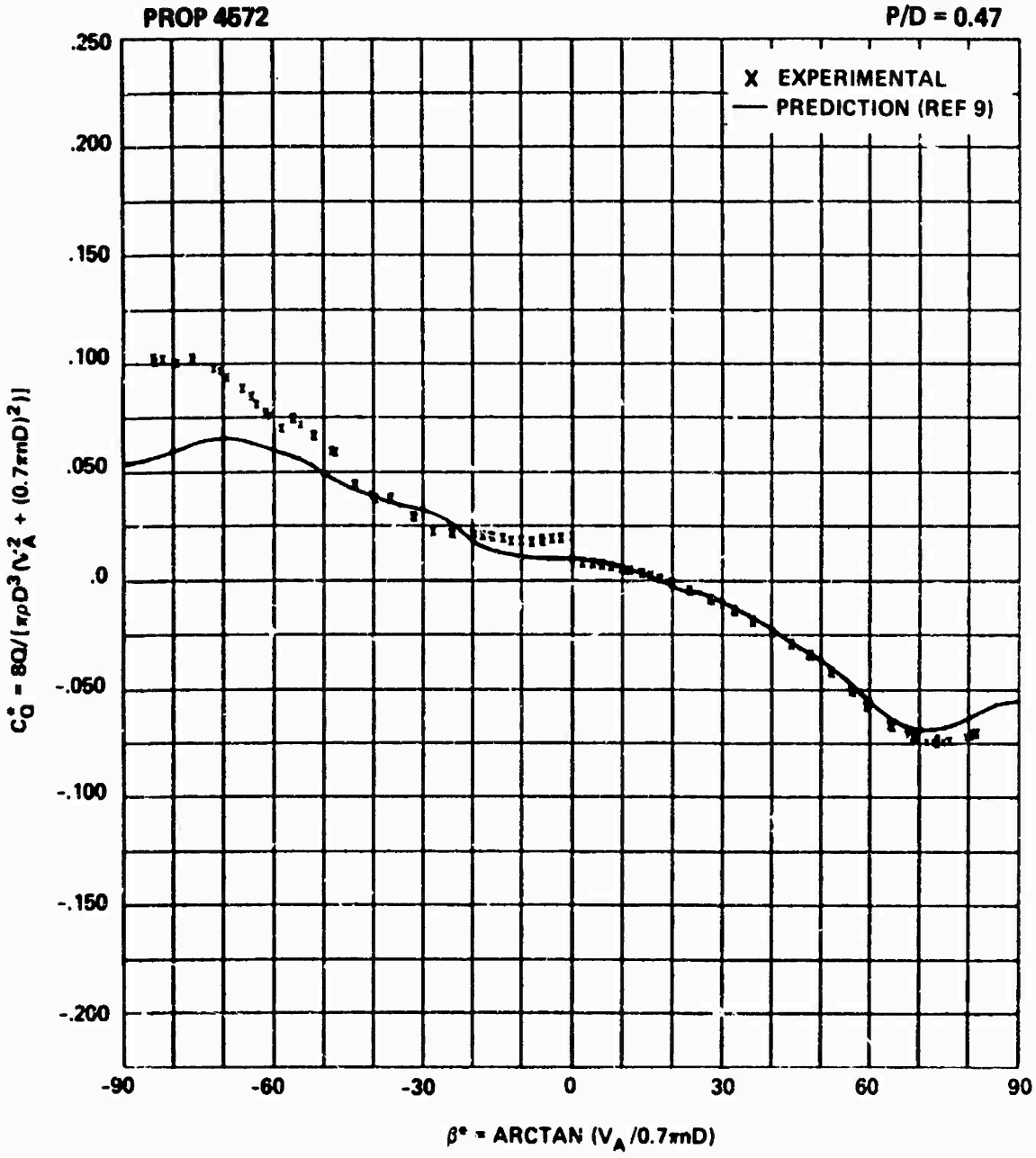

Figure 15d - At P/D = 0.47

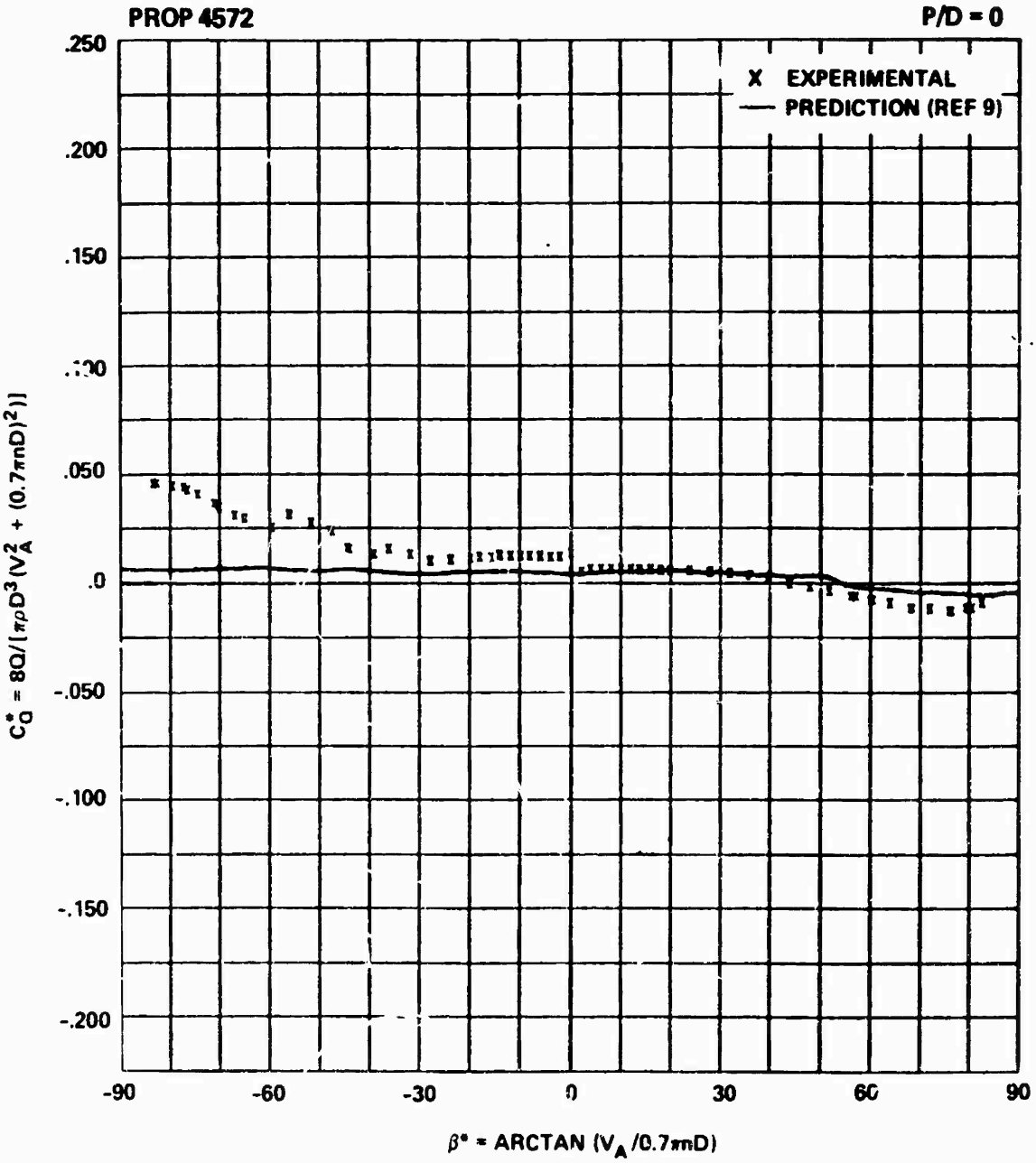

Figure 15e - At P/D = 0

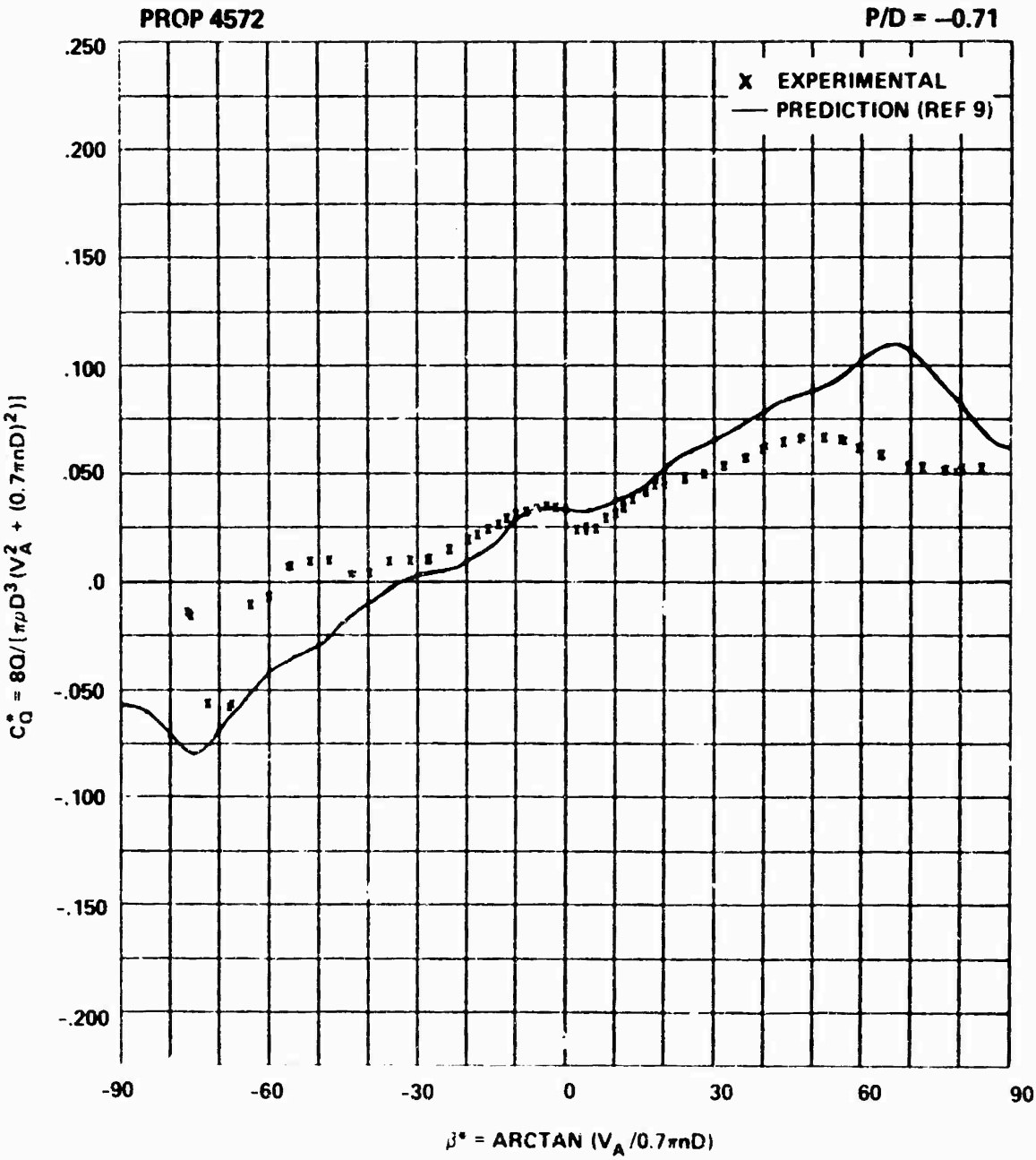

Figure 15f - At P/D = -0.71

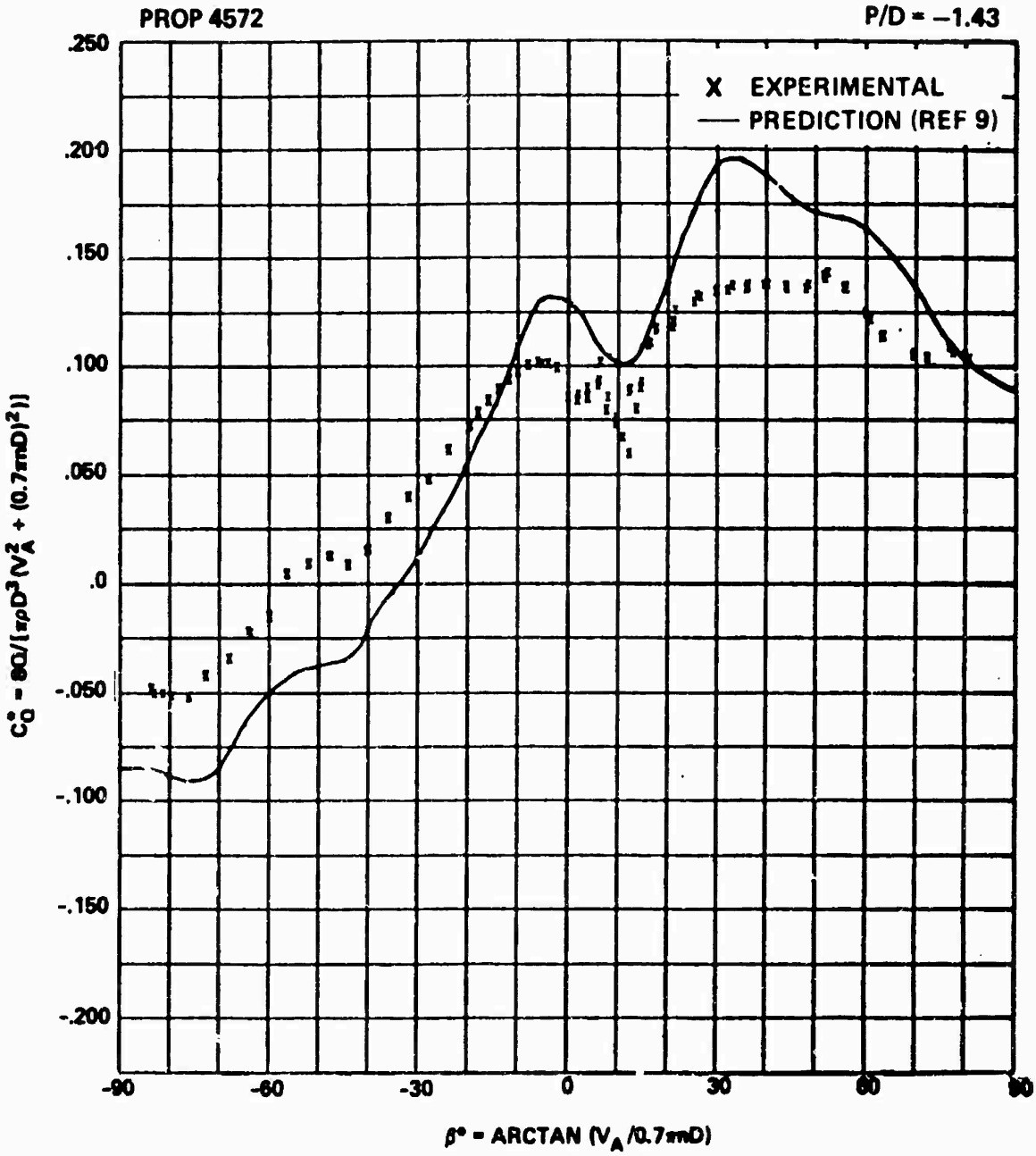

Figure 15g - At P/D = -1.43

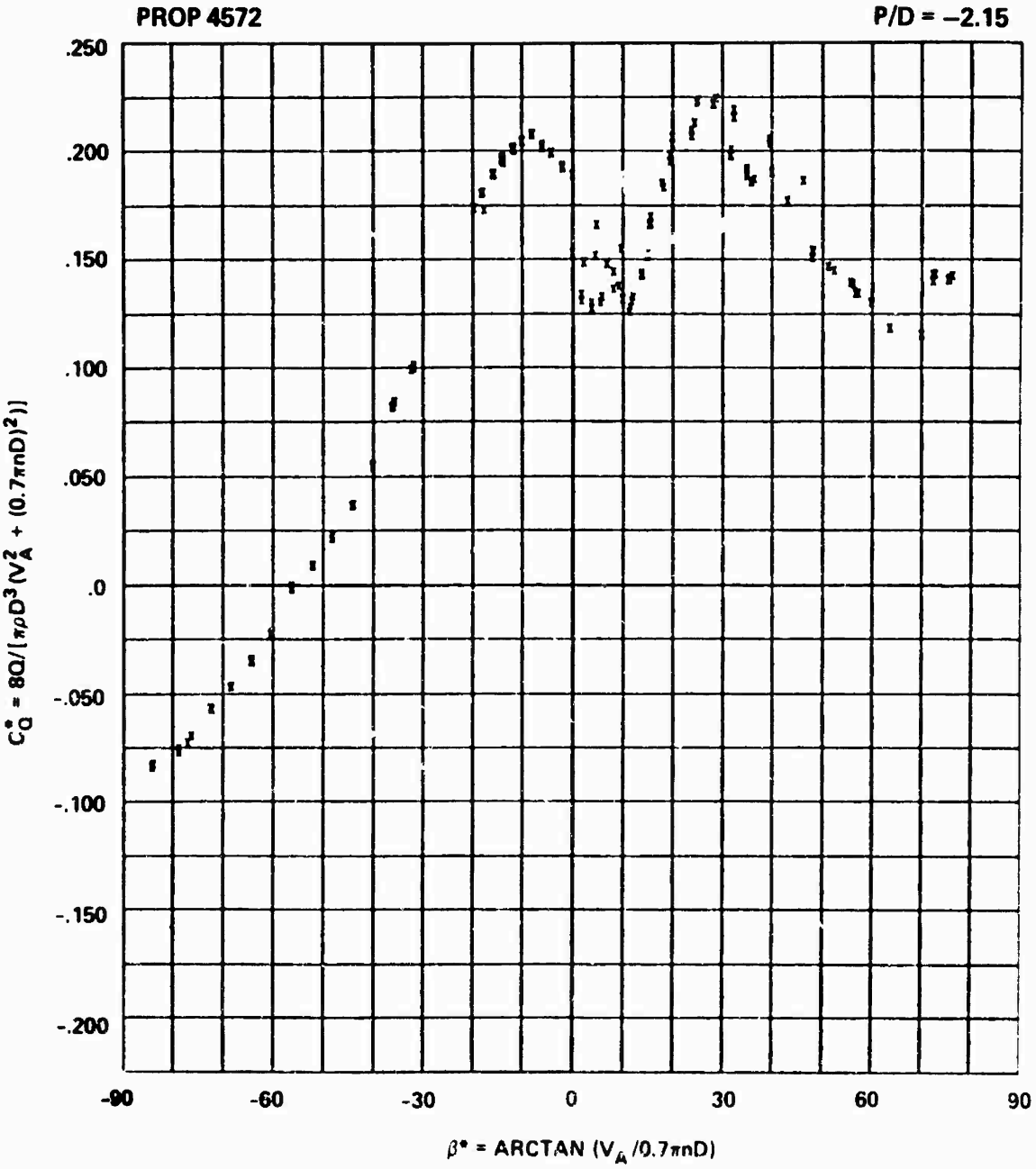

Figure 15h - At P/D = -2.15

Figure 16 - Variation of Thrust Coefficient K_T with Advance Coefficient J for Propeller 4575

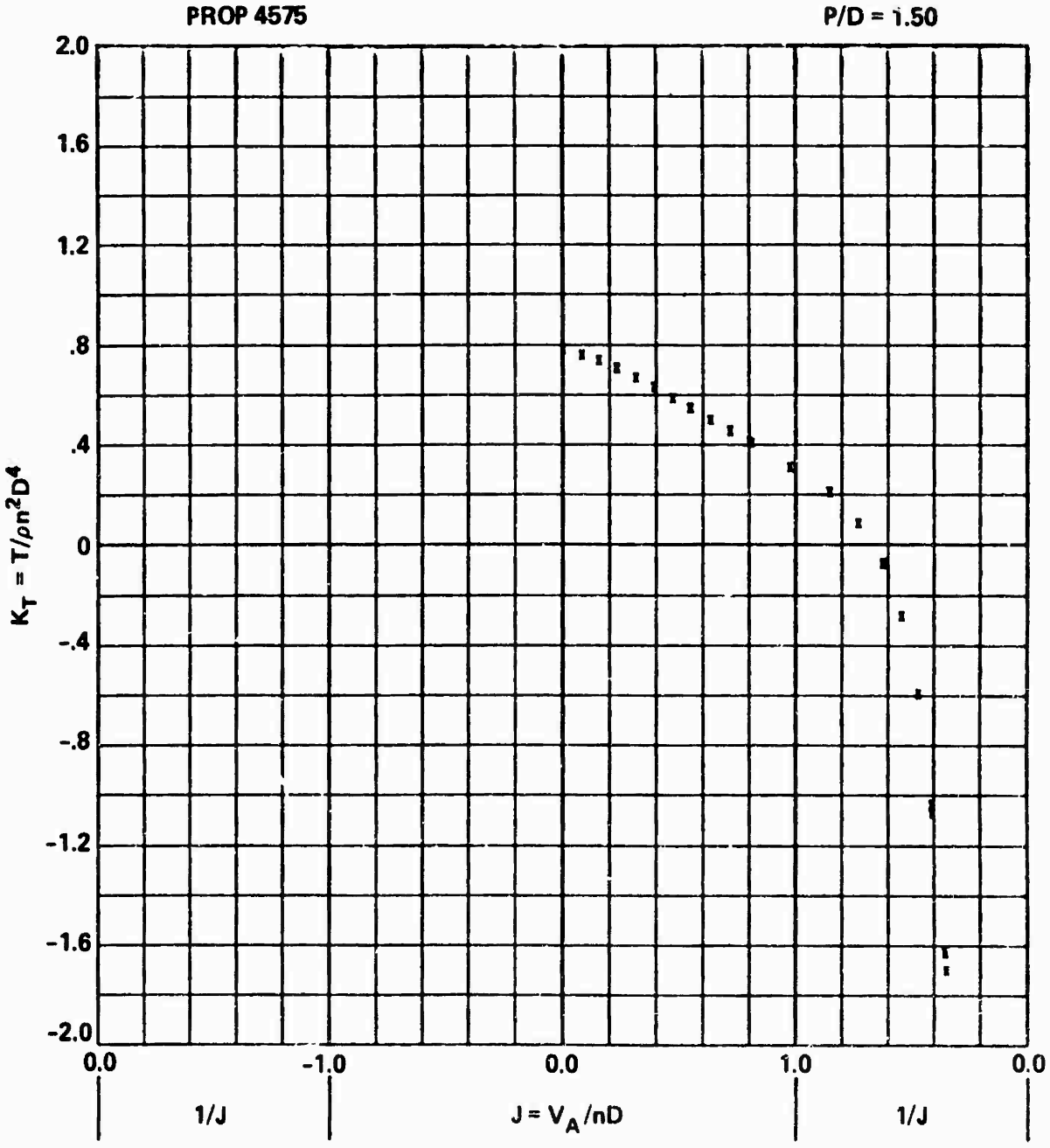

Figure 16a - At P/D = 1.50

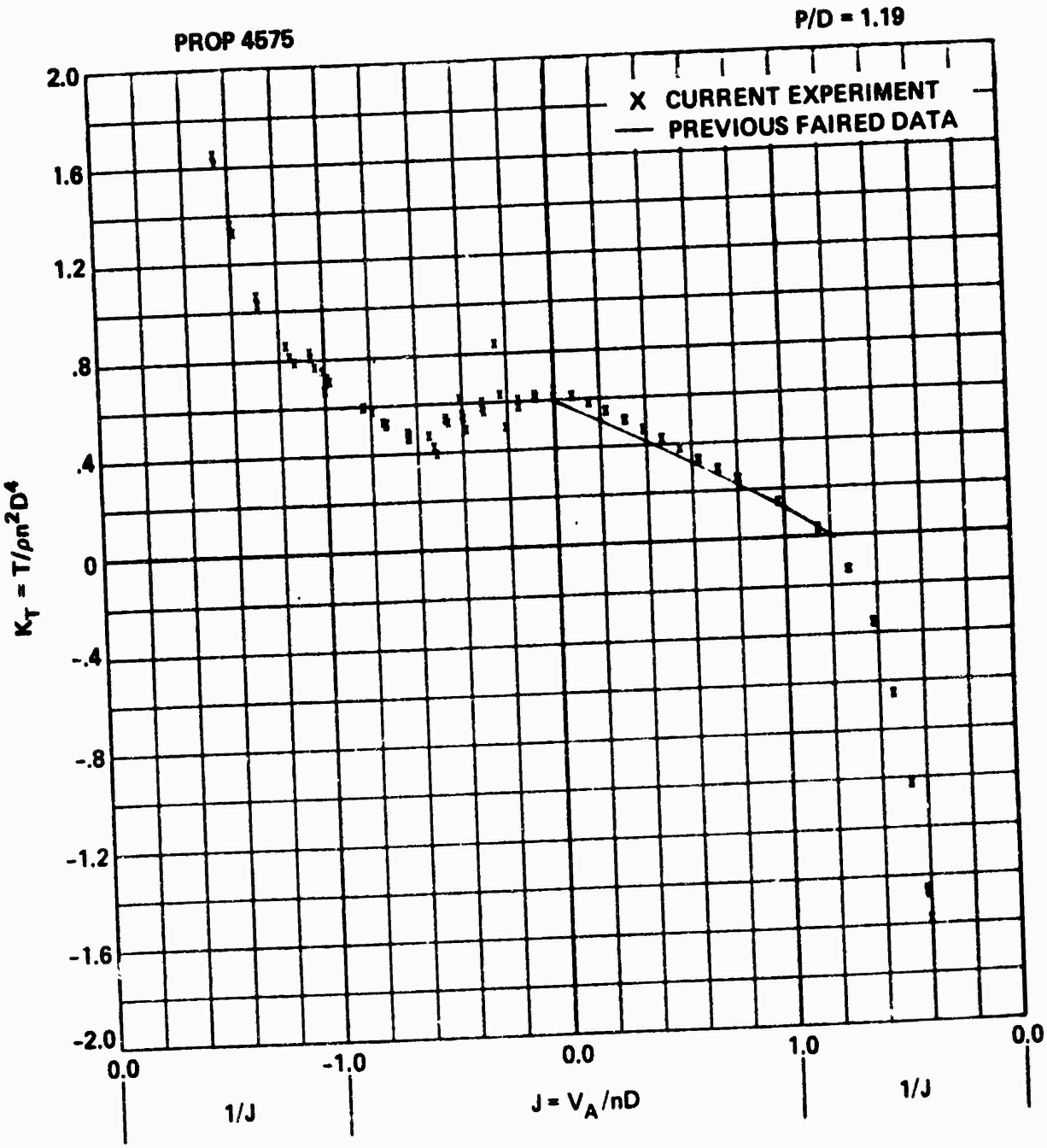

Figure 16b - At P/D = 1.19

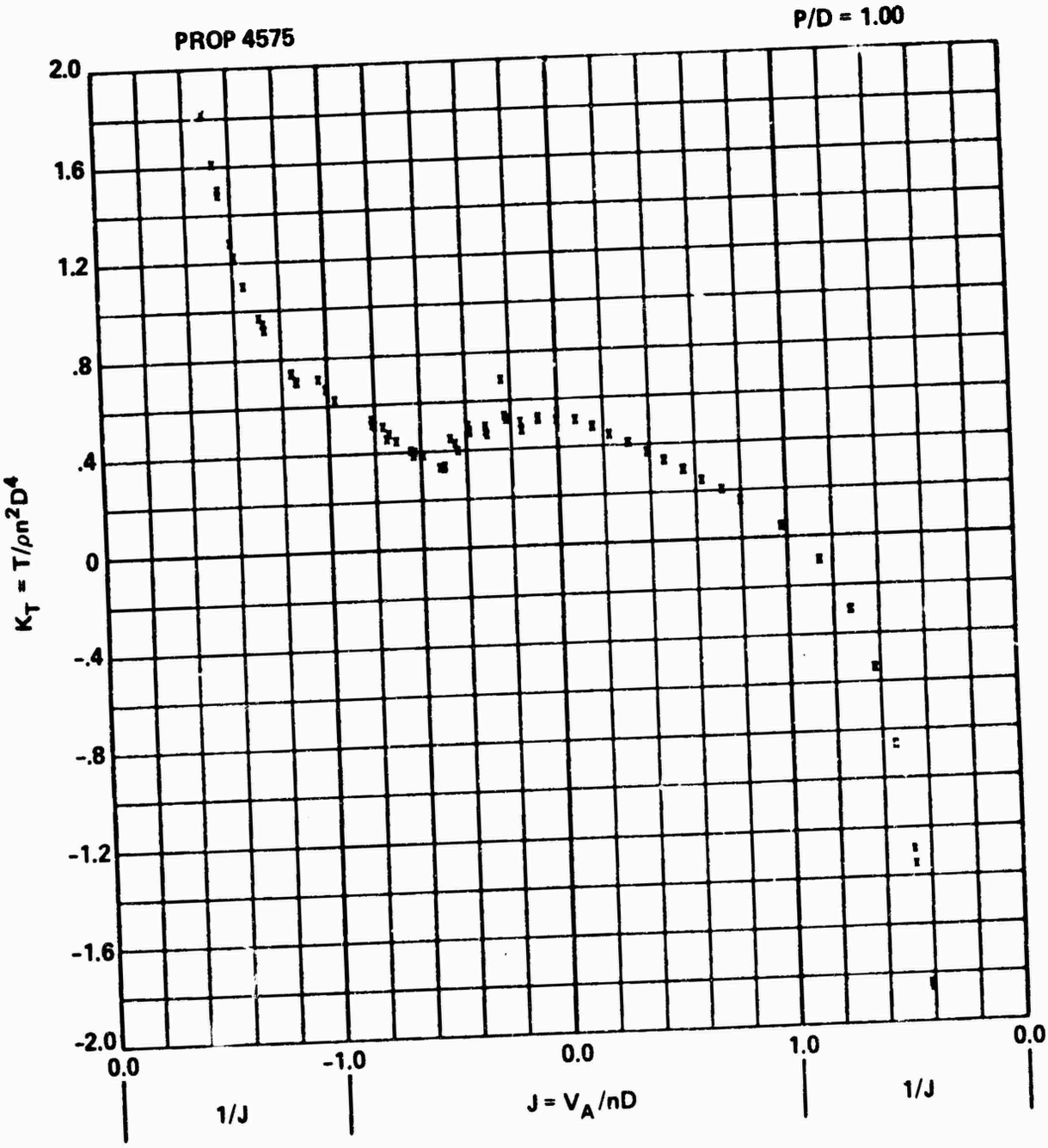

Figure 16c - At P/D = 1.00

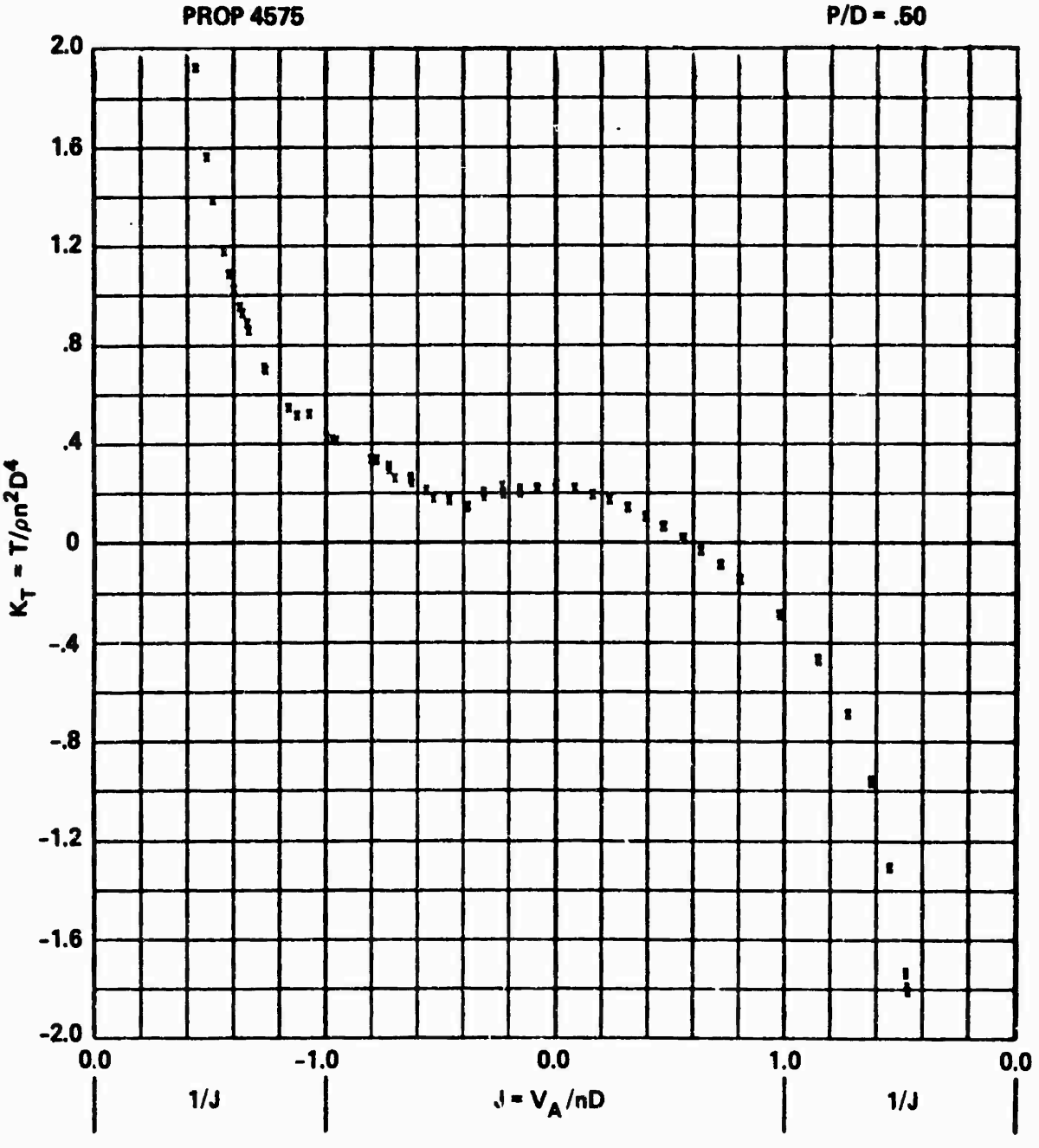

Figure 16d - At P/D = 0.50

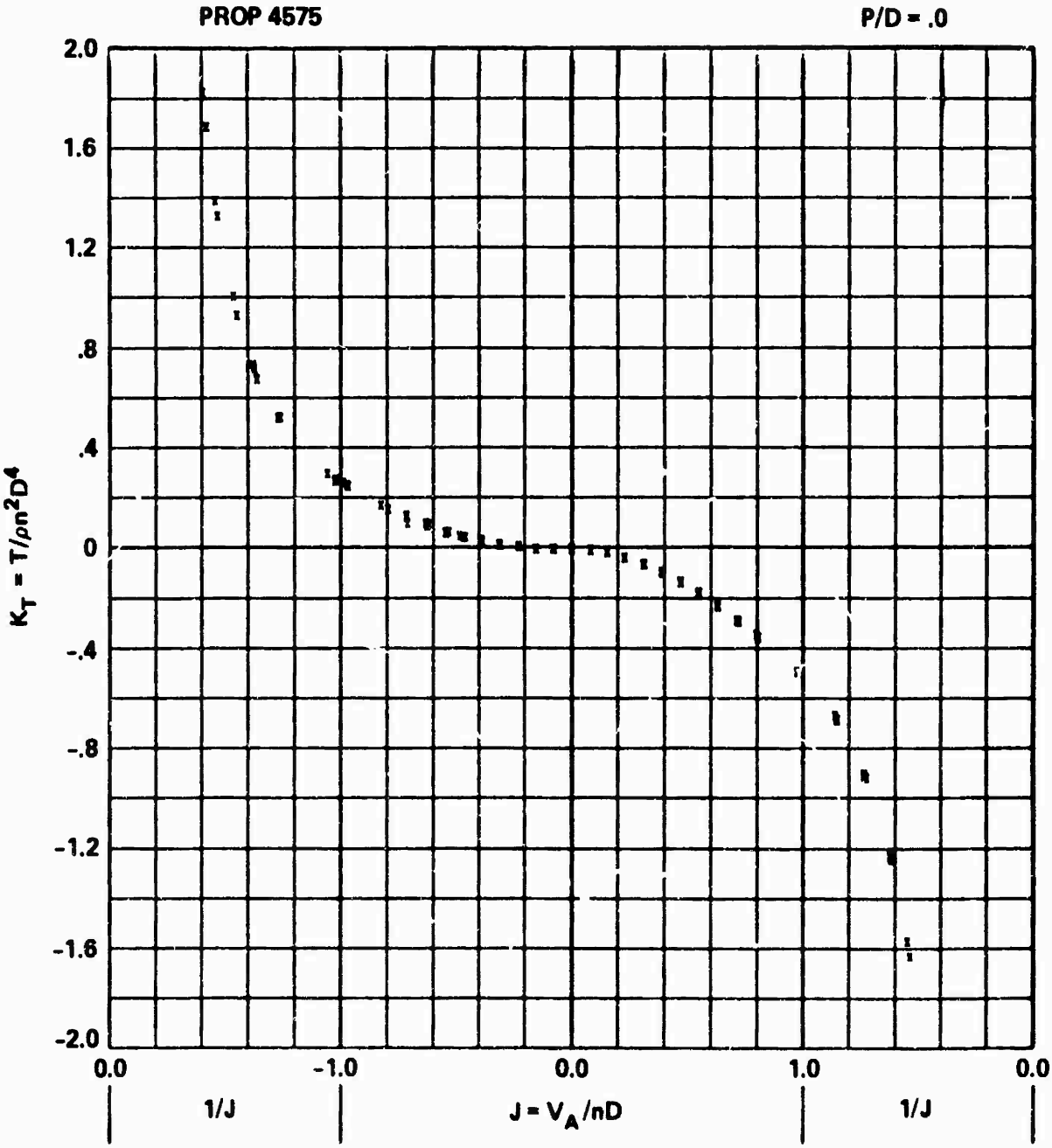

Figure 16e - At P/D = 0

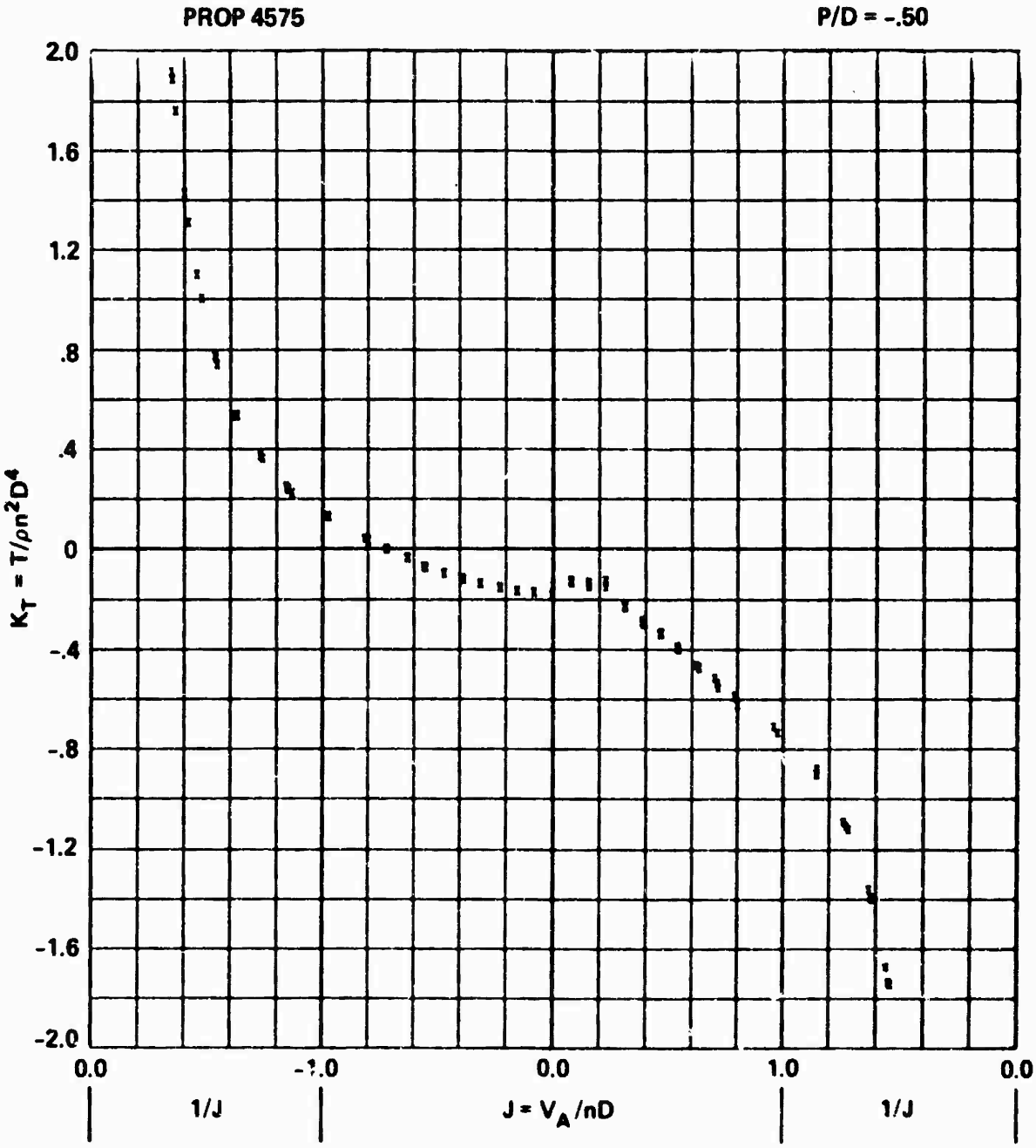

Figure 16f - At P/D = -0.50

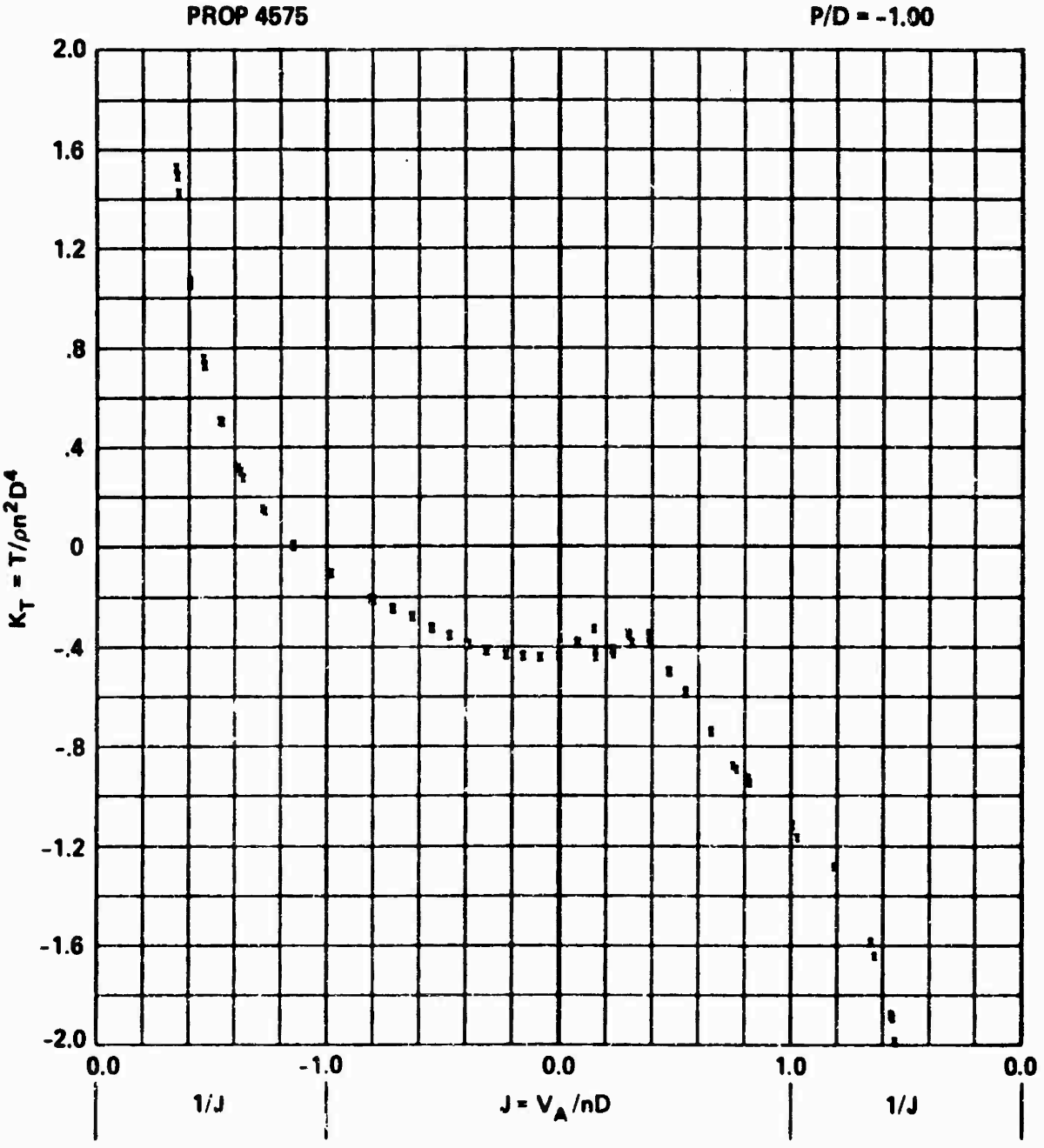

Figure 10g - At P/D = -1.00

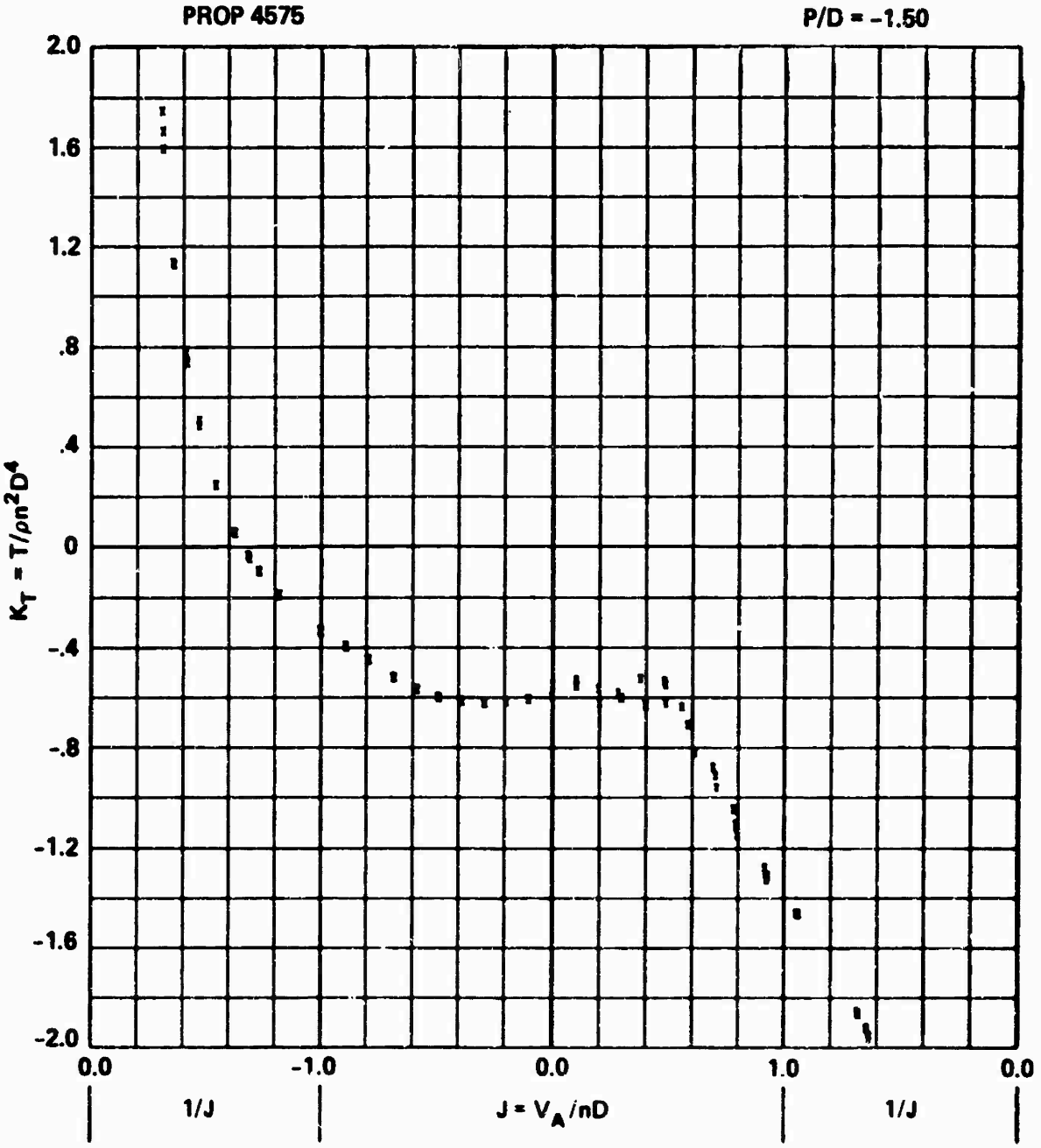

Figure 16h - At P/D = -1.50

Figure 17 - Variation of Torque Coefficient K_Q with Advance Coefficient J for Propeller 4575

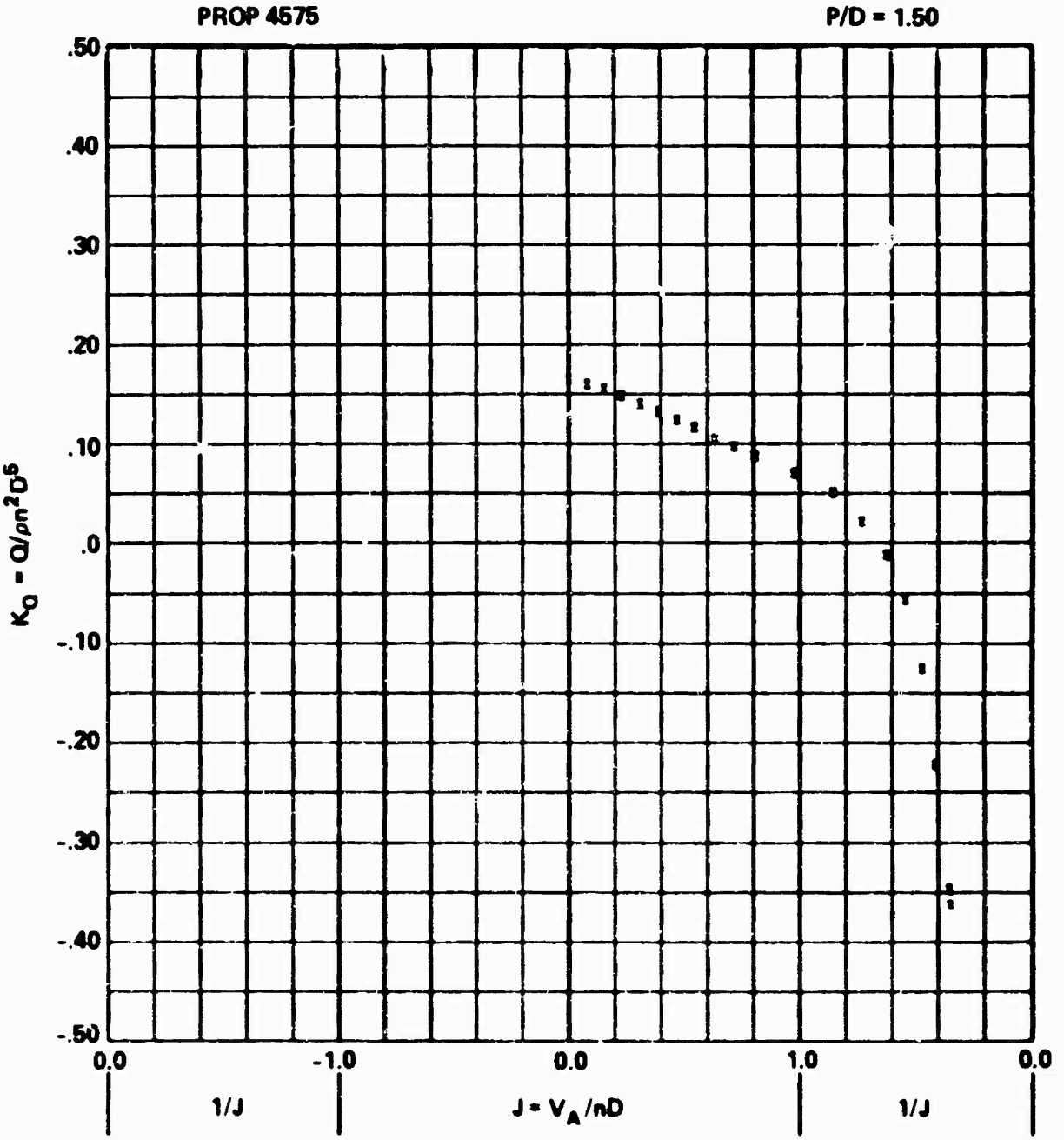

Figure 17a - At P/D = 1.50

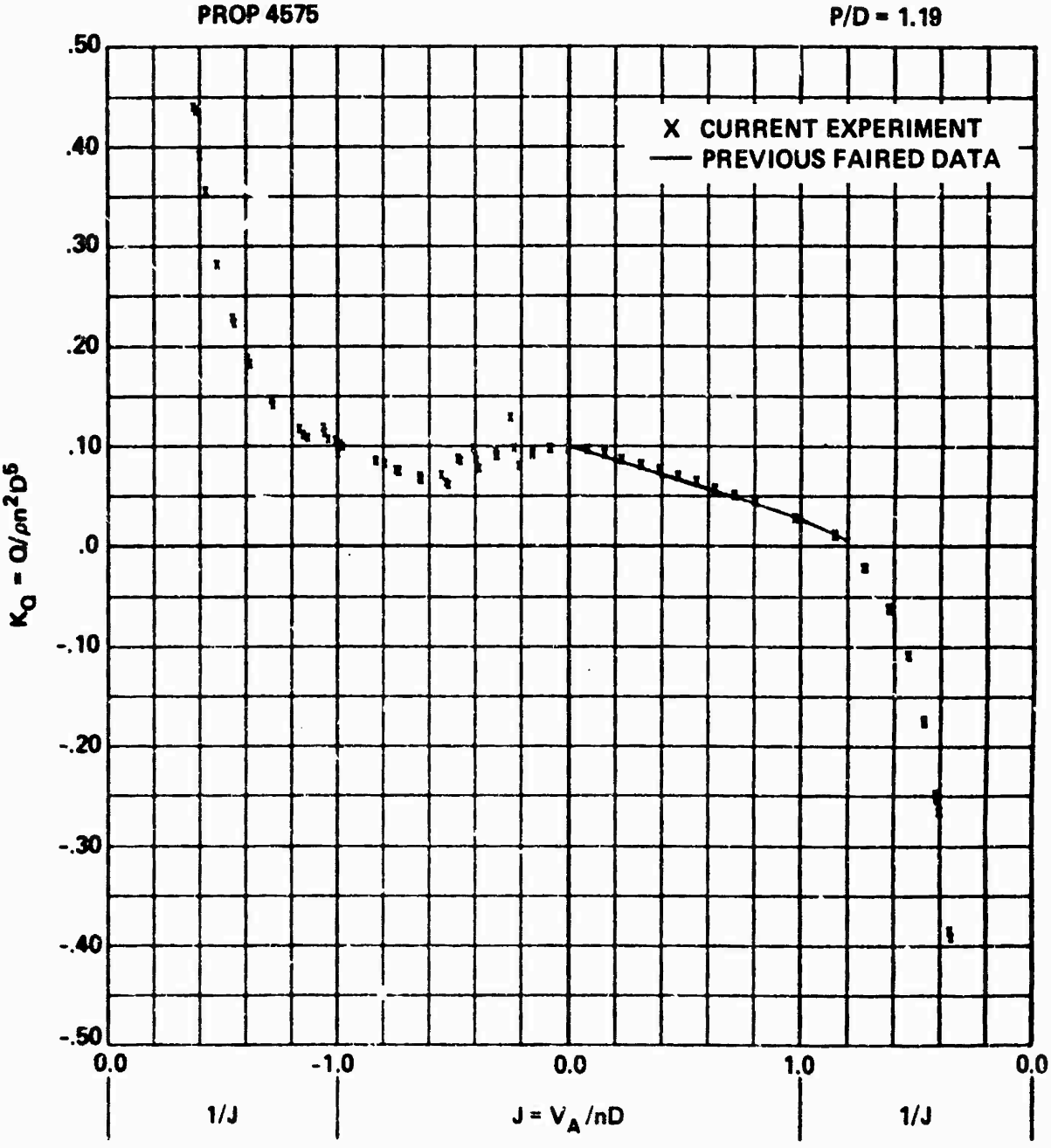

Figure 17b - At P/D = 1.19

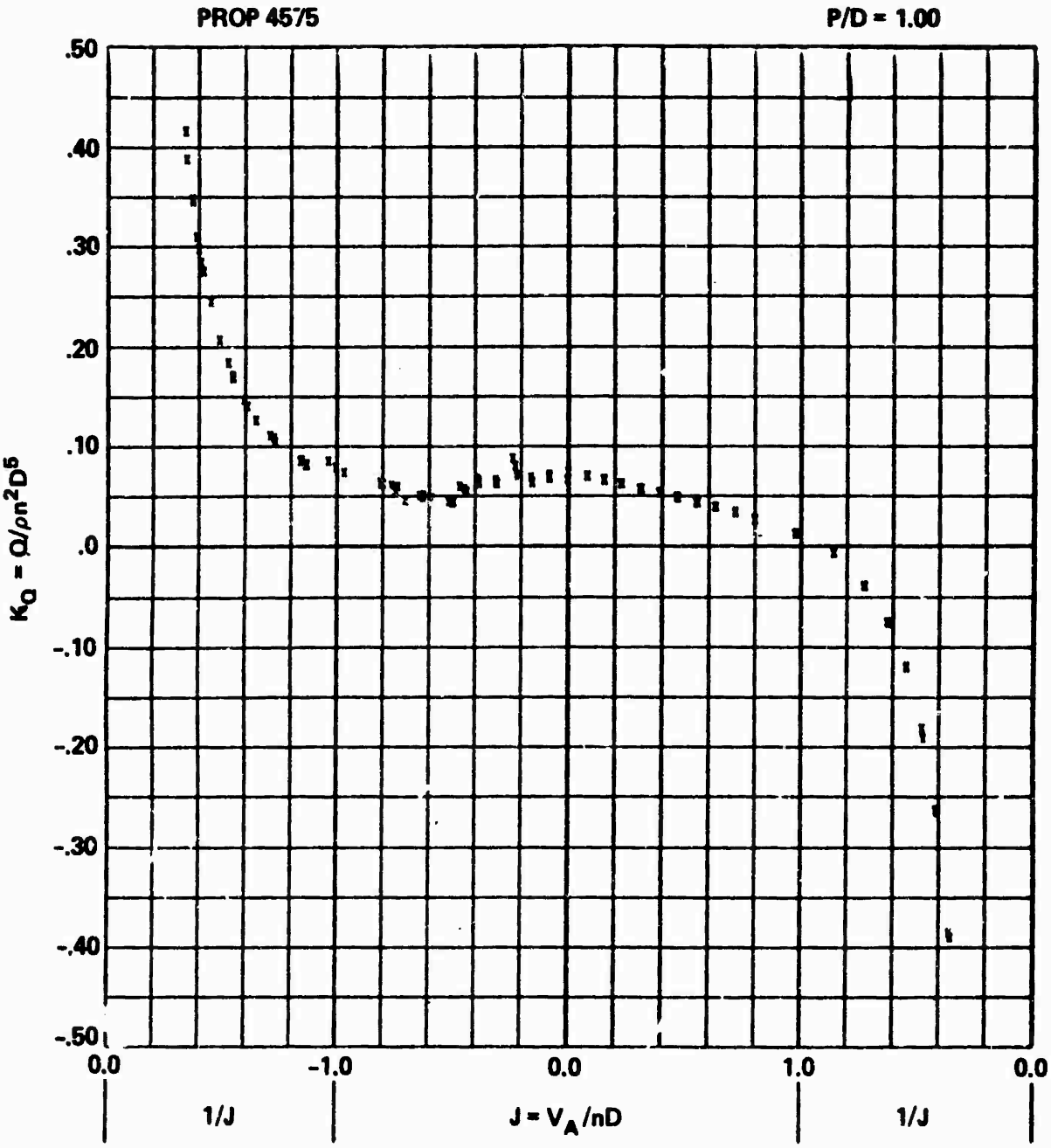

Figure 17c - At P/D = 1.00

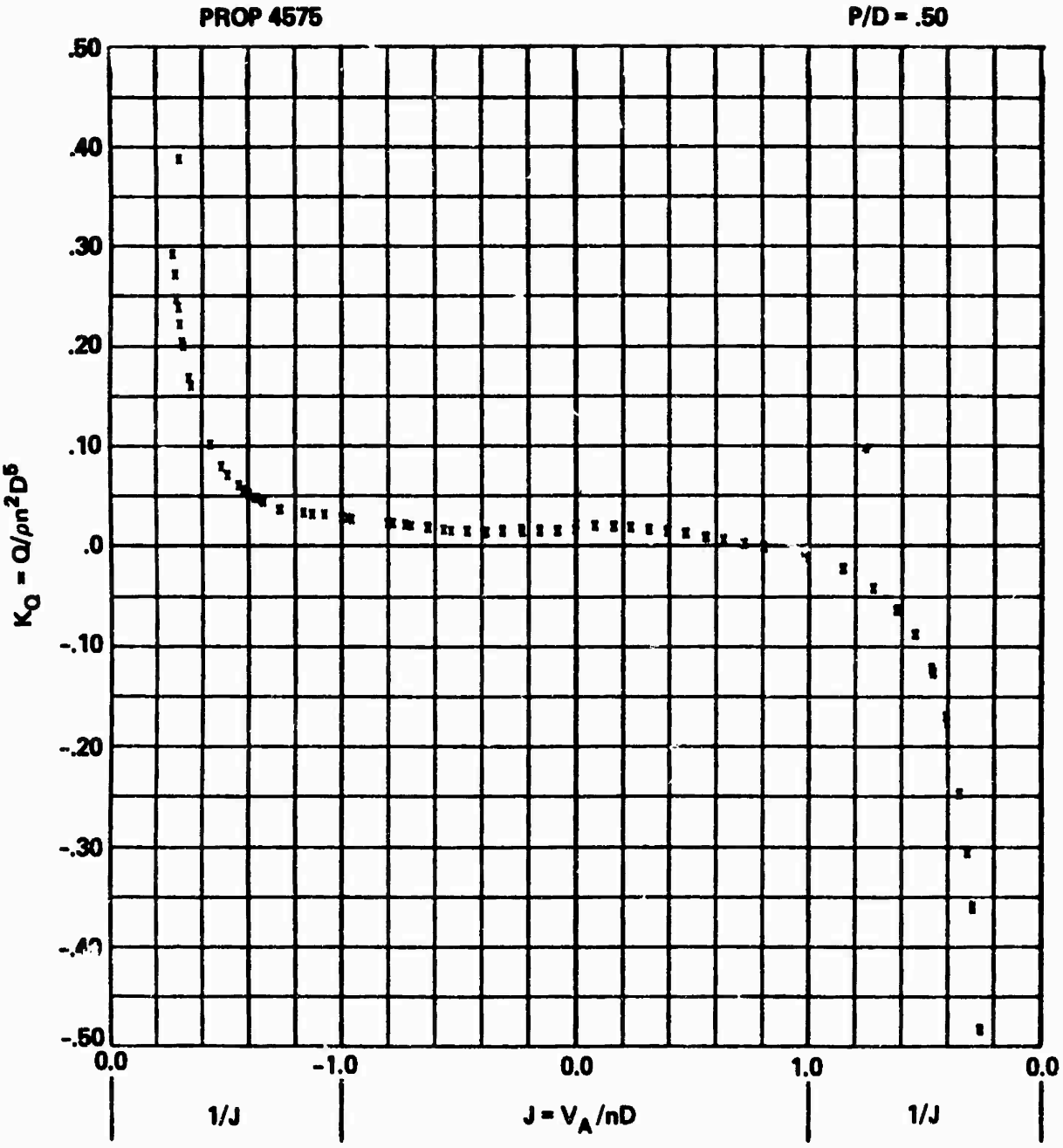

Figure 17d - At P/D = 0.50

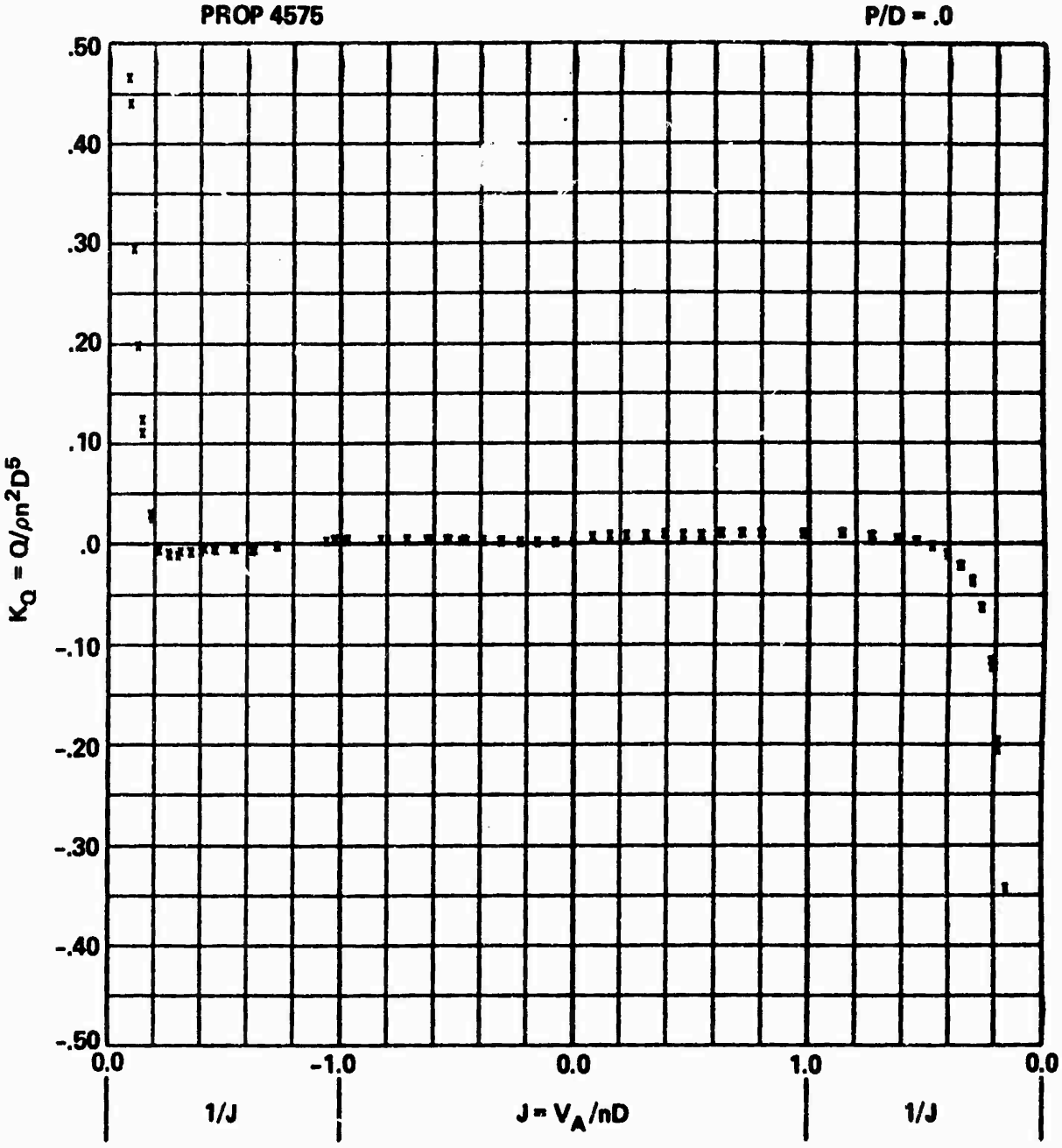

Figure 17e - At P/D = 0

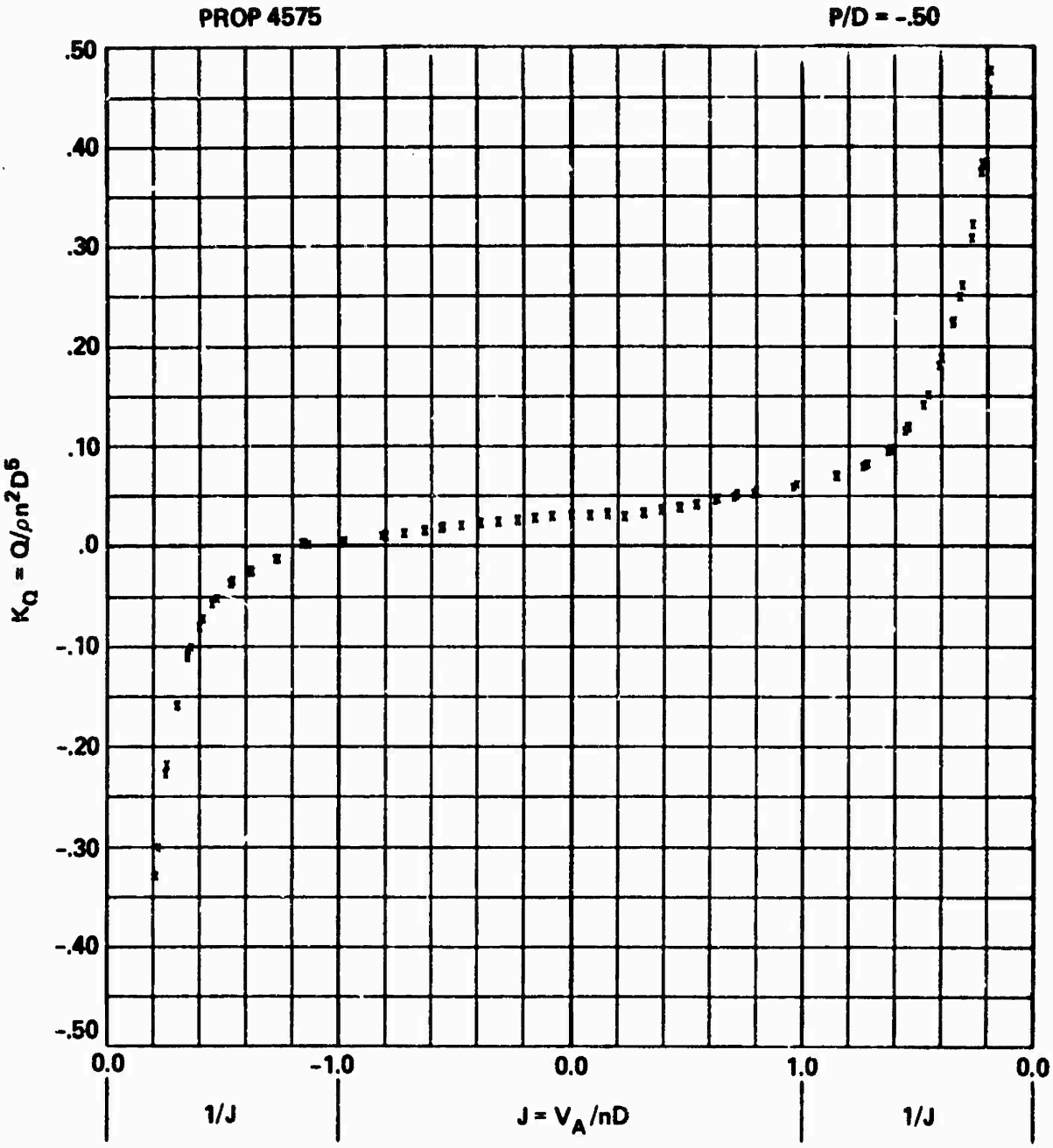

Figure 17f - At P/D = -0.50

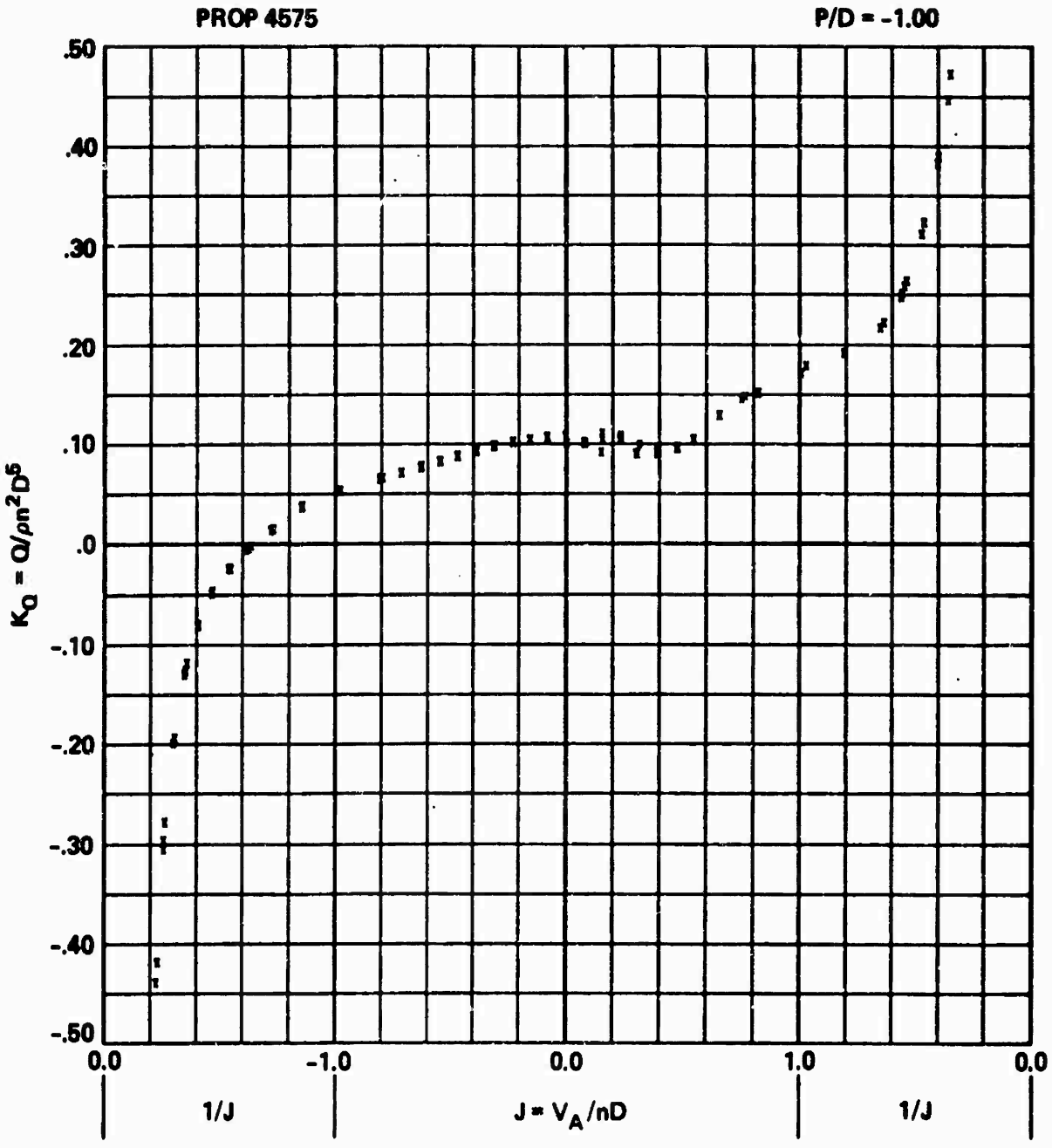

Figure 17g - At P/D = -1.00

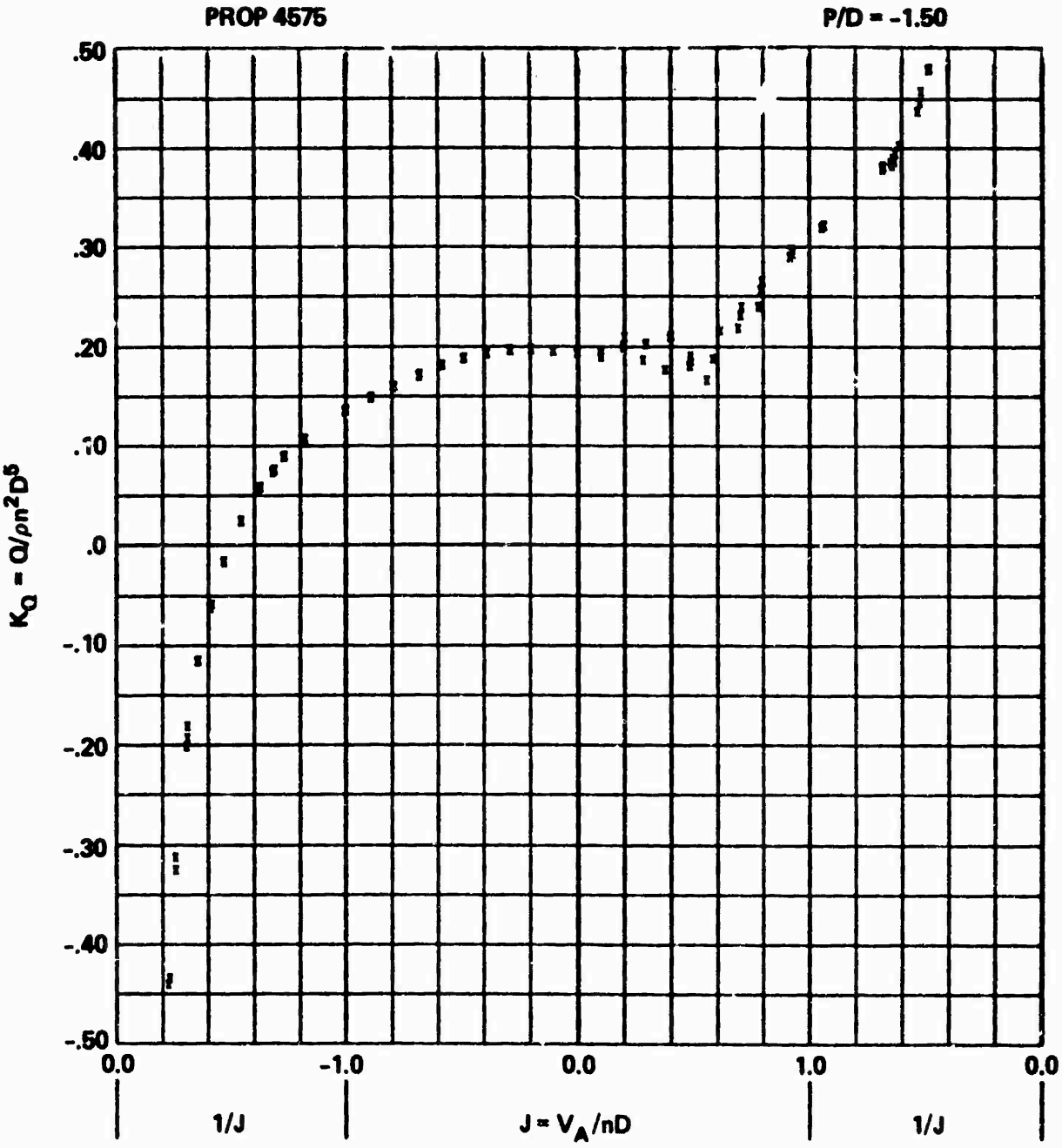

Figure 17h - At P/D = -1.50

Figure 18 - Variation of Thrust Index C_T^* with Advance Angle β^* for Propeller 4575

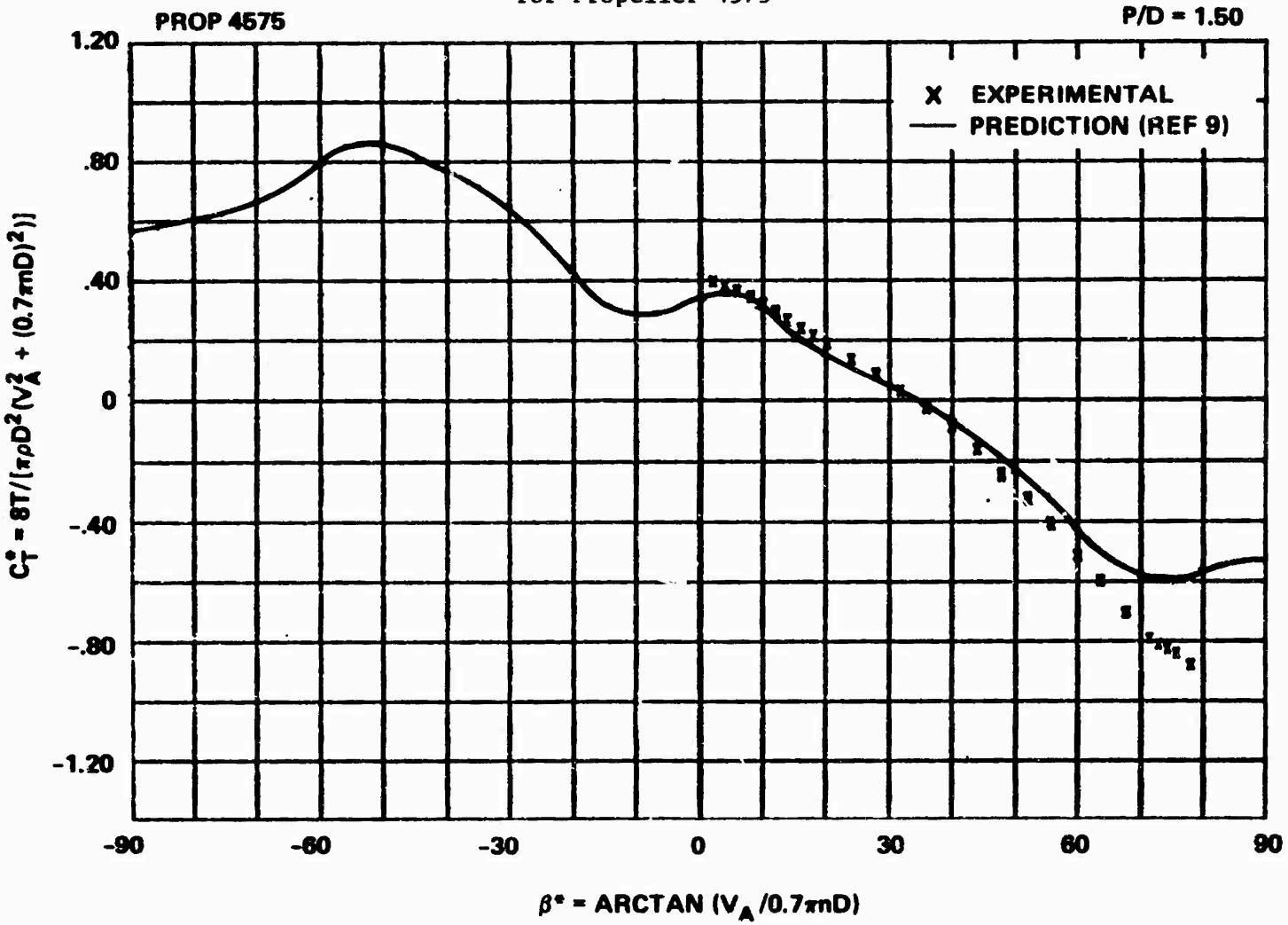

Figure 18a - At P/D = 1.50

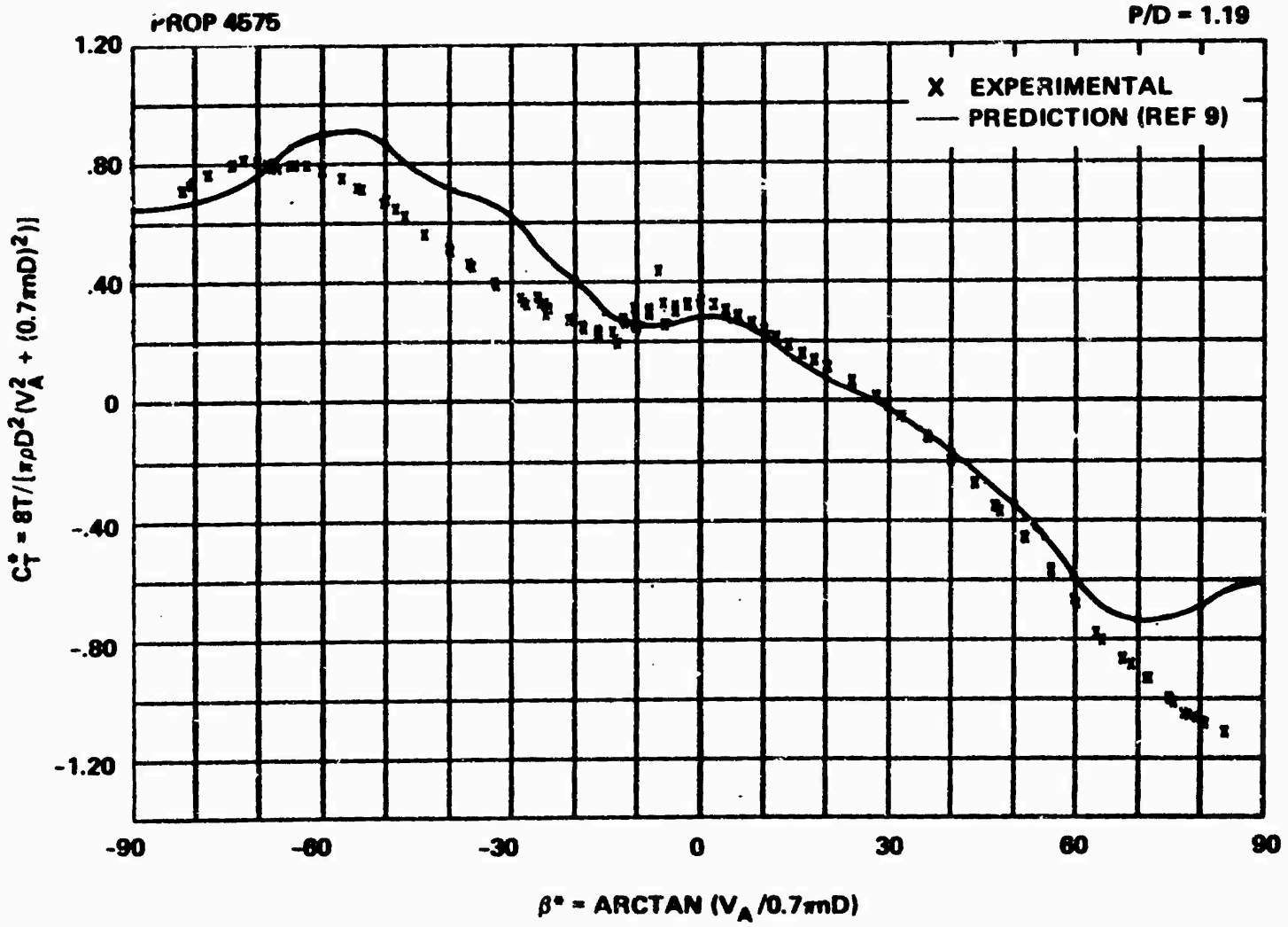

Figure 18b - At P/D = 1.19

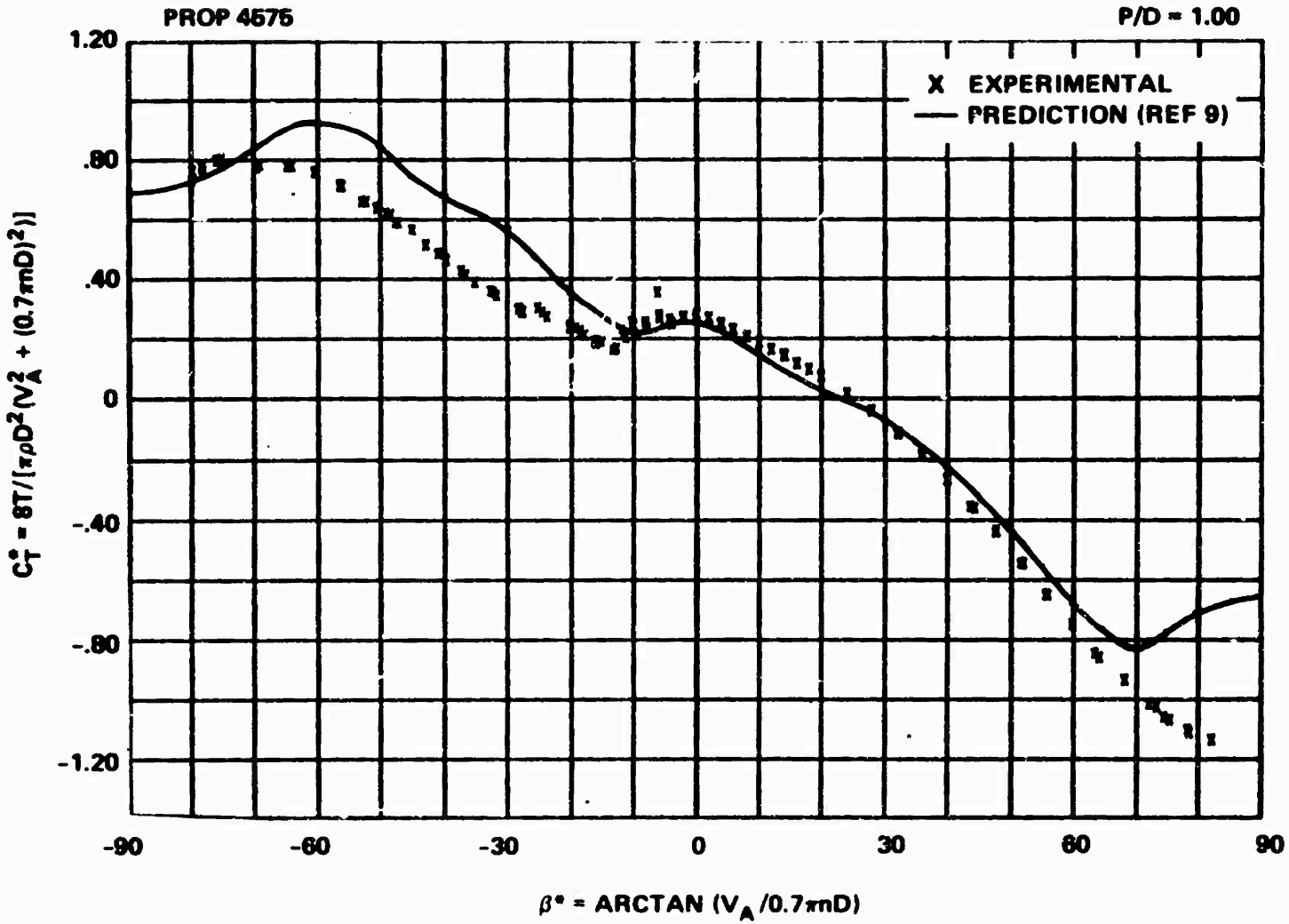

Figure 18c - At P/D = 1.00

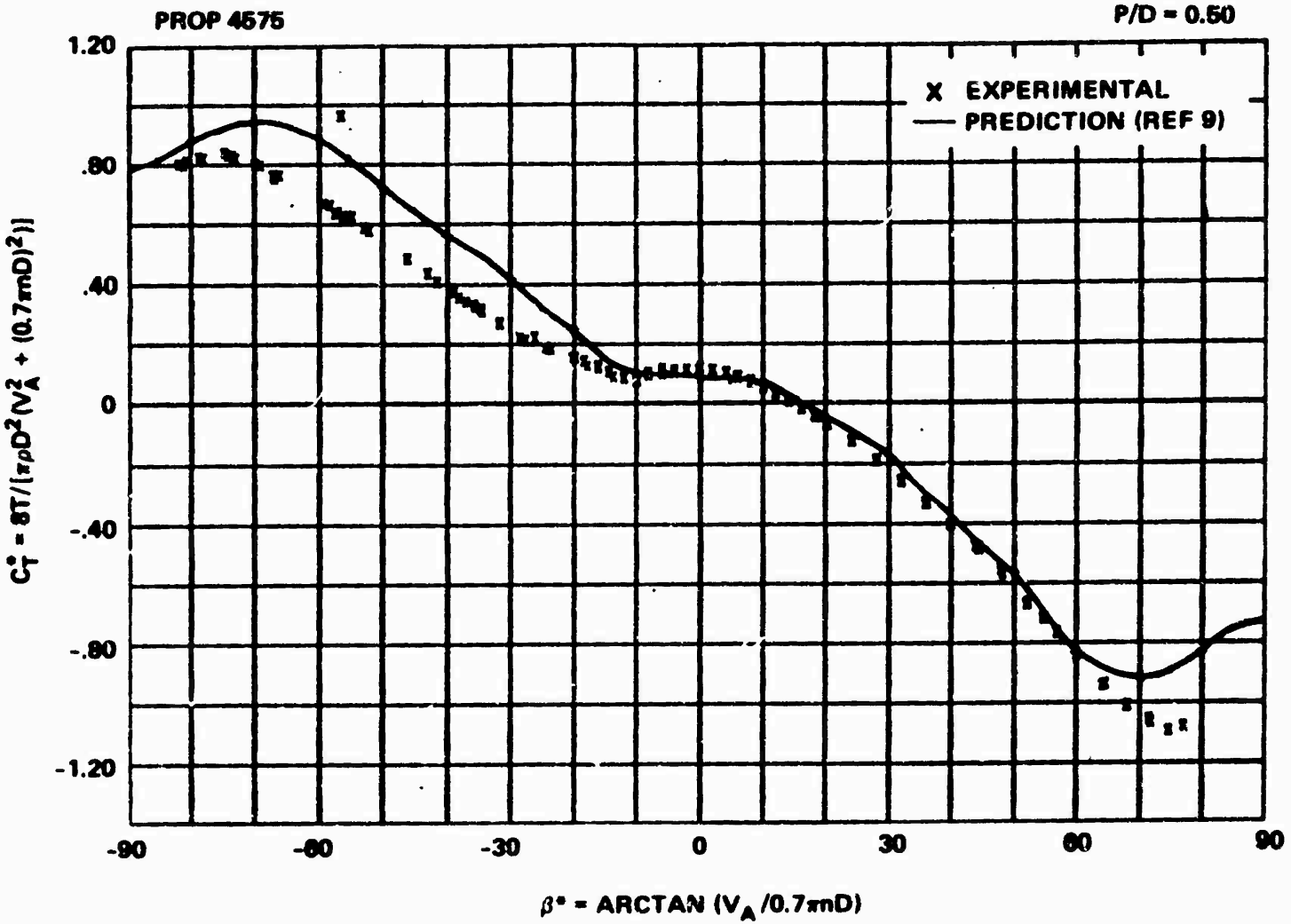

Figure 18d - At P/D = 0.50

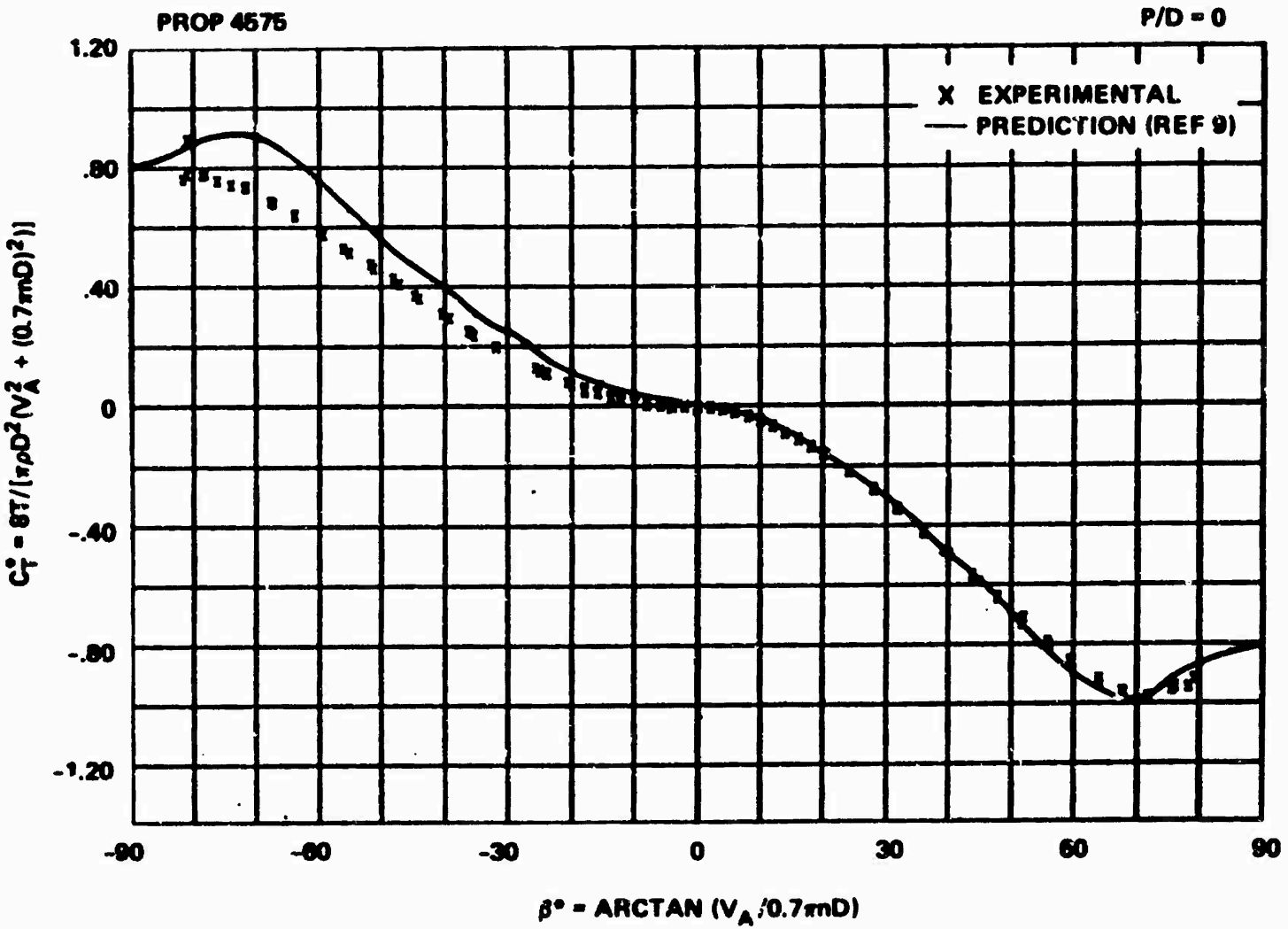

Figure 18e - At P/D = 0

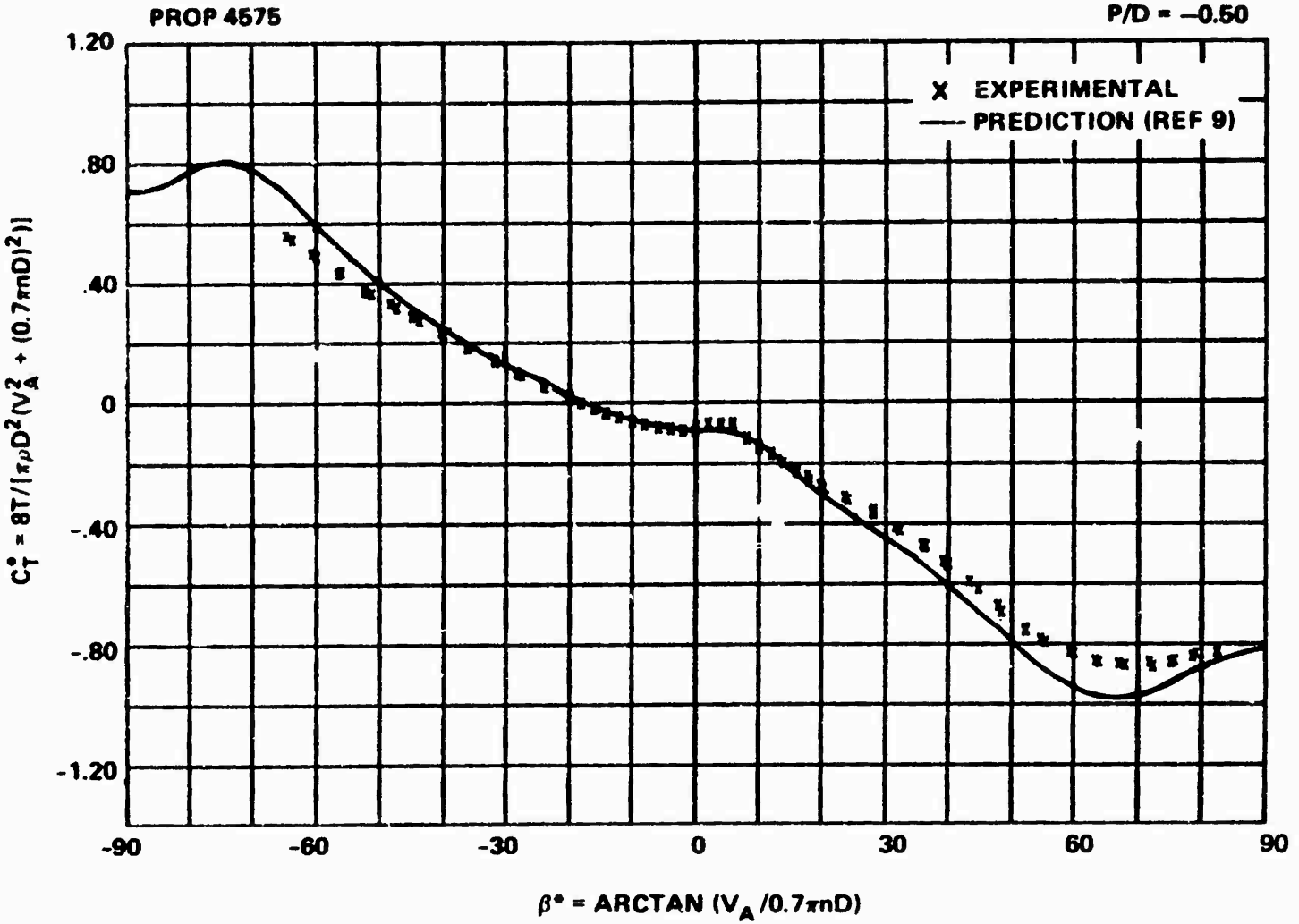

Figure 18f - At P/D = -0.50

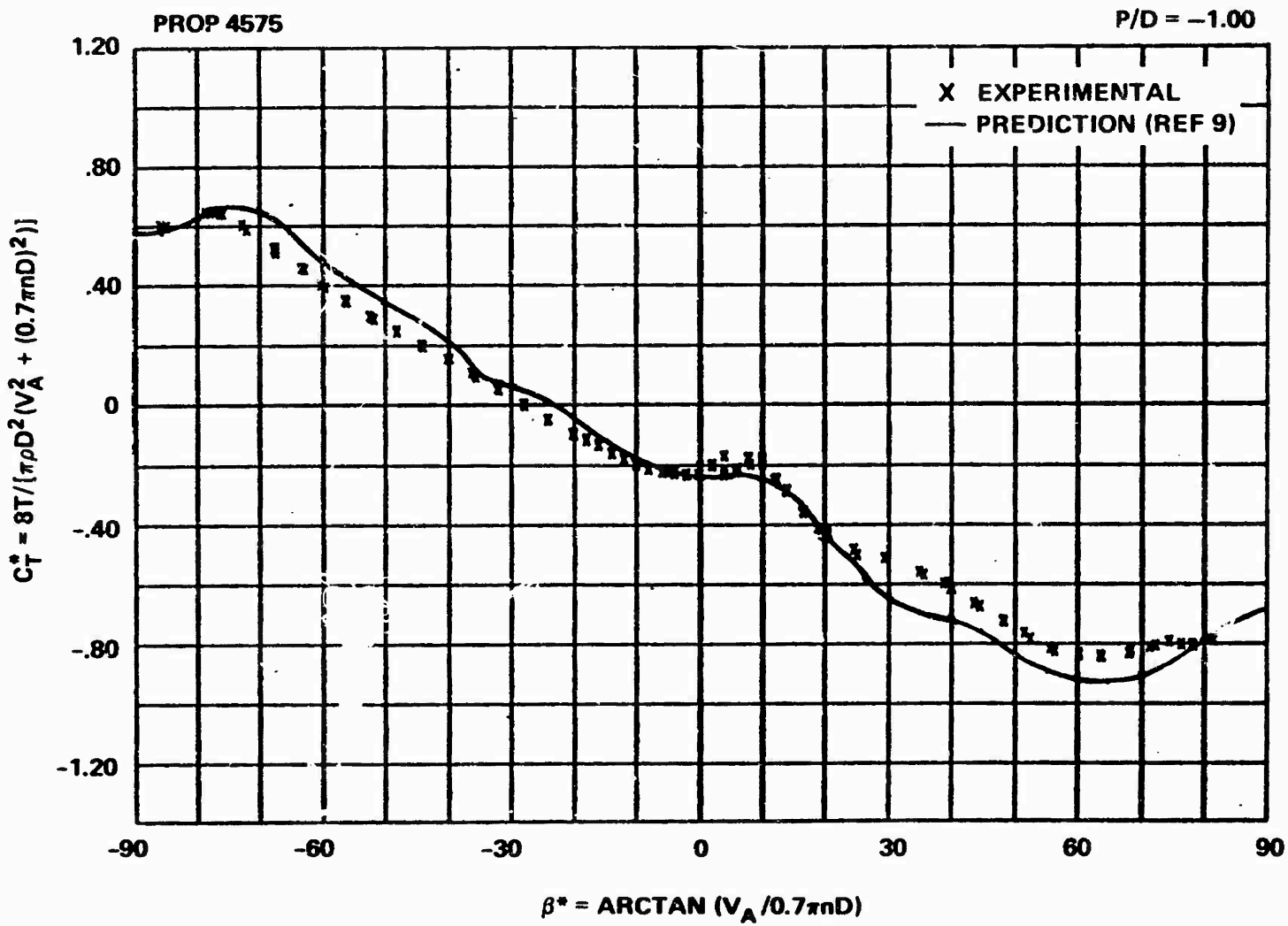

Figure 18g - At P/D = -1.00

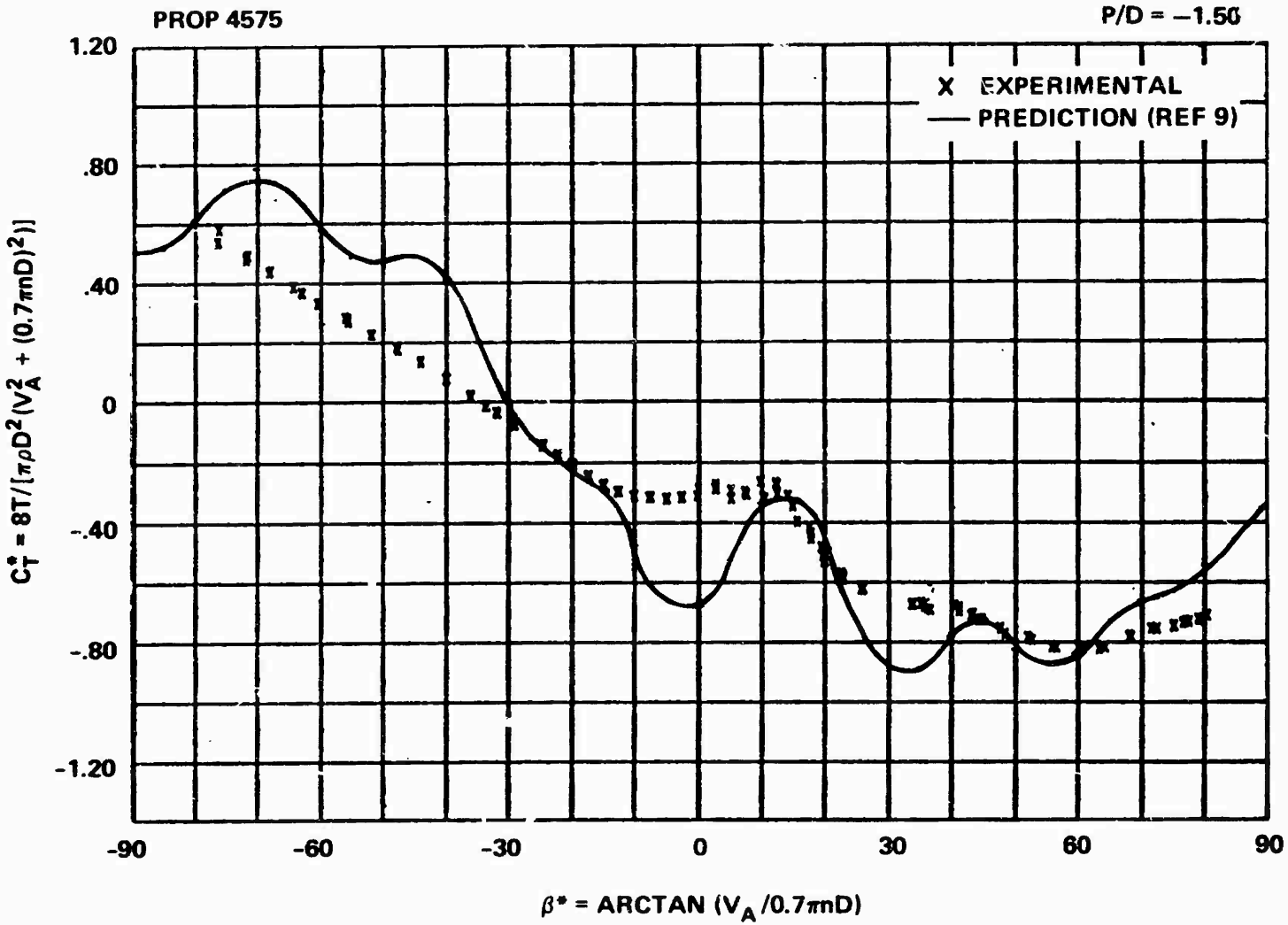

Figure 18h - At P/D = -1.50

Figure 19 - Variation of Torque Index C_Q^* with Advance Angle β^* for Propeller 4575

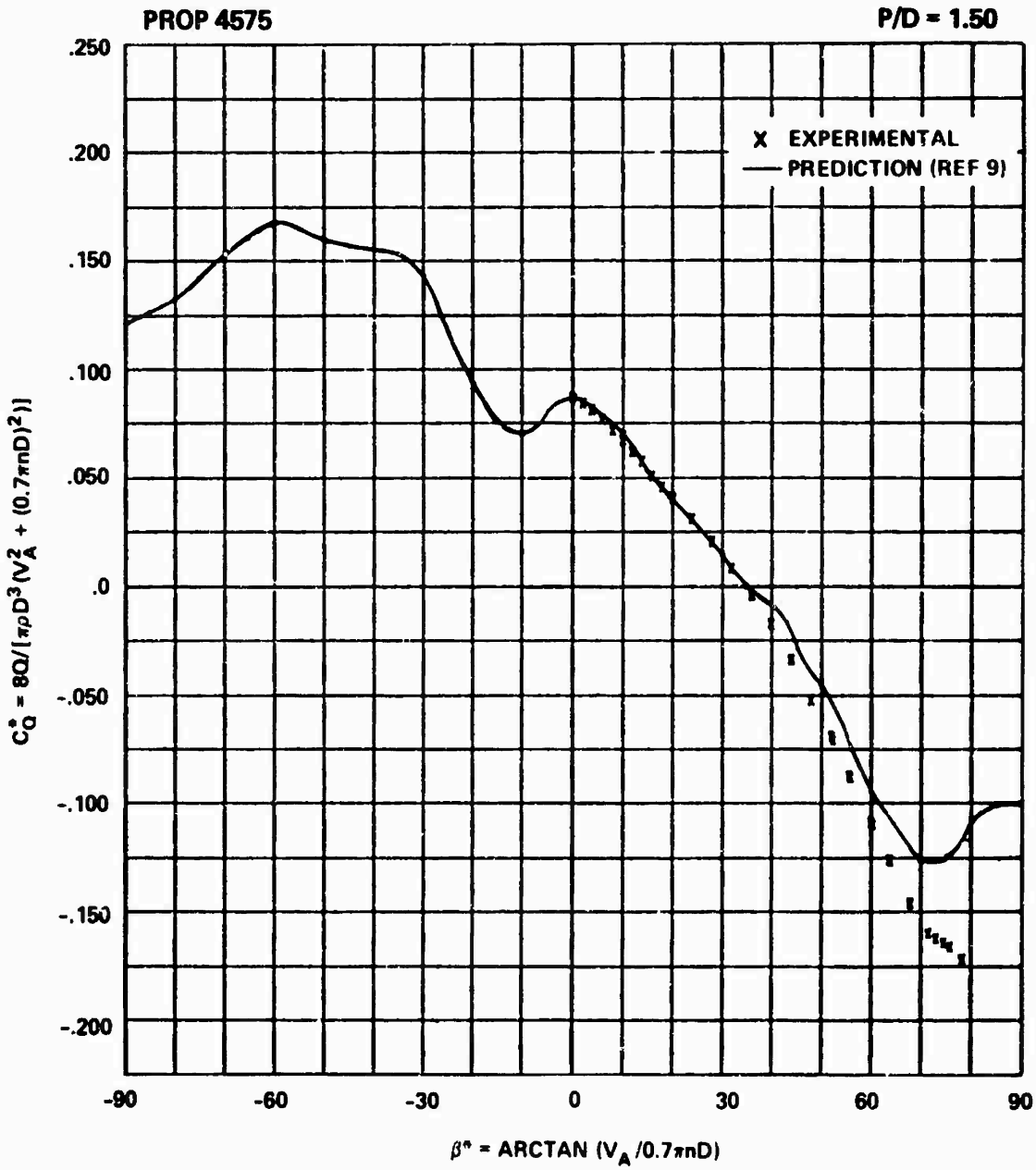

Figure 19a - At P/D = 1.50

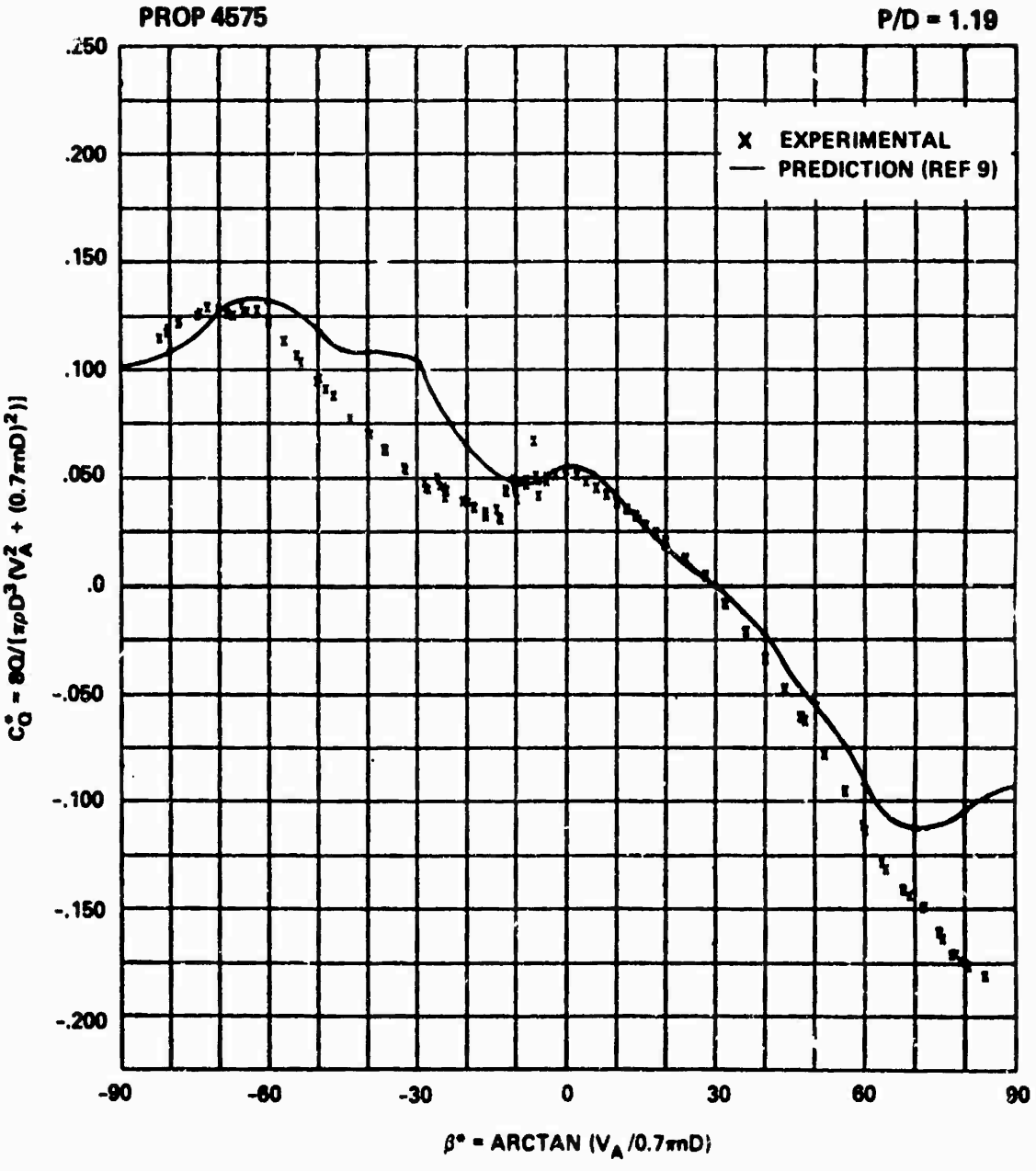

Figure 19b - At P/D = 1.19

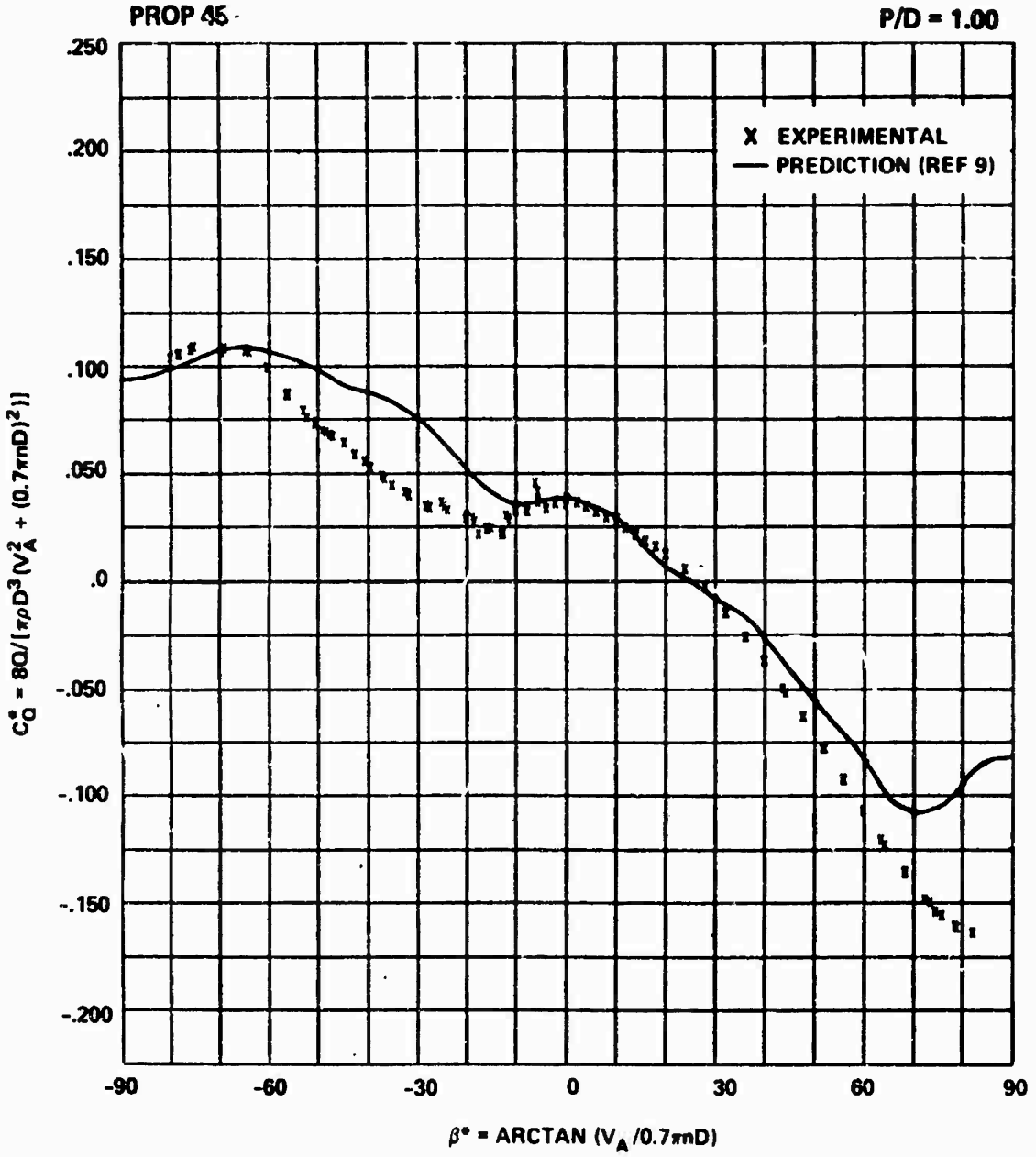

Figure 19c - At P/D = 1.00

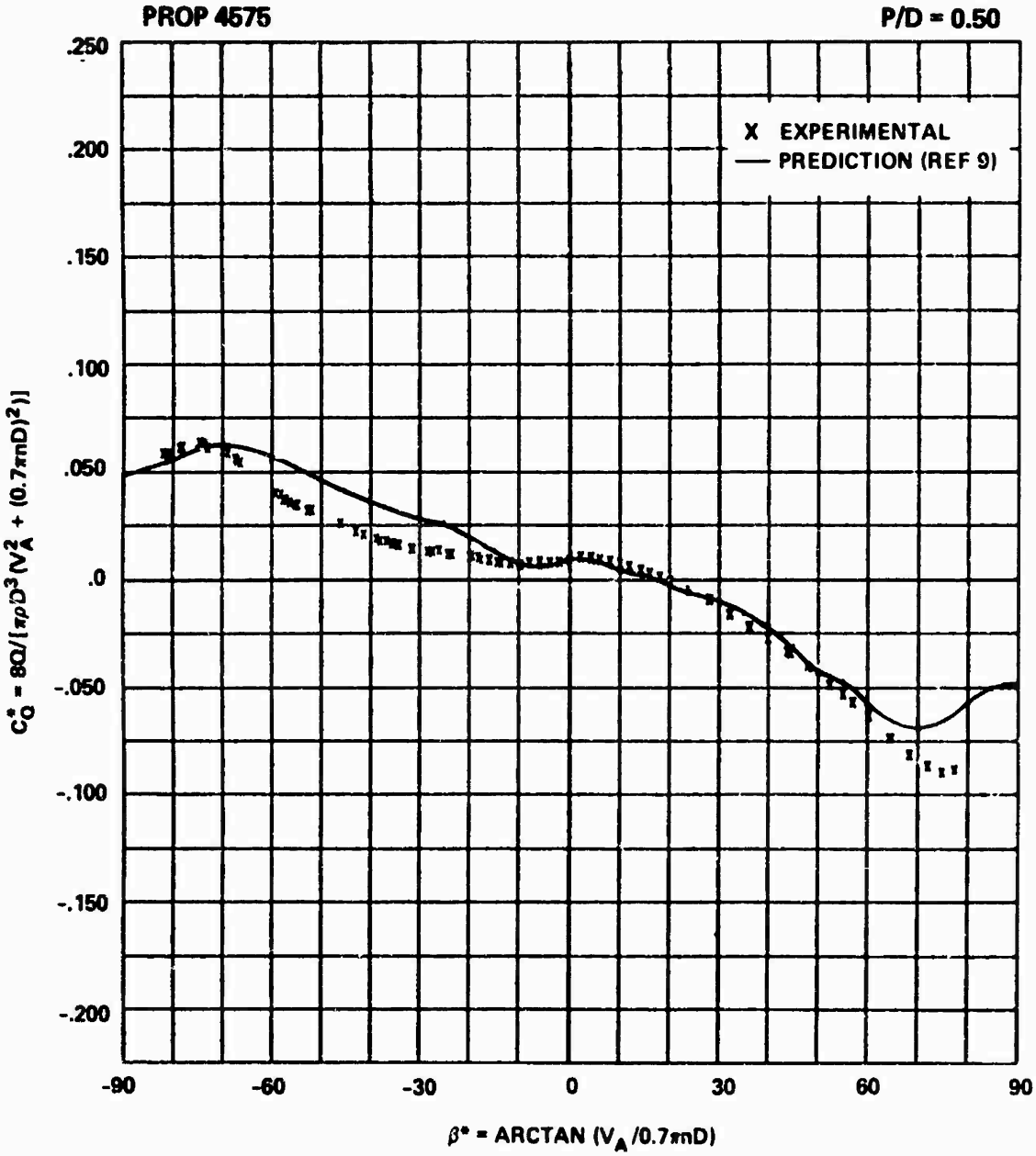

Figure 19d - At P/D = 0.50

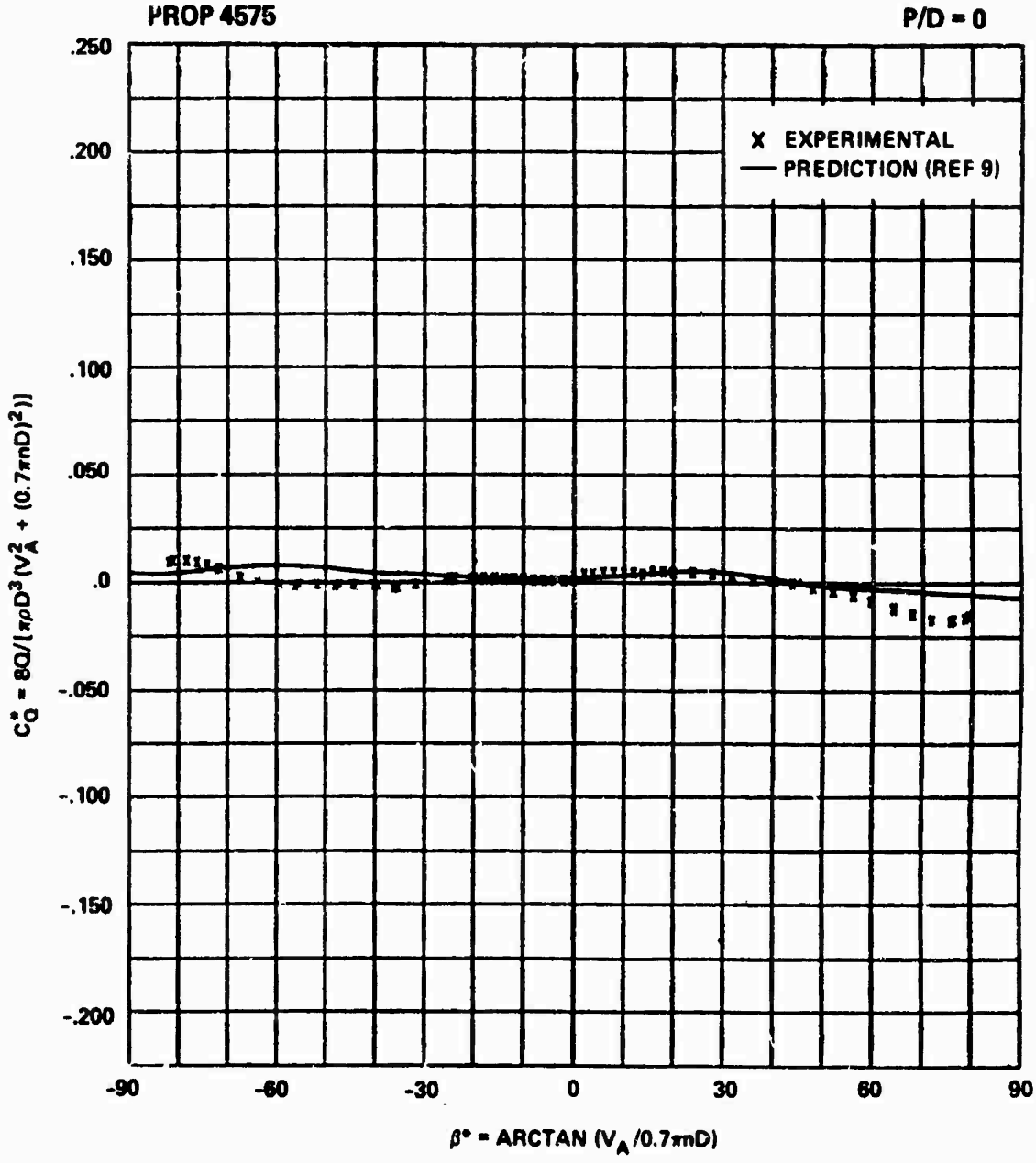

Figure 19e - At P/D = 0

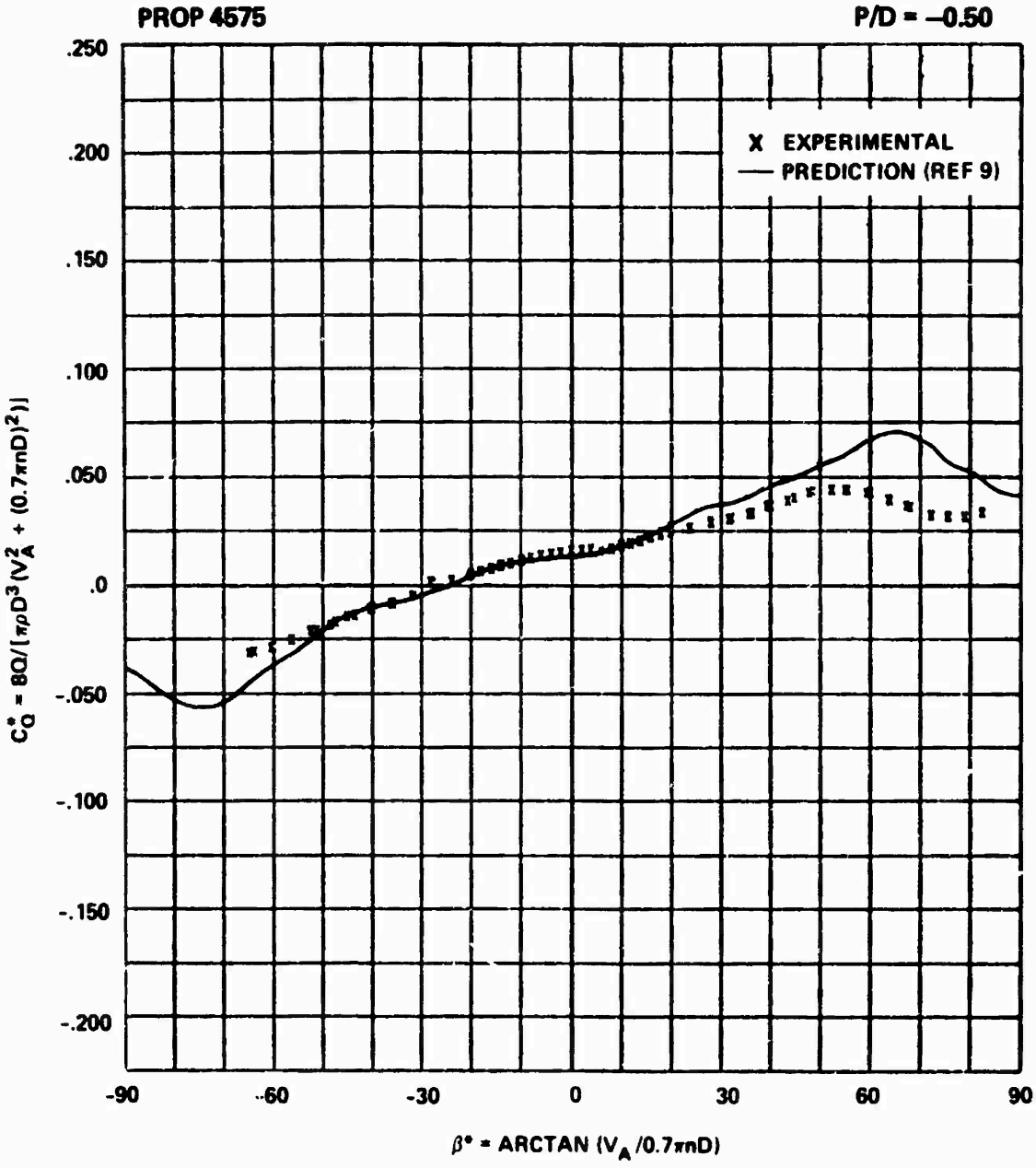

Figure 19f - At P/D = -0.50

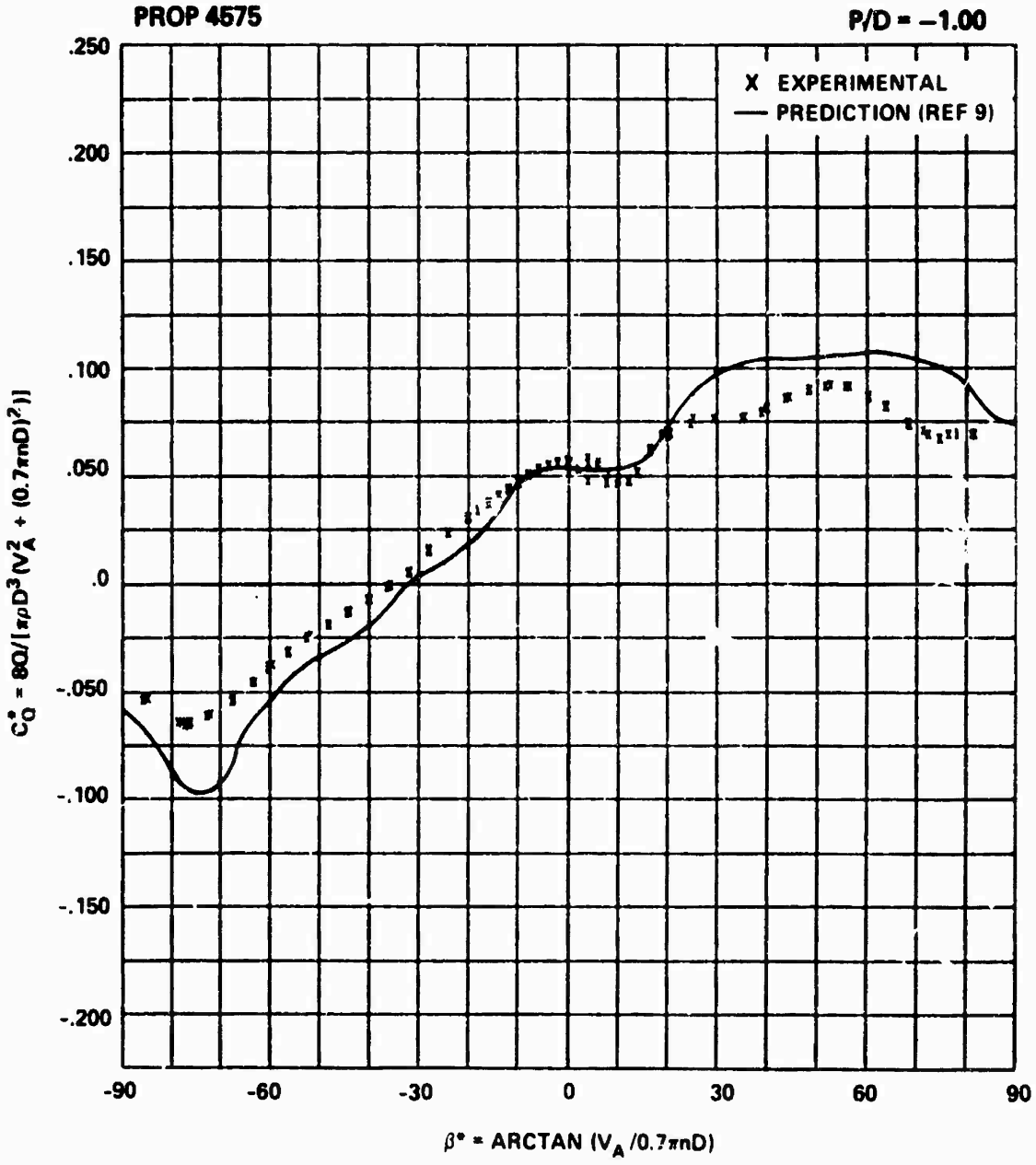

Figure 19g - At P/D = -1.00

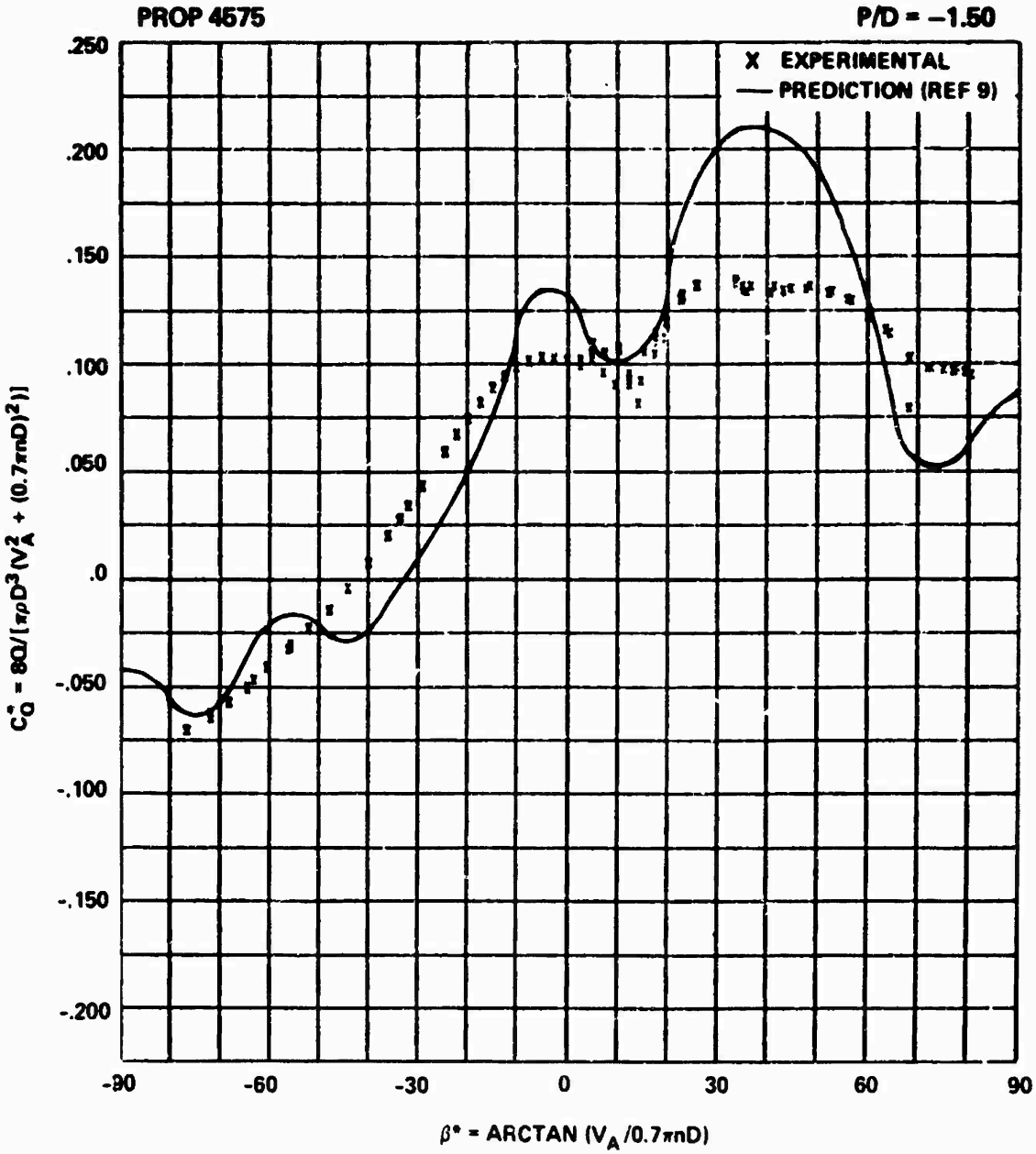

Figure 19h - At P/D = -1.50

Figure 20 - Variation of Modified Hydrodynamic Blade Spindle Torque Coefficient K'_{SH} with Modified Advance Coefficient J' for Propeller 4572

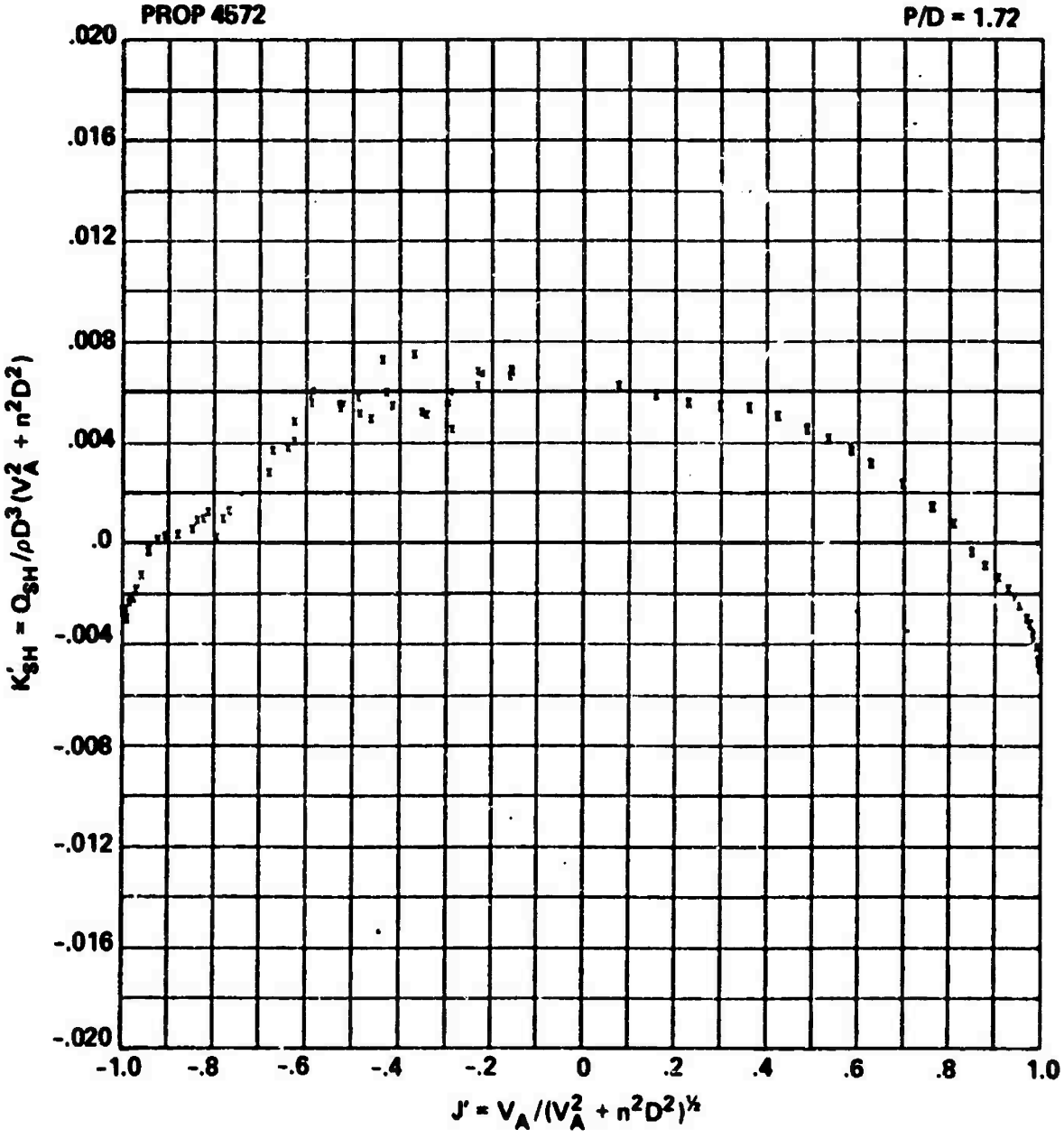

Figure 20a - At P/D = 1.72

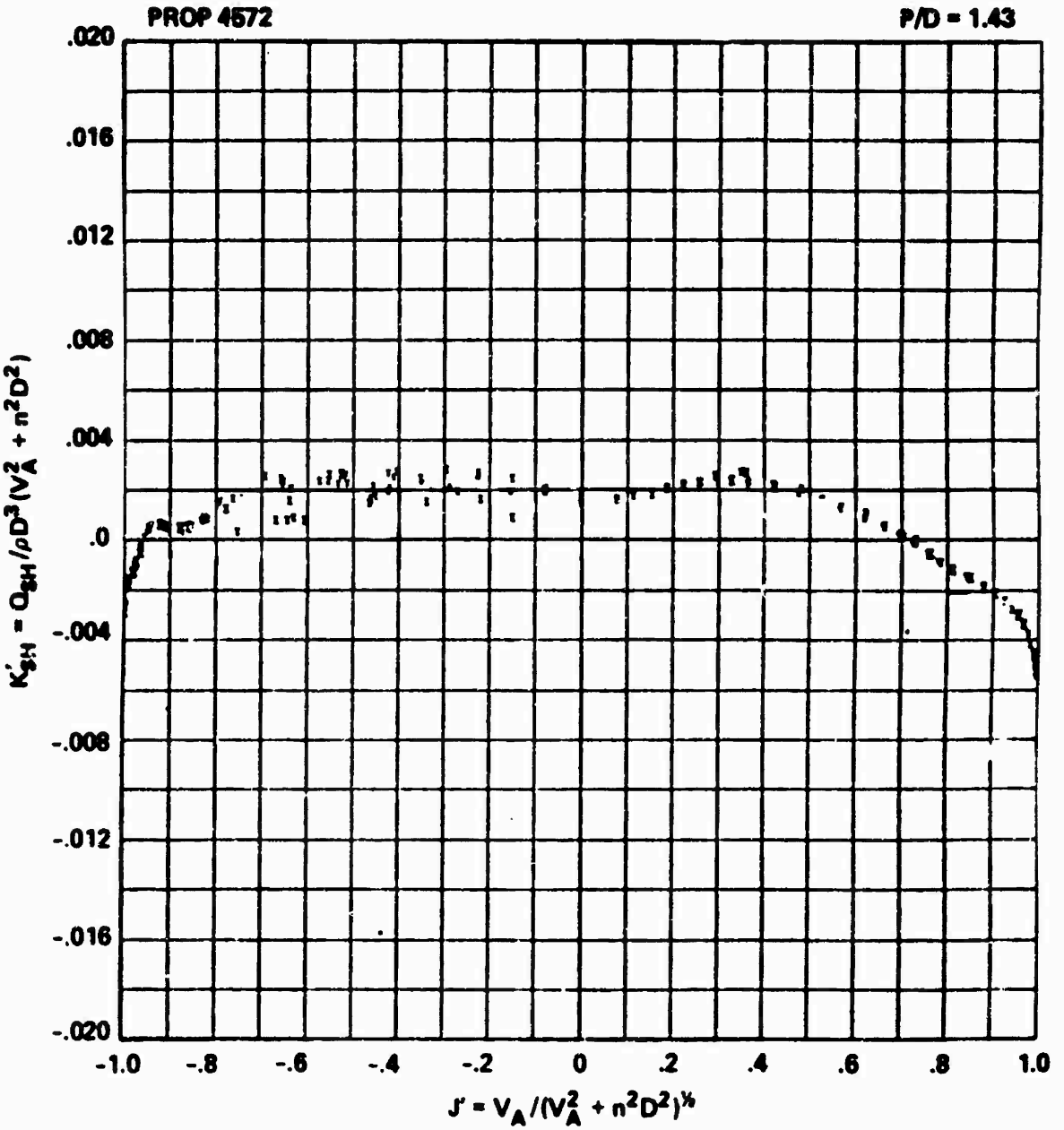

Figure 20b - At P/D = 1.43

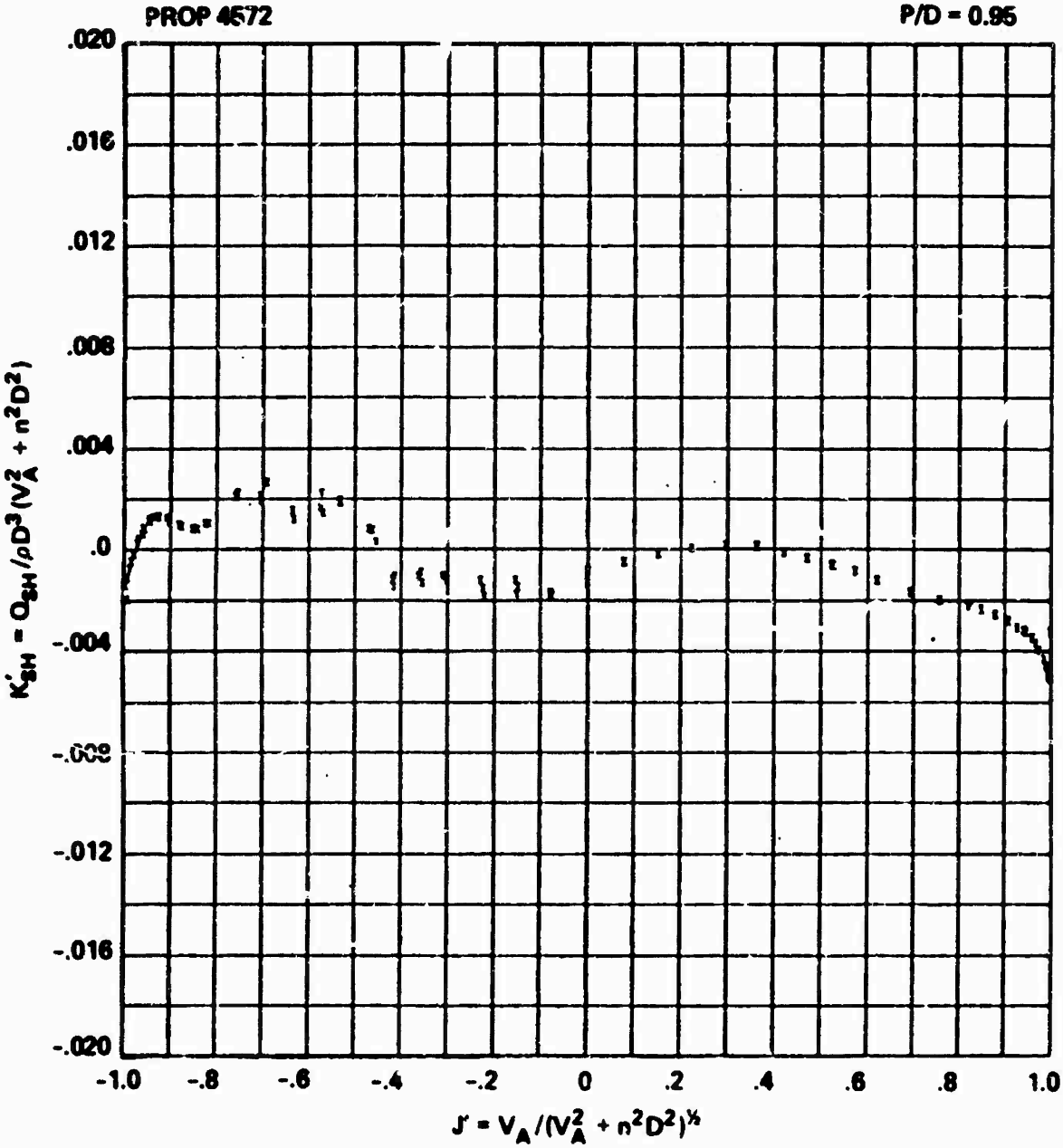

Figure 20c - At P/D = 0.95

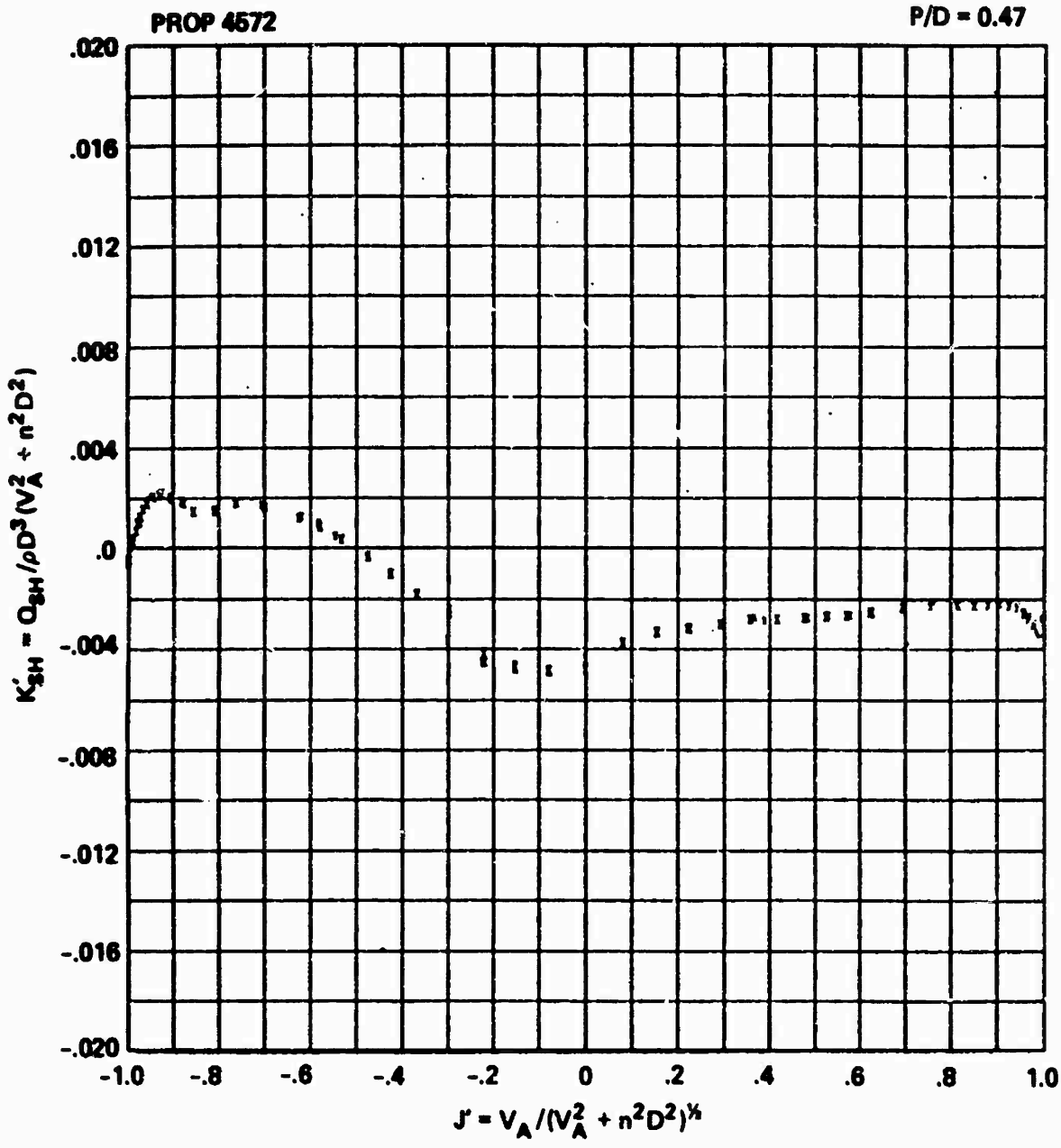

Figure 20d - At P/D = 0.47

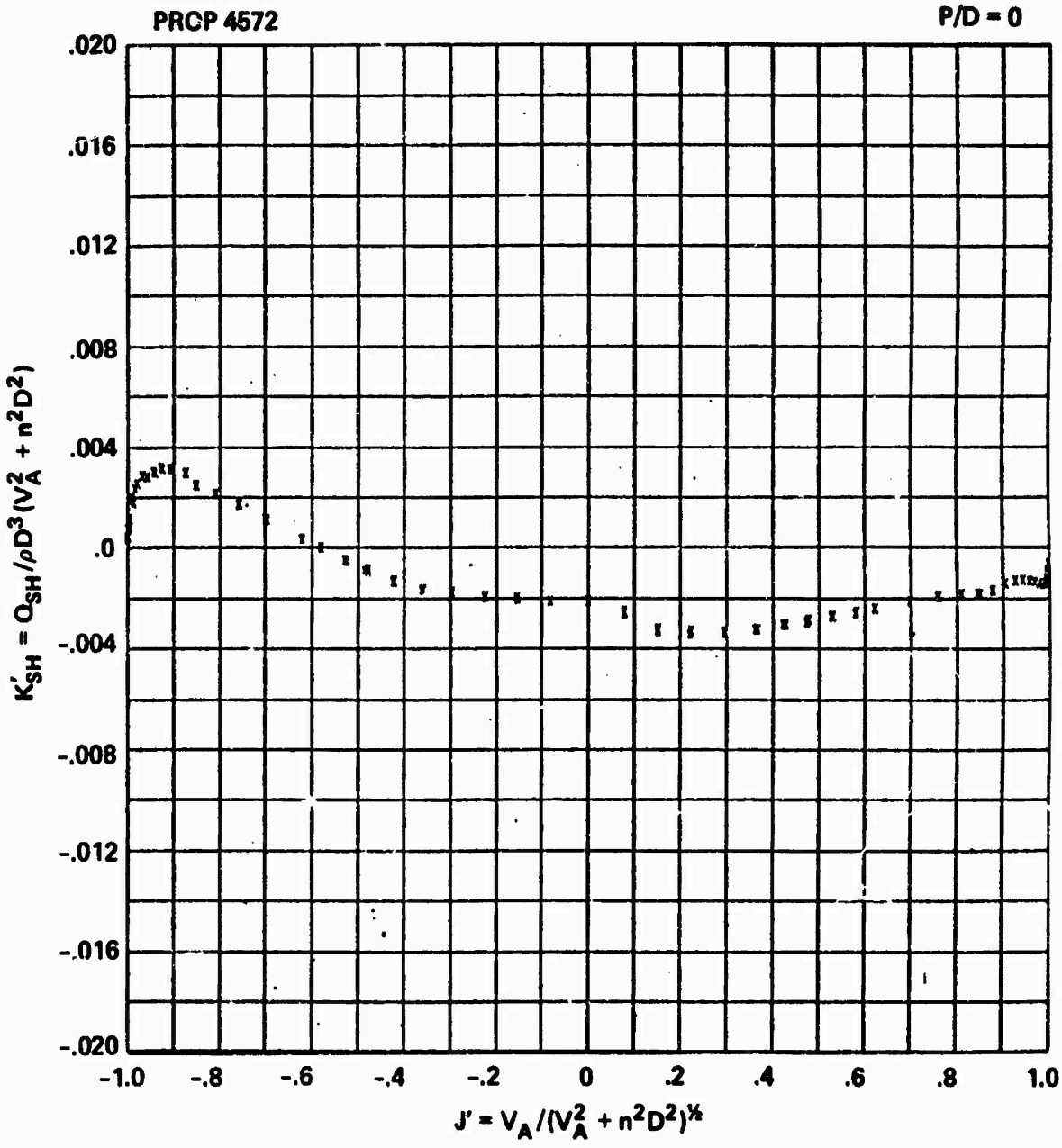

Figure 20e - At P/D = 0

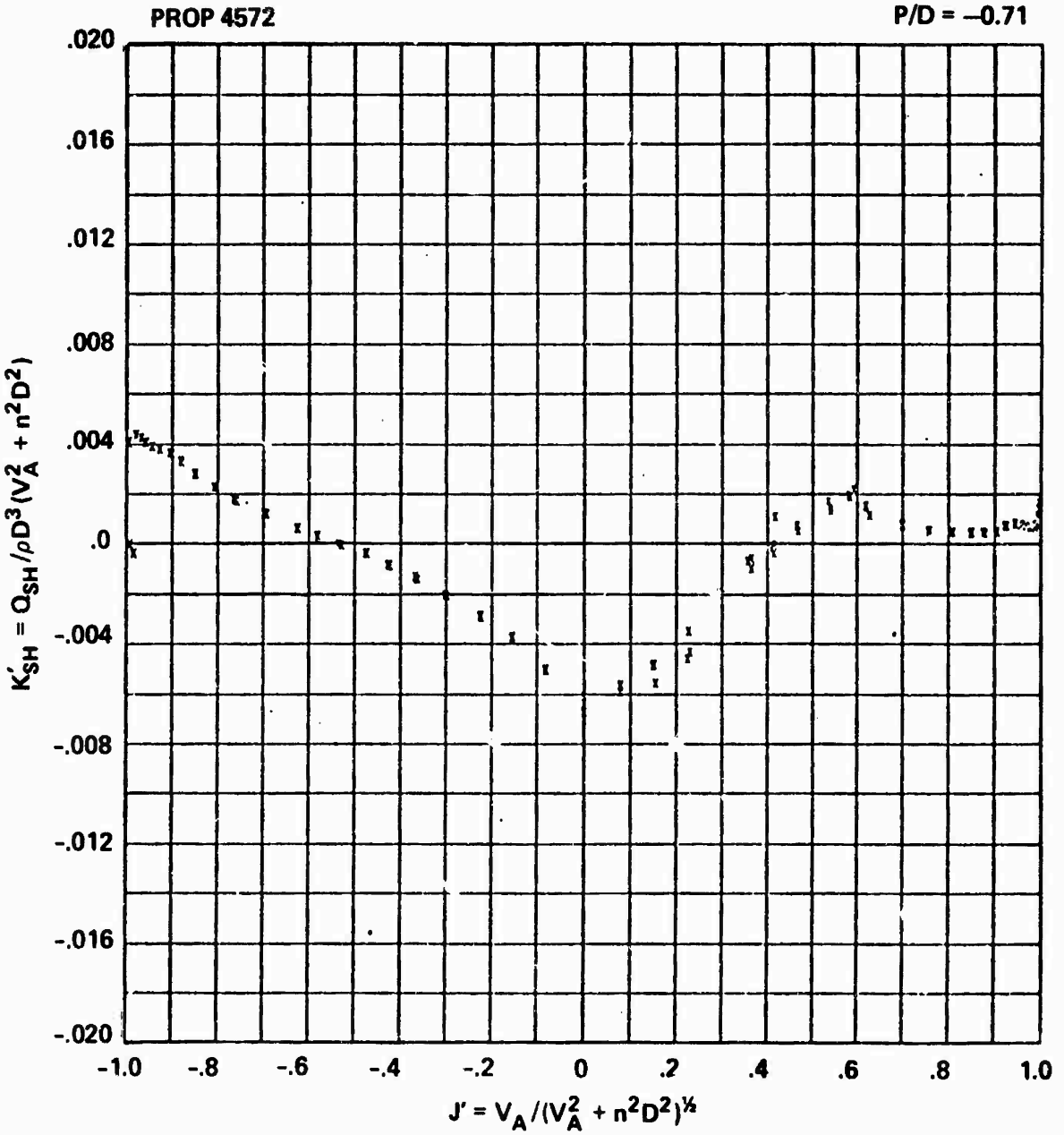

Figure 20f - At P/D = -0.71

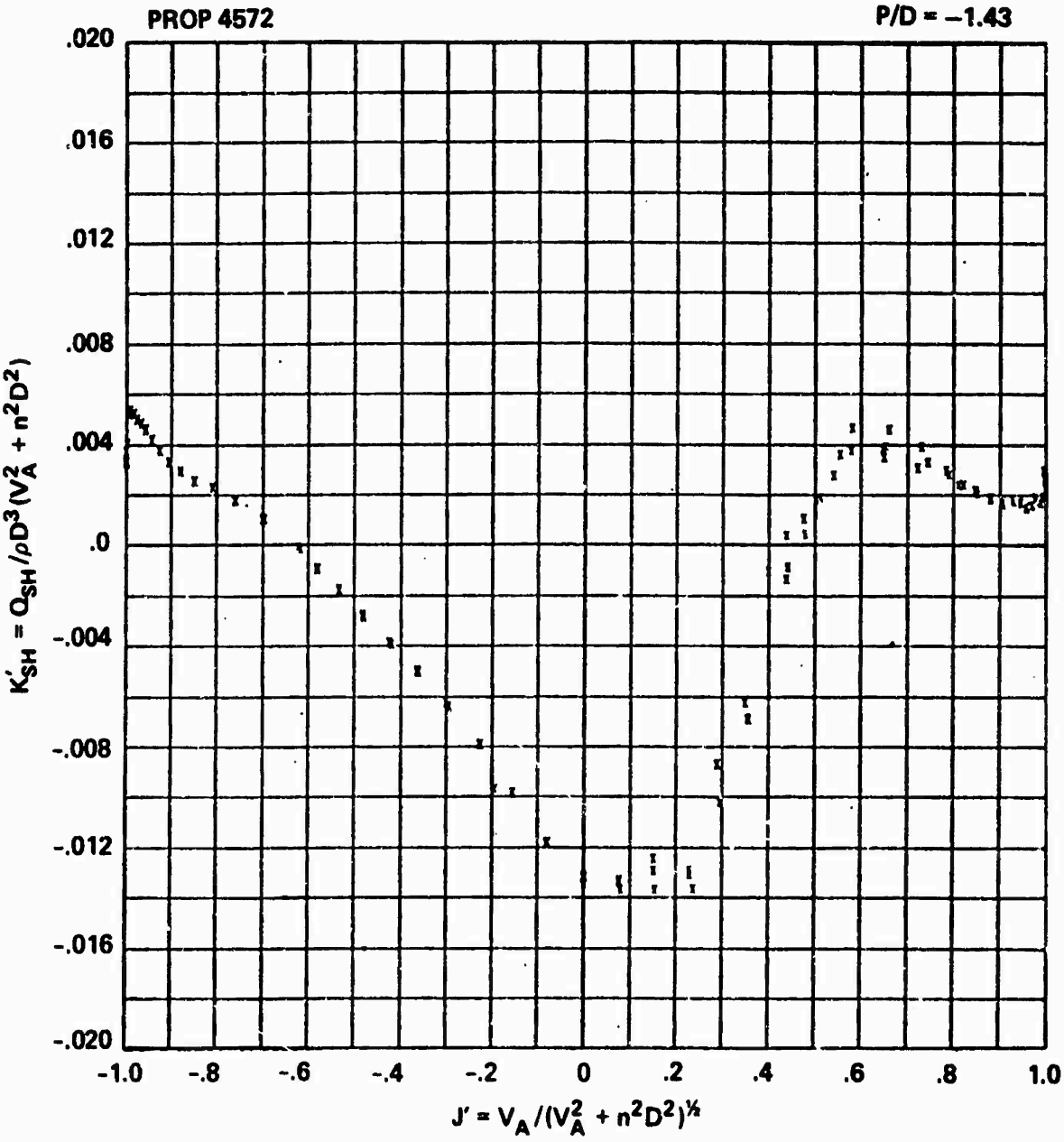

Figure 20g - At P/D = -1.43

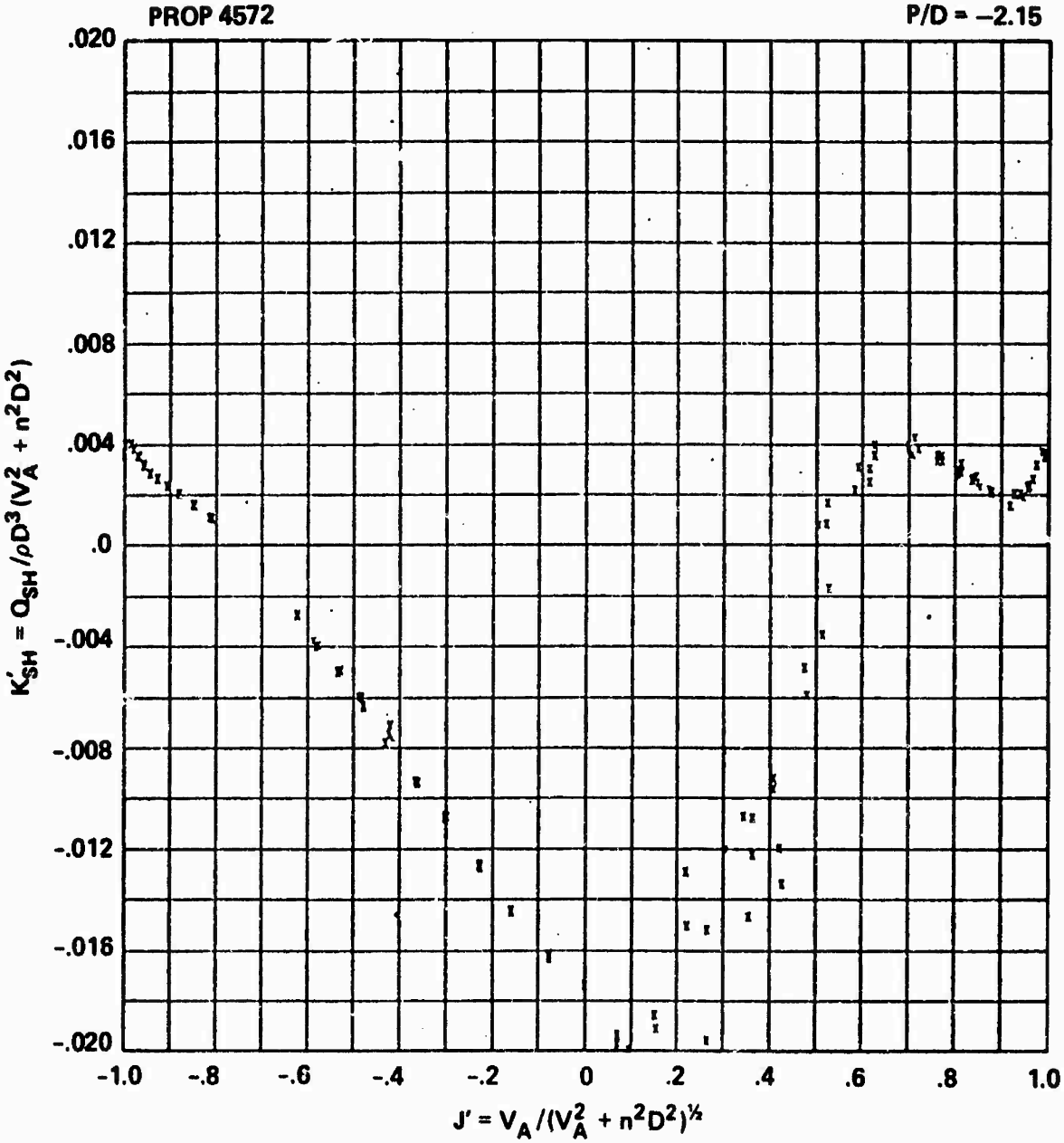

Figure 20h - At P/D = -2.15

Figure 21 - Variation of Modified Hydrodynamic Blade Spindle Torque Coefficient K'_{SH} with Modified Advance Coefficient J' for Propeller 4575

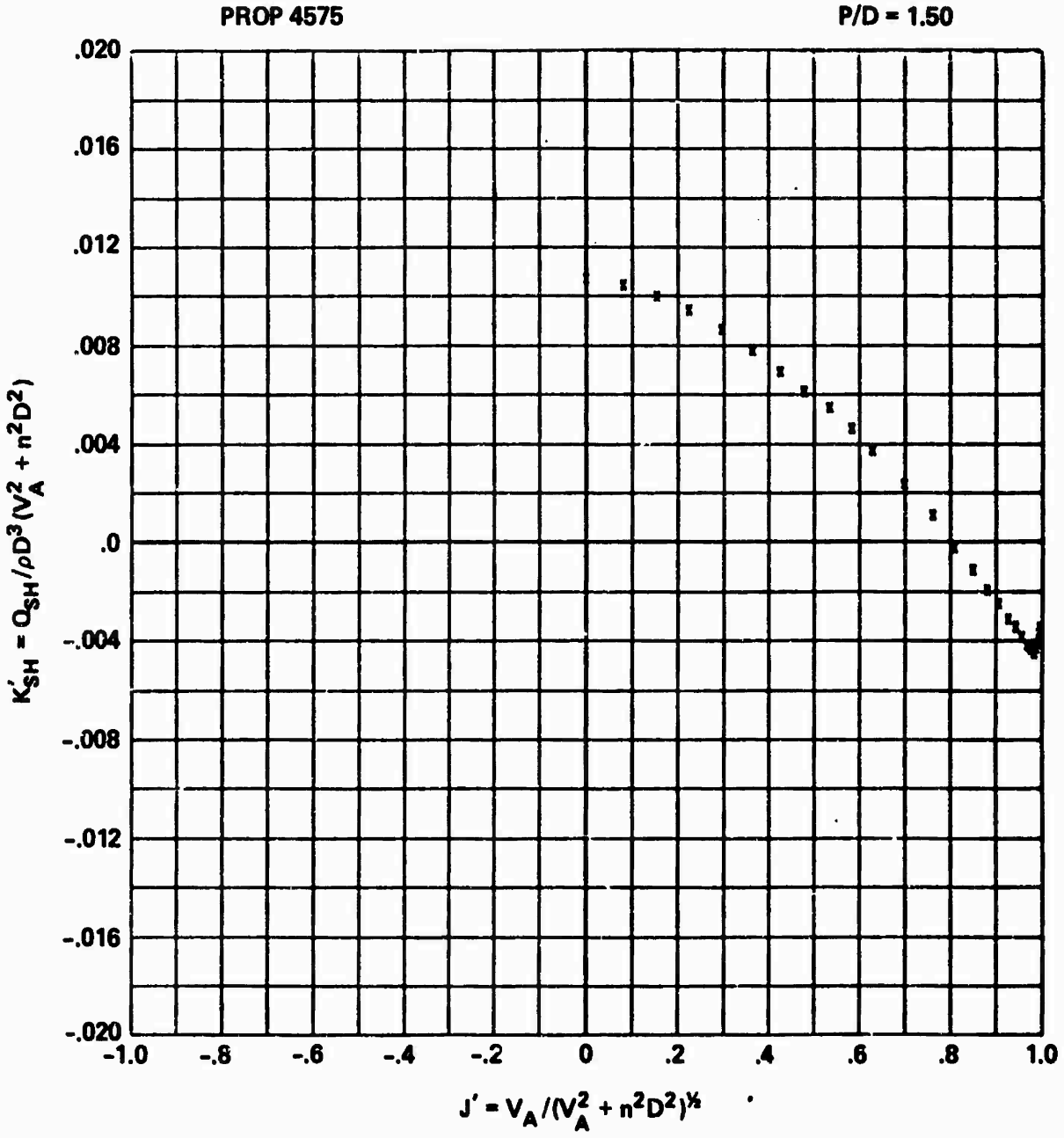

Figure 21a - At P/D = 1.50

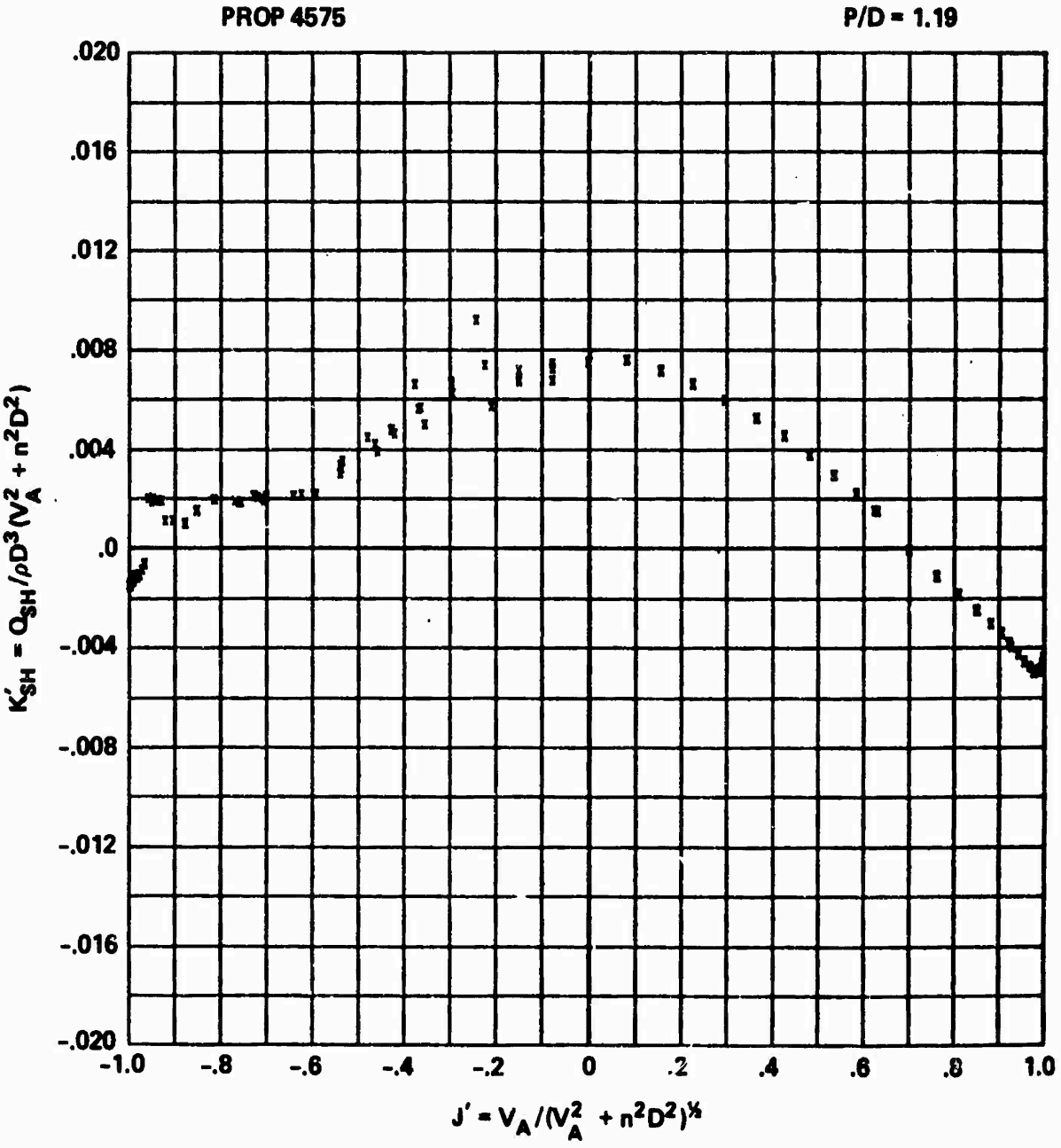

Figure 21b - At P/D = 1.19

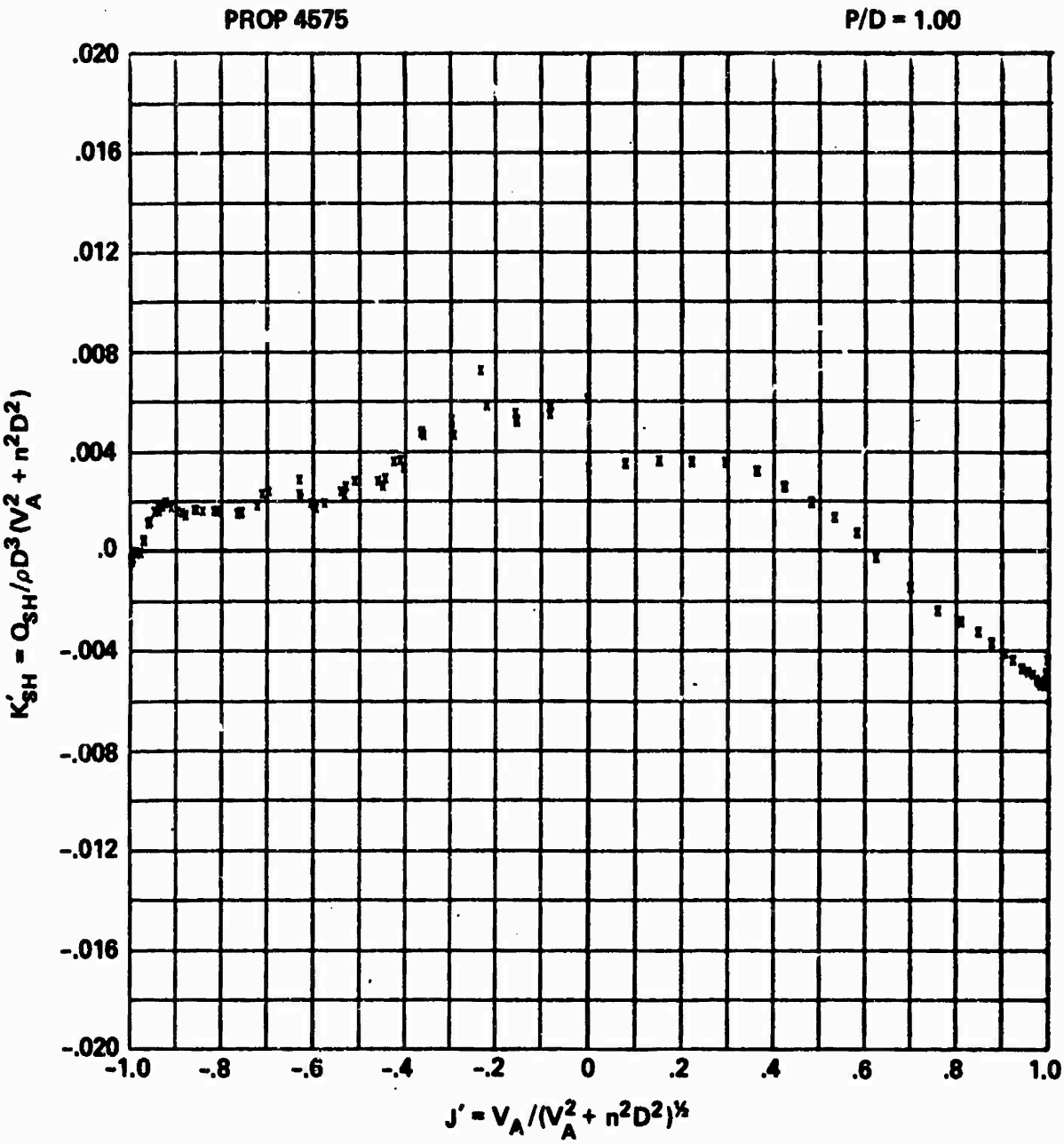

Figure 21c - At P/D = 1.00

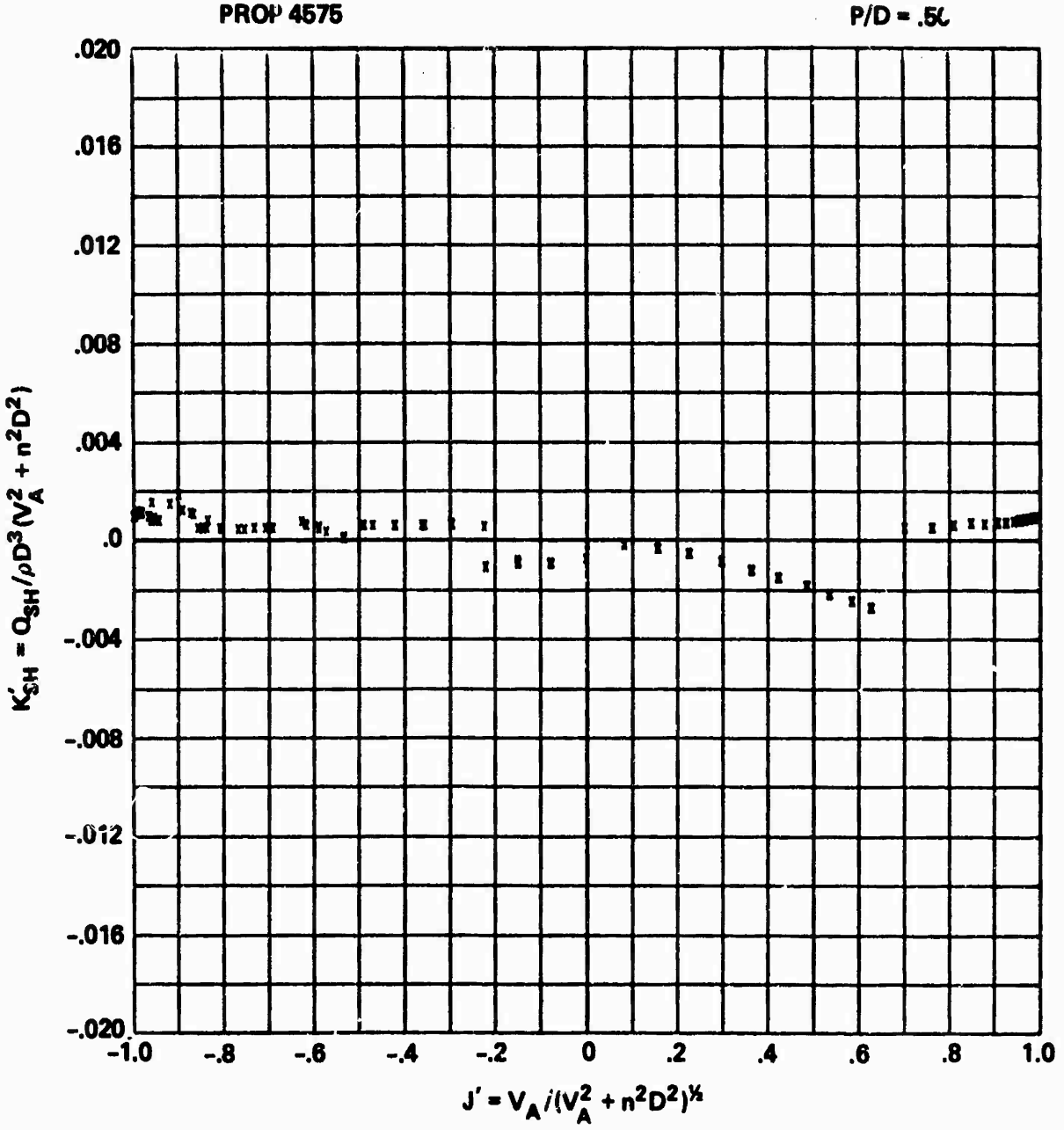

Figure 21d - At P/D = 0.50

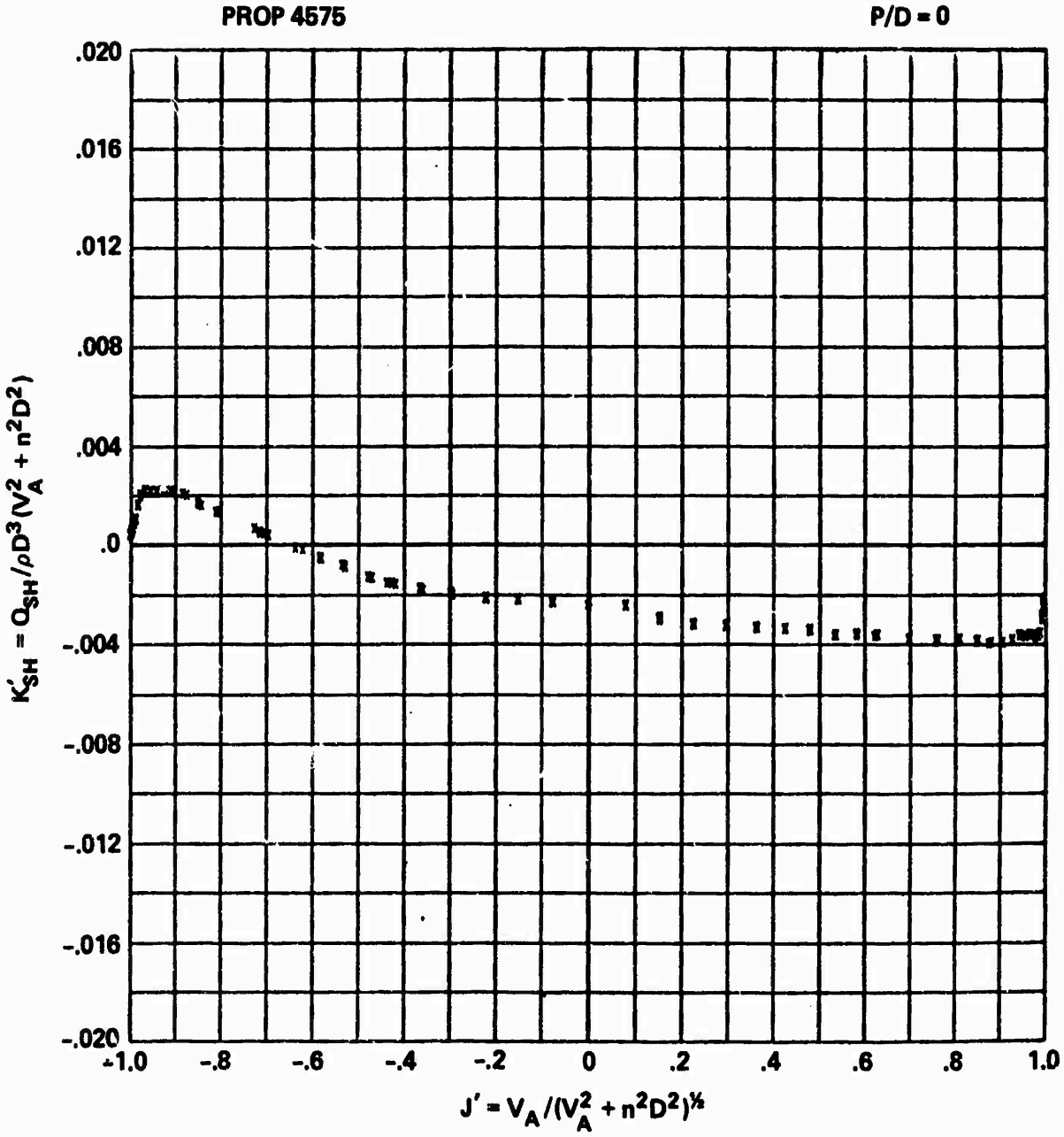

Figure 21e - At P/D = 0

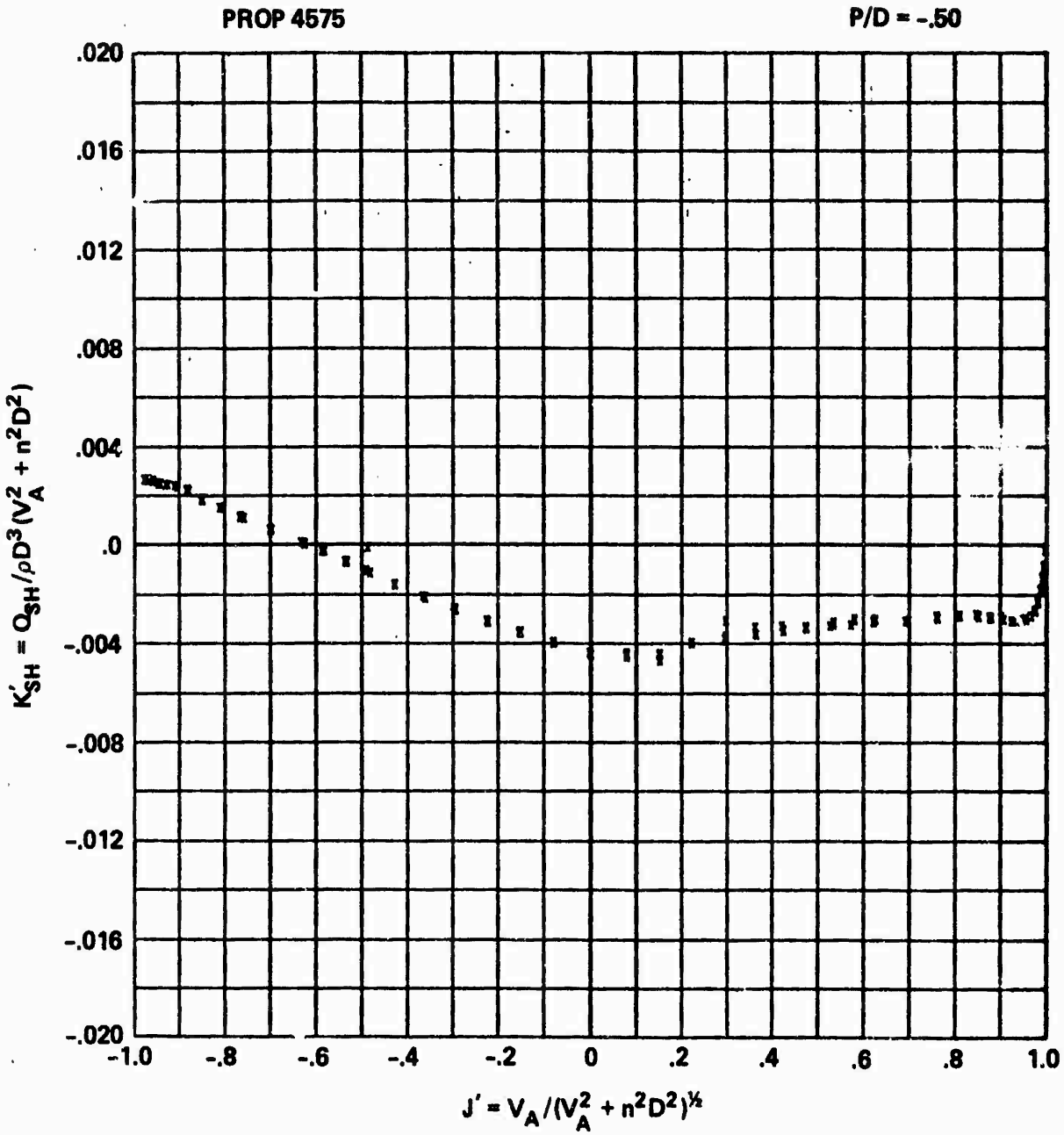

Figure 21f - At P/D = -0.50

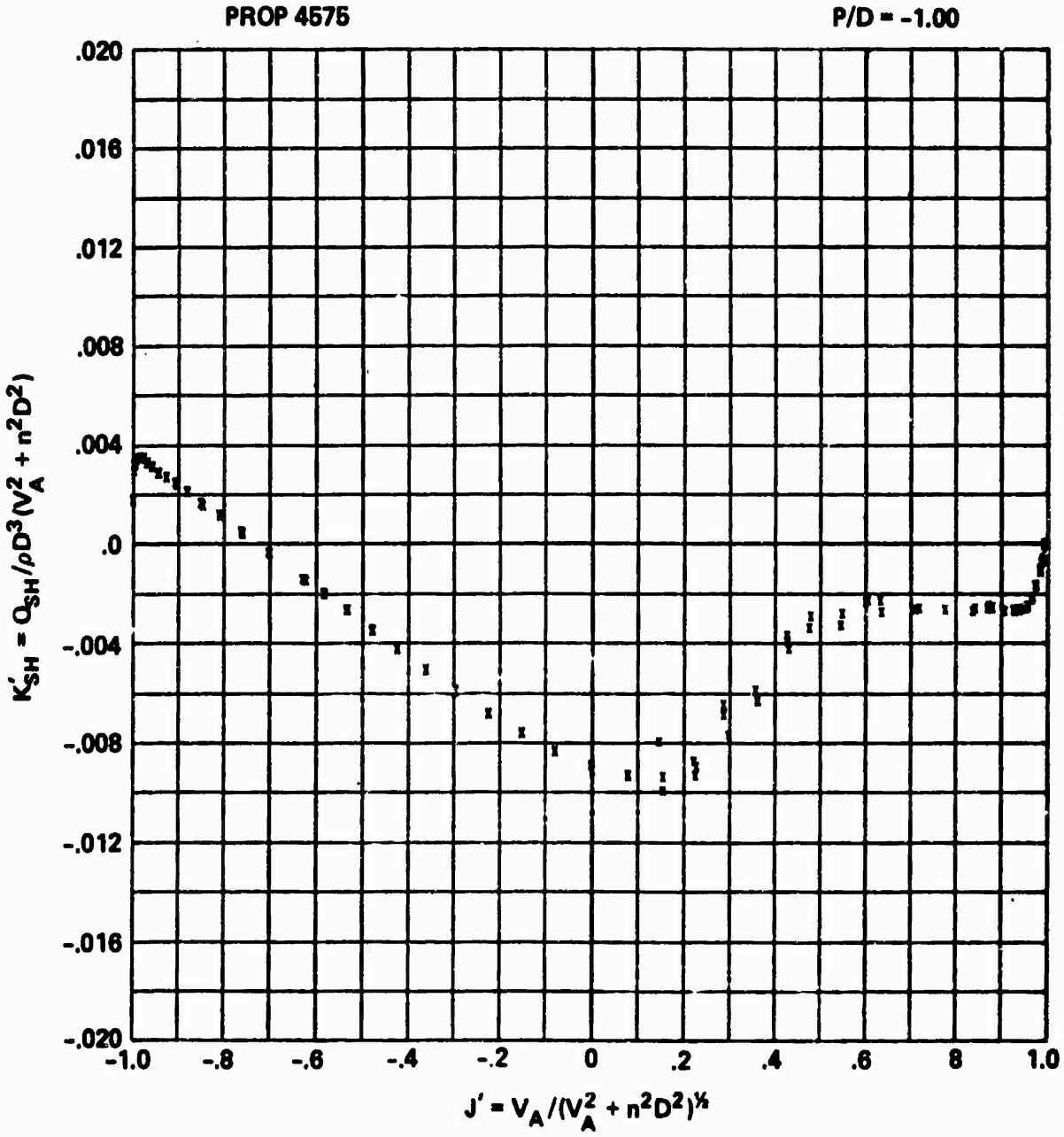

Figure 21g - At P/D = -1.00

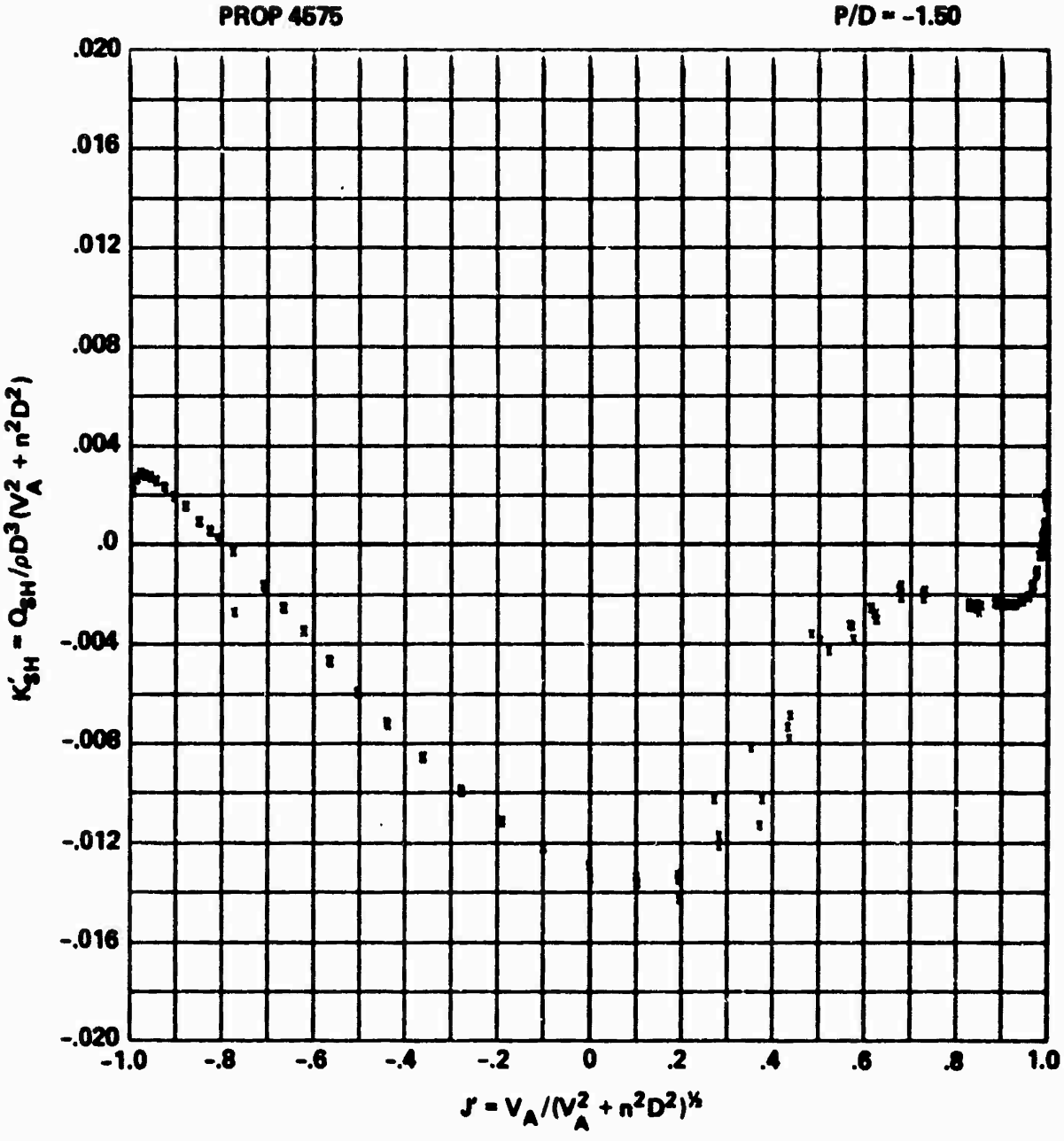

Figure 21h - At P/D = -1.50

Figure 22 - Variation of Hydrodynamic Blade Spindle Torque Index K^*_{SH} with Advance Angle β* for Propeller 4572

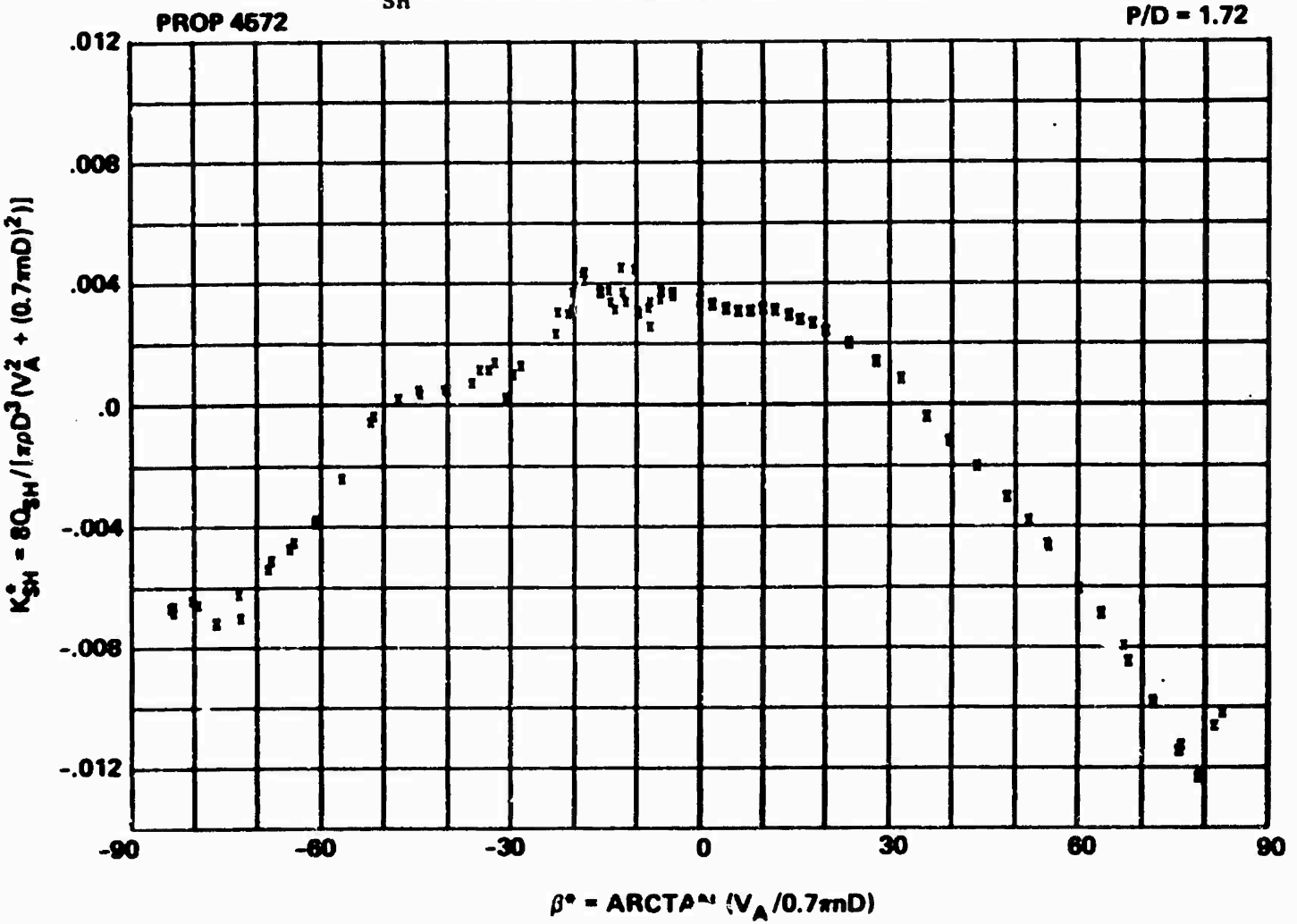

Figure 22a - At P/D = 1.72

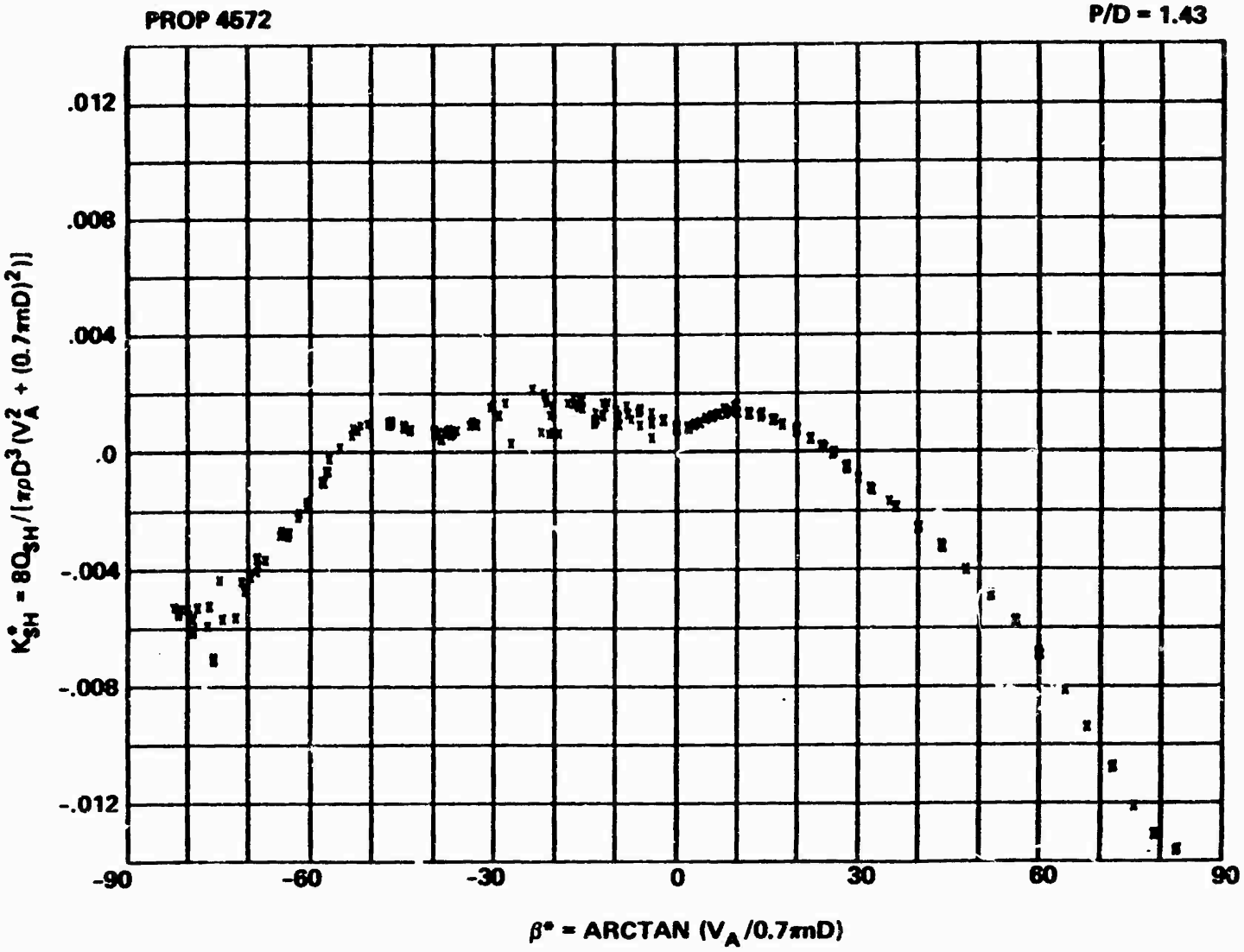

Figure 22b - At P/D = 1.43

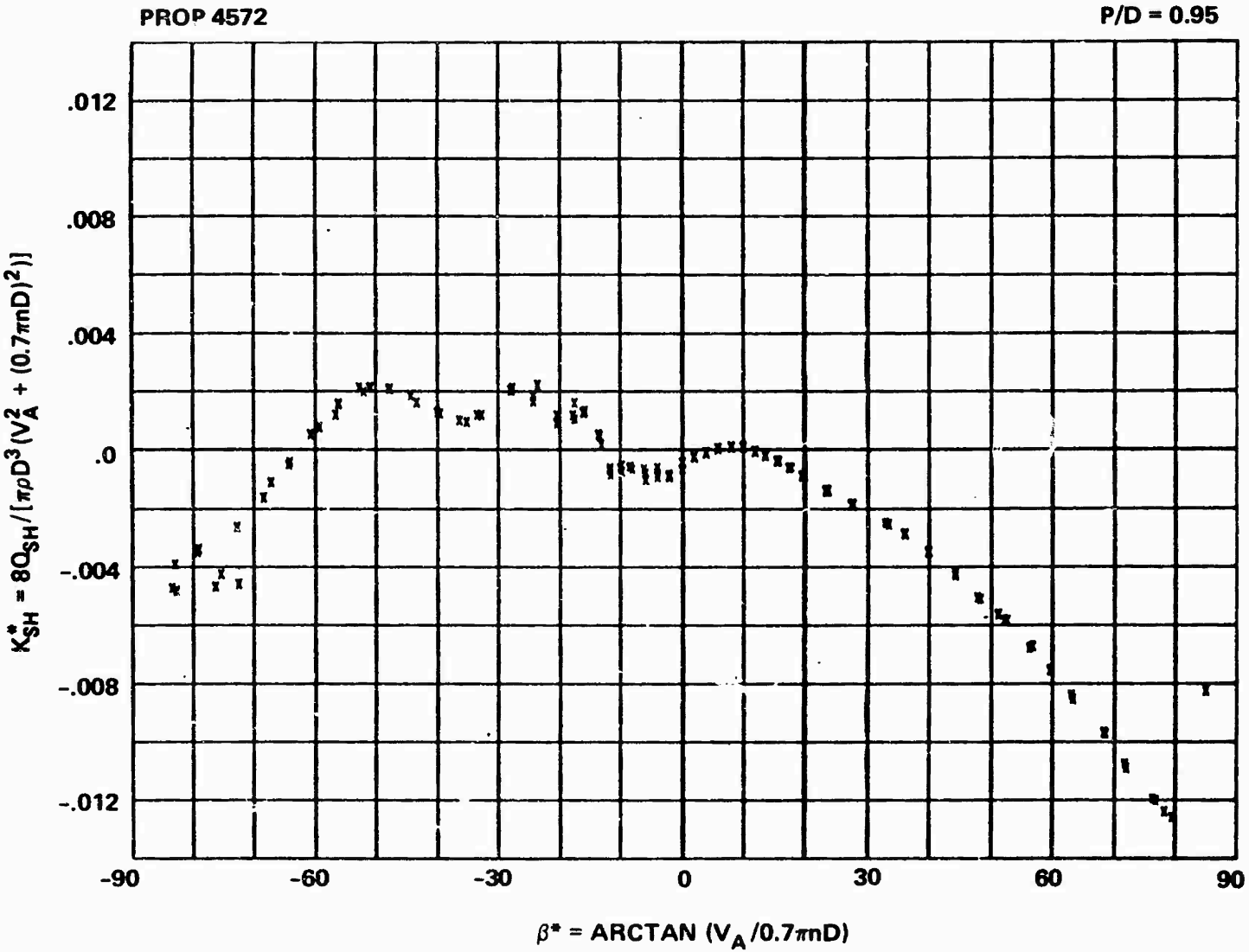

Figure 22c - At P/D = 0.95

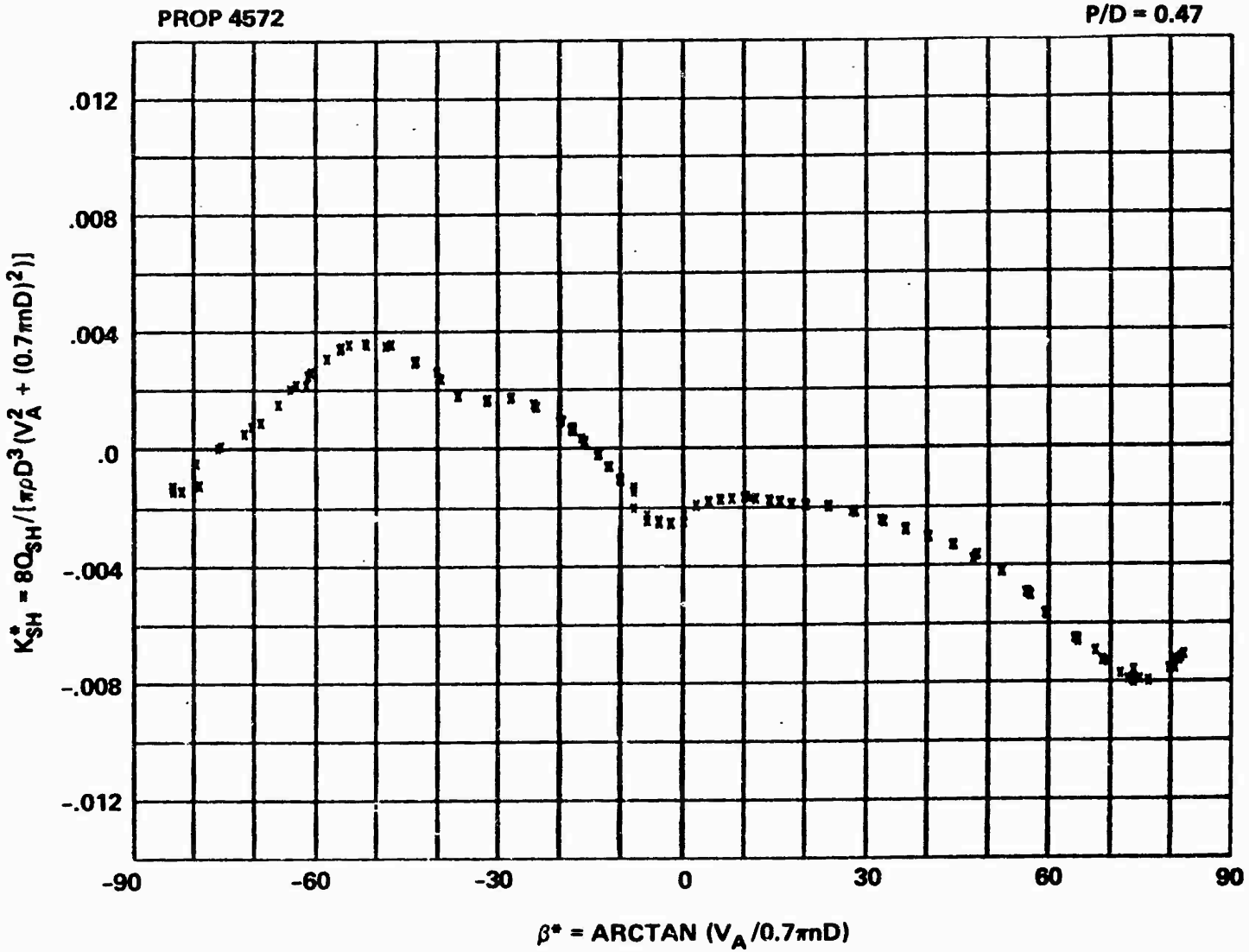

Figure 22d - At P/D = 0.47

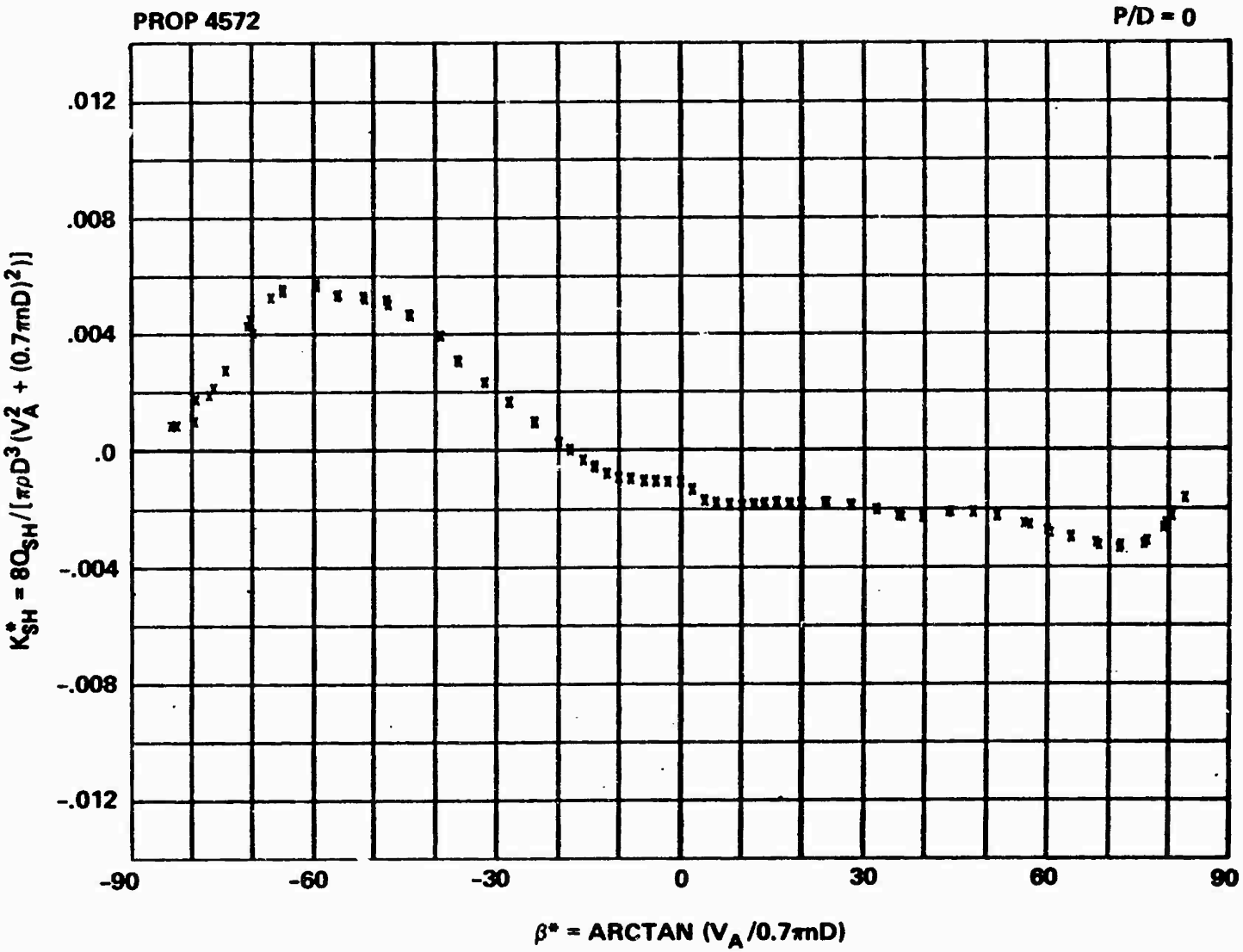

Figure 22e - At P/D = 0

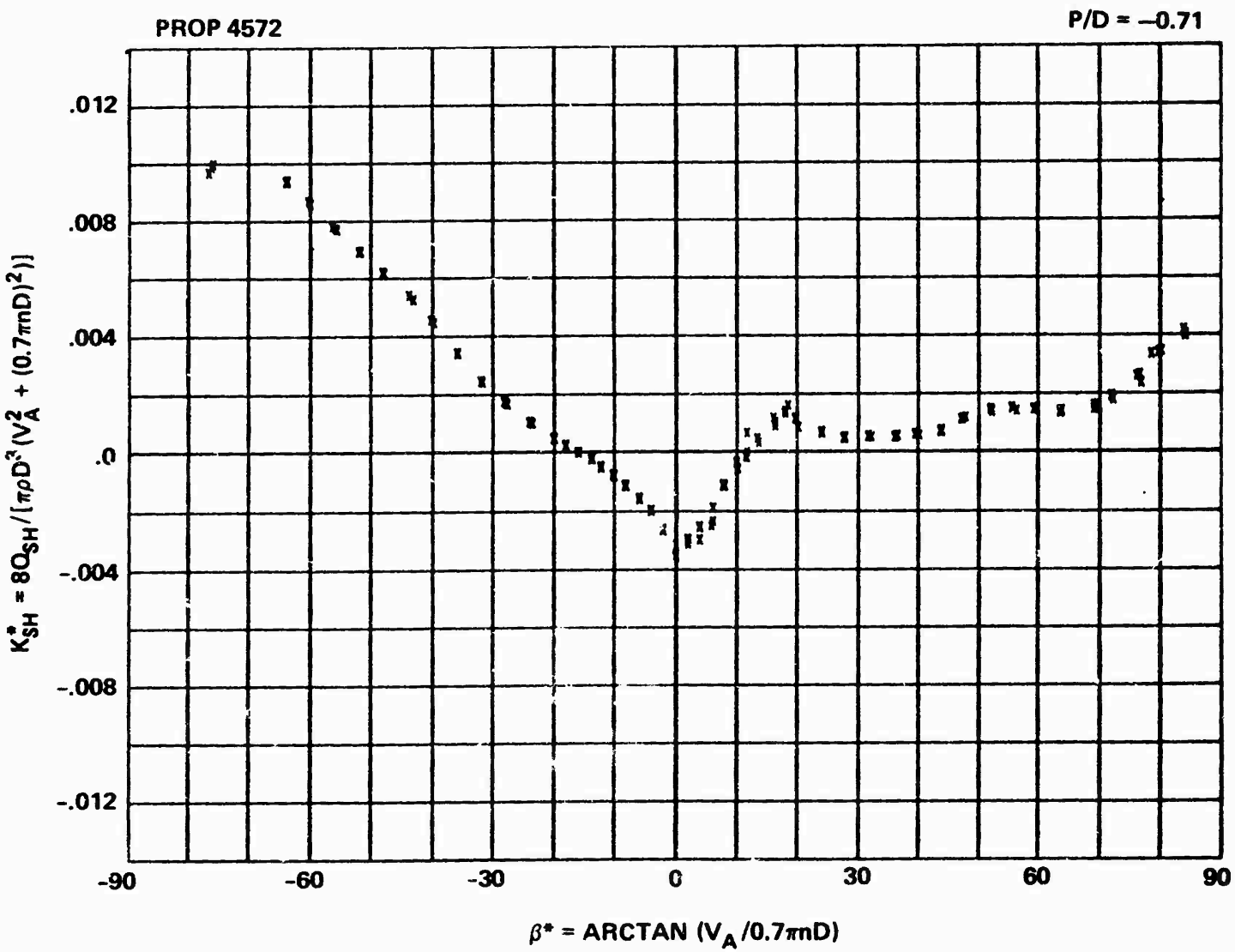

Figure 22f - At P/D = -0.71

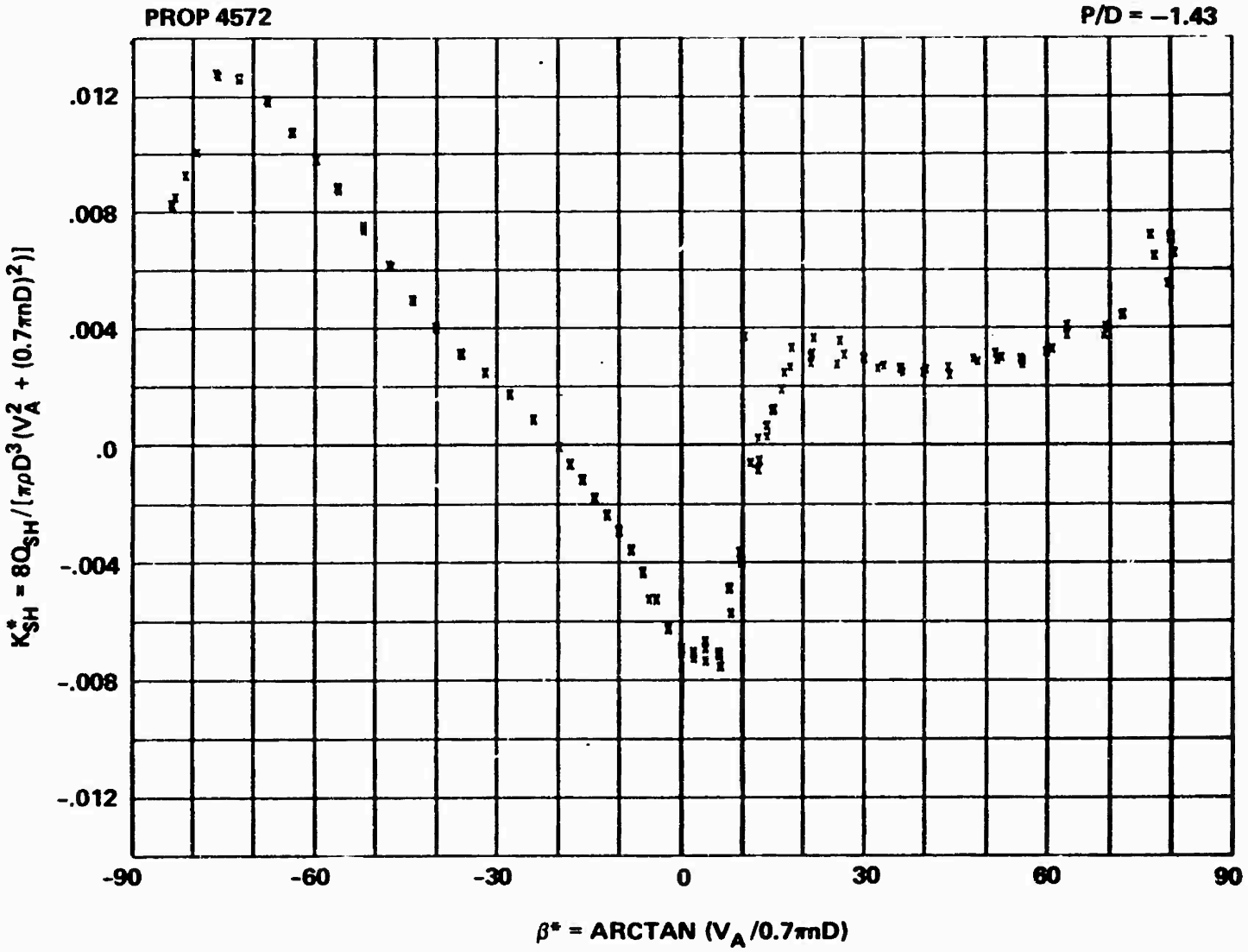

Figure 22g - At P/D = -1.43

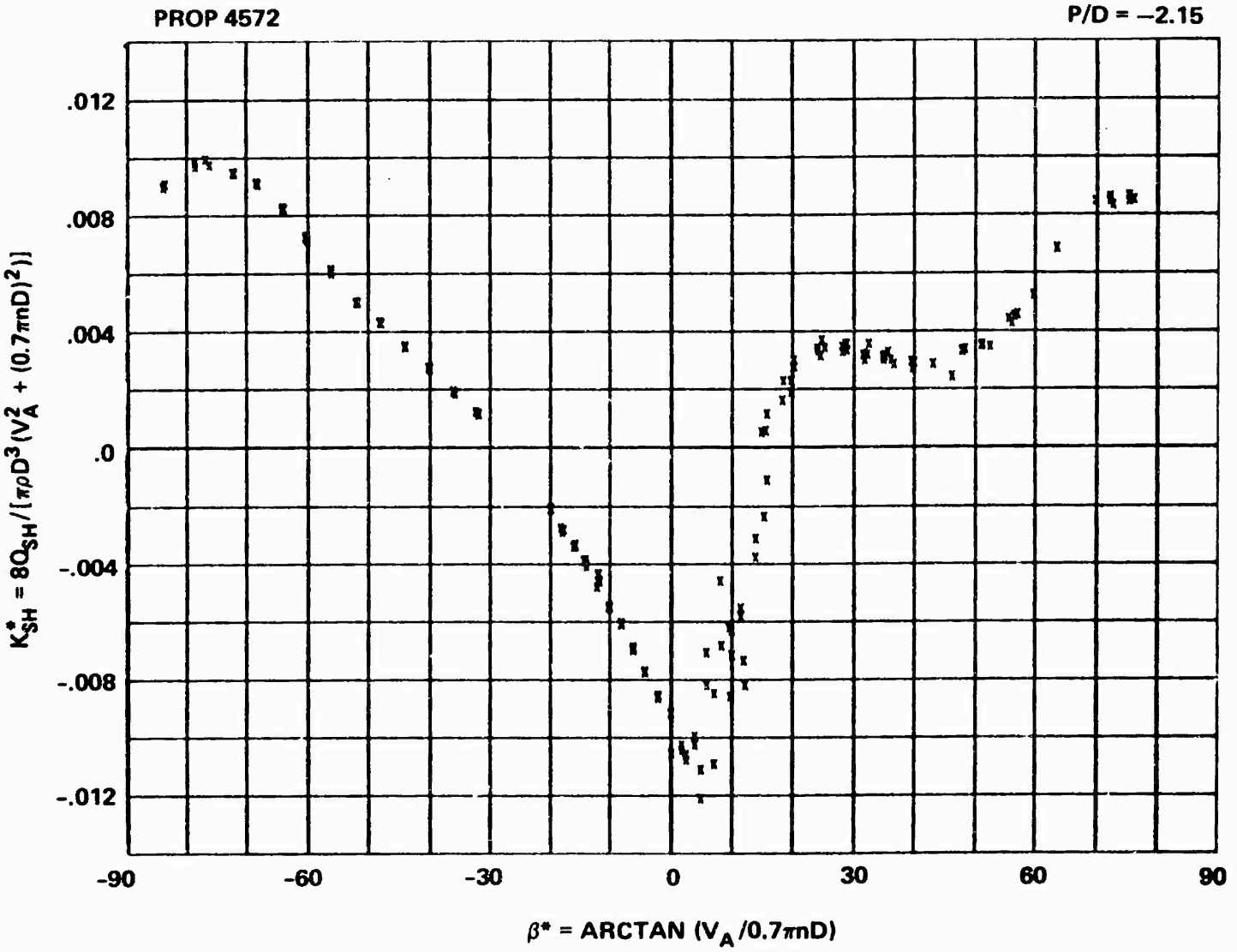

Figure 22h – At P/D = –2.15

Figure 23 - Variation of Hydrodynamic Blade Spindle Torque Index K^*_{SH} with Advance Angle β^* for Propeller 4575

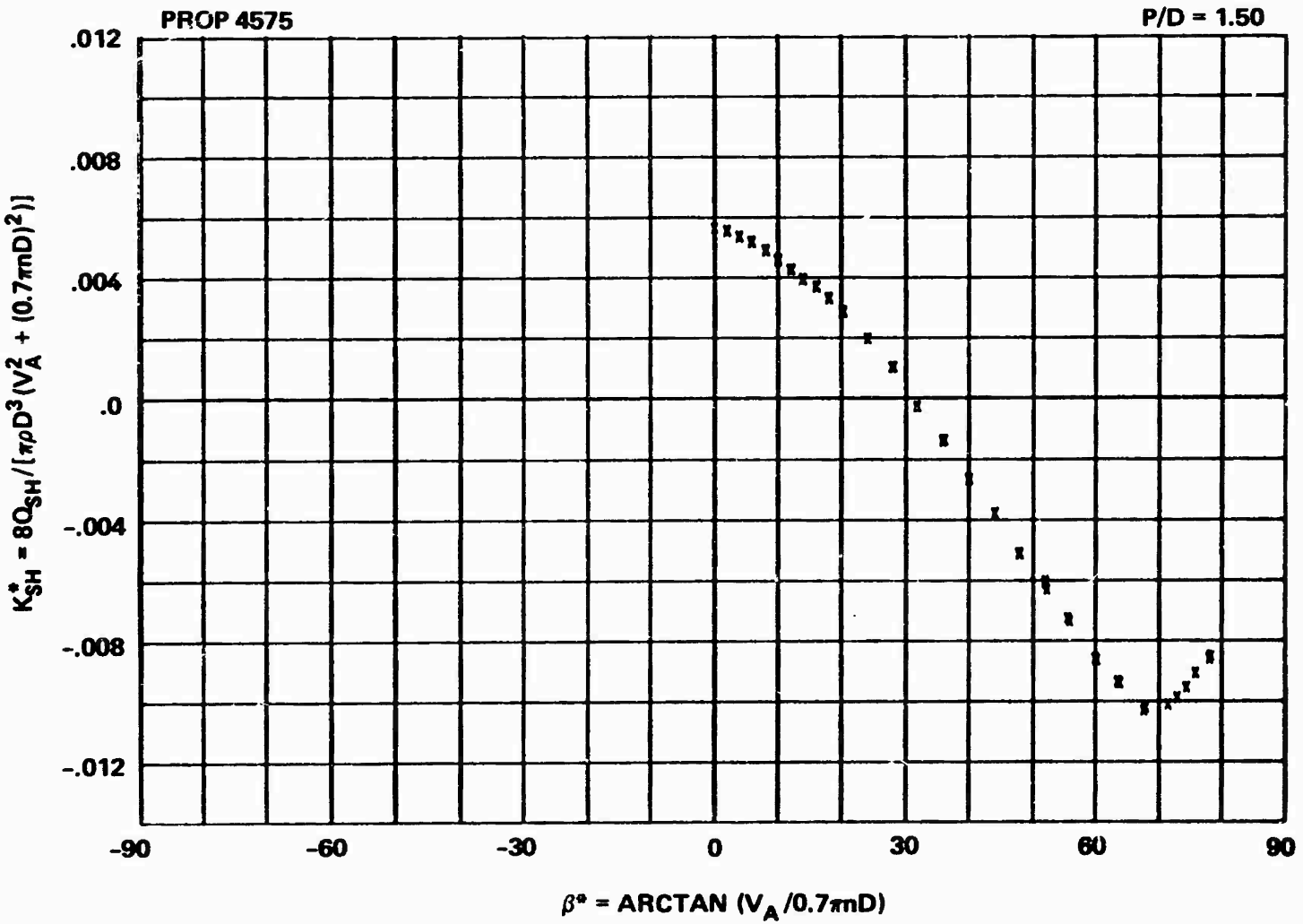

Figure 23a - At P/D = 1.50

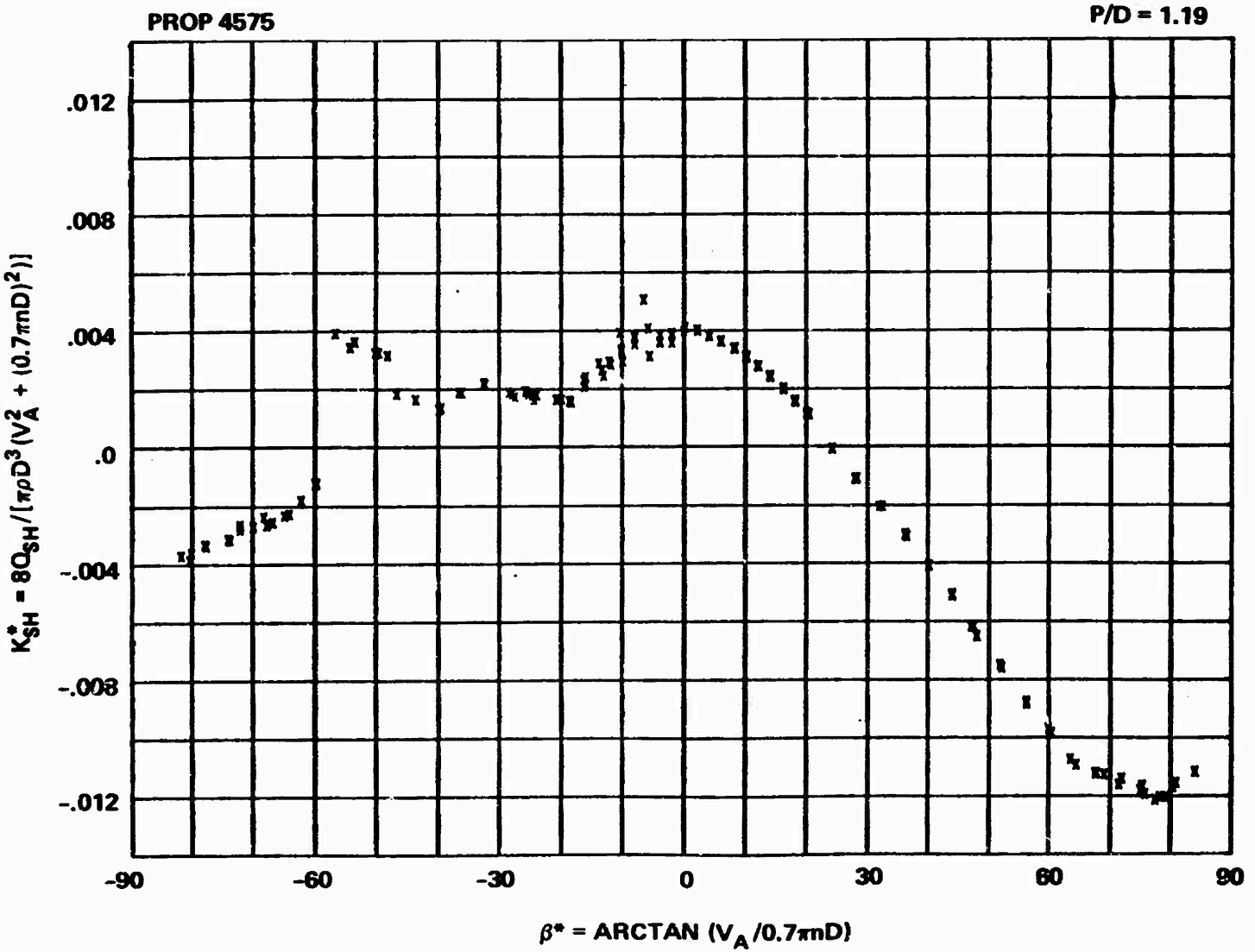

Figure 23b - At P/D = 1.19

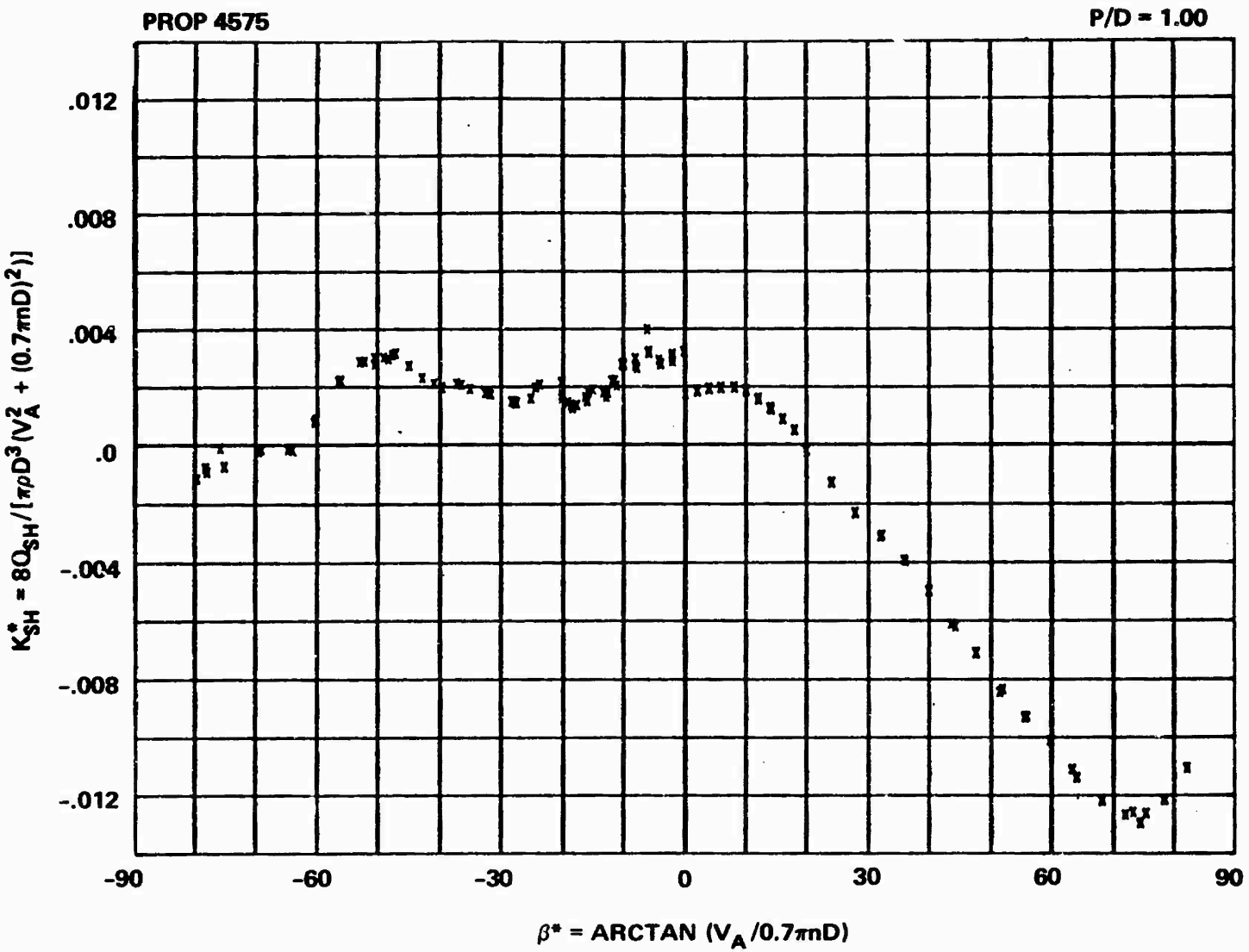

Figure 23c - At P/D = 1.00

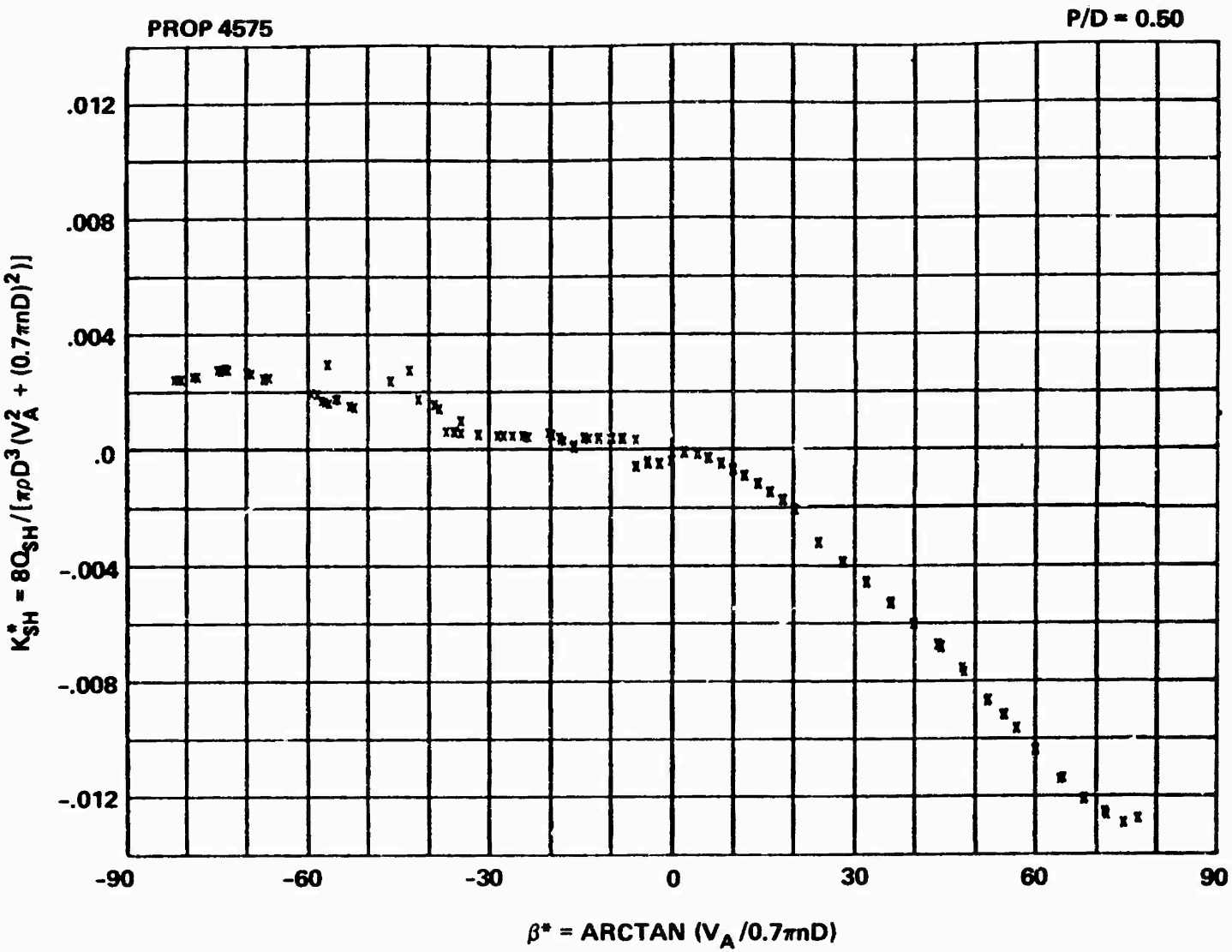

Figure 23d - At P/D = 0.50

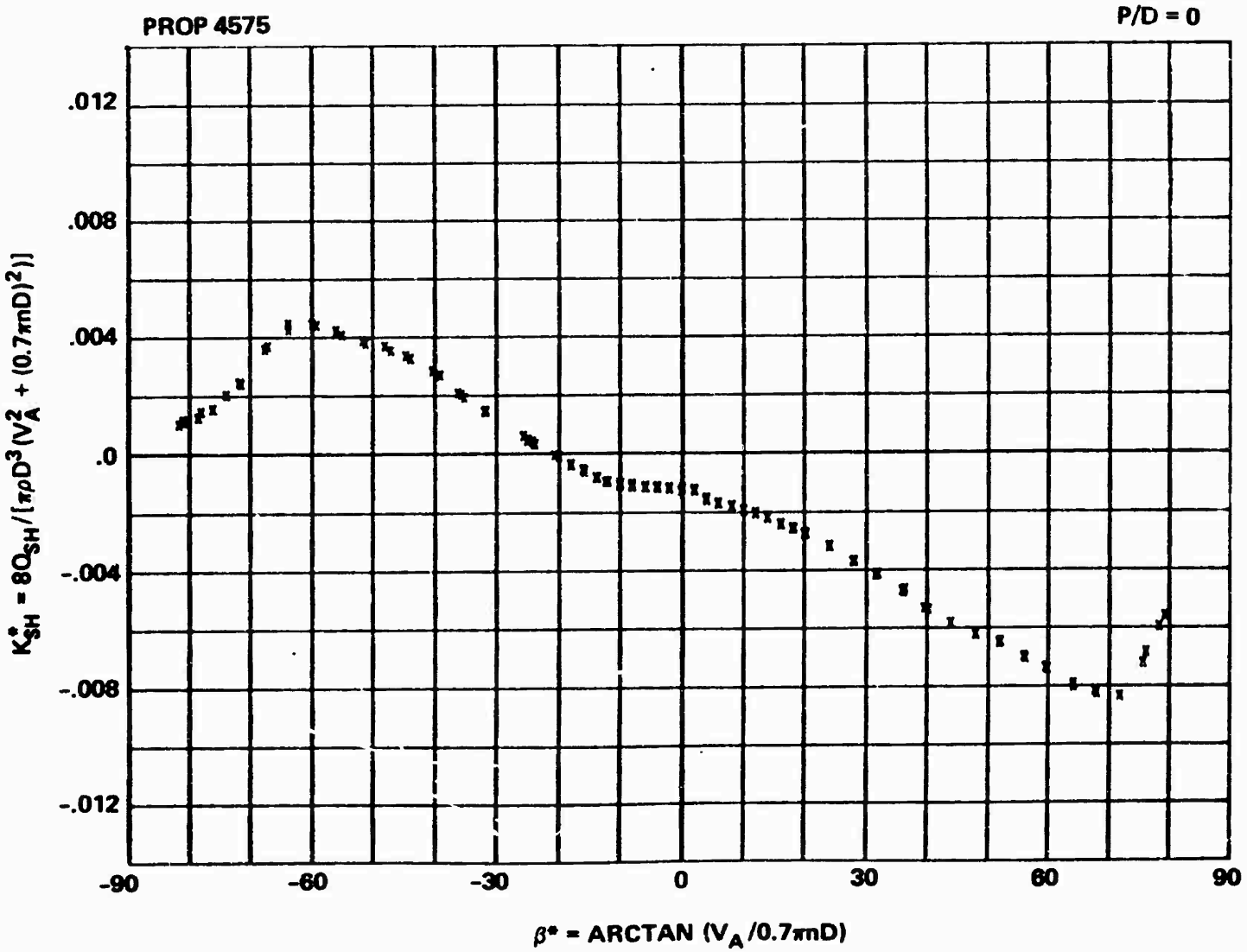

Figure 23e - At P/D = 0

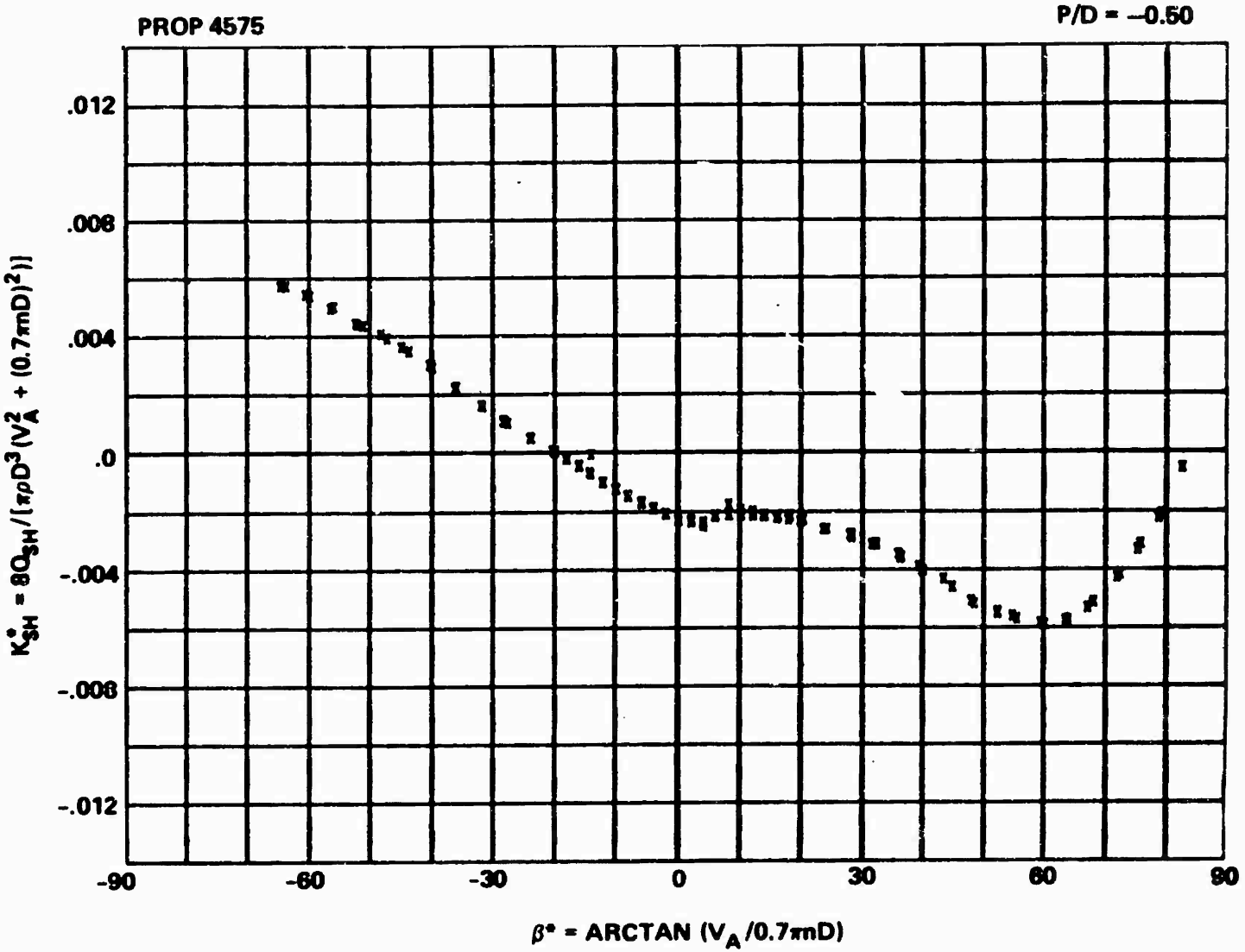

Figure 23f - At P/D = -0.50

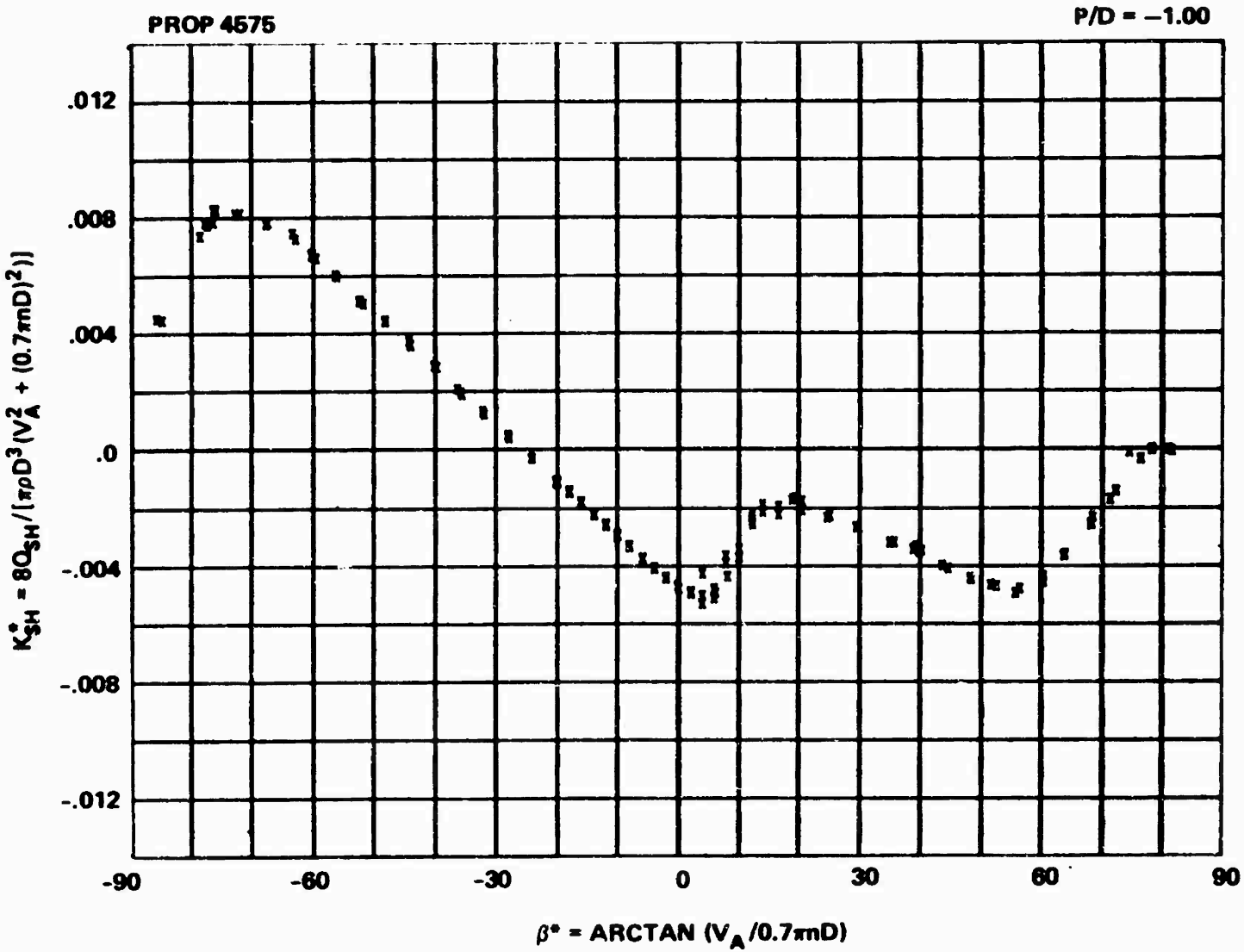

Figure 23g - At P/D = -1.00

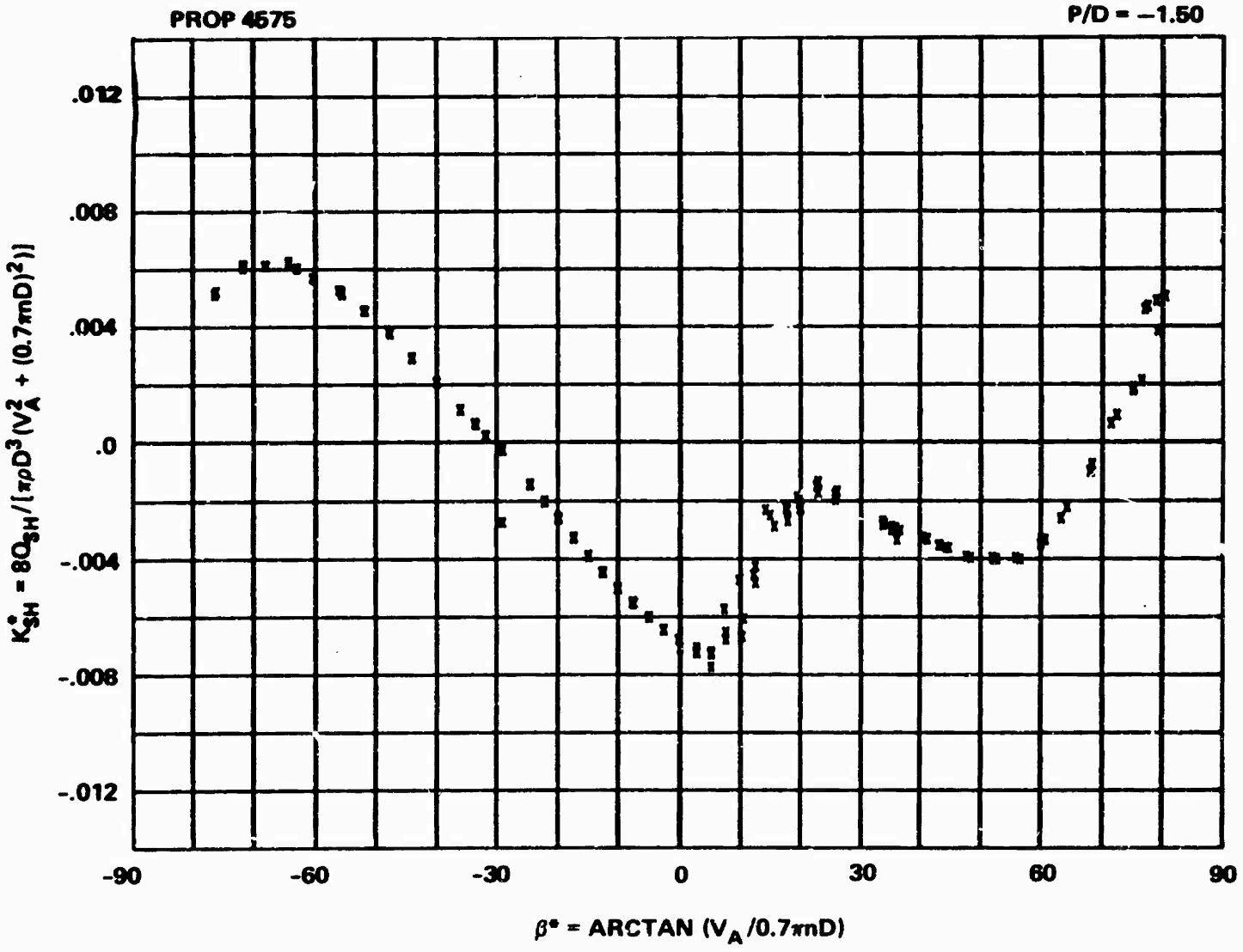

Figure 23h - At P/D = -1.50

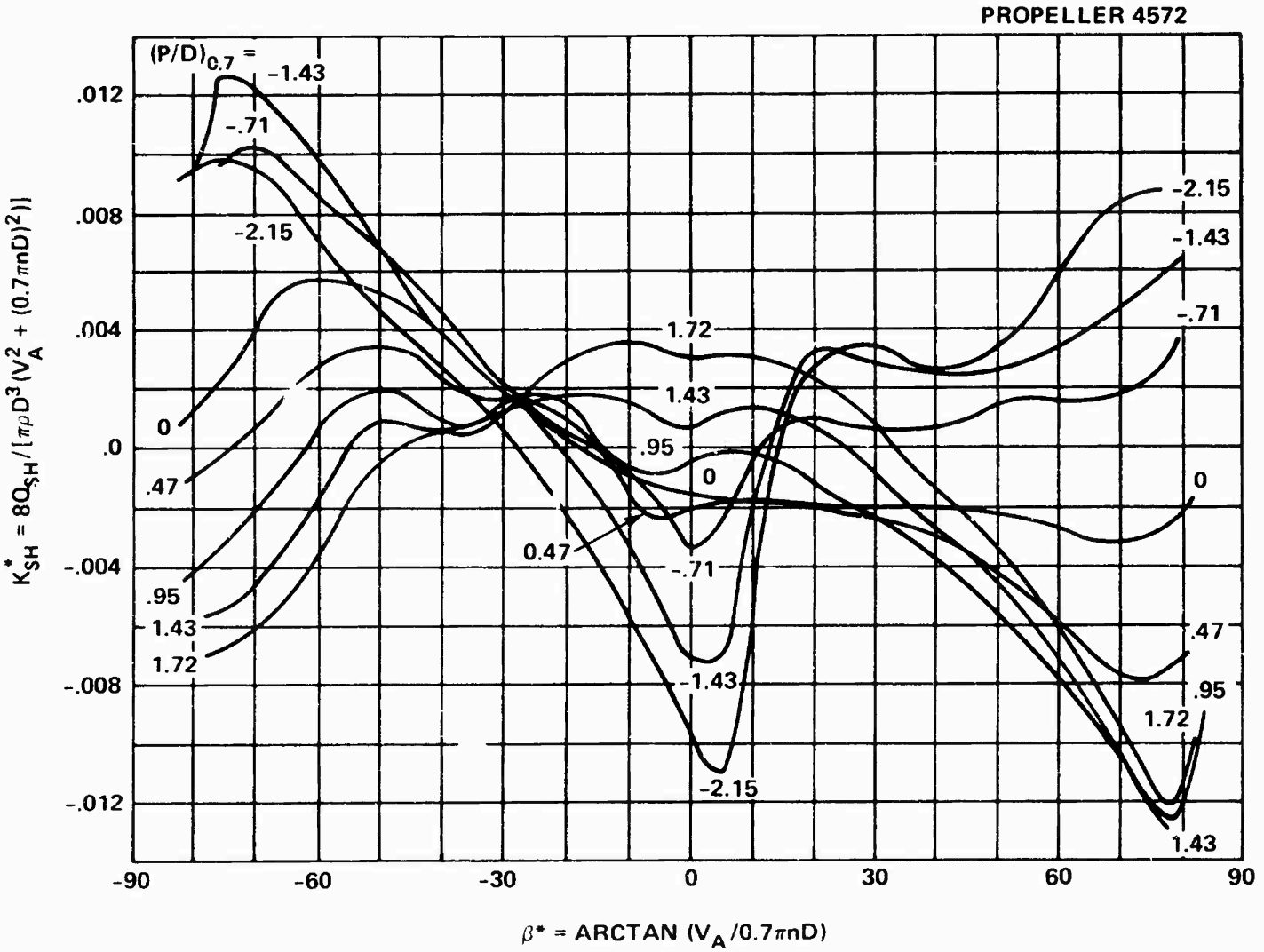

Figure 24 - Faired Experimental Results Showing Variation of Blade Spindle Torque Index K^*_{SH} with Advance Angle β^* and Pitch Ratio $(P/D)_{0.7}$ for Propeller 4572

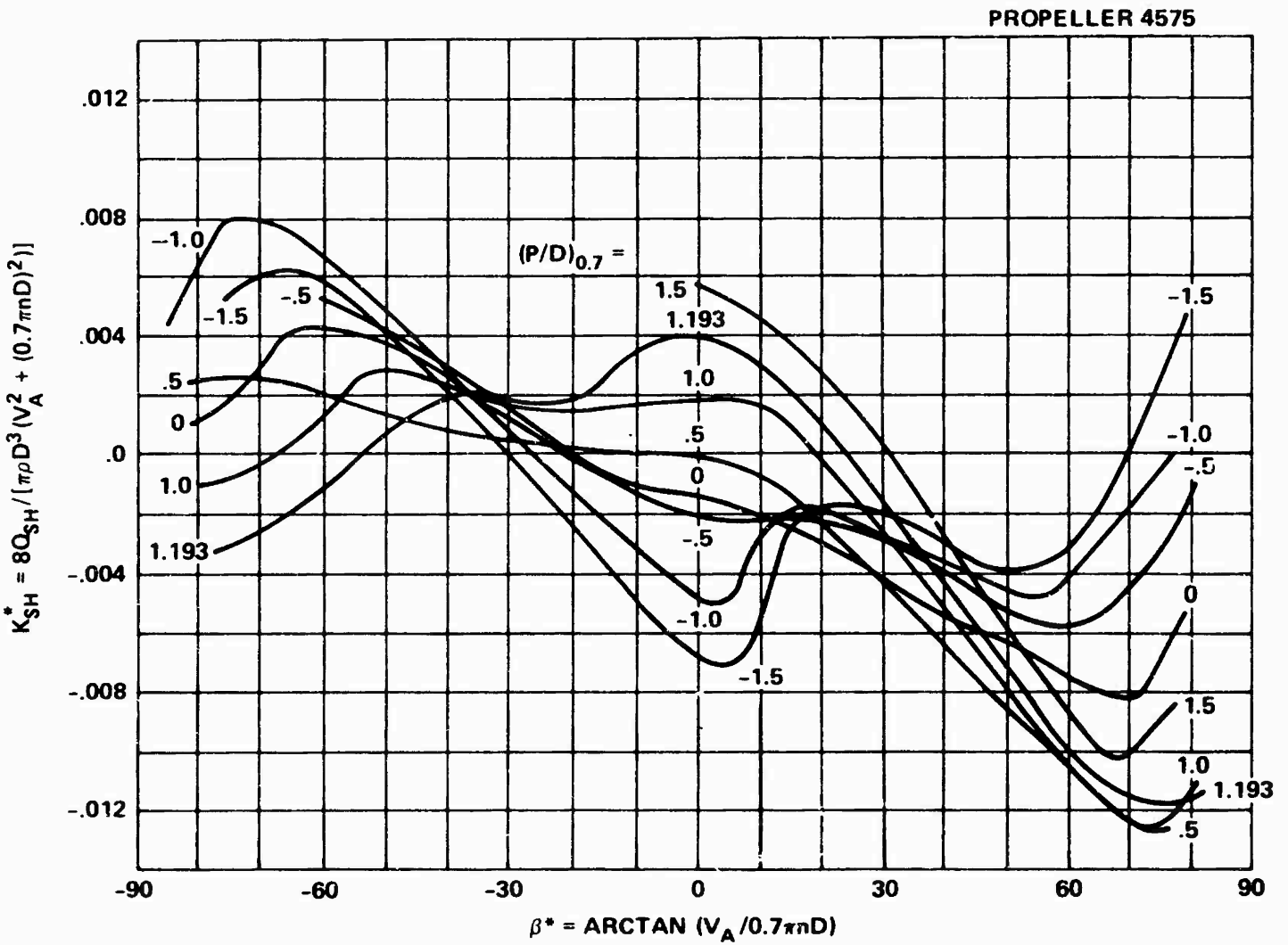

Figure 25 - Faired Experimental Results Showing Variation of Blade Spindle Torque Index K^*_{SH} with Advance Angle β^* and Pitch Ratio $(P/D)_{0.7}$ for Propeller 4575

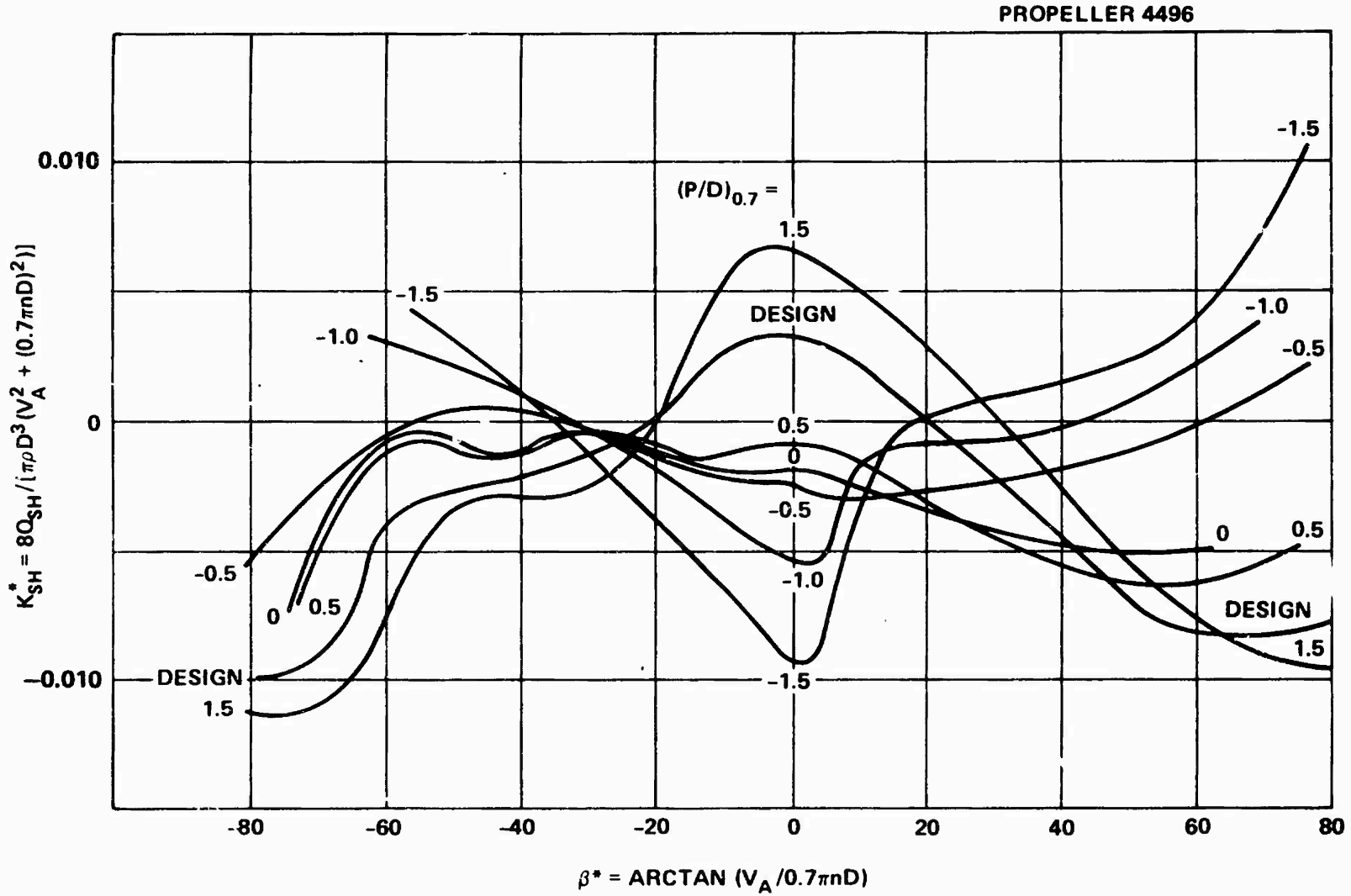

Figure 26 - Faired Experimental Results Showing Variation of Blade Spindle Torque Index K^*_{SH} with Advance Angle β^* and Pitch Ratio $(P/D)_{0.7}$ for Propeller 4496

(From Figure 7 in Denny and Stephens[16])

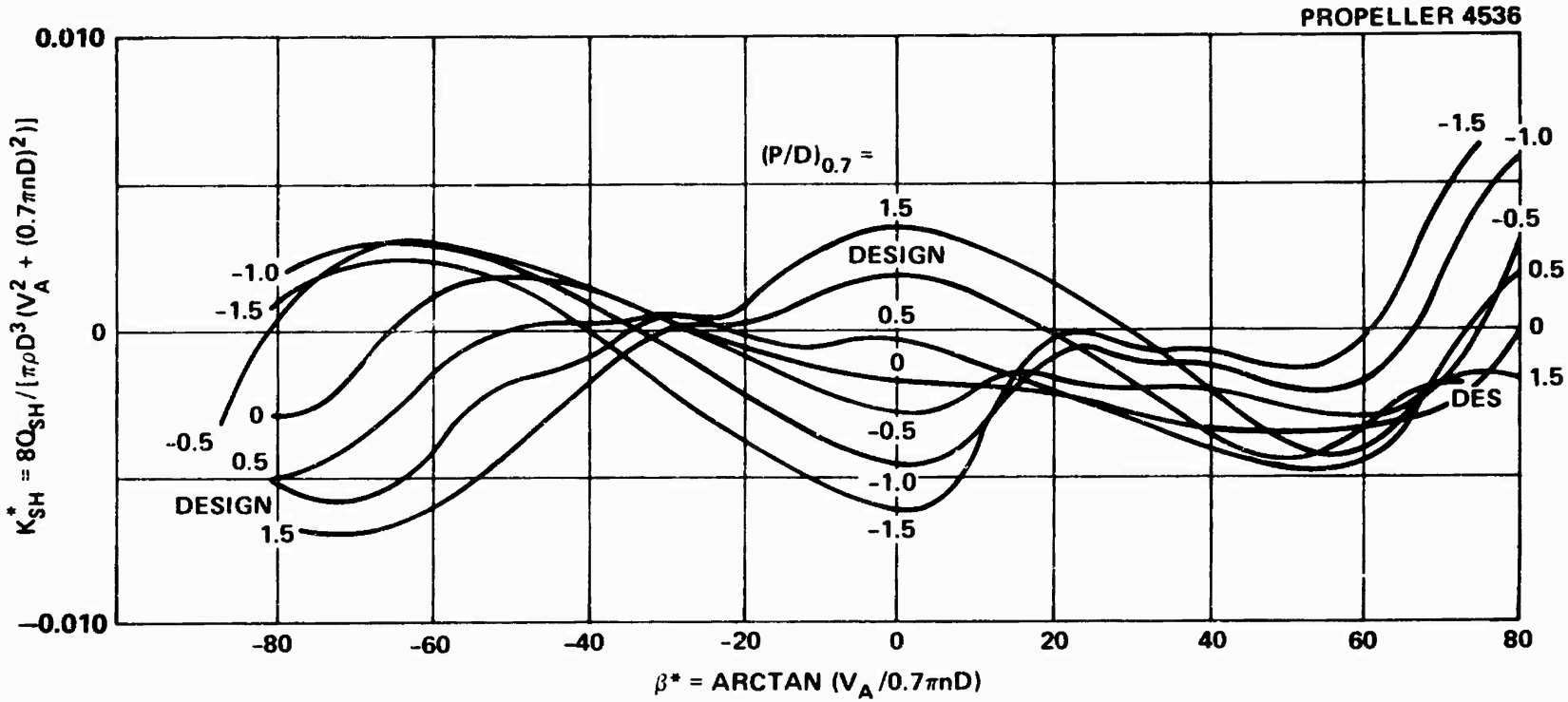

Figure 27 - Faired Experimental Results Showing Variations of Blade Spindle Torque Index K^*_{SH} with Advance Angle β* and Pitch Ratio $(P/D)_{0.7}$ for Propeller 4536

(From Figure 7 in Denny and Stephens[16])

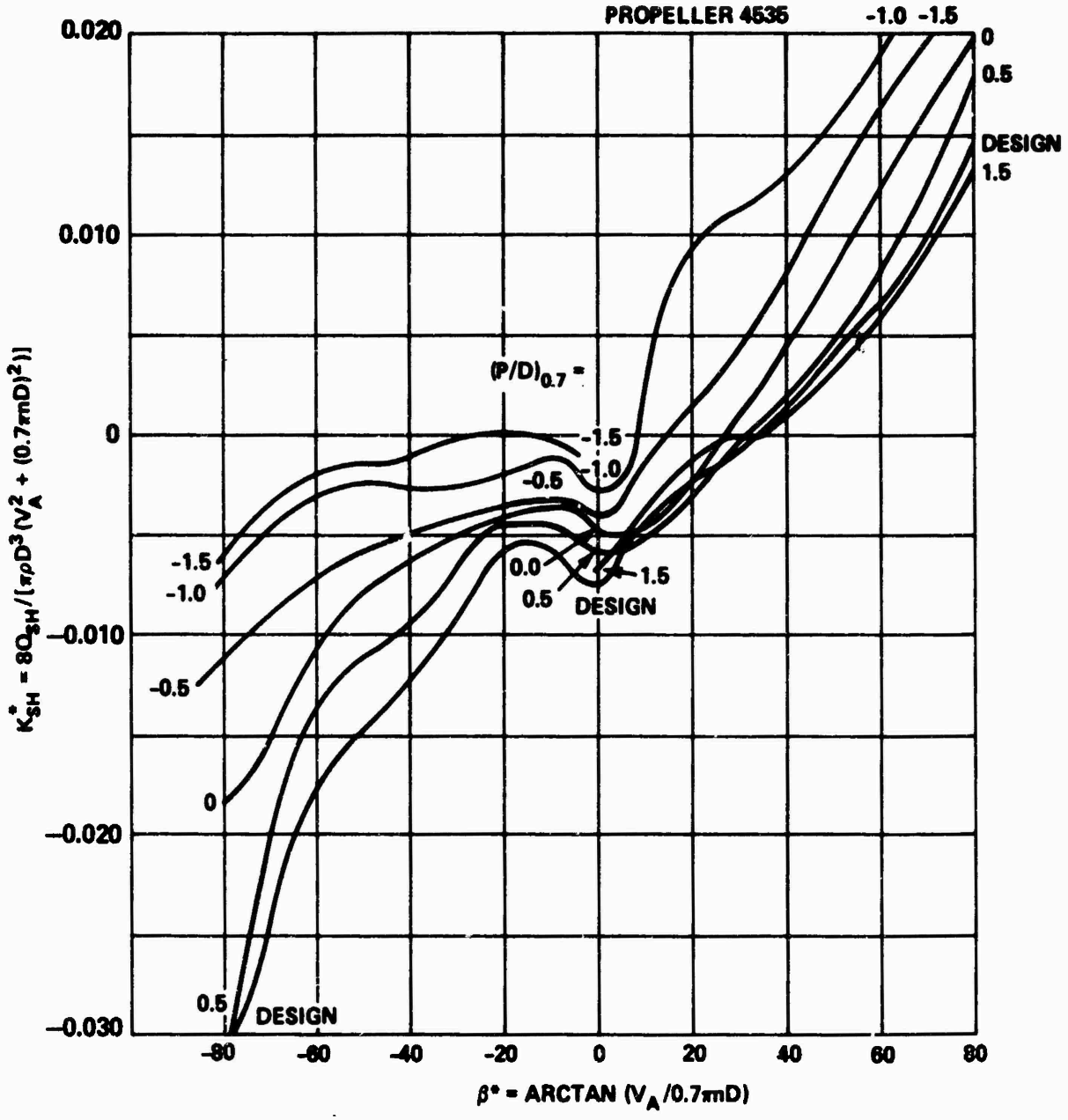

Figure 28 - Faired Experimental Results Showing Variation of Blade Spindle Torque Index K^*_{SH} with Advance Angle β^* and Pitch Ratio $(P/D)_{0.7}$ for Propeller 4535

(From Figure 7 in Denny and Stephens[16])

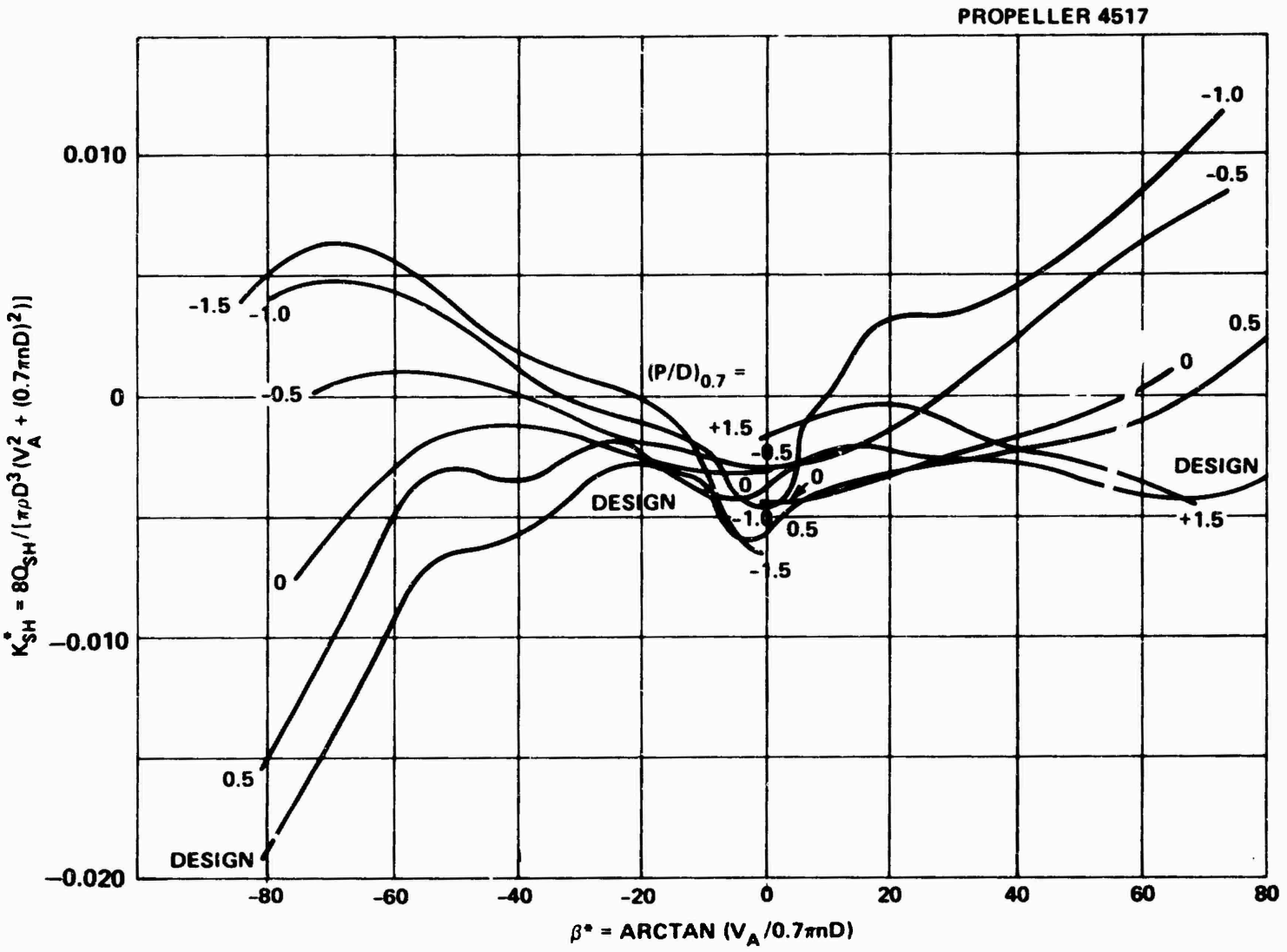

Figure 29 - Faired Experimental Results Showing Variation of Blade Spindle Torque Index K^*_{SH} with Advance Angle β^* and Pitch Ratio $(P/D)_{0.7}$ for Propeller 4517

(From Figure 7 in Denny and Stephens[16])

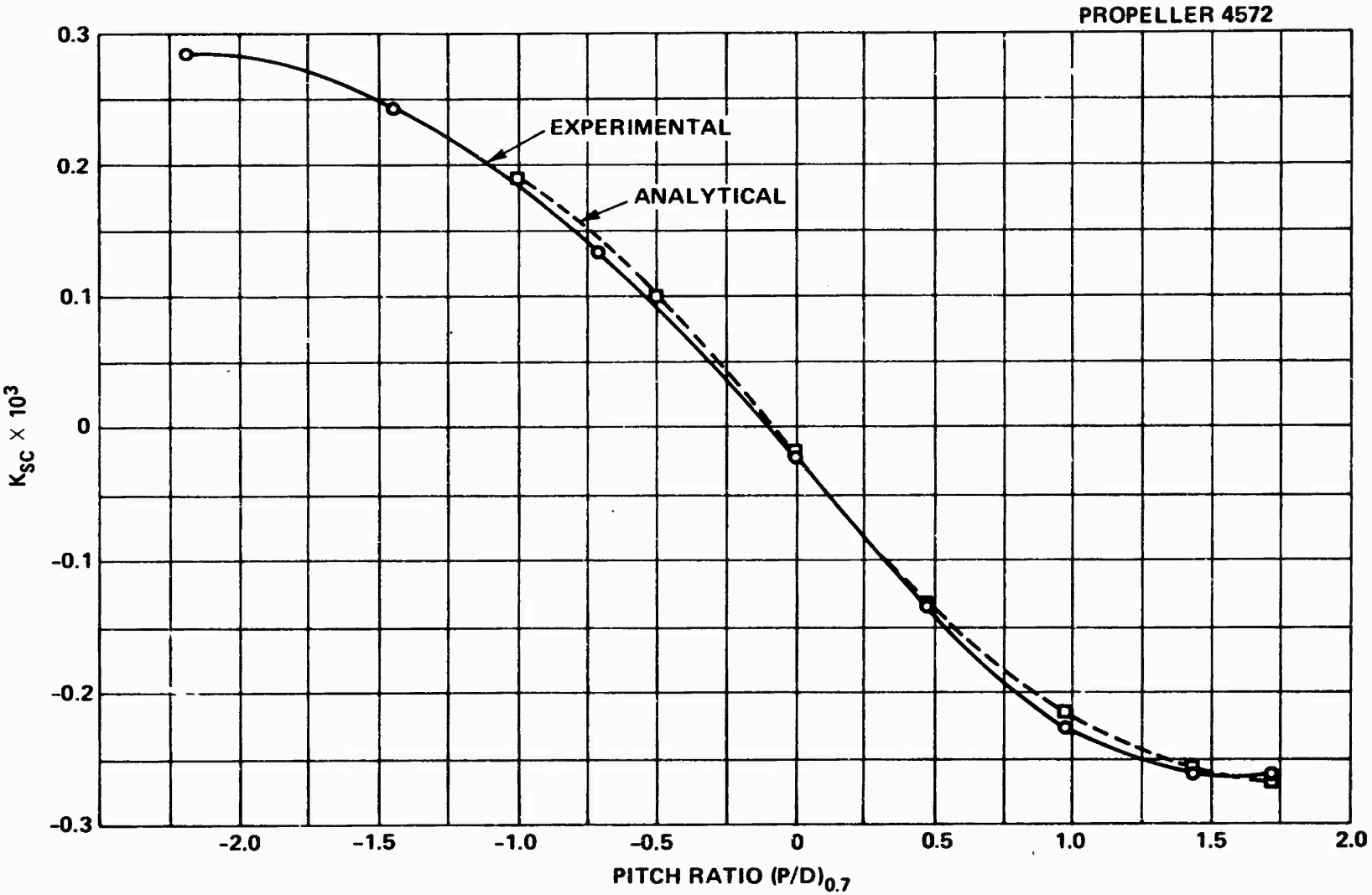

Figure 30 - Variation of Centrifugal Blade Spindle Torque Coefficient K_{SC} with Pitch Ratio $(P/D)_{0.7}$ for Propeller 4572

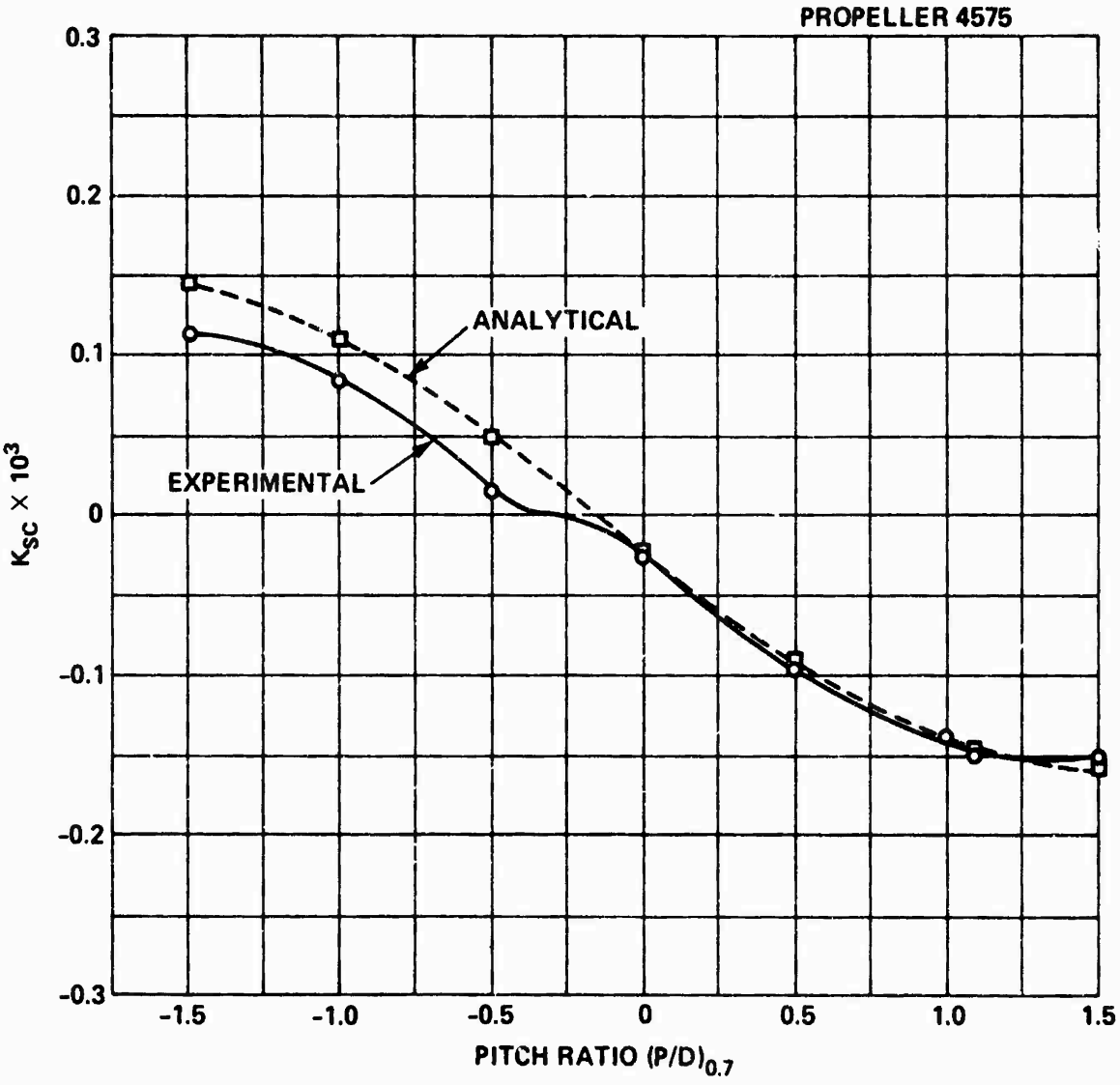

Figure 31 - Variation of Centrifugal Blade Spindle Torque Coefficient K_{SC} with Pitch Ratio $(P/D)_{0.7}$ for Propeller 4575

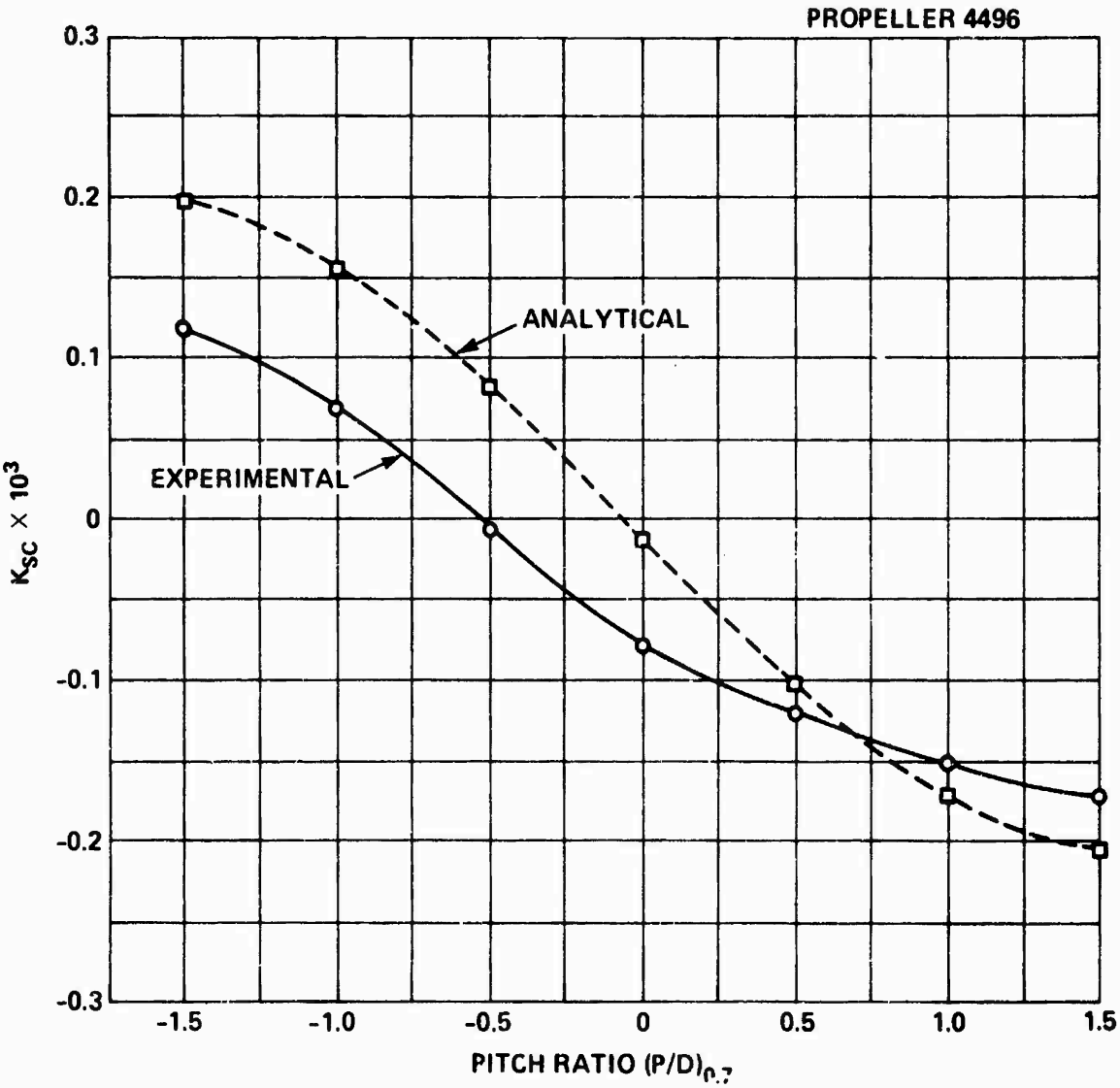

Figure 32 - Variation of Centrifugal Blade Spindle Torque Coefficient K_{SC} with Pitch Ratio $(P/D)_{0.7}$ for Propeller 4496

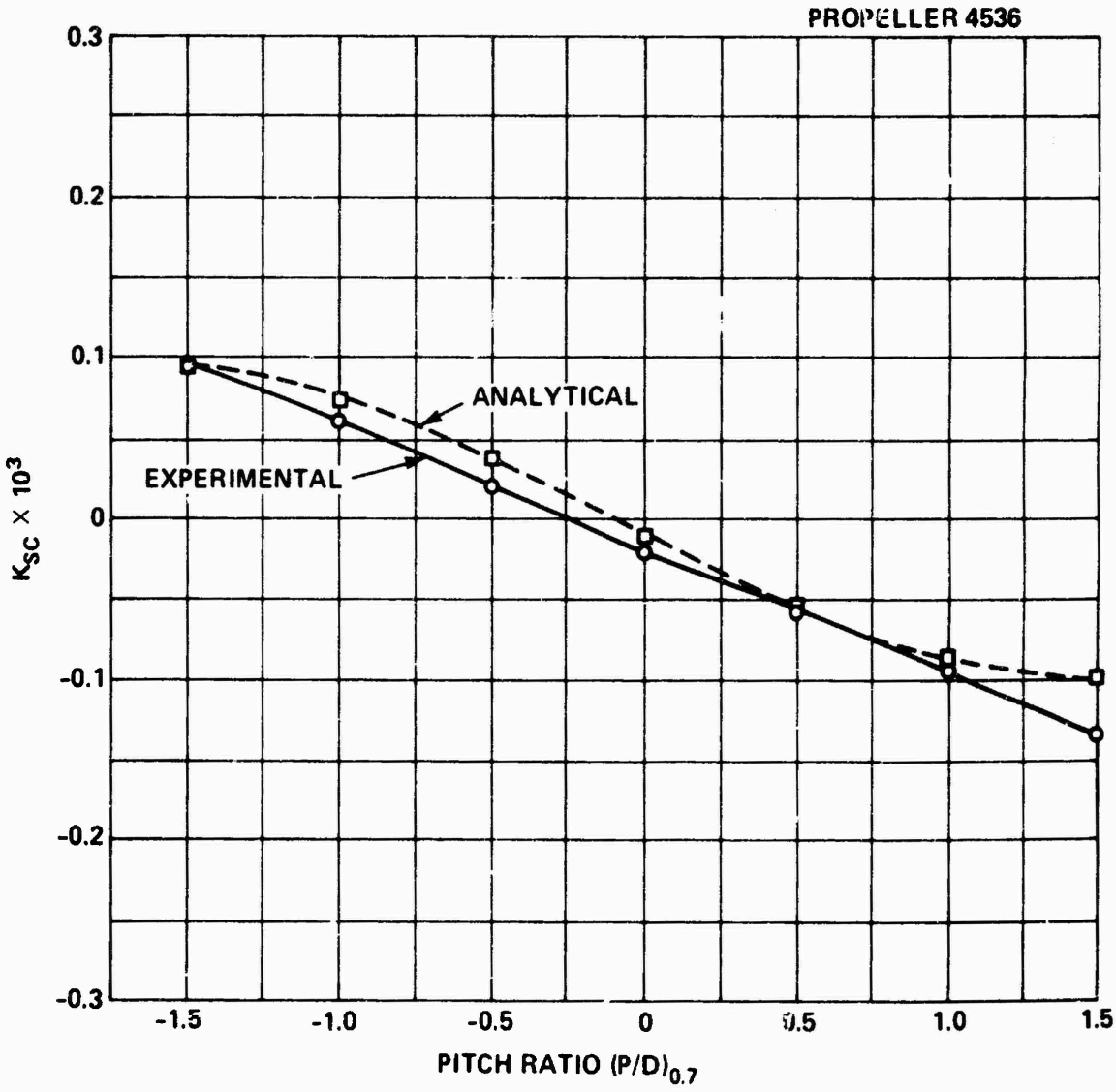

Figure 33 - Variation of Centrifugal Blade Spindle Torque Coefficient K_{SC} with Pitch Ratio $(P/D)_{0.7}$ for Propeller 4536

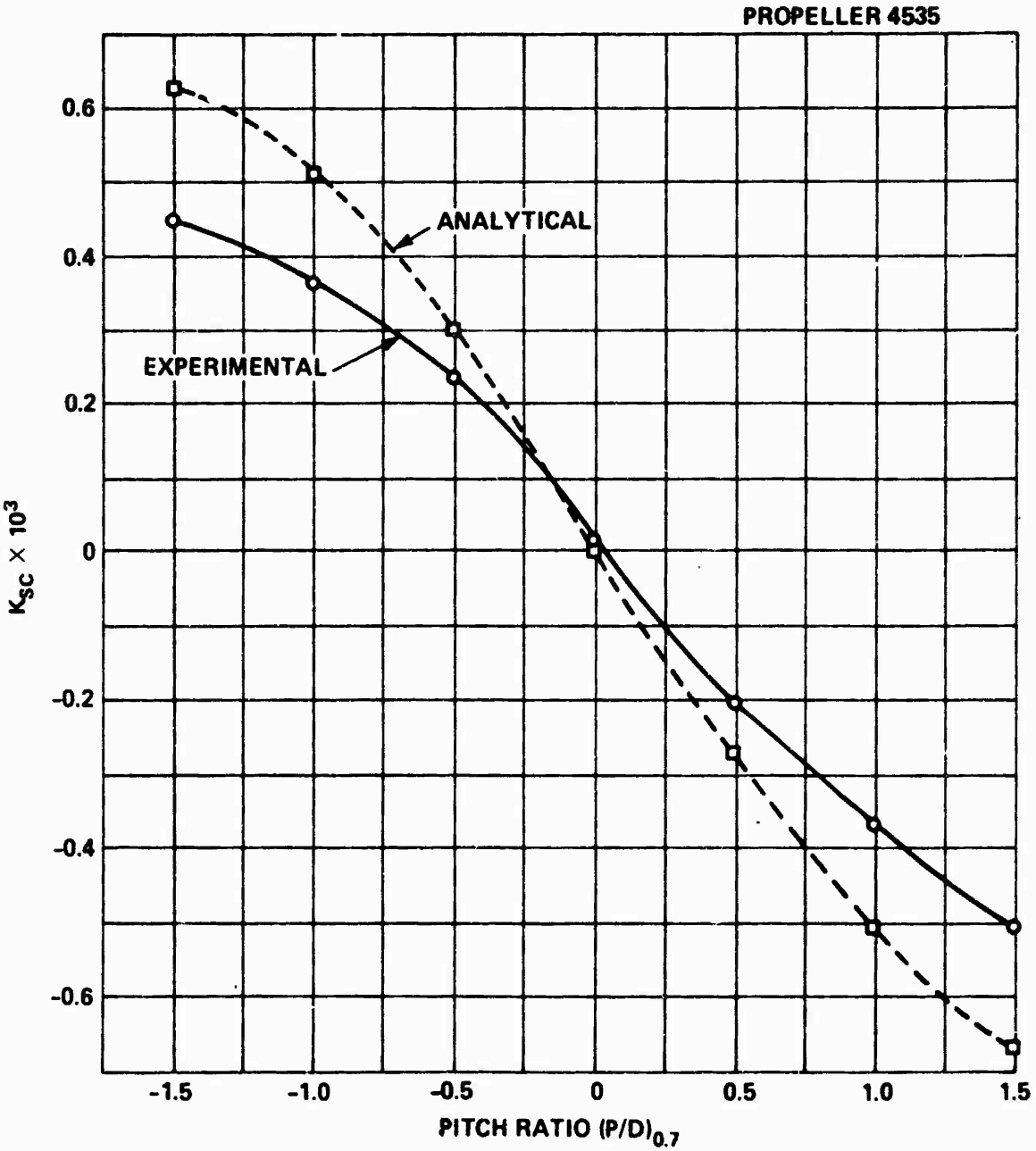

Figure 34 - Variation of Centrifugal Blade Spindle Torque Coefficient K_{SC} with Pitch Ratio $(P/D)_{0.7}$ for Propeller 4535

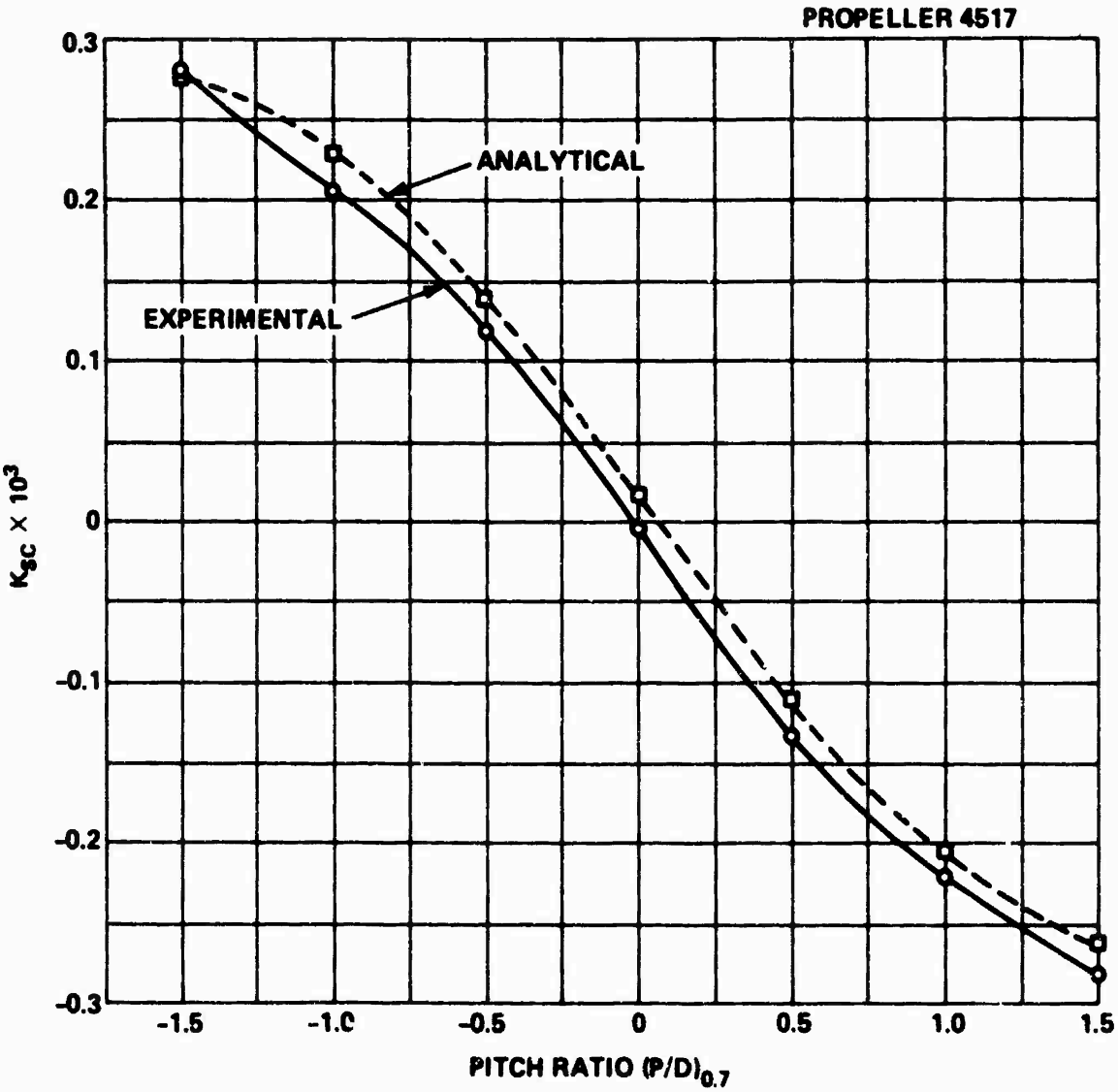

Figure 35 - Variation of Centrifugal Blade Spindle Torque Coefficient K_{SC} with Pitch Ratio $(P/D)_{0.7}$ for Propeller 4517

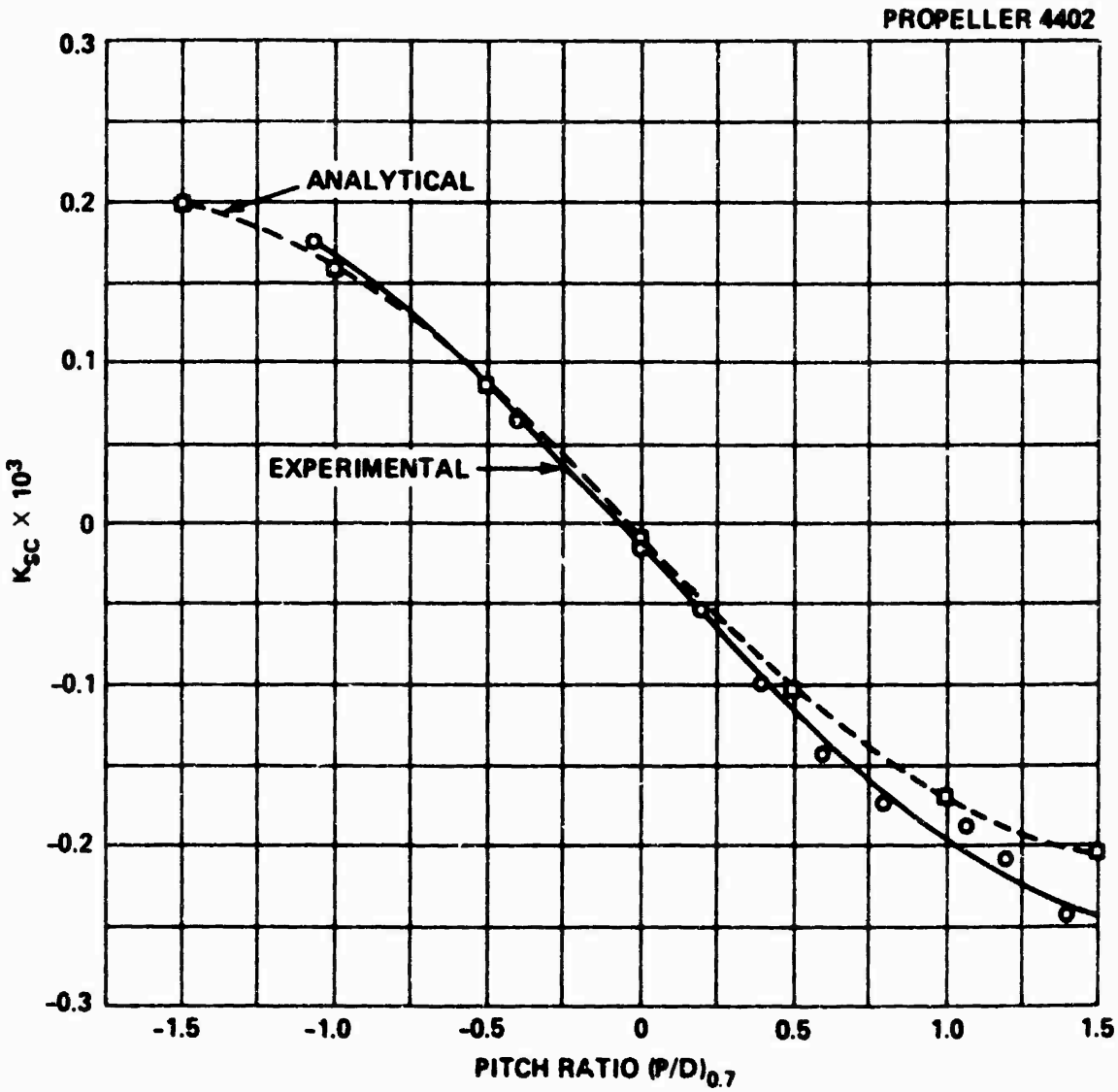

Figure 36 - Variation of Centrifugal Blade Spindle Torque Coefficient K_{SC} with Pitch Ratio $(P/D)_{0.7}$ for Propeller 4402

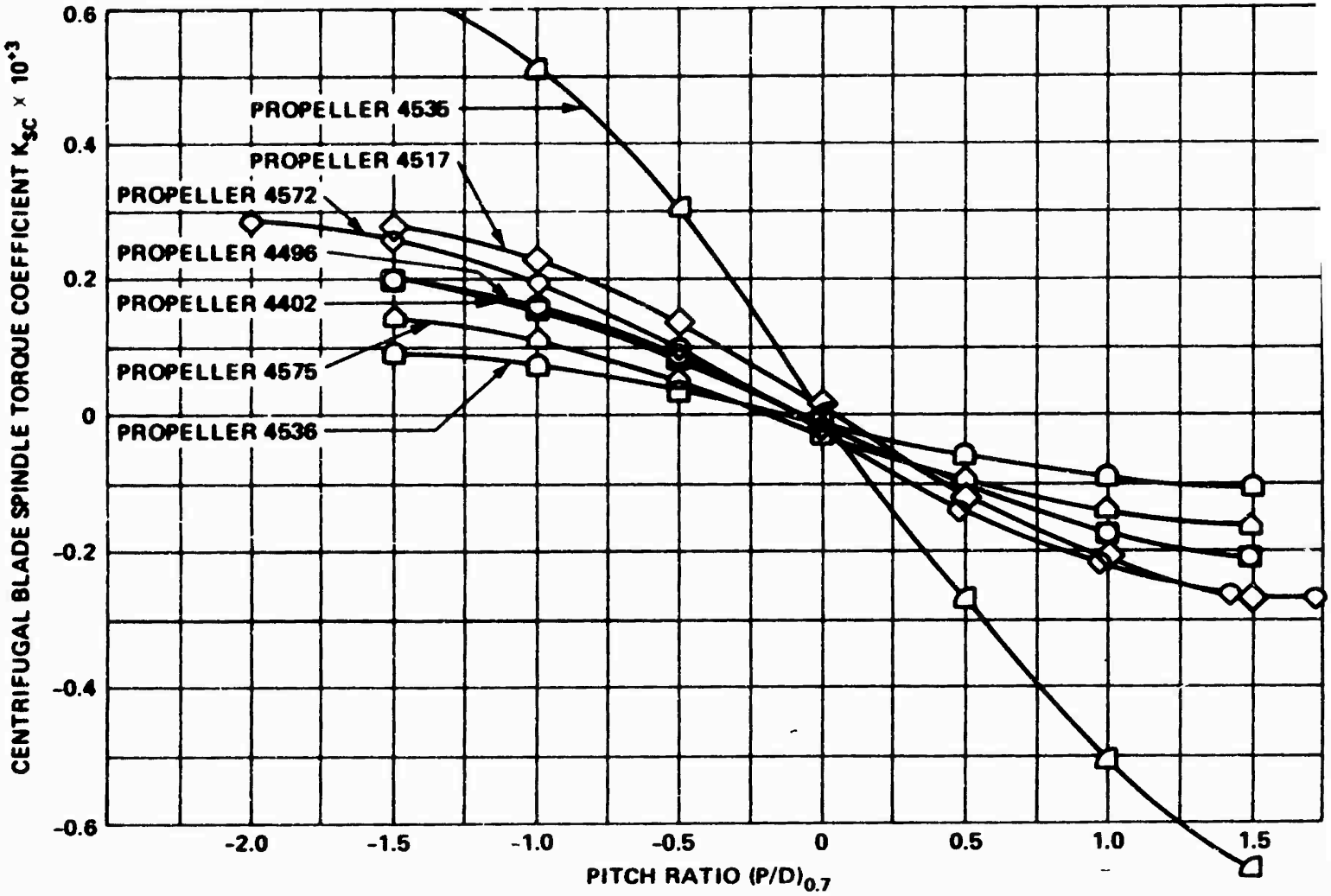

Figure 37 - Analytical Values of Centrifugal Blade Spindle Torque Coefficient over a Range of Pitch Ratio $(P/D)_{0.7}$ for Various Propellers

TABLE 1 - CHARACTERISTICS OF DTNSRDC MODEL PROPELLER 4572

Rotation	Right Hand
Number of Blades Z	5
Expanded Area Ratio A_E/A_0	0.739
Section Meanline	NACA a = 0.8
Section Thickness Distribution	NACA 66 (DTNSRDC Modified)
Design Advance Coefficient J	1.077
Design Advance Angle β*	26.09 deg
Design Thrust Loading Coefficient C_{Th}	0.414

x	c/D	P/D	S/D*	θ_s	Z_R/D	t/D	f_M/c	V_L/V_A**
0.3	0.1868	1.0798	0	0	0	0.0467	0.00574	1.007
0.4	0.2494	1.2710	-0.0347	- 7.56	0	0.0353	0.01370	1.013
0.5	0.3113	1.3956	-0.0523	- 9.73	0	0.0266	0.01851	1.011
0.6	0.3664	1.4433	-0.0485	- 7.94	0	0.0207	0.02069	0.996
0.7	0.4031	1.4253	-0.0214	- 3.14	0	0.0152	0.02100	0.991
0.8	0.4090	1.3531	0.0309	4.12	0	0.0115	0.01951	1.000
0.9	0.3651	1.2336	0.1089	13.37	0	0.0093	0.01811	0.996
0.95	0.3106	1.1533	0.1598	18.89	0	0.0080	0.01844	0.987
1.0	0.0700	1.0575	0.2169	24.71	0	0.0002	0.01900	0.977

*Measured from the propeller reference line, which coincides with the spindle axis, to the section midchord position.

**Radial distribution of circumferential mean longitudinal wake for which propeller was designed, $\frac{V_L}{V_A} = \frac{(1-w_x)}{2\int_{x_h}^{1} x(1-w_x)dx}$.

TABLE 2 - CHARACTERISTICS OF DTNSRDC MODEL PROPELLER 4575

Rotation	Right Hand
Number of Blades Z	5
Expanded Area Ratio A_E/A_0	0.65
Section Meanline	NACA a = 0.8
Section Thickness Distribution	NACA 16 (Modified)
Design Advance Coefficient J	0.888
Design Advance Angle β*	21.99 deg
Design Thrust Loading Coefficient C_{Th}	0.556

x	c/D	P/D	S/D*	θ_s	Z_R/D	t/D	f_M/c	V_L/V_A**
0.3	0.1686	1.0128	0	0	0	0.0450	0.00	1.020
0.4	0.2368	1.1399	-0.0430	- 4.649	-0.0044	0.0355	0.0177	1.010
0.5	0.2926	1.2106	-0.0637	- 5.911	-0.00875	0.0275	0.0204	1.010
0.6	0.3338	1.2237	-0.0604	- 4.920	-0.0131	0.0210	0.0205	1.005
0.7	0.3564	1.1925	-0.0319	- 2.321	-0.0175	0.0159	0.0187	1.005
0.8	0.3525	1.1253	0.0225	1.477	-0.0219	0.0119	0.0161	1.000
0.9	0.3022	1.0325	0.1038	6.194	-0.0262	0.0091	0.0137	0.995
0.95	0.1784	0.9813	0.1546	8.831	-0.0284	0.0072	0.0129	0.990
1.0	0.0	0.9282	0.2125	11.623	-0.0306	0.0	0.0	0.990

*Measured from the propeller reference line, which coincides with the spindle axis, to the section midchord position.

**Radial distribution of circumferential mean longitudinal wake for which propeller was designed, $\frac{V_L}{V_A} = \frac{(1-w_x)}{2\int_{x_h}^{1} x(1-w_x)dx}$.

TABLE 3 - CHARACTERISTICS OF DTNSRDC MODEL PROPELLER 4496

Rotation	Right Hand
Number of Blades Z	5
Expanded Area Ratio A_E/A_0	0.826
Section Meanline	NACA a = 0.8
Section Thickness Distribution	NACA 66 (DTNSRDC Modified)
Design Advance Coefficient J	0.767
Design Advance Angle β*	19.23 deg
Design Thrust Loading Coefficient C_{Th}	0.706

x	c/D	P/D	S/D*	θ_s	Z_R/D	t/D	f_M/c	V_L/V_A**
0.3	0.1853	0.9975	0.0185	4.853	0	0.0437	0.0189	1.008
0.4	0.2482	1.0696	0.0248	5.410	0	0.0328	0.0197	1.007
0.5	0.3111	1.1036	0.0311	5.832	0	0.0250	0.0190	1.006
0.6	0.3740	1.1016	0.0374	6.167	0	0.0187	0.0168	1.004
0.7	0.4369	1.0775	0.0437	6.424	0	0.0131	0.0128	1.002
0.8	0.4760	1.0354	0.0476	6.304	0	0.0089	0.0105	1.000
0.9	0.4600	0.9789	0.0460	5.535	0	0.0061	0.0098	0.997
0.95	0.4228	0.9444	0.0423	4.864	0	0.0051	0.0099	0.996
1.0	0.1500	0.9060	0.0150	1.651	0	0.0040	0.0100	0.994

*Measured from the propeller reference line, which coincides with the spindle axis, to the section midchord position.

**Radial distribution of circumferential mean longitudinal wake for which propeller was designed, $\frac{V_L}{V_A} = \frac{(1-w_x)}{2\int_{x_h}^{1} x(1-w_x)dx}$.

TABLE 4 - CHARACTERISTICS OF DTNSRDC MODEL PROPELLER 4536

Rotation	Right Hand
Number of Blades Z	5
Expanded Area Ratio A_E/A_0	0.622
Section Meanline	NACA a = 0.8
Section Thickness Distribution	NACA 66 (DTNSRDC Modified)
Design Advance Coefficient J	0.767
Design Advance Angle β*	19.23 deg
Design Thrust Loading Coefficient C_{Th}	0.706

x	c/D	P/D	S/D*	θ_s	Z_R/D	t/D	f_M/c	V_L/V_A**
0.3	0.1853	0.9850	0.0185	4.885	0	0.0440	0.0227	1.008
0.4	0.2168	1.0324	0.0217	4.804	0	0.0351	0.0235	1.007
0.5	0.2482	1.0591	0.0248	4.712	0	0.0280	0.0234	1.006
0.6	0.2797	1.0573	0.0280	4.664	0	0.0216	0.0215	1.004
0.7	0.3111	1.0319	0.0311	4.609	0	0.0155	0.0174	1.002
0.8	0.3307	0.9990	0.0331	4.406	0	0.0107	0.0139	1.000
0.9	0.3227	0.9542	0.0323	3.896	0	0.0073	0.0115	0.997
0.95	0.3041	0.9254	0.0304	3.502	0	0.0060	0.0105	0.996
1.0	0.1000	0.9050	0.0100	1.101	0	0.0050	0.0280	0.994

*Measured from the propeller reference line, which coincides with the spindle axis, to the section midchord position.

**Radial distribution of circumferential mean longitudinal wake for which propeller was designed, $\frac{V_L}{V_A} = \frac{(1-w_x)}{2\int_{x_h}^{1} x\,(1-w_x)dx}$.

TABLE 5 - CHARACTERISTICS OF DTNSRDC MODEL PROPELLER4535

Rotation	Right Hand
Number of Blades Z	5
Expanded Area Ratio A_E/A_0	0.83
Section Meanline	NACA a = 0.8
Section Thickness Distribution	NACA 66 (DTNSRDC Modified)
Design Advance Coefficient J	0.767
Design Advance Angle β*	19.23 deg
Design Thrust Loading Coefficient C_{Th}	0.706

x	c/D	P/D	S/D*	θ_s	Z_R/D	t/D	f_M/c	V_L/V_A**
0.3	0.1853	1.0740	0.0185	4.669	0	0.0437	0.0254	1.008
0.4	0.2482	1.0909	0.0450	9.730	0	0.0328	0.0230	1.007
0.5	0.3111	1.0939	0.0798	15.003	0	0.0250	0.0209	1.006
0.6	0.3740	1.0731	0.1213	20.137	0	0.0187	0.0190	1.004
0.7	0.4369	1.0321	0.1713	25.387	0	0.0131	0.0151	1.002
0.8	0.4760	0.9861	0.2285	30.479	0	0.0089	0.0126	1.000
0.9	0.4600	0.9205	0.2955	35.763	0	0.0061	0.0113	0.997
0.95	0.4228	0.8895	0.3305	38.121	0	0.0051	0.0104	0.996
1.0	0.1500	0.8540	0.3674	40.630	0	0.0040	0.0213	0.994

*Measured from the propeller reference line, which coincides with the spindle axis, to the section midchord position.

**Radial distribution of circumferential mean longitudinal wake for which propeller was designed, $\frac{V_L}{V_A} = \frac{(1-w_x)}{2\int_{x_h}^{1} x(1-w_x)dx}$.

TABLE 6 - CHARACTERISTICS OF DTNSRDC MODEL PROPELLER 4517

Rotation	Right Hand
Number of Blades Z	5
Expanded Area Ratio A_E/A_0	0.83
Section Meanline	NACA a = 0.8
Section Thickness Distribution	NACA 66 (DTNSRDC Modified)
Design Advance Coefficient J	0.767
Design Advance Angle β*	19.23 deg
Design Thrust Loading Coefficient C_{Th}	0.706

x	c/D	P/D	S/D*	θ_s	Z_R/D	t/D	f_M/c	V_L/V_A**
0.3	0.1853	0.9975	0.0185	4.853	0	0.0437	0.0232	1.008
0.4	0.2482	1.0885	-0.0020	- 0.443	0	0.0328	0.0189	1.007
0.5	0.3111	1.1354	-0.0010	- 0.186	0	0.0250	0.0167	1.006
0.6	0.3740	1.1306	+0.0134	2.195	0	0.0187	0.0150	1.004
0.7	0.4369	1.0912	0.0437	6.408	0	0.0131	0.0124	1.002
0.8	0.4760	1.0339	0.0919	12.174	0	0.0089	0.0116	1.000
0.9	0.4600	0.9517	0.1615	19.489	0	0.0061	0.0124	0.997
0.95	0.4228	0.9025	0.2128	24.570	0	0.0051	0.0154	0.996
1.0	0.1500	0.8560	0.0341	37.700	0	0.0040	0.0487	0.994

*Measured from the propeller reference line, which coincides with the spindle axis, to the section midchord position.

**Radial distribution of circumferential mean longitudinal wake for which propeller was designed, $\frac{V_L}{V_A} = \frac{(1-w_x)}{2\int_{x_h}^{1} x(1-w_x)dx}$.

TABLE 7 - CHARACTERISTICS OF DTNSRDC MODEL PROPELLER 4402

Rotation	Right Hand
Number of Blades Z	5
Expanded Area Ratio A_E/A_0	0.83
Section Meanline	NACA 65
Section Thickness Distribution	NACA 16 (Modified)
Design Advance Coefficient J	0.767
Design Advance Angle β*	19.23 deg
Design Thrust Loading Coefficient C_{Th}	0.706

x	c/D	P/D	S/D*	θ_s	Z_R/D	t/D	f_M/c	V_L/V_A**
0.3	0.1853	1.008	0.0185	4.826	0	0.0437	0.0243	1.008
0.4	0.2482	1.044	0.0248	5.465	0	0.0328	0.0302	1.007
0.5	0.3111	1.067	0.0311	5.896	0	0.0250	0.0280	1.006
0.6	0.3740	1.072	0.0374	6.209	0	0.0187	0.0240	1.004
0.7	0.4369	1.061	0.0437	6.443	0	0.0131	0.0191	1.002
0.8	0.4760	1.025	0.0476	6.313	0	0.0089	0.0140	1.000
0.9	0.4600	0.964	0.0460	5.544	0	0.0061	0.0082	0.997
0.95	0.4587	0.922	0.0459	4.750	0	0.0051	0.0042	0.996
1.0	0.3400	0.878	0.0340	2.372	0	0.0040	0.0000	0.994

*Measured from the propeller reference line, which coincides with the spindle axis, to the section midchord position.

**Radial distribution of circumferential mean longitudinal wake for which propeller was designed, $\frac{V_L}{V_A} = \frac{(1-w_x)}{2\int_{x_h}^{1} x(1-w_x)dx}$.

TABLE 8 - EXPERIMENTAL SPINDLE TORQUE AT DESIGN ADVANCE COEFFICIENT FOR VARIOUS PROPELLERS
(Propellers scaled to full-scale conditions indicated in the table. All values of spindle torque are given in pounds-feet x 10^{-3})

Diameter D	16.0 feet
Speed of Advance V_A	20.0 knots
Propeller Material	Nickle-Aluminum-Bronze
Mass Density of Propeller Blades	484 lb/ft^3
Advance Coefficient	Design value

Propeller	J_D	n(rpm)	Q_{SH}	Q_{SC}	Q_s
4572	1.077	117.5	- 1.9	-15.8	- 17.7
4575	0.888	142.6	15.6	-13.4	+ 2.2
4496	0.767	165.0	10.1	-18.6	- 8.5
4536	0.767	165.0	3.4	-11.7	- 8.3
4535	0.767	165.0	-89.2	-44.7	-133.9
4517	0.767	165.0	-77.4	-28.0	-105.4

REFERENCES

1. Rusetskiy, A.A., "Hydrodynamics of Controllable-Pitch Propellers," Shipbuilding Publishing House, Leningrad (1968) (in Russian).

2. Gunsteren, L.A., van, "Hydrodynamics of Controllable-Pitch-Propellers," in "Design and Economical Consideration on Shipbuilding and Shipping," Report of Postgraduate Course, May 1969, University of Delft, the Netherlands, H. Veenman En Zonen N.V., Wageningen, the Netherlands (1970) pp. 212-252; also, presented as "Design and Performance of Controllable-Pitch Propellers," New York Metropoliten Section of the Society of Naval Architects and Marine Engineers (Mar 1970).

3. Schanz, F., "The Controllable-Pitch Propeller as an Integral Part of the Ship's Propulsion System," Transactions of Society of Naval Architects and Marine Engineers, Vol. 75, pp. 194-223 (1967).

4. Boatwright, G.M. and J. Strandell, "Controllable Pitch Propellers," Fourth Annual Technical Symposium, Association of Senior Engineers, Naval Ship Systems Command, Washington, D.C. (31 Mar 1967).

5. Tsuchida, K., "Design Diagrams of Three-Bladed Controllable Pitch Propellers," Proceedings, Fourth ONR Symposium on Naval Hydrodynamics, Washington, D.C. (Aug 1962).

6. Yazaki, A., "Model Tests on Four-Bladed Controllable-Pitch Propellers," Ship Research Institute, Tokyo, Japan, Paper 1 (Mar 1964).

7. Yazaki, A. and S. Nobuo, "Further Model Tests on Four-Bladed Controllable-Pitch Propellers," Ship Research Institute, Tokyo, Japan, Paper 16 (Aug 1966).

8. Gutsche, F. and G. Schroeder, "Freifahrversuche an Propellern mit festen und verstellbaren Flugeln voraus and zuruck (Open Water Tests on Fixed-Bladed and Controllable-Pitch Propellers in Forward and Backing Operations), Schiffbauforschung, Vol. 2, No. 4 (1963).

9. Strom-Tejsen, J. and R.R. Porter, "Prediction of Controllable-Pitch Propeller Performance in Off-Design Conditions," Third Ship Control Systems Symposium, Bath, England (Aug 1972).

10. Tsao, S.S., "Documentation of Programs for the Analysis of Performance and Spindle Torque of Controllable-Pitch Propellers," Massachusetts Institute of Technology, Department of Ocean Engineering Report 75-8 (May 1975).

11. Boswell, R.J., "A Method of Calculating the Spindle Torque of a Controllable-Pitch Propeller at Design Conditions," NSRDC Report 1529 (Aug 1961).

12. Klaasen and Arnoldus, "Actuating Forces in Controllable Pitch Propellers," Transactions Institute of Marine Engineers, Vol. 76, No. 6 (Jun 1964).

13. Miller, M.L., "Spindle Torque Tests of Four CRP Propeller Blade Designs for MSO-421," NSRDC Report 1837 (Jul 1964).

14. Hansen, E.O., "Thrust and Blade Spindle Torque Measurements of Five Controllable-Pitch Propeller Designs for MSO-421," NSRDC Report 2325 (Apr 1967).

15. Denny, S.B. and J.J. Nelka, "Blade Spindle Moment on a Five-Bladed Controllable-Pitch Propeller," NSRDC Report 3729 (Jan 1972).

16. Denny, S.B. and H.G. Stephens, "Blade Spindle Moment on Controllable-Pitch Propellers," NSRDC Report SPD-011-14 (Jul 1974).

17. Stephens, H.G., "Open Water Performance of a Controllable-Pitch (C-P) Propeller Series," NSRDC Report SPD-011-13 (Jul 1974).

18. Cheng, H.M., "Hydrodynamic Aspect of Propeller Design Based on Lifting-Surface Theory," Part 1 David Taylor Model Basin Report 1802 (Sep 1964) and Part 2 DTMB Report 1803 (Jun 1965).

19. Kerwin, J.E. and R. Leopold, "A Design Theory for Subcavitating Propellers," Transactions Society of Naval Architects and Marine Engineers, Vol. 72, pp. 294-335 (1964).

20. Denny, S.B. et al., "Hydrodynamic Design Considerations for the Controllable-Pitch Propeller for the Guided Missile Frigate," Naval Engineers Journal, pp. 72-81 (Apr 1975).

21. Cumming, R.A. et al., "Highly Skewed Propellers," Transactions Society of Naval Architects and Marine Engineers, Vol. 80 (1972).

22. Boswell, R.J. and G.G. Cox, "Design and Model Evaluation of a Highly Skewed Propeller for a Cargo Ship," Marine Technology, Vol. 11, No. 1, pp. 73-89 (Jan 1974).

23. Van Lammerman, W.P.A. et al., "The Wageningen B-Screw Series," Transactions Society of Naval Architects and Marine Engineers, Vol. 77, pp. 269-317 (1969).

24. Kerwin, J.E., "Computer Techniques for Propeller Blade Section Design," Proceedings Second LIPS Propeller Symposium, Drunen, Holland, pp. 7-31 (May 1973).

25. Nelka, J.J., "Experimental Evaluation of a Series of Skewed Propellers with Forward Rake: Open Water Performance, Cavitation Performance, Field-Point Pressures, and Unsteady Propeller Loading," NSRDC Report 4113 (Jul 1974).